

Appendix E-2e

**Regional Haze Modeling for Southeastern VISTAS II
Regional Haze Analysis Project 2028elv3 CAMx
Version 6.40 12km VISTAS and EPA 12km
Continental Grid Comparison Report**

Benchmark Run #6

August 17, 2020

This page intentionally left blank.

**Regional Haze Modeling for Southeastern
VISTAS II Regional Haze Analysis Project
2028elv3 CAMx Version 6.40 12km VISTAS
and EPA 12km Continental Grid Comparison
Report**

Task 6 Benchmark Report #5
Covering Benchmark Run #6

Prepared for:

**Southeastern States Air Resource Managers, Inc.
(SESARM)**

205 Corporate Center Drive, Suite D
Stockbridge, GA 30281-7383

Under Contract No. V-2018-03-01

Prepared by:
Alpine Geophysics, LLC
387 Pollard Mine Road
Burnsville, NC 28714

and

Eastern Research Group, Inc.
1600 Perimeter Park Dr., Suite 200
Morrisville, NC 27560

Final – August 17, 2020

Alpine Project Number: TS-527
ERG Project Number: 4133.00.006

This page is intentionally blank.

Contents

	Page
1.0 INTRODUCTION	1
1.1 Overview.....	1
1.2 CAMx 6.40 2028elv3 VISTAS12 and EPA 12US2 Comparison	3
2.0 DEVELOPMENT OF VISTAS12 INPUTS.....	4
3.0 CONFIRMATION METHODOLOGY.....	4
3.1 CAMx Species Mapping.....	6
4.0 VISTAS12 AND 12US2 CAMX 6.40 2018ELV3 COMPARISON.....	6
4.1 Ozone	6
4.2 PM _{2.5}	30
4.3 Sulfate	53
4.4 Nitrate	76
4.5 Organic Matter (OM).....	99
5.0 CONCLUSIONS.....	122

This page is intentionally blank.

TABLES

Table 1-1. VISTAS II Modeling Domain Specifications	3
Table 3-1. Species Mapping from CAMx into Aggregated Species	6
Table 4-1. Comparison of 2028elv3 CAMx 6.40 VISTAS12 and 12US2 Simulation of Ozone Concentrations (ppb). Hours with the top 10 maximum positive and maximum negative differences are shown.....	8
Table 4-2. Comparison of 2028elv3 CAMx 6.40 VISTAS12 and 12US2 Simulation of PM _{2.5} Concentrations ($\mu\text{g}/\text{m}^3$). Hours with the top 10 maximum positive and maximum negative differences are shown.....	31
Table 4-3. Comparison of 2028elv3 CAMx 6.40 VISTAS12 and 12US2 Simulation of Sulfate Concentrations ($\mu\text{g}/\text{m}^3$). Hours with the top 10 maximum positive and maximum negative differences are shown.....	54
Table 4-4. Comparison of 2028elv3 CAMx 6.40 VISTAS12 and 12US2 Simulation of Nitrate Concentrations ($\mu\text{g}/\text{m}^3$). Hours with the top 10 maximum positive and maximum negative differences are shown.....	77
Table 4-5. Comparison of 2028elv3 CAMx 6.40 VISTAS12 and 12US2 Simulation of Organic Matter Concentrations ($\mu\text{g}/\text{m}^3$). Hours with the top 10 maximum positive and maximum negative differences are shown.....	100

FIGURES

Figure 1-1. Map of 12km CAMx Modeling Domains. VISTAS12 Domain Represented as Inner Red Domain.....	3
Figure 4-1: Comparison of Ozone Concentrations (ppb) for CAMx 6.40 on VISTAS12 and 12US2 Domains 2028elv3 Simulations (Maximum Positive Difference).....	9
Figure 4-2: Comparison of Ozone Concentrations (ppb) for CAMx 6.40 on VISTAS12 and 12US2 Domains 2028elv3 Simulations (Second Highest Positive Difference)	10
Figure 4-3: Comparison of Ozone Concentrations (ppb) for CAMx 6.40 on VISTAS12 and 12US2 Domains 2028elv3 Simulations (Third Highest Positive Difference)	11
Figure 4-4: Comparison of Ozone Concentrations (ppb) for CAMx 6.40 on VISTAS12 and 12US2 Domains 2028elv3 Simulations (Fourth Highest Positive Difference)	12
Figure 4-5: Comparison of Ozone Concentrations (ppb) for CAMx 6.40 on VISTAS12 and 12US2 Domains 2028elv3 Simulations (Fifth Highest Positive Difference)	13
Figure 4-6: Comparison of Ozone Concentrations (ppb) for CAMx 6.40 on VISTAS12 and 12US2 Domains 2028elv3 Simulations (Sixth Highest Positive Difference)	14

Figure 4-7: Comparison of Ozone Concentrations (ppb) for CAMx 6.40 on VISTAS12 and 12US2 Domains 2028elv3 Simulations (Seventh Highest Positive Difference)	15
Figure 4-8: Comparison of Ozone Concentrations (ppb) for CAMx 6.40 on VISTAS12 and 12US2 Domains 2028elv3 Simulations (Eighth Highest Positive Difference)	16
Figure 4-9: Comparison of Ozone Concentrations (ppb) for CAMx 6.40 on VISTAS12 and 12US2 Domains 2028elv3 Simulations (Ninth Highest Positive Difference)	17
Figure 4-10: Comparison of Ozone Concentrations (ppb) for CAMx 6.40 on VISTAS12 and 12US2 Domains 2028elv3 Simulations (Tenth Highest Positive Difference)	18
Figure 4-11: Comparison of Ozone Concentrations (ppb) for CAMx 6.40 on VISTAS12 and 12US2 Domains 2028elv3 Simulations (Maximum Negative Difference)	19
Figure 4-12: Comparison of Ozone Concentrations (ppb) for CAMx 6.40 on VISTAS12 and 12US2 Domains 2028elv3 Simulations (Second Highest Negative Difference)	20
Figure 4-13: Comparison of Ozone Concentrations (ppb) for CAMx 6.40 on VISTAS12 and 12US2 Domains 2028elv3 Simulations (Third Highest Negative Difference)	21
Figure 4-14: Comparison of Ozone Concentrations (ppb) for CAMx 6.40 on VISTAS12 and 12US2 Domains 2028elv3 Simulations (Fourth Highest Negative Difference)	22
Figure 4-15: Comparison of Ozone Concentrations (ppb) for CAMx 6.40 on VISTAS12 and 12US2 Domains 2028elv3 Simulations (Fifth Highest Negative Difference)	23
Figure 4-16: Comparison of Ozone Concentrations (ppb) for CAMx 6.40 on VISTAS12 and 12US2 Domains 2028elv3 Simulations (Sixth Highest Negative Difference)	24
Figure 4-17: Comparison of Ozone Concentrations (ppb) for CAMx 6.40 on VISTAS12 and 12US2 Domains 2028elv3 Simulations (Seventh Highest Negative Difference)	25
Figure 4-18: Comparison of Ozone Concentrations (ppb) for CAMx 6.40 on VISTAS12 and 12US2 Domains 2028elv3 Simulations (Eighth Highest Negative Difference)	26
Figure 4-19: Comparison of Ozone Concentrations (ppb) for CAMx 6.40 on VISTAS12 and 12US2 Domains 2028elv3 Simulations (Ninth Highest Negative Difference)	27
Figure 4-20: Comparison of Ozone Concentrations (ppb) for CAMx 6.40 on VISTAS12 and 12US2 Domains 2028elv3 Simulations (Tenth Highest Negative Difference)	28
Figure 4-21: Scatterplot Comparing 24-hour Average Predicted Ozone Concentrations (ppb) for All Days at all IMPROVE Monitor Locations for CAMx 6.40 on VISTAS12 and 12US2 Domains 2028elv3 Simulations Performed by VISTAS (Alpine)	29
Figure 4-22: Comparison of PM _{2.5} Concentrations ($\mu\text{g}/\text{m}^3$) for CAMx 6.40 on VISTAS12 and 12US2 Domains 2028elv3 Simulations (Maximum Positive Difference)	32
Figure 4-23: Comparison of PM _{2.5} Concentrations ($\mu\text{g}/\text{m}^3$) for CAMx 6.40 on VISTAS12 and 12US2 Domains 2028elv3 Simulations (Second Highest Positive Difference)	33
Figure 4-24: Comparison of PM _{2.5} Concentrations ($\mu\text{g}/\text{m}^3$) for CAMx 6.40 on VISTAS12 and 12US2 Domains 2028elv3 Simulations (Third Highest Positive Difference)	34

Figure 4-25: Comparison of PM _{2.5} Concentrations ($\mu\text{g}/\text{m}^3$) for CAMx 6.40 on VISTAS12 and 12US2 Domains 2028elv3 Simulations (Fourth Highest Positive Difference)	35
Figure 4-26: Comparison of PM _{2.5} Concentrations ($\mu\text{g}/\text{m}^3$) for CAMx 6.40 on VISTAS12 and 12US2 Domains 2028elv3 Simulations (Fifth Highest Positive Difference)	36
Figure 4-27: Comparison of PM _{2.5} Concentrations ($\mu\text{g}/\text{m}^3$) for CAMx 6.40 on VISTAS12 and 12US2 Domains 2028elv3 Simulations (Sixth Highest Positive Difference).....	37
Figure 4-28: Comparison of PM _{2.5} Concentrations ($\mu\text{g}/\text{m}^3$) for CAMx 6.40 on VISTAS12 and 12US2 Domains 2028elv3 Simulations (Seventh Highest Positive Difference)	38
Figure 4-29: Comparison of PM _{2.5} Concentrations ($\mu\text{g}/\text{m}^3$) for CAMx 6.40 on VISTAS12 and 12US2 Domains 2028elv3 Simulations (Eighth Highest Positive Difference)	39
Figure 4-30: Comparison of PM _{2.5} Concentrations ($\mu\text{g}/\text{m}^3$) for CAMx 6.40 on VISTAS12 and 12US2 Domains 2028elv3 Simulations (Ninth Highest Positive Difference)	40
Figure 4-31: Comparison of PM _{2.5} Concentrations ($\mu\text{g}/\text{m}^3$) for CAMx 6.40 on VISTAS12 and 12US2 Domains 2028elv3 Simulations (Tenth Highest Positive Difference).....	41
Figure 4-32: Comparison of PM _{2.5} Concentrations ($\mu\text{g}/\text{m}^3$) for CAMx 6.40 on VISTAS12 and 12US2 Domains 2028elv3 Simulations (Maximum Negative Difference)	42
Figure 4-33: Comparison of PM _{2.5} Concentrations ($\mu\text{g}/\text{m}^3$) for CAMx 6.40 on VISTAS12 and 12US2 Domains 2028elv3 Simulations (Second Highest Negative Difference).....	43
Figure 4-34: Comparison of PM _{2.5} Concentrations ($\mu\text{g}/\text{m}^3$) for CAMx 6.40 on VISTAS12 and 12US2 Domains 2028elv3 Simulations (Third Highest Negative Difference).....	44
Figure 4-35: Comparison of PM _{2.5} Concentrations ($\mu\text{g}/\text{m}^3$) for CAMx 6.40 on VISTAS12 and 12US2 Domains 2028elv3 Simulations (Fourth Highest Negative Difference)	45
Figure 4-36: Comparison of PM _{2.5} Concentrations ($\mu\text{g}/\text{m}^3$) for CAMx 6.40 on VISTAS12 and 12US2 Domains 2028elv3 Simulations (Fifth Highest Negative Difference).....	46
Figure 4-37: Comparison of PM _{2.5} Concentrations ($\mu\text{g}/\text{m}^3$) for CAMx 6.40 on VISTAS12 and 12US2 Domains 2028elv3 Simulations (Sixth Highest Negative Difference)	47
Figure 4-38: Comparison of PM _{2.5} Concentrations ($\mu\text{g}/\text{m}^3$) for CAMx 6.40 on VISTAS12 and 12US2 Domains 2028elv3 Simulations (Seventh Highest Negative Difference).....	48
Figure 4-39: Comparison of PM _{2.5} Concentrations ($\mu\text{g}/\text{m}^3$) for CAMx 6.40 on VISTAS12 and 12US2 Domains 2028elv3 Simulations (Eighth Highest Negative Difference)	49
Figure 4-40: Comparison of PM _{2.5} Concentrations ($\mu\text{g}/\text{m}^3$) for CAMx 6.40 on VISTAS12 and 12US2 Domains 2028elv3 Simulations (Ninth Highest Negative Difference)	50
Figure 4-41: Comparison of PM _{2.5} Concentrations ($\mu\text{g}/\text{m}^3$) for CAMx 6.40 on VISTAS12 and 12US2 Domains 2028elv3 Simulations (Tenth Highest Negative Difference)	51
Figure 4-42: Scatterplot Comparing 24-hour Average Predicted PM _{2.5} Concentrations ($\mu\text{g}/\text{m}^3$) for All Days at all IMPROVE Monitor Locations for CAMx 6.40 on	

VISTAS12 and 12US2 Domains 2028elv3 Simulations Performed by VISTAS (Alpine).....	52
Figure 4-43: Comparison of Sulfate Concentrations ($\mu\text{g}/\text{m}^3$) for CAMx 6.40 on VISTAS12 and 12US2 Domains 2028elv3 Simulations (Maximum Positive Difference).....	55
Figure 4-44: Comparison of Sulfate Concentrations ($\mu\text{g}/\text{m}^3$) for CAMx 6.40 on VISTAS12 and 12US2 Domains 2028elv3 Simulations (Second Highest Positive Difference)	56
Figure 4-45: Comparison of Sulfate Concentrations ($\mu\text{g}/\text{m}^3$) for CAMx 6.40 on VISTAS12 and 12US2 Domains 2028elv3 Simulations (Third Highest Positive Difference)	57
Figure 4-46: Comparison of Sulfate Concentrations ($\mu\text{g}/\text{m}^3$) for CAMx 6.40 on VISTAS12 and 12US2 Domains 2028elv3 Simulations (Fourth Highest Positive Difference)	58
Figure 4-47: Comparison of Sulfate Concentrations ($\mu\text{g}/\text{m}^3$) for CAMx 6.40 on VISTAS12 and 12US2 Domains 2028elv3 Simulations (Fifth Highest Positive Difference)	59
Figure 4-48: Comparison of Sulfate Concentrations ($\mu\text{g}/\text{m}^3$) for CAMx 6.40 on VISTAS12 and 12US2 Domains 2028elv3 Simulations (Sixth Highest Positive Difference).....	60
Figure 4-49: Comparison of Sulfate Concentrations ($\mu\text{g}/\text{m}^3$) for CAMx 6.40 on VISTAS12 and 12US2 Domains 2028elv3 Simulations	61
Figure 4-50: Comparison of Sulfate Concentrations ($\mu\text{g}/\text{m}^3$) for CAMx 6.40 on VISTAS12 and 12US2 Domains 2028elv3 Simulations (Eighth Highest Positive Difference)	62
Figure 4-51: Comparison of Sulfate Concentrations ($\mu\text{g}/\text{m}^3$) for CAMx 6.40 on VISTAS12 and 12US2 Domains 2028elv3 Simulations (Ninth Highest Positive Difference)	63
Figure 4-52: Comparison of Sulfate Concentrations ($\mu\text{g}/\text{m}^3$) for CAMx 6.40 on VISTAS12 and 12US2 Domains 2028elv3 Simulations (Tenth Highest Positive Difference).....	64
Figure 4-53: Comparison of Sulfate Concentrations ($\mu\text{g}/\text{m}^3$) for CAMx 6.40 on VISTAS12 and 12US2 Domains 2028elv3 Simulations (Maximum Negative Difference)	65
Figure 4-54: Comparison of Sulfate Concentrations ($\mu\text{g}/\text{m}^3$) for CAMx 6.40 on VISTAS12 and 12US2 Domains 2028elv3 Simulations (Second Highest Negative Difference).....	66
Figure 4-55: Comparison of Sulfate Concentrations ($\mu\text{g}/\text{m}^3$) for CAMx 6.40 on VISTAS12 and 12US2 Domains 2028elv3 Simulations (Third Highest Negative Difference).....	67
Figure 4-56: Comparison of Sulfate Concentrations ($\mu\text{g}/\text{m}^3$) for CAMx 6.40 on VISTAS12 and 12US2 Domains 2028elv3 Simulations (Fourth Highest Negative Difference)	68
Figure 4-57: Comparison of Sulfate Concentrations ($\mu\text{g}/\text{m}^3$) for CAMx 6.40 on VISTAS12 and 12US2 Domains 2028elv3 Simulations (Fifth Highest Negative Difference).....	69
Figure 4-58: Comparison of Sulfate Concentrations ($\mu\text{g}/\text{m}^3$) for CAMx 6.40 on VISTAS12 and 12US2 Domains 2028elv3 Simulations (Sixth Highest Negative Difference)	70
Figure 4-59: Comparison of Sulfate Concentrations ($\mu\text{g}/\text{m}^3$) for CAMx 6.40 on VISTAS12 and 12US2 Domains 2028elv3 Simulations (Seventh Highest Negative Difference).....	71

Figure 4-60: Comparison of Sulfate Concentrations ($\mu\text{g}/\text{m}^3$) for CAMx 6.40 on VISTAS12 and 12US2 Domains 2028elv3 Simulations (Eighth Highest Negative Difference)	72
Figure 4-61: Comparison of Sulfate Concentrations ($\mu\text{g}/\text{m}^3$) for CAMx 6.40 on VISTAS12 and 12US2 Domains 2028elv3 Simulations (Ninth Highest Negative Difference)	73
Figure 4-62: Comparison of Sulfate Concentrations ($\mu\text{g}/\text{m}^3$) for CAMx 6.40 on VISTAS12 and 12US2 Domains 2028elv3 Simulations (Tenth Highest Negative Difference)	74
Figure 4-63: Scatterplot Comparing 24-hour Average Predicted Sulfate Concentrations ($\mu\text{g}/\text{m}^3$) for All Days at all IMPROVE Monitor Locations for CAMx 6.40 on VISTAS12 and 12US2 Domains 2028elv3 Simulations Performed by VISTAS (Alpine).....	75
Figure 4-64: Comparison of Nitrate Concentrations ($\mu\text{g}/\text{m}^3$) for CAMx 6.40 on VISTAS12 and 12US2 Domains 2028elv3 Simulations (Maximum Positive Difference)	78
Figure 4-65: Comparison of Nitrate Concentrations ($\mu\text{g}/\text{m}^3$) for CAMx 6.40 on VISTAS12 and 12US2 Domains 2028elv3 Simulations (Second Highest Positive Difference)	79
Figure 4-66: Comparison of Nitrate Concentrations ($\mu\text{g}/\text{m}^3$) for CAMx 6.40 on VISTAS12 and 12US2 Domains 2028elv3 Simulations (Third Highest Positive Difference)	80
Figure 4-67: Comparison of Nitrate Concentrations ($\mu\text{g}/\text{m}^3$) for CAMx 6.40 on VISTAS12 and 12US2 Domains 2028elv3 Simulations (Fourth Highest Positive Difference)	81
Figure 4-68: Comparison of Nitrate Concentrations ($\mu\text{g}/\text{m}^3$) for CAMx 6.40 on VISTAS12 and 12US2 Domains 2028elv3 Simulations (Fifth Highest Positive Difference)	82
Figure 4-69: Comparison of Nitrate Concentrations ($\mu\text{g}/\text{m}^3$) for CAMx 6.40 on VISTAS12 and 12US2 Domains 2028elv3 Simulations (Sixth Highest Positive Difference).....	83
Figure 4-70: Comparison of Nitrate Concentrations ($\mu\text{g}/\text{m}^3$) for CAMx 6.40 on VISTAS12 and 12US2 Domains 2028elv3 Simulations (Seventh Highest Positive Difference)	84
Figure 4-71: Comparison of Nitrate Concentrations ($\mu\text{g}/\text{m}^3$) for CAMx 6.40 on VISTAS12 and 12US2 Domains 2028elv3 Simulations (Eighth Highest Positive Difference)	85
Figure 4-72: Comparison of Nitrate Concentrations ($\mu\text{g}/\text{m}^3$) for CAMx 6.40 on VISTAS12 and 12US2 Domains 2028elv3 Simulations (Ninth Highest Positive Difference)	86
Figure 4-73: Comparison of Nitrate Concentrations ($\mu\text{g}/\text{m}^3$) for CAMx 6.40 on VISTAS12 and 12US2 Domains 2028elv3 Simulations (Tenth Highest Positive Difference).....	87
Figure 4-74: Comparison of Nitrate Concentrations ($\mu\text{g}/\text{m}^3$) for CAMx 6.40 on VISTAS12 and 12US2 Domains 2028elv3 Simulations (Maximum Negative Difference)	88
Figure 4-75: Comparison of Nitrate Concentrations ($\mu\text{g}/\text{m}^3$) for CAMx 6.40 on VISTAS12 and 12US2 Domains 2028elv3 Simulations (Second Highest Negative Difference).....	89
Figure 4-76: Comparison of Nitrate Concentrations ($\mu\text{g}/\text{m}^3$) for CAMx 6.40 on VISTAS12 and 12US2 Domains 2028elv3 Simulations (Third Highest Negative Difference).....	90

Figure 4-77: Comparison of Nitrate Concentrations ($\mu\text{g}/\text{m}^3$) for CAMx 6.40 on VISTAS12 and 12US2 Domains 2028elv3 Simulations (Fourth Highest Negative Difference)	91
Figure 4-78: Comparison of Nitrate Concentrations ($\mu\text{g}/\text{m}^3$) for CAMx 6.40 on VISTAS12 and 12US2 Domains 2028elv3 Simulations (Fifth Highest Negative Difference)	92
Figure 4-79: Comparison of Nitrate Concentrations ($\mu\text{g}/\text{m}^3$) for CAMx 6.40 on VISTAS12 and 12US2 Domains 2028elv3 Simulations (Sixth Highest Negative Difference)	93
Figure 4-80: Comparison of Nitrate Concentrations ($\mu\text{g}/\text{m}^3$) for CAMx 6.40 on VISTAS12 and 12US2 Domains 2028elv3 Simulations (Seventh Highest Negative Difference)	94
Figure 4-81: Comparison of Nitrate Concentrations ($\mu\text{g}/\text{m}^3$) for CAMx 6.40 on VISTAS12 and 12US2 Domains 2028elv3 Simulations (Eighth Highest Negative Difference)	95
Figure 4-82: Comparison of Nitrate Concentrations ($\mu\text{g}/\text{m}^3$) for CAMx 6.40 on VISTAS12 and 12US2 Domains 2028elv3 Simulations (Ninth Highest Negative Difference)	96
Figure 4-83: Comparison of Nitrate Concentrations ($\mu\text{g}/\text{m}^3$) for CAMx 6.40 on VISTAS12 and 12US2 Domains 2028elv3 Simulations (Tenth Highest Negative Difference)	97
Figure 4-84: Scatterplot Comparing 24-hour Average Predicted Nitrate Concentrations ($\mu\text{g}/\text{m}^3$) for All Days at all IMPROVE Monitor Locations for CAMx 6.40 on VISTAS12 and 12US2 Domains 2028elv3 Simulations Performed by VISTAS (Alpine)	98
Figure 4-85: Comparison of Organic Matter Concentrations ($\mu\text{g}/\text{m}^3$) for CAMx 6.40 on VISTAS12 and 12US2 Domains 2028elv3 Simulations (Maximum Positive Difference)	101
Figure 4-86: Comparison of Organic Matter Concentrations ($\mu\text{g}/\text{m}^3$) for CAMx 6.40 on VISTAS12 and 12US2 Domains 2028elv3 Simulations (Second Highest Positive Difference)	102
Figure 4-87: Comparison of Organic Matter Concentrations ($\mu\text{g}/\text{m}^3$) for CAMx 6.40 on VISTAS12 and 12US2 Domains 2028elv3 Simulations (Third Highest Positive Difference)	103
Figure 4-88: Comparison of Organic Matter Concentrations ($\mu\text{g}/\text{m}^3$) for CAMx 6.40 on VISTAS12 and 12US2 Domains 2028elv3 Simulations (Fourth Highest Positive Difference)	104
Figure 4-89: Comparison of Organic Matter Concentrations ($\mu\text{g}/\text{m}^3$) for CAMx 6.40 on VISTAS12 and 12US2 Domains 2028elv3 Simulations (Fifth Highest Positive Difference)	105
Figure 4-90: Comparison of Organic Matter Concentrations ($\mu\text{g}/\text{m}^3$) for CAMx 6.40 on VISTAS12 and 12US2 Domains 2028elv3 Simulations (Sixth Highest Positive Difference)	106
Figure 4-91: Comparison of Organic Matter Concentrations ($\mu\text{g}/\text{m}^3$) for CAMx 6.40 on VISTAS12 and 12US2 Domains 2028elv3 Simulations (Seventh Highest Positive Difference)	107

Figure 4-92: Comparison of Organic Matter Concentrations ($\mu\text{g}/\text{m}^3$) for CAMx 6.40 on VISTAS12 and 12US2 Domains 2028elv3 Simulations (Eighth Highest Positive Difference)	108
Figure 4-93: Comparison of Organic Matter Concentrations ($\mu\text{g}/\text{m}^3$) for CAMx 6.40 on VISTAS12 and 12US2 Domains 2028elv3 Simulations (Ninth Highest Positive Difference)	109
Figure 4-94: Comparison of Organic Matter Concentrations ($\mu\text{g}/\text{m}^3$) for CAMx 6.40 on VISTAS12 and 12US2 Domains 2028elv3 Simulations (Tenth Highest Positive Difference)	110
Figure 4-95: Comparison of Organic Matter Concentrations ($\mu\text{g}/\text{m}^3$) for CAMx 6.40 on VISTAS12 and 12US2 Domains 2028elv3 Simulations (Maximum Negative Difference)	111
Figure 4-96: Comparison of Organic Matter Concentrations ($\mu\text{g}/\text{m}^3$) for CAMx 6.40 on VISTAS12 and 12US2 Domains 2028elv3 Simulations (Second Highest Negative Difference)	112
Figure 4-97: Comparison of Organic Matter Concentrations ($\mu\text{g}/\text{m}^3$) for CAMx 6.40 on VISTAS12 and 12US2 Domains 2028elv3 Simulations (Third Highest Negative Difference)	113
Figure 4-98: Comparison of Organic Matter Concentrations ($\mu\text{g}/\text{m}^3$) for CAMx 6.40 on VISTAS12 and 12US2 Domains 2028elv3 Simulations (Fourth Highest Negative Difference)	114
Figure 4-99: Comparison of Organic Matter Concentrations ($\mu\text{g}/\text{m}^3$) for CAMx 6.40 on VISTAS12 and 12US2 Domains 2028elv3 Simulations (Fifth Highest Negative Difference)	115
Figure 4-100: Comparison of Organic Matter Concentrations ($\mu\text{g}/\text{m}^3$) for CAMx 6.40 on VISTAS12 and 12US2 Domains 2028elv3 Simulations (Sixth Highest Negative Difference)	116
Figure 4-101: Comparison of Organic Matter Concentrations ($\mu\text{g}/\text{m}^3$) for CAMx 6.40 on VISTAS12 and 12US2 Domains 2028elv3 Simulations (Seventh Highest Negative Difference)	117
Figure 4-102: Comparison of Organic Matter Concentrations ($\mu\text{g}/\text{m}^3$) for CAMx 6.40 on VISTAS12 and 12US2 Domains 2028elv3 Simulations (Eighth Highest Negative Difference)	118
Figure 4-103: Comparison of Organic Matter Concentrations ($\mu\text{g}/\text{m}^3$) for CAMx 6.40 on VISTAS12 and 12US2 Domains 2028elv3 Simulations (Ninth Highest Negative Difference)	119
Figure 4-104: Comparison of Organic Matter Concentrations ($\mu\text{g}/\text{m}^3$) for CAMx 6.40 on VISTAS12 and 12US2 Domains 2028elv3 Simulations (Tenth Highest Negative Difference)	120

Figure 4-105: Scatterplot Comparing 24-hour Average Predicted Organic Matter Concentrations ($\mu\text{g}/\text{m}^3$) for All Days at all IMPROVE Monitor Locations for CAMx 6.40 on VISTAS12 and 12US2 Domains 2028elv3 Simulations Performed by VISTAS (Alpine) 121

This page is intentionally blank.

Abbreviations/Acronym List

Alpine	Alpine Geophysics, LLC
BNDEXTR	Boundary extraction program
CAMx	Comprehensive Air quality Model with eXtensions
CONUS	Continental U.S.
dv	Deciview
ERG	Eastern Research Group, Inc.
EPA	Environmental Protection Agency
FCRS	Crustal fraction of PM
FLM	Federal Land Manager
FORTRAN	Formula Translation programming language
FPRM	Fine other primary (diameter $\leq 2.5\mu\text{m}$)
FR	Federal Register
IMPROVE	Interagency Monitoring of Protected Visual Environments
km	kilometer
$\mu\text{g}/\text{m}^3$	microgram per cubic meter
NA	Sodium
NAAQS	National Ambient Air Quality Standard
OAQPS	Office of Air Quality Planning and Standards
O ₃	Ozone
OM	Organic matter
PCL	Particulate chlorine
PEC	Primary elemental carbon
PM _{2.5}	Fine particle; primary particulate matter less than or equal to 2.5 microns in aerodynamic diameter
PNH4	Particulate ammonium
PNO ₃	Particulate nitrate
POA	Primary Organic Aerosol
ppb	Parts per billion
PSO ₄	Particulate sulfate
R ²	Pearson correlation coefficient squared
RHR	Regional Haze Rule
SESARM	Southeastern States Air Resource Managers, Inc.
SIP	State Implementation Plan
SO ₂	Sulfur dioxide
SOA	Secondary organic aerosol
U.S.	United States
VISTAS	Visibility Improvement – State and Tribal Association of the Southeast

1.0 INTRODUCTION

1.1 Overview

Southeastern States Air Resource Managers, Inc. (SESARM) has been designated by the United States Environmental Protection Agency (EPA) as the entity responsible for coordinating regional haze evaluations for the ten Southeastern states of Alabama, Florida, Georgia, Kentucky, Mississippi, North Carolina, South Carolina, Tennessee, Virginia, and West Virginia. The Eastern Band of Cherokee Indians and the Knox County, Tennessee local air pollution control agency are also participating agencies. These parties are collaborating through the Regional Planning Organization known as Visibility Improvement - State and Tribal Association of the Southeast (VISTAS) in the technical analyses and planning activities associated with visibility and related regional air quality issues. VISTAS analyses will support the VISTAS states in their responsibility to develop, adopt, and implement their State Implementation Plans (SIPs) for regional haze.

The state and local air pollution control agencies in the Southeast are mandated to protect human health and the environment from the impacts of air pollutants. They are responsible for air quality planning and management efforts including the evaluation, development, adoption, and implementation of strategies controlling and managing all criteria air pollutants including fine particles and ozone as well as regional haze. This project will focus on regional haze and regional haze precursor emissions. Control of regional haze precursor emissions will have the additional benefit of reducing criteria pollutants as well.

The 1999 Regional Haze Rule (RHR) identified 18 Class I Federal areas (national parks greater than 6,000 acres and wilderness areas greater than 5,000 acres) in the VISTAS region. The 1999 RHR required states to define long-term strategies to improve visibility in Federal Class I national parks and wilderness areas. States were required to establish baseline visibility conditions for the period 2000-2004, natural visibility conditions in the absence of anthropogenic influences, and an expected rate of progress to reduce emissions and incrementally improve visibility to natural conditions by 2064. The original RHR required states to improve visibility on the 20% most impaired days and protect visibility on the 20% least impaired days.¹ The RHR

¹ RHR summary data is available at: <http://vista.cira.colostate.edu/Improve/rhr-summary-data/>

requires states to evaluate progress toward visibility improvement goals every five years and submit revised SIPs every ten years.

EPA finalized revisions to various requirements of the RHR in January 2017 (82 FR 3078) that were designed to strengthen, streamline, and clarify certain aspects of the agency's regional haze program including:

- A. Strengthening the Federal Land Manager (FLM) consultation requirements to ensure that issues and concerns are brought forward early in the planning process.
- B. Updating the SIP submittal deadlines for the second planning period from July 31, 2018 to July 31, 2021 to ensure that they align where applicable with other state obligations under the Clean Air Act. The end date for the second planning period remains 2028; that is, the focus of state planning will be to establish reasonable progress goals for each Class I area against which progress will be measured during the second planning period. This extension will allow states to incorporate planning for other Federal programs while conducting their regional haze planning. These other programs include: the Mercury and Air Toxics Standards, the 2010 1-hour sulfur dioxide (SO₂) National Ambient Air Quality Standards (NAAQS); the 2012 annual fine particle (PM_{2.5}) NAAQS; and the 2008 and 2015 ozone NAAQS.
- C. Adjusting interim progress report submission deadlines so that second and subsequent progress reports will be due by: January 31, 2025; July 31, 2033; and every ten years thereafter. This means that one progress report will be required midway through each planning period.
- D. Removing the requirement for progress reports to take the form of SIP revisions. States will be required to consult with FLMs and obtain public comment on their progress reports before submission to the EPA. EPA will be reviewing but not formally approving or disapproving these progress reports.

The RHR defines "clearest days" as the 20% of monitored days in a calendar year with the lowest deciview (dv) index values. "Most impaired days" are defined as the 20% of

monitored days in a calendar year with the highest amounts of anthropogenic visibility impairment. The long-term strategy and the reasonable progress goals must provide for an improvement in visibility for the most impaired days since the baseline period and ensure no degradation in visibility for the clearest days since the baseline period.

1.2 CAMx 6.40 2028elv3 VISTAS12 and EPA 12US2 Comparison

The VISTAS II air quality modeling is being performed on a smaller computational grid than EPA used in developing the 2011el platform. The use of the smaller domain is designed to allow SESARM to more efficiently look at air quality issues in the southeastern US.

Alpine has executed two air quality simulations for the 2028elv3 base year modeling platform; one run with CAMx 6.40 over the EPA continental US domain (12US2) and one for the VISTAS12 domain. The domains are presented in Figure 1-1 with the 12US2 domain as the outer grid and the VISTAS12 domain is shown as the red box. The domain definitions for the two domains are presented in Table 1-1.

Table 1-1. VISTAS II Modeling Domain Specifications

Domain	Columns	Rows	Vertical Layers	X Origin (km)	Y Origin (km)
CONUS_12	396	246	25	-2,412	-1,620
VISTAS_12	269	242	25	-912	-1,596

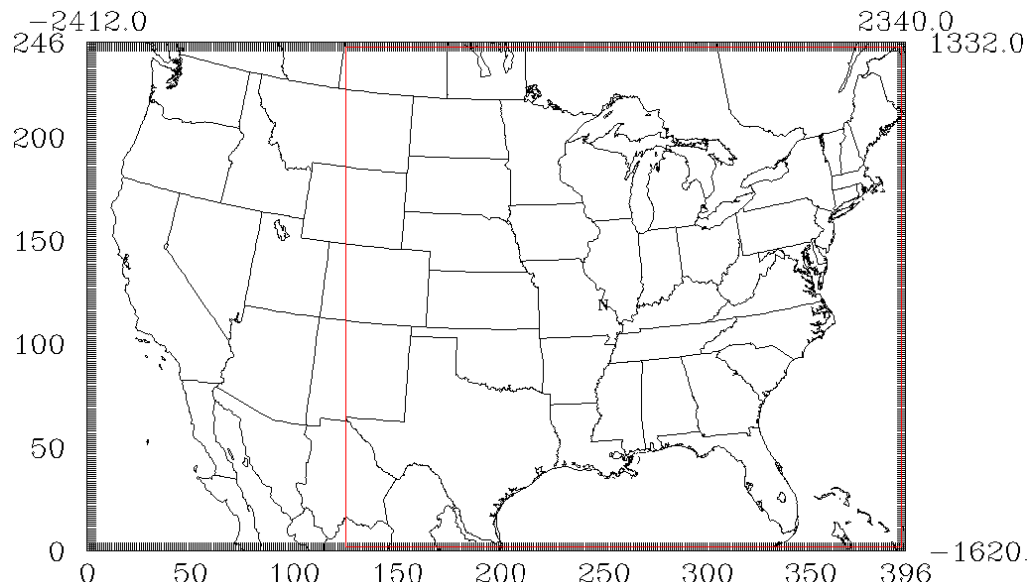


Figure 1-1. Map of 12km CAMx Modeling Domains. VISTAS12 Domain Represented as Inner Red Domain.

2.0 DEVELOPMENT OF VISTAS12 INPUTS

The inputs for the VISTAS12 domain were developed by extracting a subdomain from the CAMx ready model inputs (commonly referred to as windowing). The meteorology and emissions inputs were windowed using a slightly modified version of the CAMx utility program “window”.² The only required change to the distributed version program is to allow the program to window three-dimension files instead of just two-dimensional files. The CAMx ozone column and watermask inputs were windowed using new FORTRAN programs using the same windowing algorithm as is contained in the “window” code. The windowing code was checked graphically to assure that the VISTAS12 results were consistent with the 12US2 results. The boundary and initial conditions for the VISTAS12 domain will be extracted from the 12US2 three-dimensional output files using the CAMx BNDEXTR program.

Two issues have been identified that have noted impact on the use of the VISTAS12 domain relative to the 12US2 domain.³ The first, and likely the most significant, noted issue is a time-step difference at the boundary where concentration conditions from outside of the domain are injected into the modeling domain at one hour intervals compared to the model generated (sub-hourly) time-step interval within the modeling domain. These differences can create initial, significant concentration gradients along the boundary that can be carried through the episode and transported to grid cells within the modeling domain. The second issue is related to the time step in the model. The time step is determined by the maximum wind in the modeling domain. If the highest wind in the 12US2 domain occurs somewhere outside the VISTAS12 domain, the time step in the 12US2 simulation will be longer than in the VISTAS12 domain.

We note that in modeling the VISTAS12 domain with 12US2 boundary conditions, both of these issues are exacerbated in the modeling due to large emission sources located near the boundary of the 12US2/VISTAS12 boundary, particularly in Canada.

3.0 CONFIRMATION METHODOLOGY

The presented comparisons of model simulations are based on hourly differences in ozone, PM_{2.5}, Organic Matter (OM), Particulate Nitrate (PNO₃), and Particulate Sulfate (PSO₄).

² http://www.camx.com/getmedia/88755b80-6992-4f07-bcaa-596d05e1b4b8/window-6may13_1.tgz

³ Brian Timin, EPA Office of Air Quality Planning and Standards (OAQPS) personal communication October 11, 2018.

The metric for comparison are the absolute difference (Equation 1) and percent difference (Equation 2) defined as:

$$(Equation\ 1) \quad (C_{VISTAS12} - C_{12US2})$$

$$(Equation\ 2) \quad \frac{(C_{VISTAS12} - C_{12US2})}{(C_{12US2})}$$

Where $C_{VISTAS12}$ is the concentration at each grid cell hour for the CAMx simulation over the VISTAS12 simulation and C_{12US2} is the concentration at each grid cell hour for the CAMx simulation over the 12US2.

To facilitate the comparison of the results over the same spatial domain, the 12US2 simulation output files were windowed onto the VISTAS2 domain using the I/O API⁴ m3wndw code.

The results are presented for the hours with the largest difference between the simulations. Each table presents the hours with the top 10 positive and negative absolute differences. Spatial maps are presented for the hours with the top 10 highest positive and negative differences. To provide context for the differences, the concentration maps are also presented for each of the hours of high difference. On each spatial plot the maximum positive and negative values, along with the grid cell in which these occur, are presented at the top of the graphic. The coordinates refer to the row and columns of the cell referenced to the cell coordinates on the bottom (column) and left (row) of the graphic. Because the CAMx results are unduly influenced by the boundary concentrations around the edges, the analysis does not include the edge rows and columns of the CAMx domain.

Hourly animations have also been prepared and are available on the VISTAS II project ftp site. Where appropriate, this report also reports and interprets on the animations.

⁴ <https://www.cmascenter.org/ioapi/>

3.1 CAMx Species Mapping

Several of the key particulate matter species of interest are combinations of CAMx output variable. The CAMx 6.40 species mapping are presented in Table 3-1.

Table 3-1. Species Mapping from CAMx into Aggregated Species

Aggregated Species	CAMx 6.40 Species
Ozone	O3
PM _{2.5}	PSO4+PNO3+PNH4+SOA1+SOA2+SOA3+SOA4+SOPA+SOPB+POA+PEC+FPRM+FCRS+NA+PCL
Sulfate	PSO4
Nitrate	PNO3
Organic Matter (OM)	SOA1+SOA2+SOA3+SOA4+SOPA+SOPB+POA

4.0 VISTAS12 AND 12US2 CAMX 6.40 2018ELV3 COMPARISON

This section presents comparisons of the simulations using CAMx 6.40 performed on the Alpine computer system using the SESARM 2028elv3 modeling platform over the VISTAS12 and 12US2 domains.

4.1 Ozone

Ozone results for the top 10 positive and negative hours are presented in tabular format in Table 4-1. The maximum positive difference is 18.00 ppb falling to 11.76 ppb for the 10th high. The maximum negative difference is -17.43 ppb falling to -12.19 for the 10th high. Generally the highest positive and negative differences are occurring on relatively high ozone hours with concentrations up to 144.19 ppb for the VISTAS12 simulation. The maximum positive and negative percent differences are 82.1% and -16.0%, respectively.

As expected, the maximum impacts on the top 10 positive and negative hours are occurring very near the border (Rows close to 1 or 268 and Columns near 1 or 241). As was described in Section 2, the two CAMx simulations used the same input data, except that the pollutant concentrations on in-flow boundary cells. For the simulation on the VISTAS12 domain the in-flow concentrations are specified in hourly average boundary conditions extracted from the 12US2 simulation. For the 12US2 simulation the in-flow concentrations were continuously updated at every model-generated timestep from the cells outside the VISTAS12 domain. Additionally, as noted in an earlier section, the CAMx model does not include emissions in the

border cells. It would be expected that concentration differences would occur from the differences in hourly average concentrations, versus in the instantaneous model-determined concentrations and the CAMx model excluding emissions along the border.

The top ten positive impact hours are presented in Figures 4-1 through 4-10. The top ten negative impact hours are presented in Figures 4-11 through 4-20. The regions of highest differences tend to occur along the northern and western boundary and during short-term periods of time.

Scatterplots of the daily average ozone concentrations in local standard time at the IMPROVE monitors across all modeled days are presented in Figure 4-21. The 12US2 results are plotted on the x-axis and the VISTAS12 results are plotted on the y-axis. The data has a high degree of correlation with a line of best fit with a slope of 1.0002, an intercept of 0.0090 ppb and an R^2 of 0.9999.

Examination of the difference animations shows some interesting results. On many hours the differences are fairly smooth without much horizontal difference, as seen in Figure 4-10. Then, in a single hour, regions of small local gradients occur and the spatial field resembles Figure 4-8. Often, over a period of several hours, these small differences disappear and the smooth structure is restored.

These differences are likely caused by a combination of factors. The first, and likely the most significant, noted issue is a time-step difference at the boundary where concentration conditions from outside of the domain are injected into the modeling domain at one hour intervals compared to the model generated (sub-hourly) time-step interval within the modeling domain. The other difference is the time step in the integration of the CAMx model. The CAMx model determines the time step based on the highest wind speed in the domain. When the highest wind speed is located in the VISTAS12 region, the time step for the VISTAS12 and 12US2 simulations are the same. When the highest wind speed in the 12US2 domain occurs outside the VISTAS12 domain, the time steps are different in the two simulations. This difference in the time step will yield slightly different concentrations between the two region simulations.

Table 4-1. Comparison of 2028elv3 CAMx 6.40 VISTAS12 and 12US2 Simulation of Ozone Concentrations (ppb). Hours with the top 10 maximum positive and maximum negative differences are shown.

Year	Month	Day	Hour	VISTAS12 Conc.	12US2 Conc.	Difference (ppb)	Percent Difference	Column	Row
Maximum Positive									
2011	7	20	15	144.19	126.19	18.00	14.3%	108	240
2011	7	20	16	127.78	112.36	15.42	13.7%	107	240
2011	7	20	17	81.19	66.76	14.43	21.6%	121	241
2011	5	17	8	30.48	17.32	13.17	76.0%	60	6
2011	5	17	7	28.95	15.90	13.05	82.1%	60	5
2011	7	20	21	56.21	43.52	12.69	29.2%	107	241
2011	9	6	8	39.02	26.46	12.56	47.5%	51	2
2011	5	17	9	30.86	18.65	12.21	65.4%	267	107
2011	2	24	0	46.52	34.54	11.98	34.7%	49	3
2011	9	6	9	38.17	26.41	11.76	44.5%	51	2
Maximum Negative									
2011	7	17	16	110.95	128.38	-17.43	-13.6%	92	241
2011	7	17	15	124.11	141.25	-17.14	-12.1%	90	241
2011	7	17	14	127.73	142.75	-15.03	-10.5%	90	241
2011	7	17	18	83.33	98.35	-15.02	-15.3%	93	240
2011	7	17	17	96.46	111.21	-14.74	-13.3%	92	241
2011	7	17	19	78.65	92.71	-14.06	-15.2%	92	240
2011	7	18	19	70.35	83.73	-13.38	-16.0%	89	241
2011	7	18	18	74.07	87.43	-13.36	-15.3%	89	241
2011	7	18	15	94.25	107.58	-13.34	-12.4%	88	241
2011	7	18	20	68.25	80.44	-12.19	-15.2%	90	240

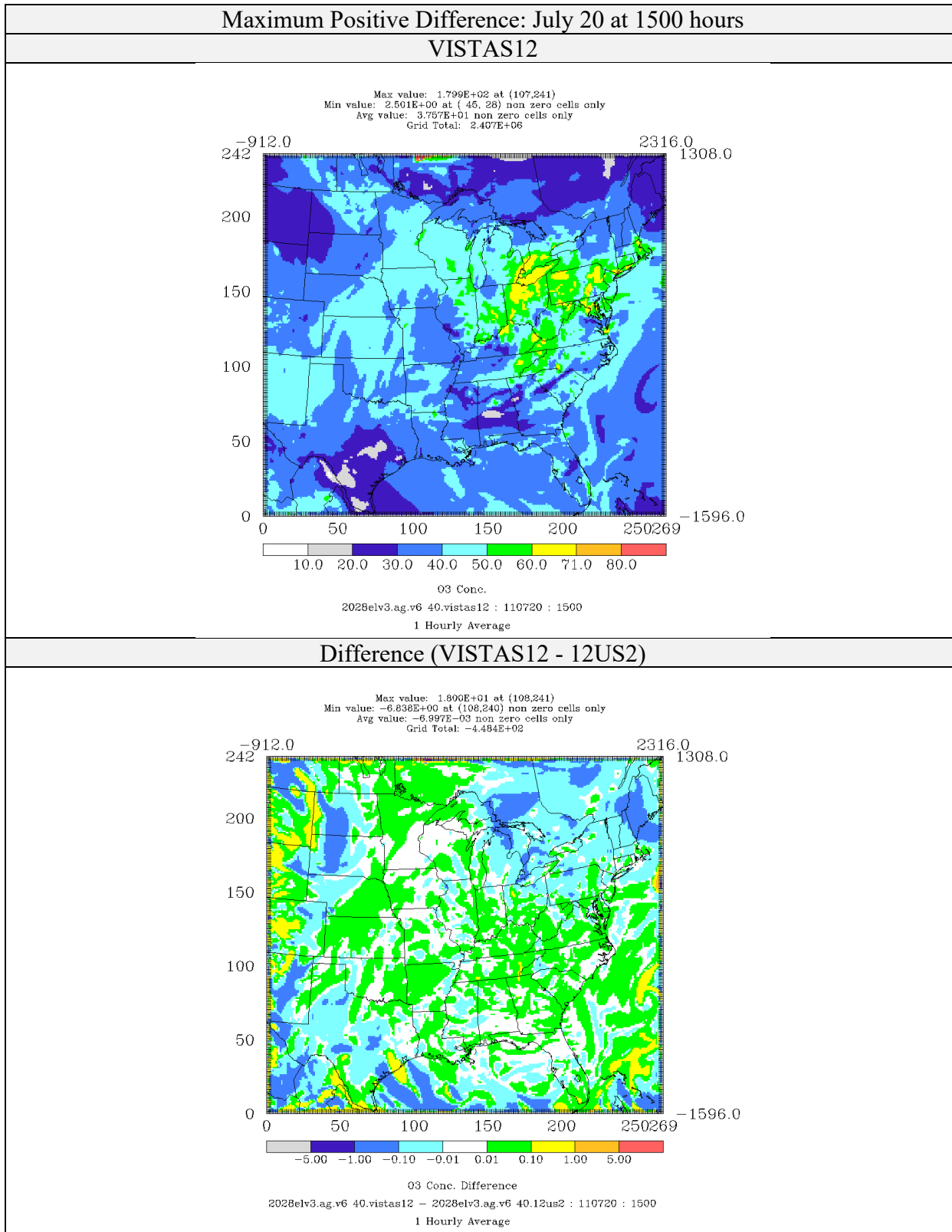


Figure 4-1: Comparison of Ozone Concentrations (ppb) for CAMx 6.40 on VISTAS12 and 12US2 Domains 2028elv3 Simulations (Maximum Positive Difference)

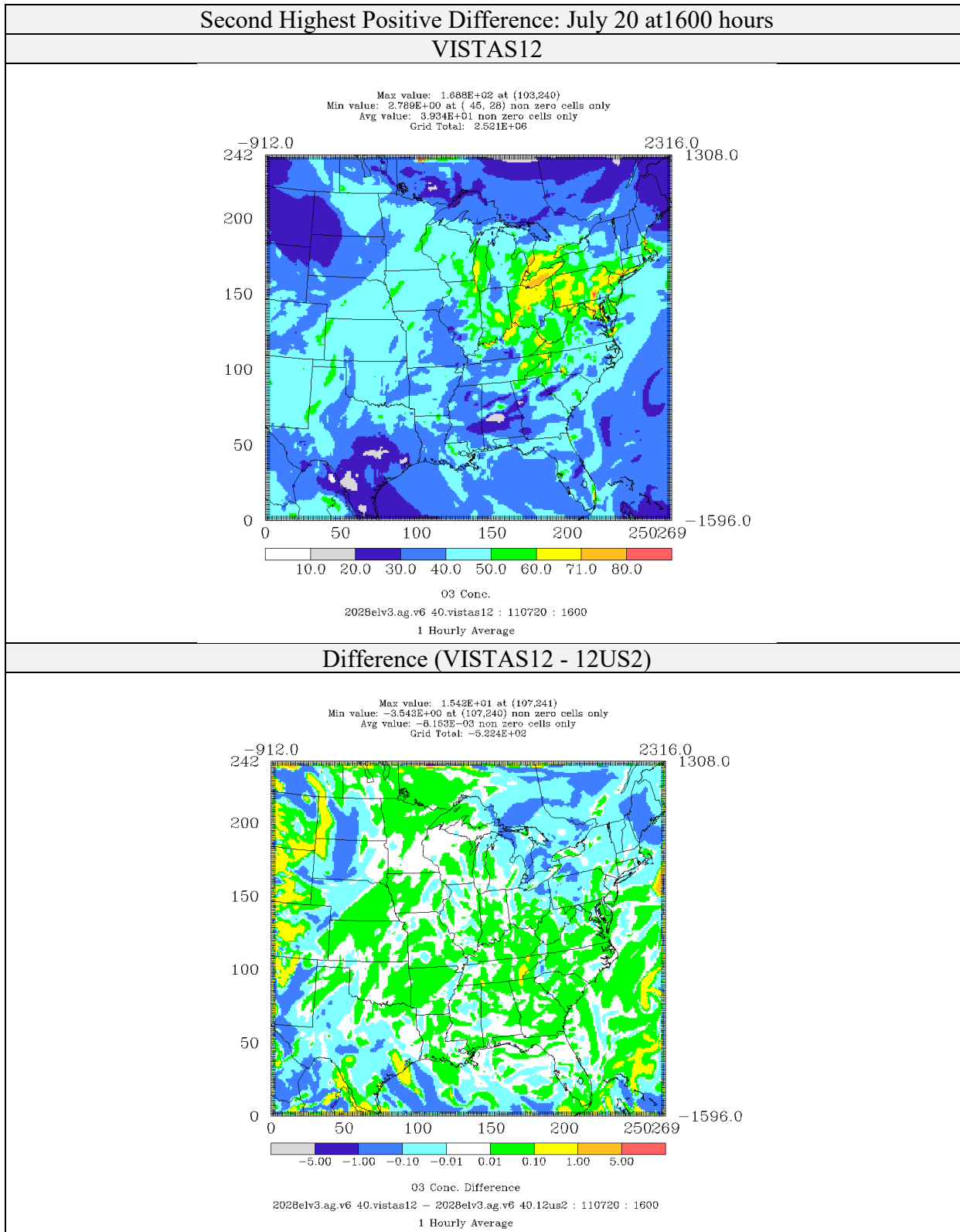


Figure 4-2: Comparison of Ozone Concentrations (ppb) for CAMx 6.40 on VISTAS12 and 12US2 Domains 2028elv3 Simulations (Second Highest Positive Difference)

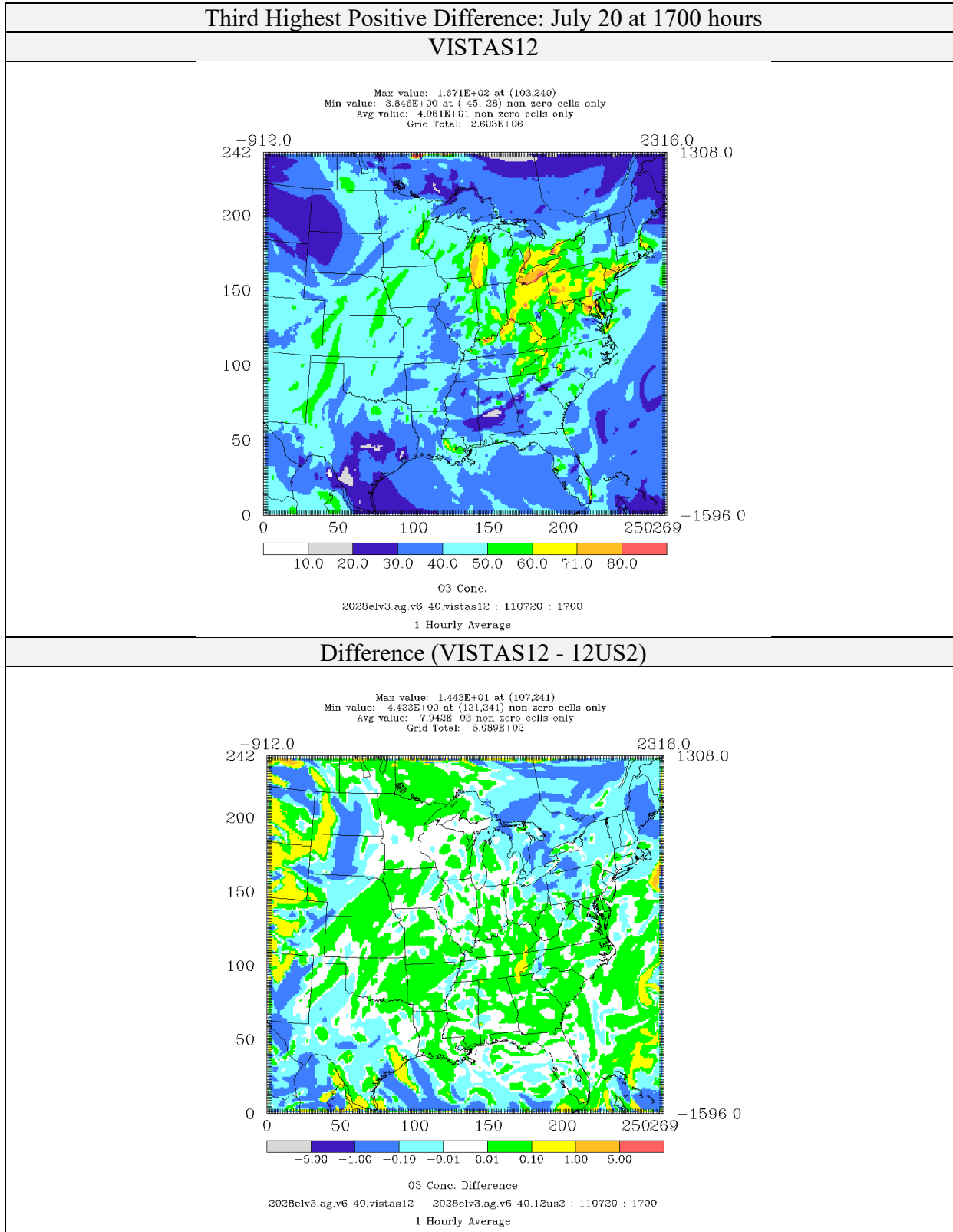


Figure 4-3: Comparison of Ozone Concentrations (ppb) for CAMx 6.40 on VISTAS12 and 12US2 Domains 2028elv3 Simulations (Third Highest Positive Difference)

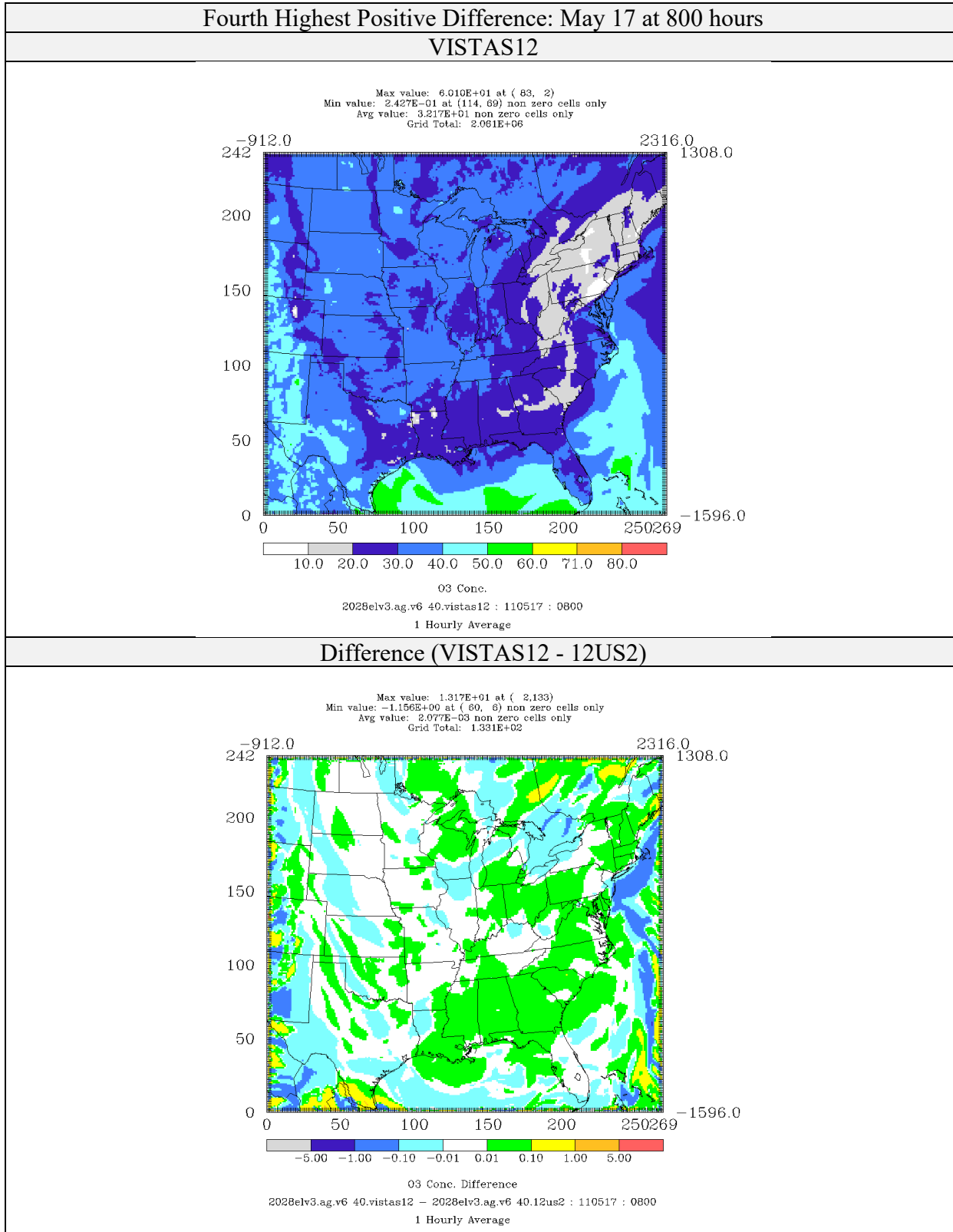


Figure 4-4: Comparison of Ozone Concentrations (ppb) for CAMx 6.40 on VISTAS12 and 12US2 Domains 2028elv3 Simulations (Fourth Highest Positive Difference)

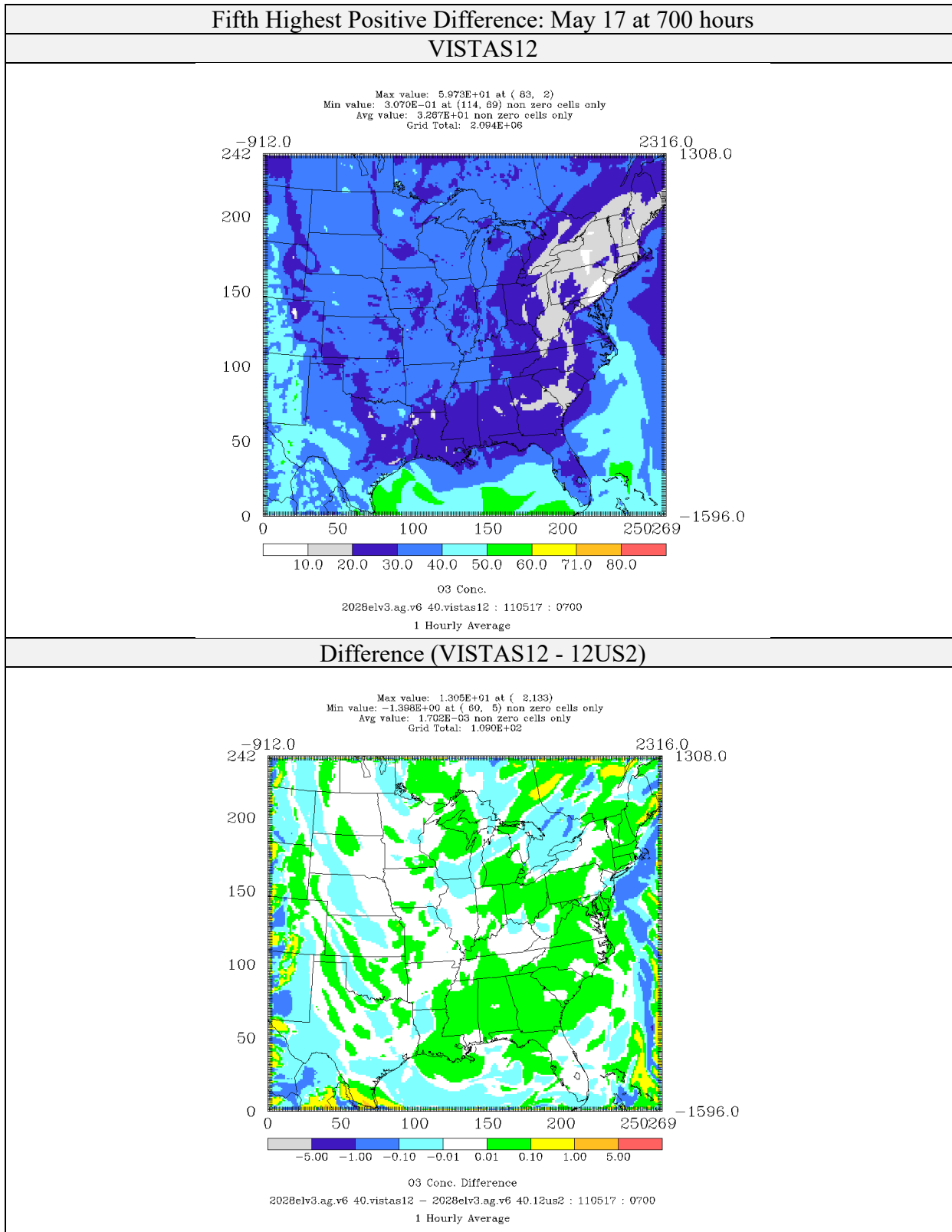


Figure 4-5: Comparison of Ozone Concentrations (ppb) for CAMx 6.40 on VISTAS12 and 12US2 Domains 2028elv3 Simulations (Fifth Highest Positive Difference)

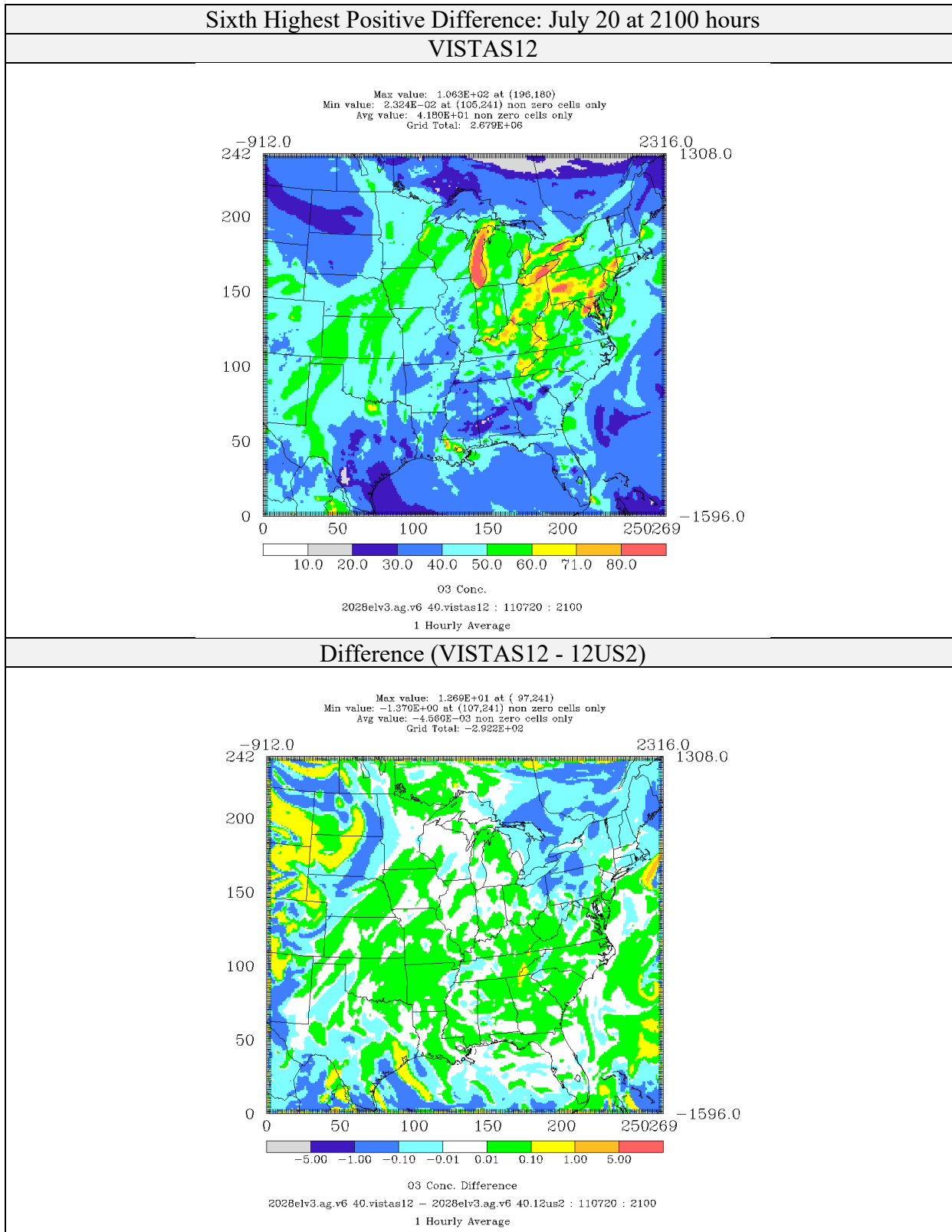


Figure 4-6: Comparison of Ozone Concentrations (ppb) for CAMx 6.40 on VISTAS12 and 12US2 Domains 2028elv3 Simulations (Sixth Highest Positive Difference)

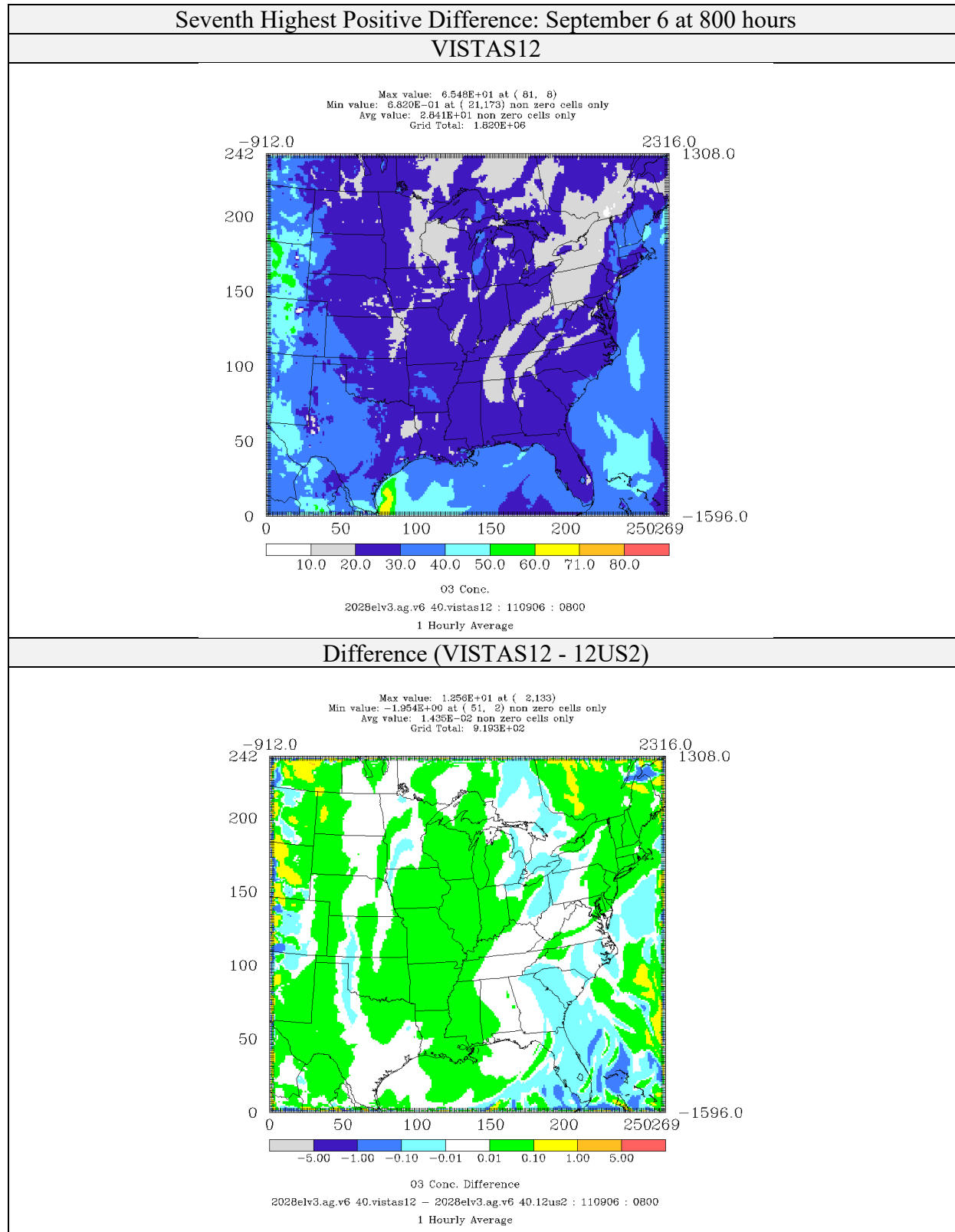


Figure 4-7: Comparison of Ozone Concentrations (ppb) for CAMx 6.40 on VISTAS12 and 12US2 Domains 2028elv3 Simulations (Seventh Highest Positive Difference)

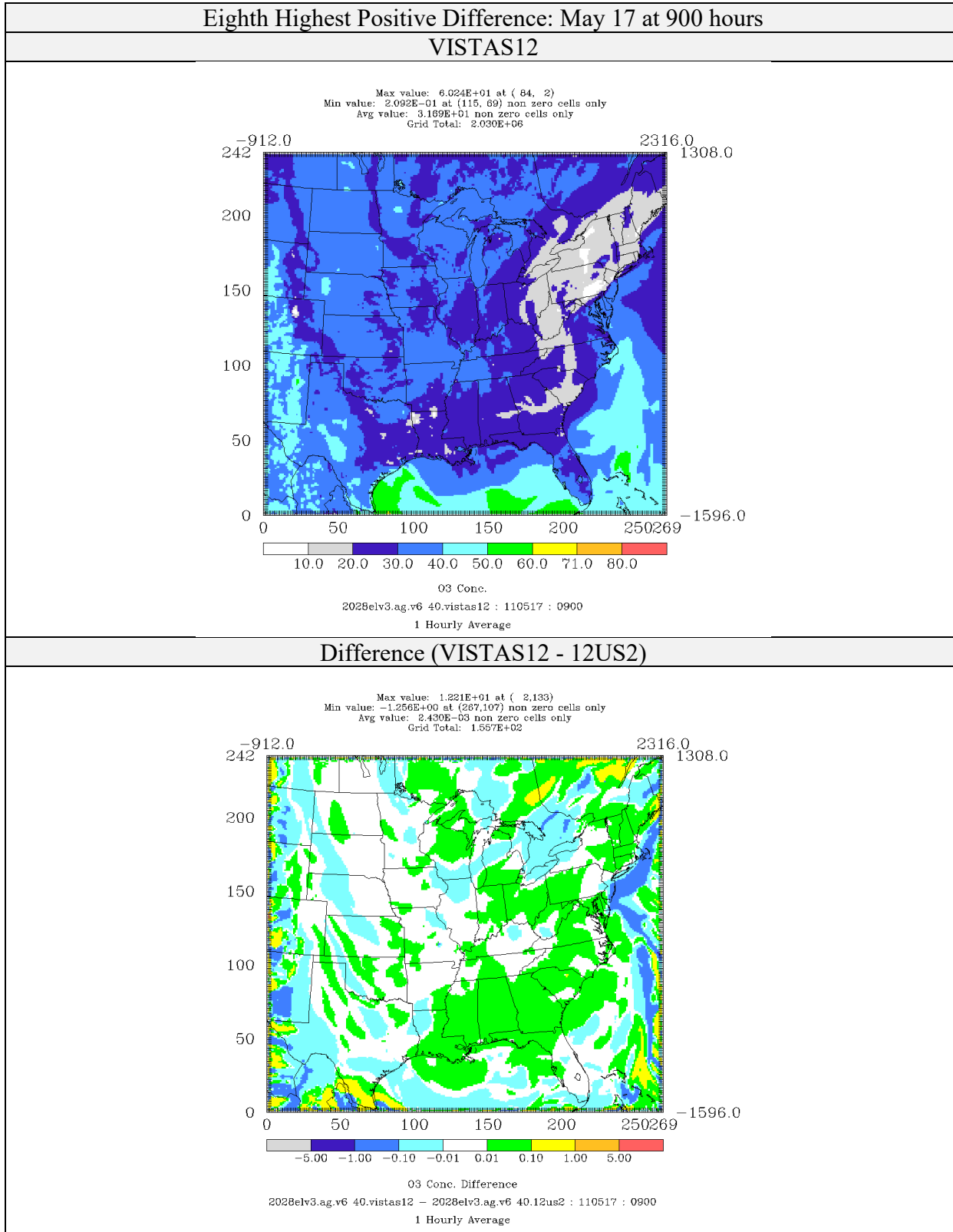


Figure 4-8: Comparison of Ozone Concentrations (ppb) for CAMx 6.40 on VISTAS12 and 12US2 Domains 2028elv3 Simulations (Eighth Highest Positive Difference)

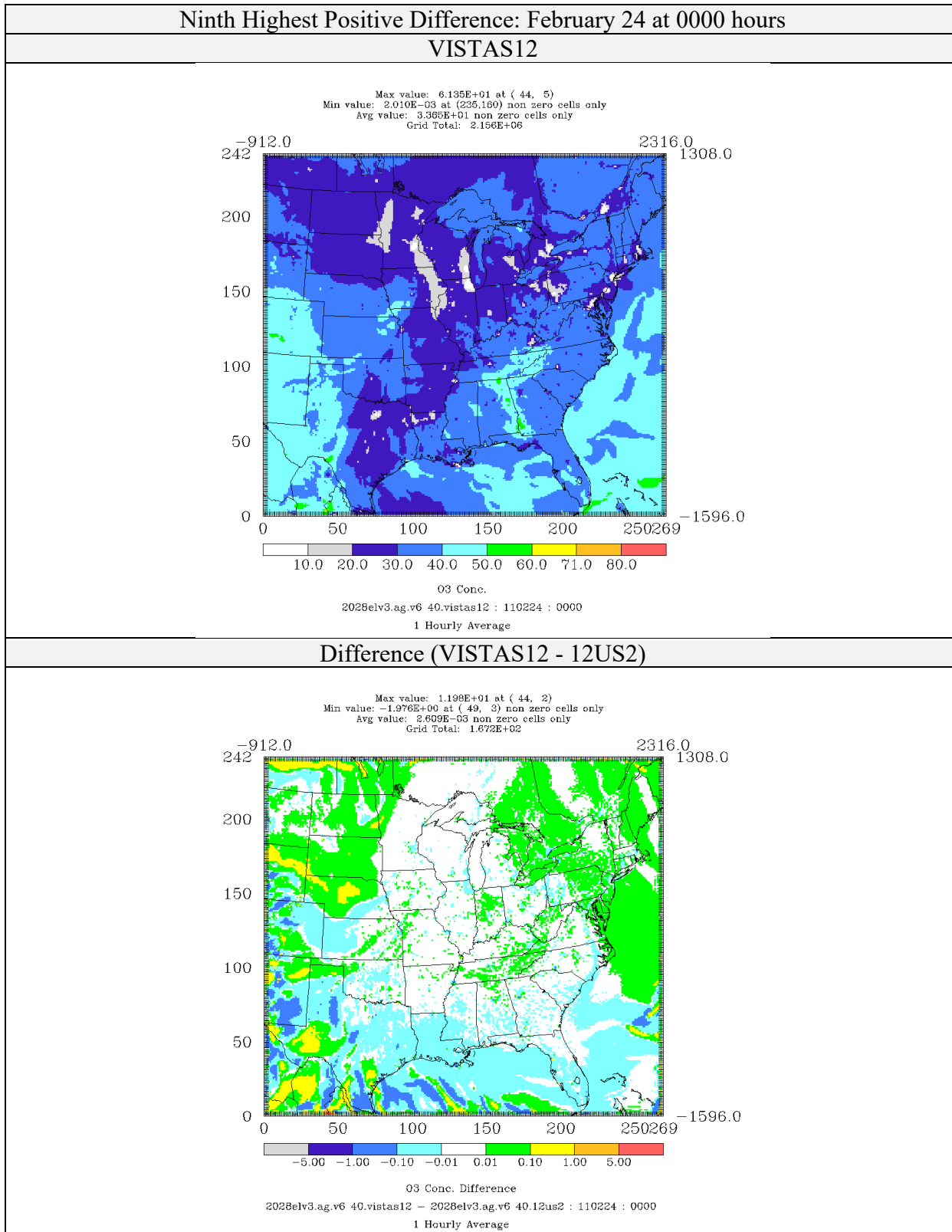


Figure 4-9: Comparison of Ozone Concentrations (ppb) for CAMx 6.40 on VISTAS12 and 12US2 Domains 2028elv3 Simulations (Ninth Highest Positive Difference)

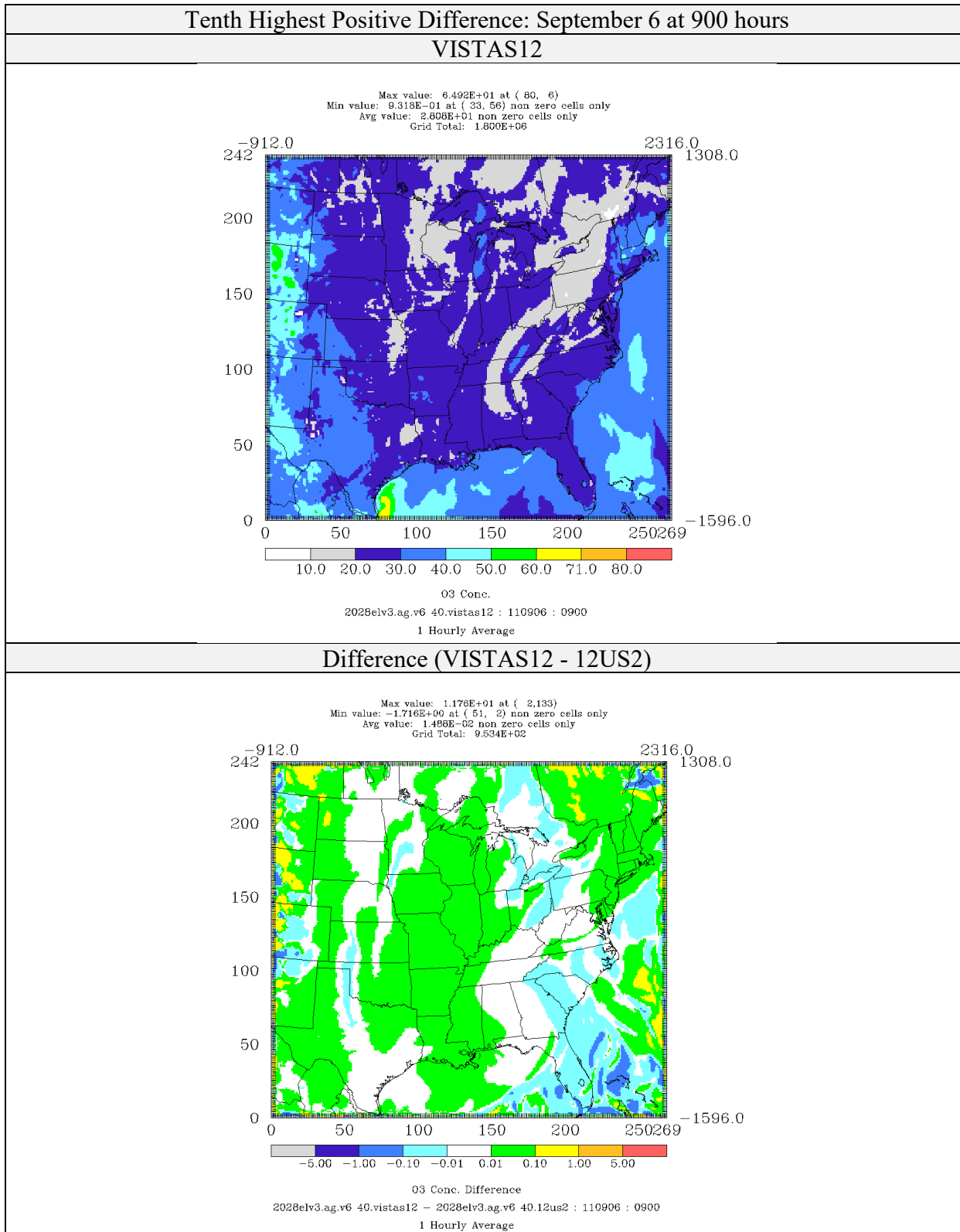


Figure 4-10: Comparison of Ozone Concentrations (ppb) for CAMx 6.40 on VISTAS12 and 12US2 Domains 2028elv3 Simulations (Tenth Highest Positive Difference)

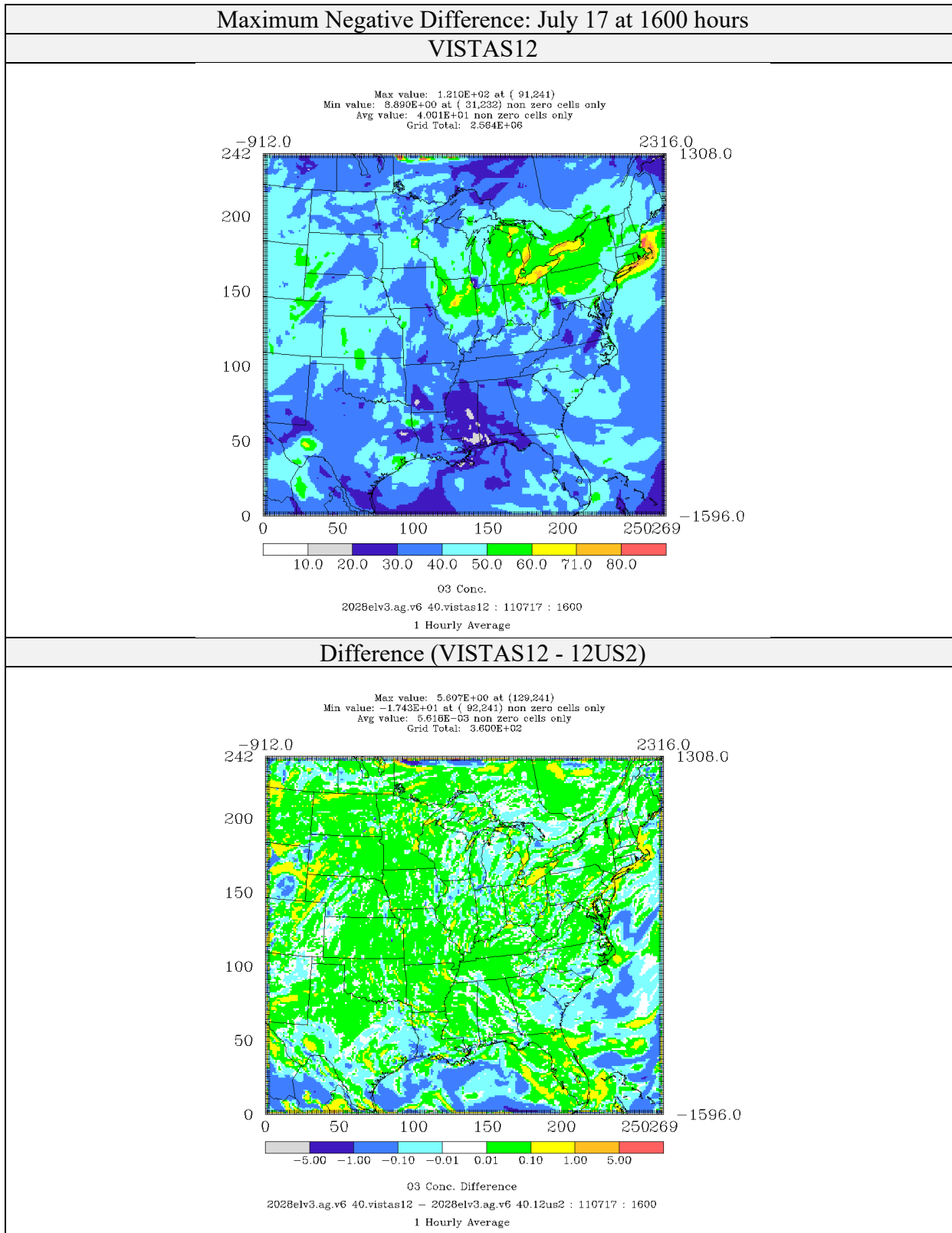


Figure 4-11: Comparison of Ozone Concentrations (ppb) for CAMx 6.40 on VISTAS12 and 12US2 Domains 2028elv3 Simulations (Maximum Negative Difference)

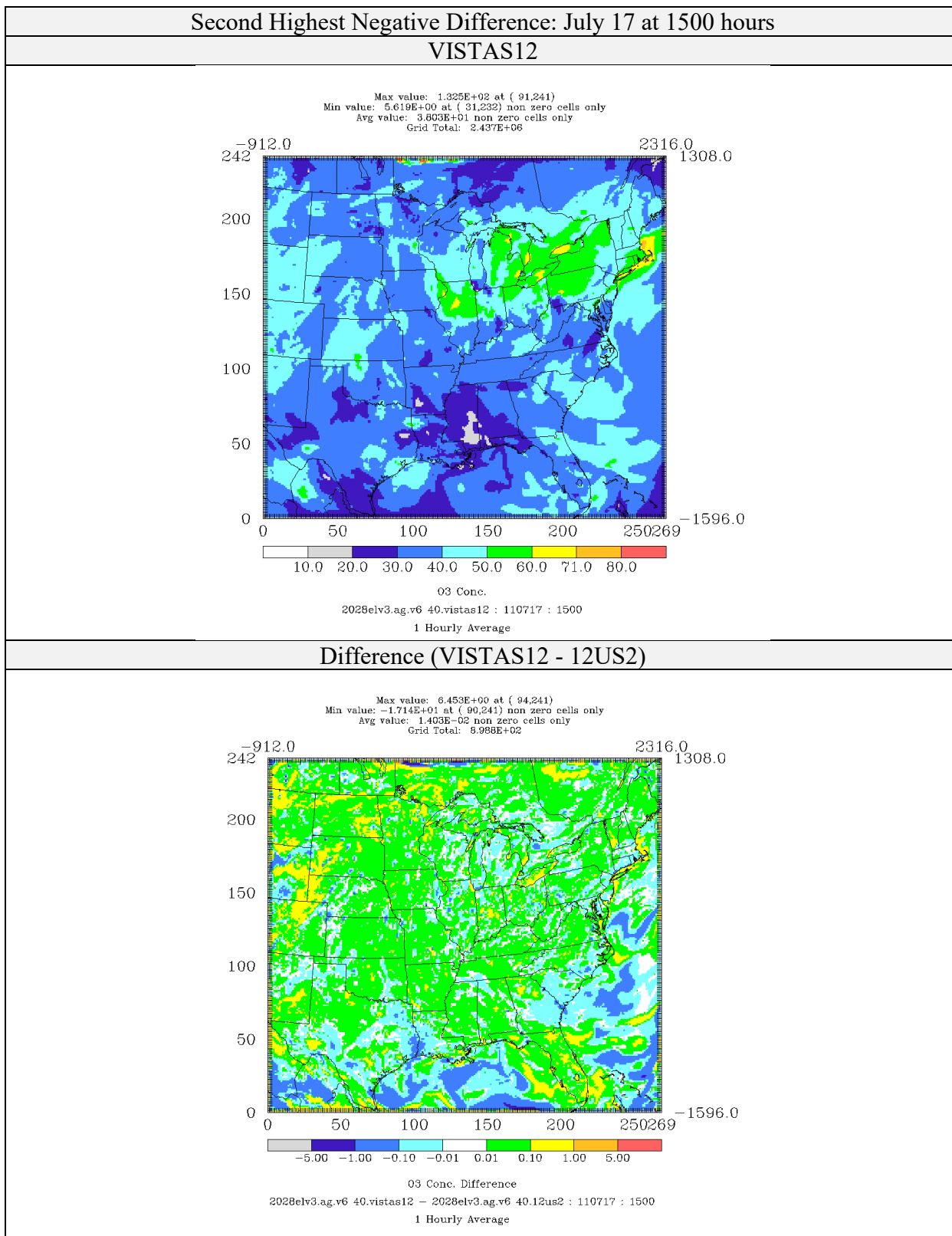


Figure 4-12: Comparison of Ozone Concentrations (ppb) for CAMx 6.40 on VISTAS12 and 12US2 Domains 2028elv3 Simulations (Second Highest Negative Difference)

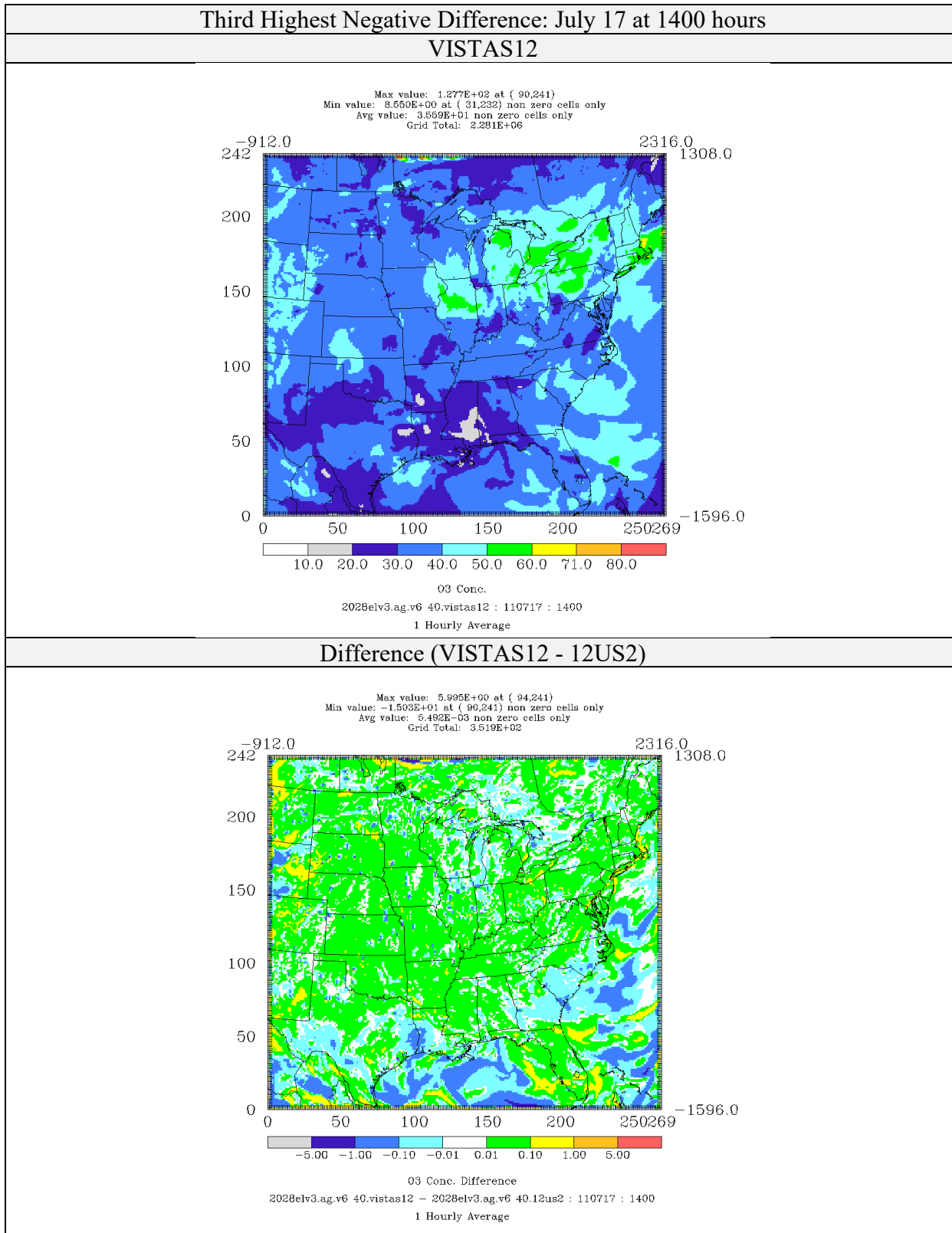


Figure 4-13: Comparison of Ozone Concentrations (ppb) for CAMx 6.40 on VISTAS12 and 12US2 Domains 2028elv3 Simulations (Third Highest Negative Difference)

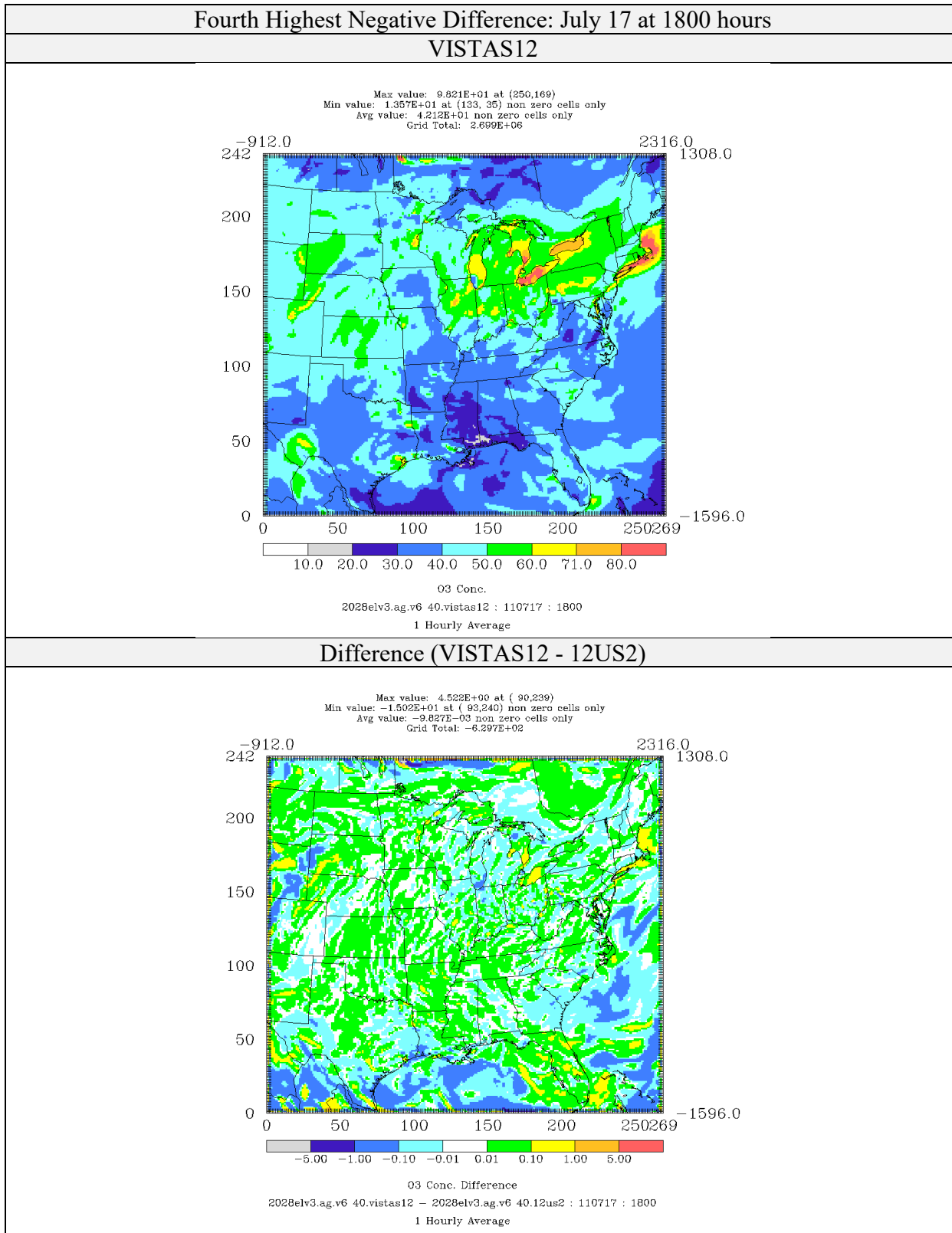


Figure 4-14: Comparison of Ozone Concentrations (ppb) for CAMx 6.40 on VISTAS12 and 12US2 Domains 2028elv3 Simulations (Fourth Highest Negative Difference)

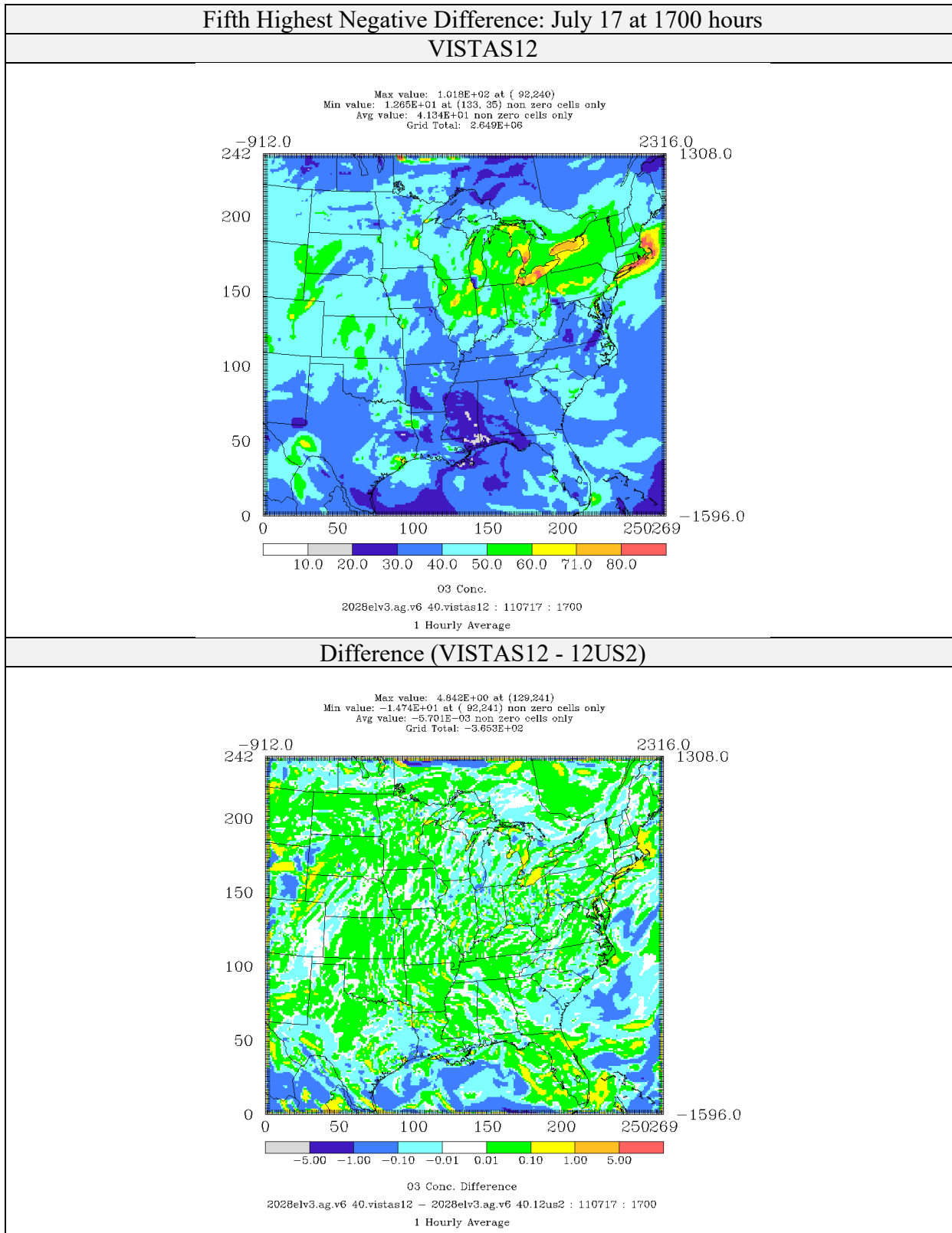


Figure 4-15: Comparison of Ozone Concentrations (ppb) for CAMx 6.40 on VISTAS12 and 12US2 Domains 2028elv3 Simulations (Fifth Highest Negative Difference)

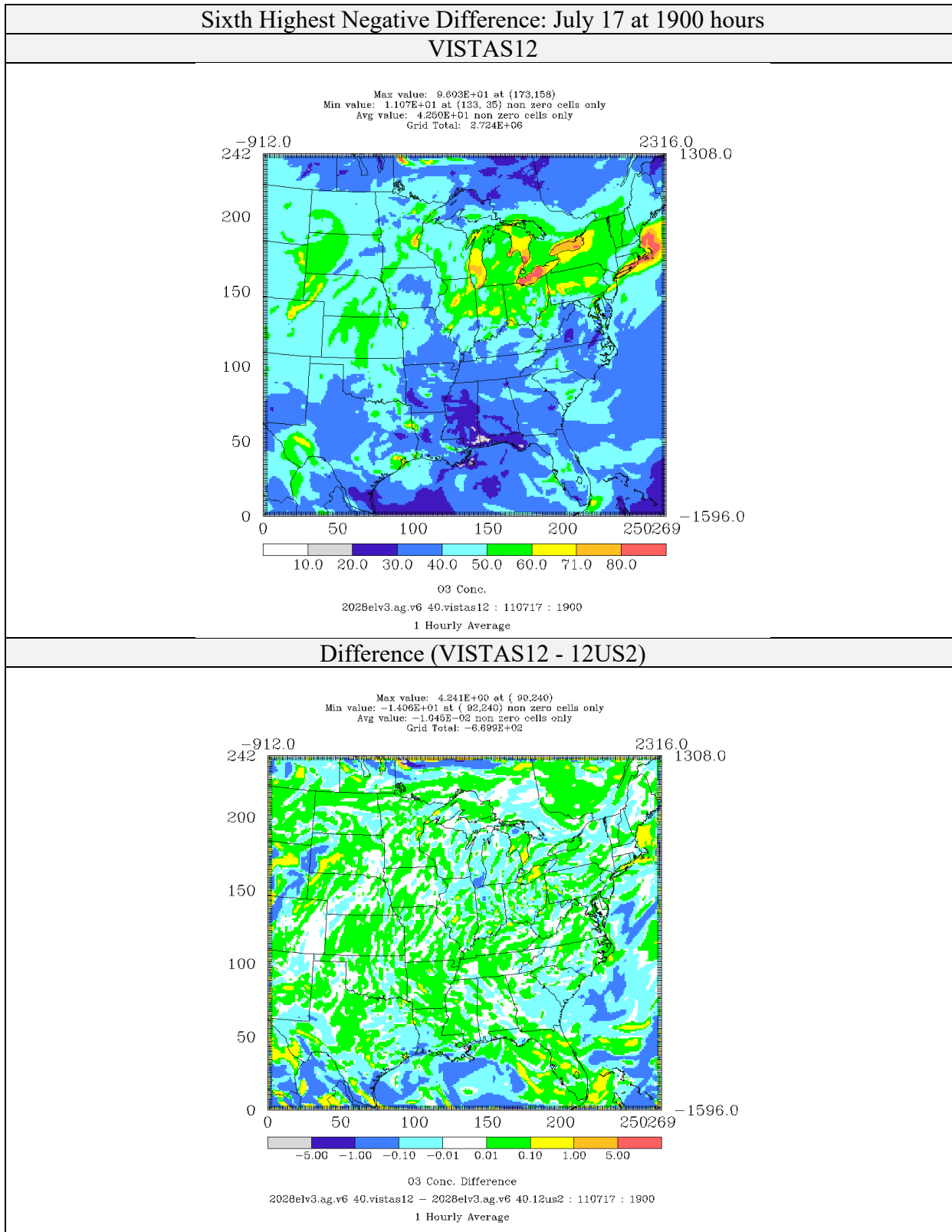


Figure 4-16: Comparison of Ozone Concentrations (ppb) for CAMx 6.40 on VISTAS12 and 12US2 Domains 2028elv3 Simulations (Sixth Highest Negative Difference)

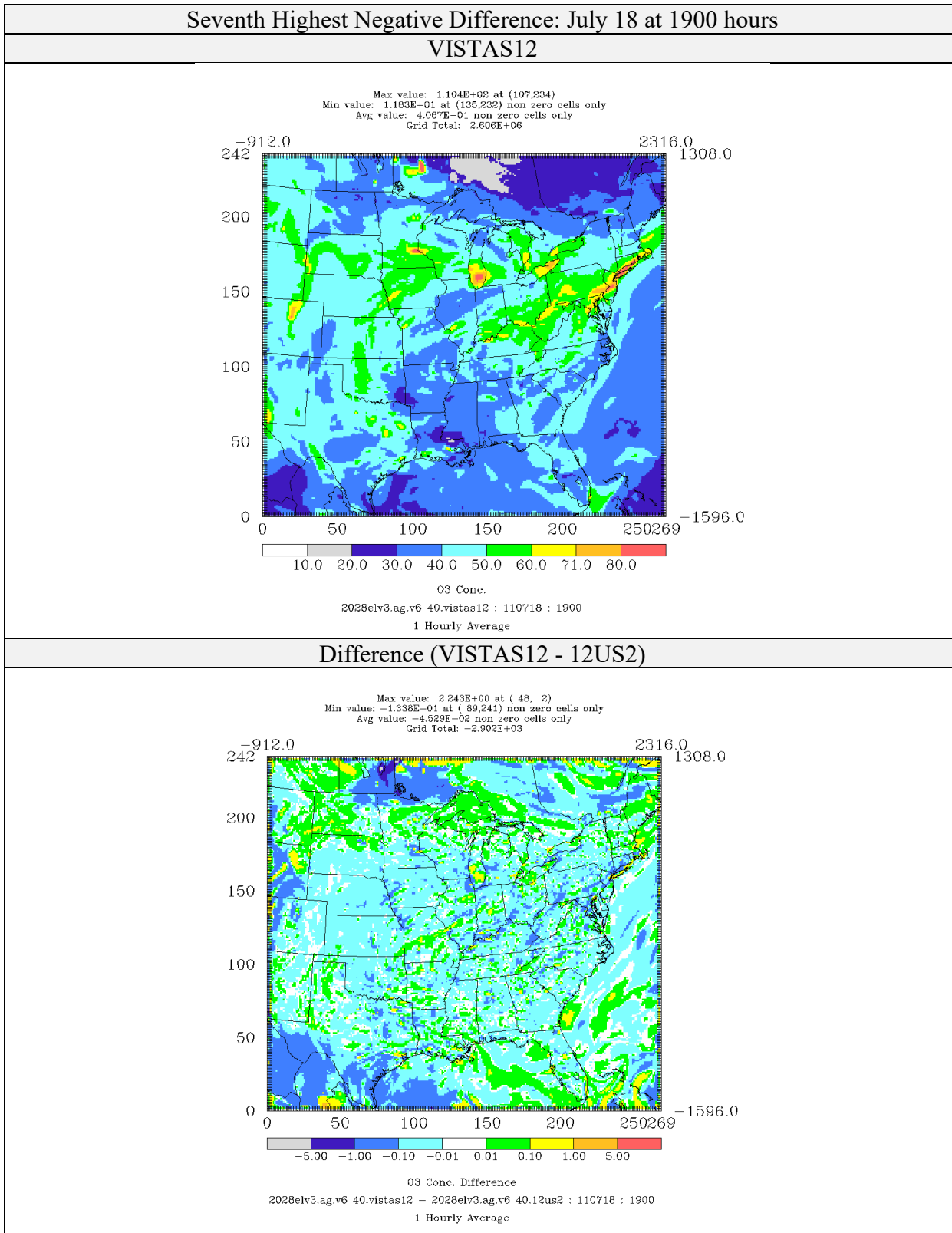


Figure 4-17: Comparison of Ozone Concentrations (ppb) for CAMx 6.40 on VISTAS12 and 12US2 Domains 2028elv3 Simulations (Seventh Highest Negative Difference)

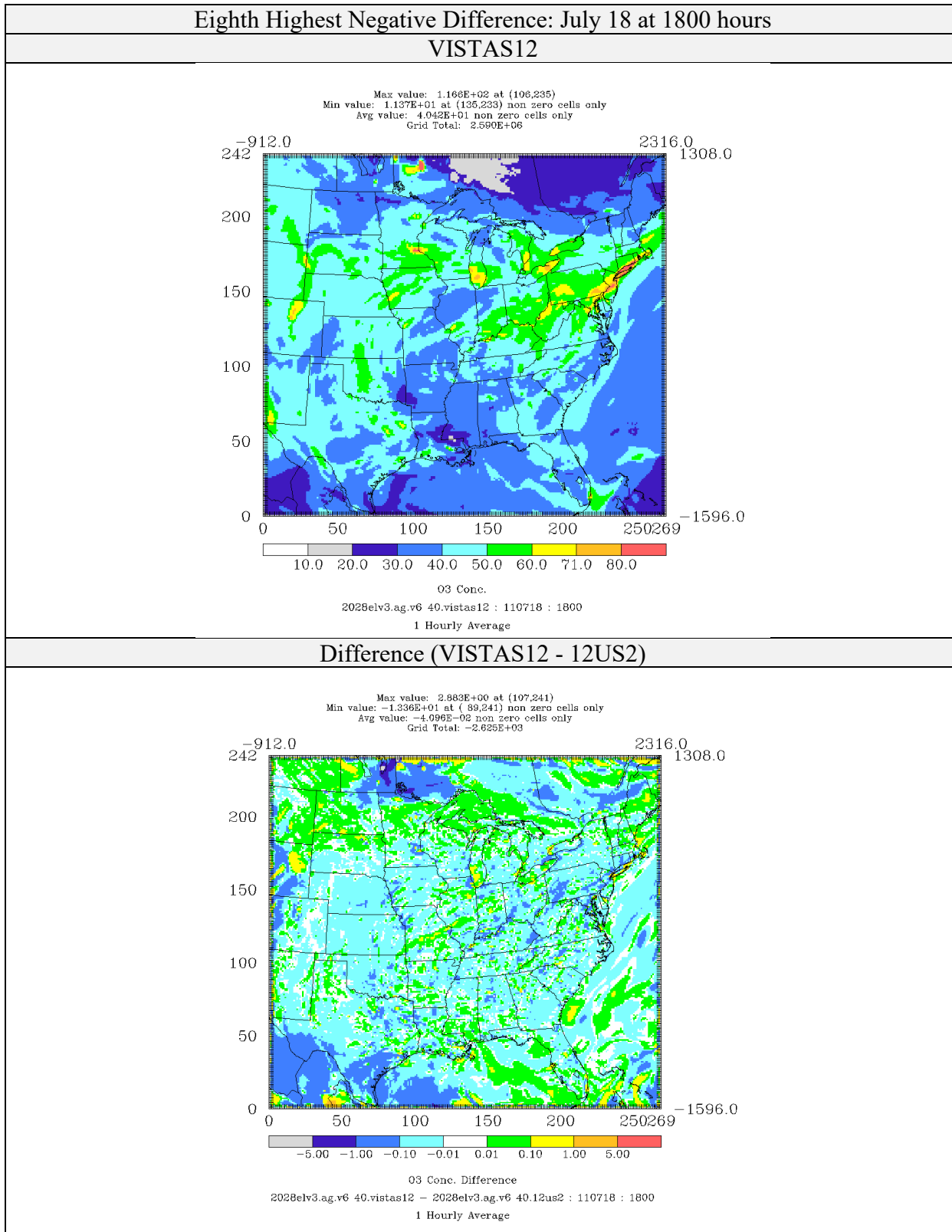


Figure 4-18: Comparison of Ozone Concentrations (ppb) for CAMx 6.40 on VISTAS12 and 12US2 Domains 2028elv3 Simulations (Eighth Highest Negative Difference)

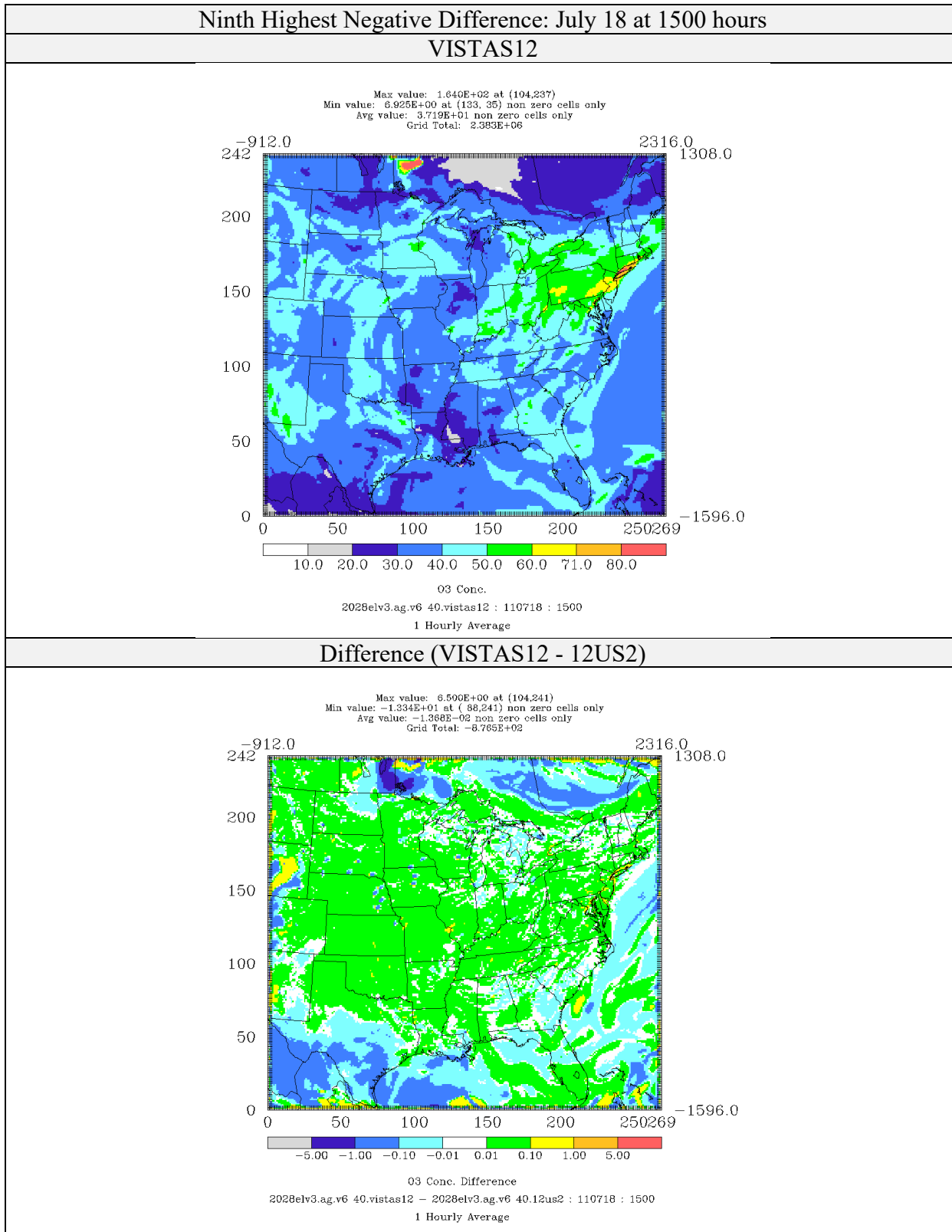


Figure 4-19: Comparison of Ozone Concentrations (ppb) for CAMx 6.40 on VISTAS12 and 12US2 Domains 2028elv3 Simulations (Ninth Highest Negative Difference)

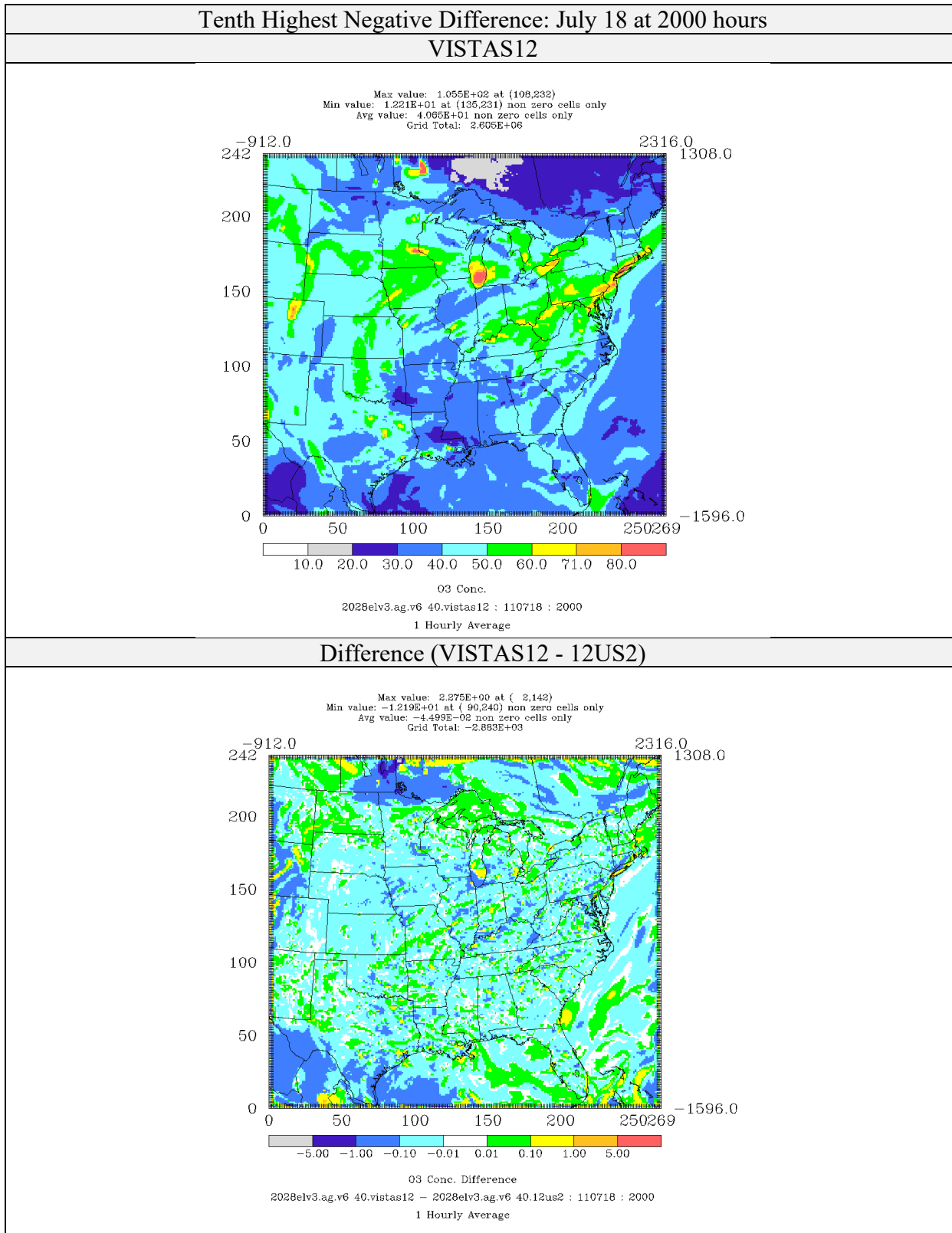


Figure 4-20: Comparison of Ozone Concentrations (ppb) for CAMx 6.40 on VISTAS12 and 12US2 Domains 2028elv3 Simulations (Tenth Highest Negative Difference)

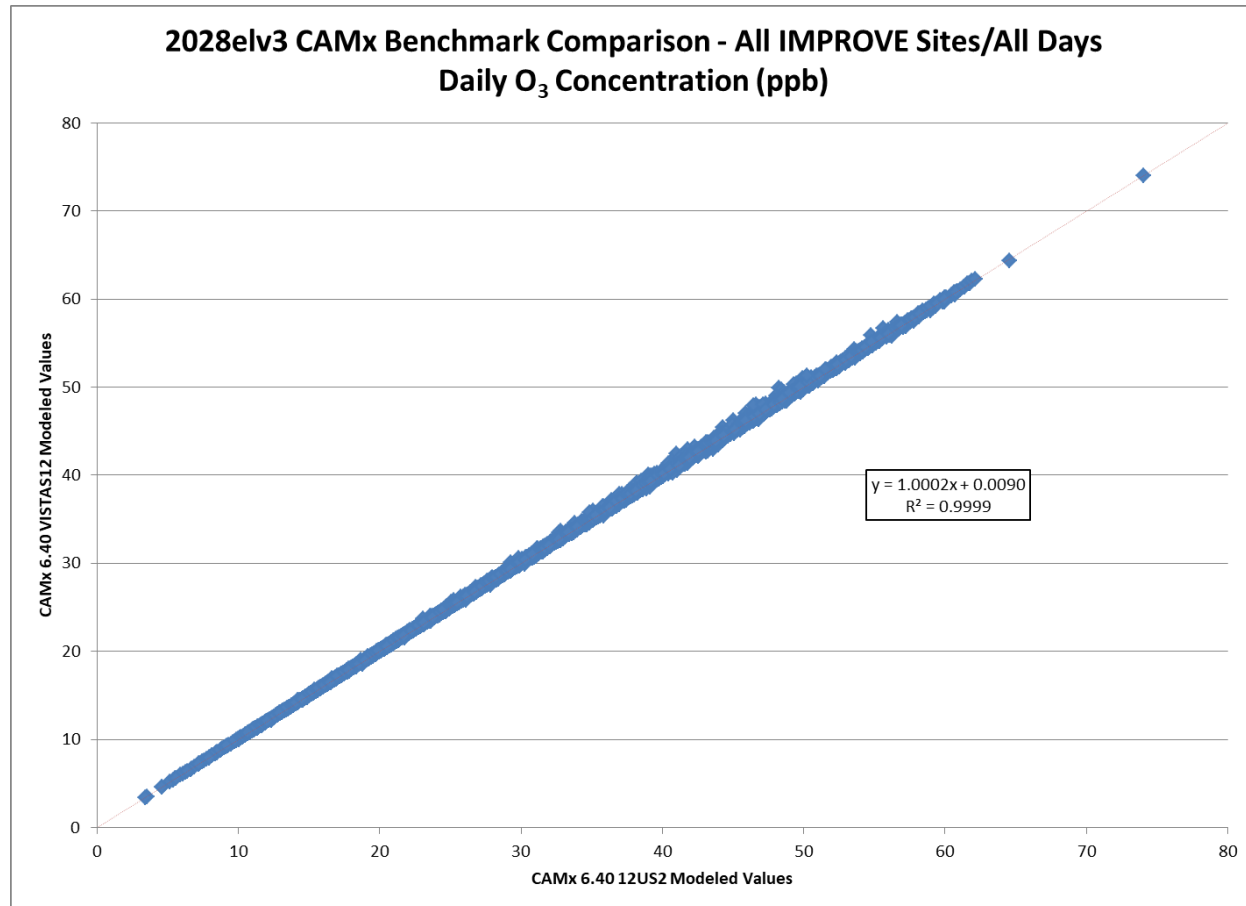


Figure 4-21: Scatterplot Comparing 24-hour Average Predicted Ozone Concentrations (ppb) for All Days at all IMPROVE Monitor Locations for CAMx 6.40 on VISTAS12 and 12US2 Domains 2028elv3 Simulations Performed by V ISTAS (Alpine).

4.2 PM_{2.5}

PM_{2.5} results for the top 10 positive and negative hours are presented in tabular format in Table 4-2. The maximum positive difference is 383.37 µg/m³ falling to 211.49 µg/m³ for the 10th high. The maximum negative difference is -296.69 µg/m³ falling to -174.08 µg/m³ for the 10th high. The maximum positive percent difference from these days is 102.4% and negative percent difference of -33.5%.

As expected and consistent with our ozone findings in the previous section, the maximum impacts on the top 10 positive and negative hours are occurring very near the border. As was described in Section 2, the two CAMx simulations used the same input data, except that the pollutant concentrations on in-flow boundary cells. For the simulation on the VISTAS12 domain the in-flow concentrations are specified in hourly boundary conditions extracted from the 12US2 simulation. For the 12US2 simulation the in-flow concentrations were continuously updated from the cells outside the VISTAS12 domain. It would be expected that concentration differences would occur from the differences in hourly average concentrations, versus in the instantaneous concentrations. Additionally, and likely more significant to concentration differences, the CAMx model does not include emissions from the boundary cells.

The top 10 positive difference hours are presented in Figures 4-22 through 4-31 and the top 10 negative impact hours are presented in Tables 4-32 through 4-41. The hours of the maximum differences are tending to occur in July 17-21. There were wildfires in Canada in the area of the maximum difference during this period. It is not surprising that the largest difference is occurring where noted large source emissions are input into the model near a boundary where the time averaging of the pollutants flowing into the cells are different. On the day of the maximum positive difference (July 21 at 0400) the maximum difference in PM_{2.5} concentration was 383.43 µg/m³ ppb. At this hour at this grid cell the difference in the sulfate, nitrate, and OM concentrations were 5.762 µg/m³, 0.835 µg/m³, 295.99 µg/m³, respectively with the difference dominated by the differences in the OM estimates. The high local emissions dominated by OM as is expected from wildfire emissions.

Scatterplots of the daily average PM_{2.5} concentrations in local standard time at the IMPROVE monitors are presented in Figure 4-42. The 12US2 results are plotted on the x-axis

and the VISTAS12 results are plotted on the y-axis. The data has a high degree of correlation with a line of best fit with a slope of 1.0003, an intercept of 0.0031 $\mu\text{g}/\text{m}^3$ and an R^2 of 1.0000.

Examination of the difference animations often show differences along the boundary becoming lower as the plumes along the boundary move into the domain.

Table 4-2. Comparison of 2028elv3 CAMx 6.40 VISTAS12 and 12US2 Simulation of PM_{2.5} Concentrations ($\mu\text{g}/\text{m}^3$). Hours with the top 10 maximum positive and maximum negative differences are shown.

Year	Month	Day	Hour	VISTAS12 Conc.	12US2 Conc.	Difference ($\mu\text{g}/\text{m}^3$)	Percent Difference	Column	Row
Maximum Positive									
2011	7	21	4	949.91	566.54	383.37	67.7%	104	241
2011	7	20	14	1660.05	1353.59	306.46	22.6%	107	241
2011	7	20	15	839.18	559.74	279.44	49.9%	107	241
2011	7	20	11	2740.11	2470.87	269.24	10.9%	107	241
2011	7	21	3	3176.80	2914.06	262.74	9.0%	104	241
2011	7	21	1	2369.71	2110.12	259.59	12.3%	104	241
2011	7	20	12	3022.91	2785.90	237.01	8.5%	107	241
2011	7	20	23	448.18	221.41	226.78	102.4%	102	241
2011	7	21	0	732.17	508.25	223.92	44.1%	103	241
2011	7	20	9	6964.26	6752.77	211.49	3.1%	105	241
Maximum Negative									
2011	7	20	15	4857.63	5154.32	-296.69	-5.8%	105	241
2011	7	20	16	4003.88	4266.41	-262.54	-6.2%	105	241
2011	7	20	14	5167.65	5429.55	-261.90	-4.8%	106	241
2011	7	17	11	508.55	761.67	-253.12	-33.2%	89	241
2011	7	20	13	6146.56	6389.86	-243.30	-3.8%	106	241
2011	7	17	12	496.56	725.04	-228.48	-31.5%	89	241
2011	7	20	12	7718.44	7943.32	-224.88	-2.8%	106	241
2011	7	19	10	815.91	1032.49	-216.58	-21.0%	104	241
2011	7	17	10	429.07	644.79	-215.71	-33.5%	89	241
2011	7	19	9	828.90	1002.97	-174.08	-17.4%	103	241

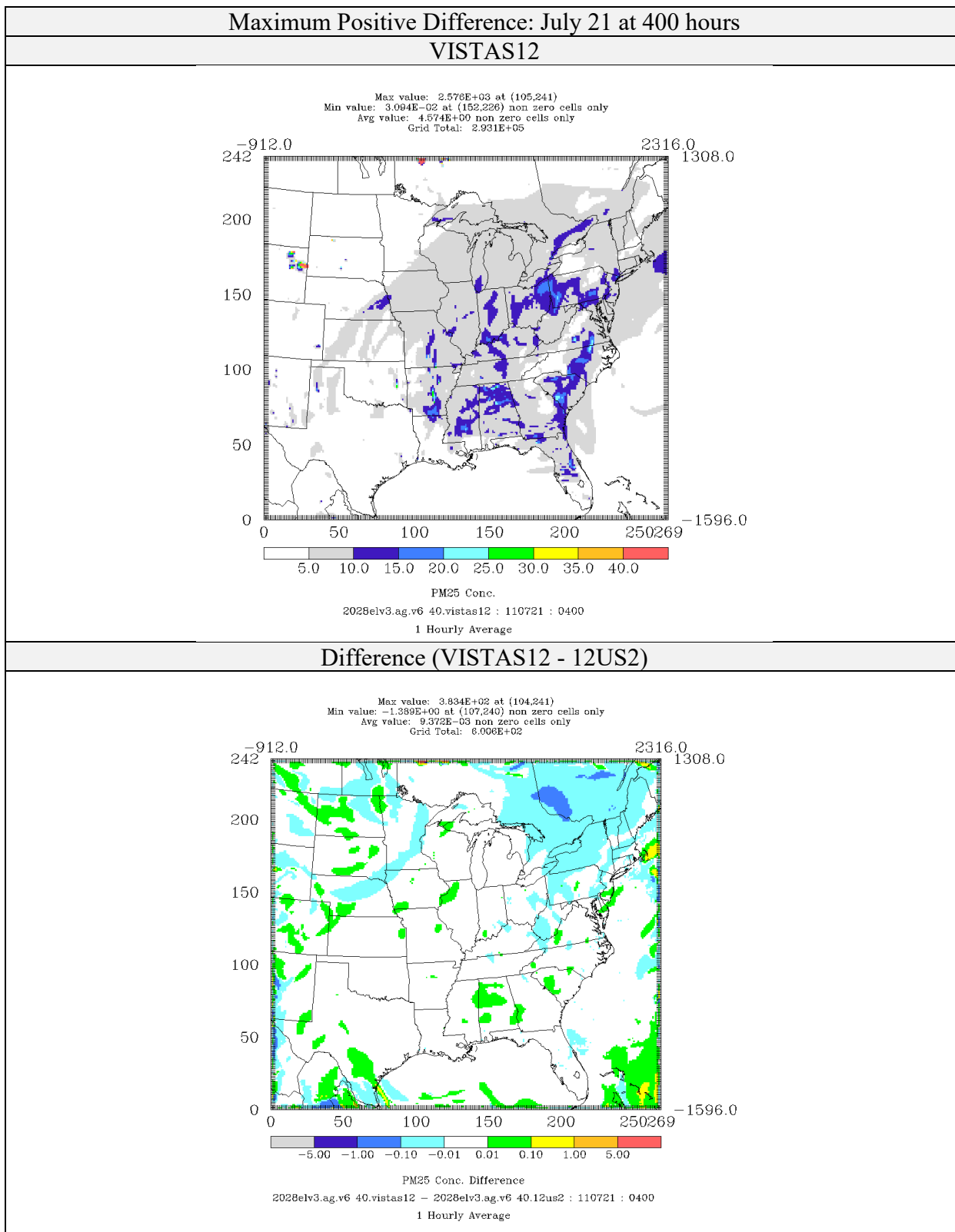


Figure 4-22: Comparison of PM_{2.5} Concentrations ($\mu\text{g}/\text{m}^3$) for CAMx 6.40 on VISTAS12 and 12US2 Domains 2028elv3 Simulations (Maximum Positive Difference)

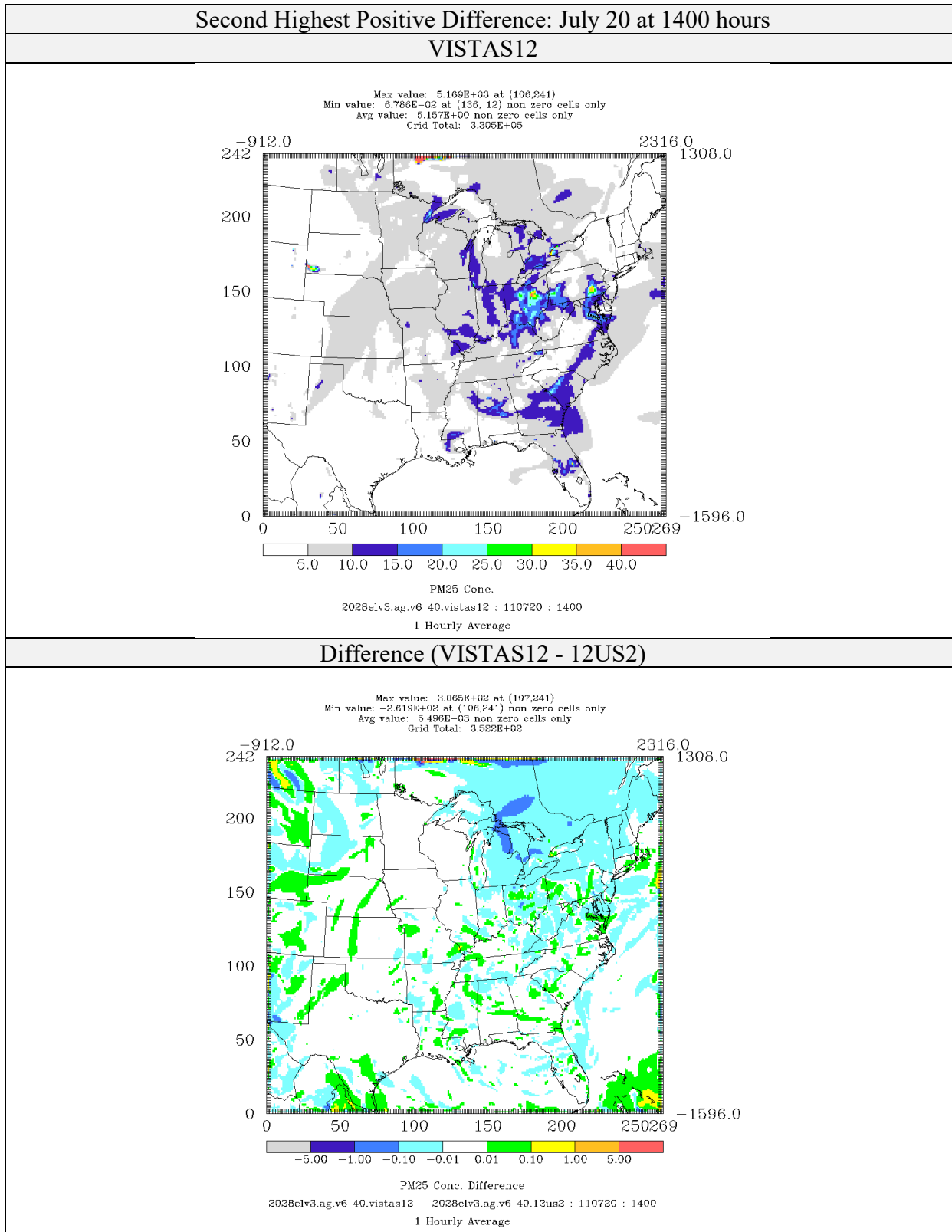


Figure 4-23: Comparison of PM_{2.5} Concentrations ($\mu\text{g}/\text{m}^3$) for CAMx 6.40 on VISTAS12 and 12US2 Domains 2028elv3 Simulations (Second Highest Positive Difference)

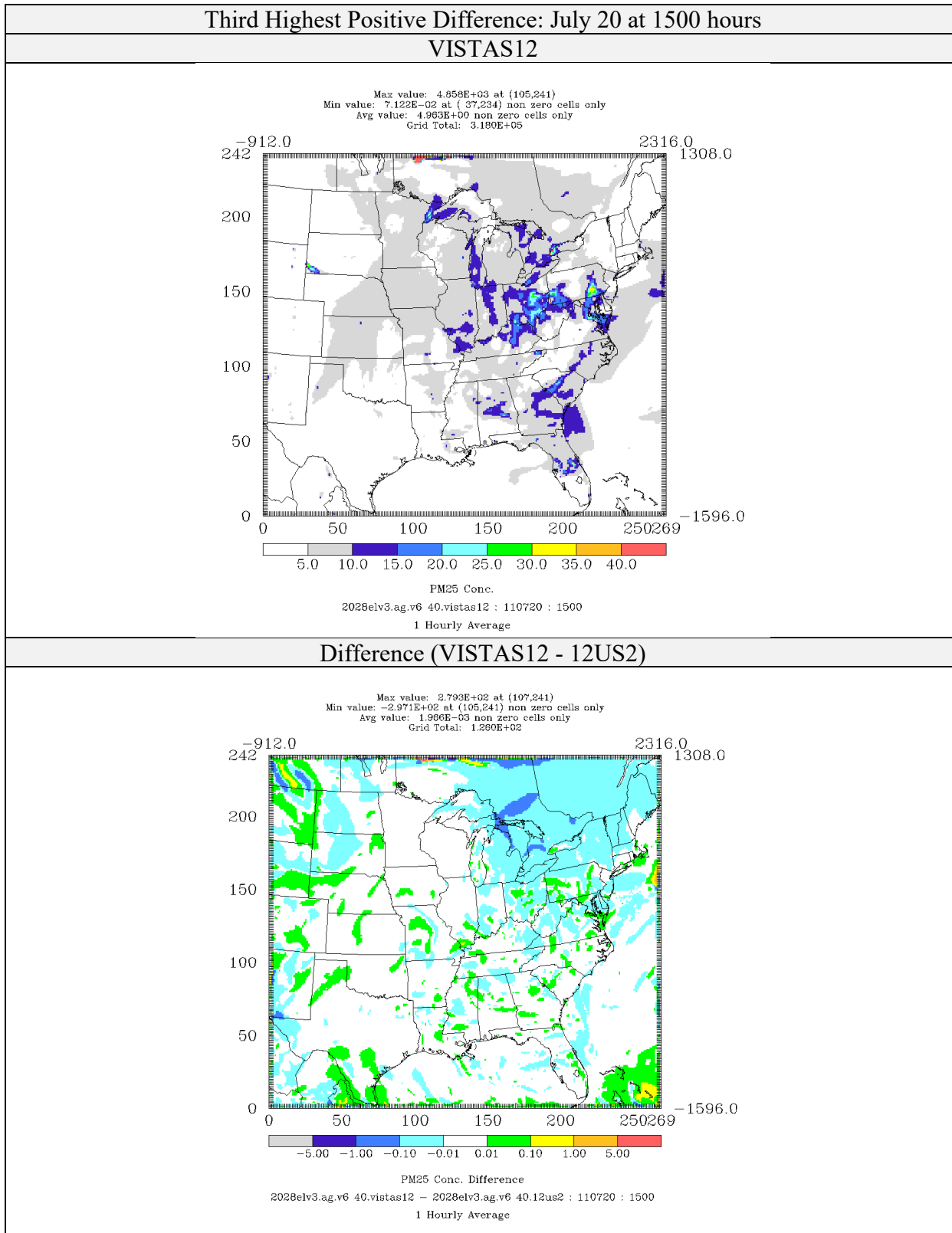


Figure 4-24: Comparison of PM_{2.5} Concentrations ($\mu\text{g}/\text{m}^3$) for CAMx 6.40 on VISTAS12 and 12US2 Domains 2028elv3 Simulations (Third Highest Positive Difference)

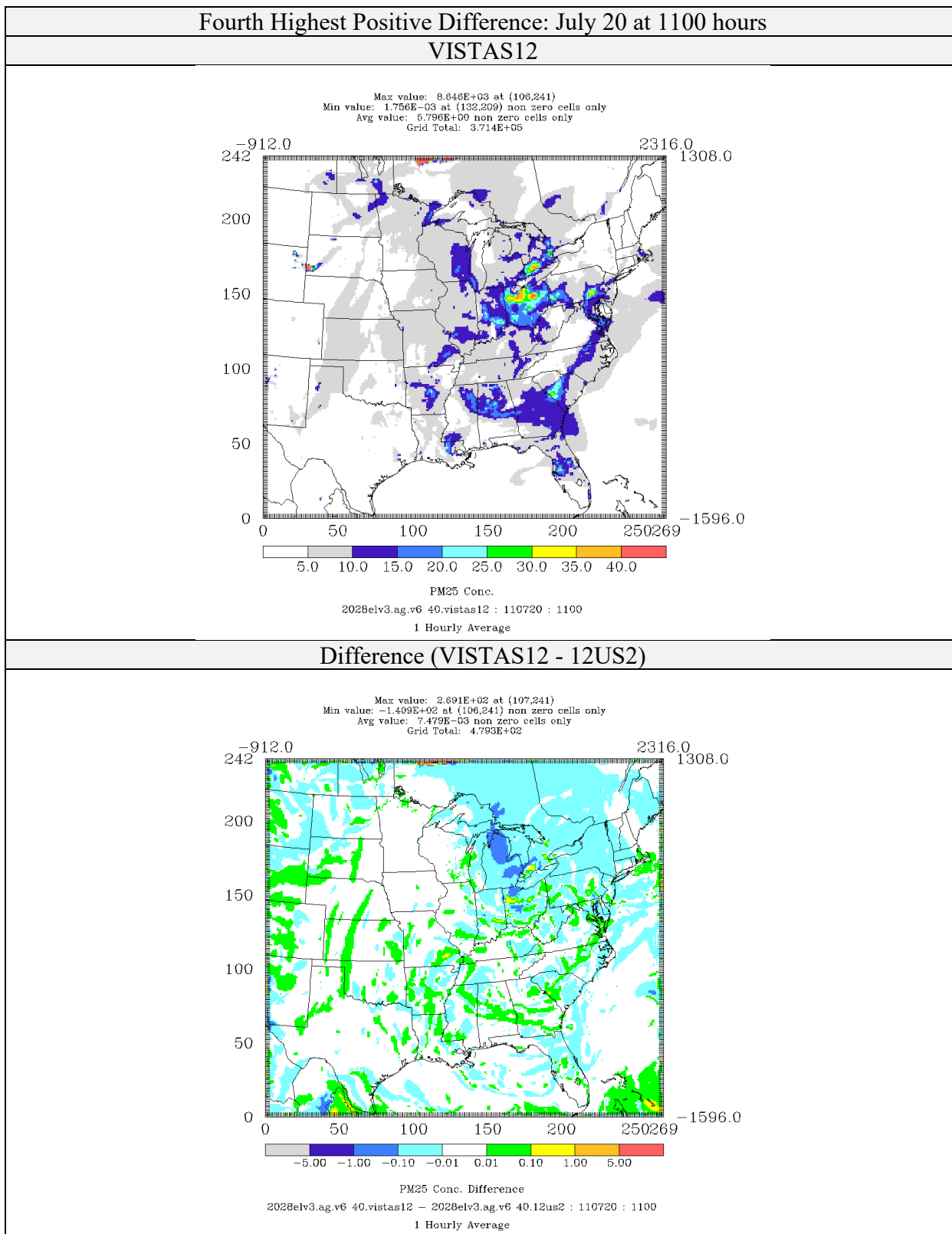


Figure 4-25: Comparison of PM_{2.5} Concentrations ($\mu\text{g}/\text{m}^3$) for CAMx 6.40 on VISTAS12 and 12US2 Domains 2028elv3 Simulations (Fourth Highest Positive Difference)

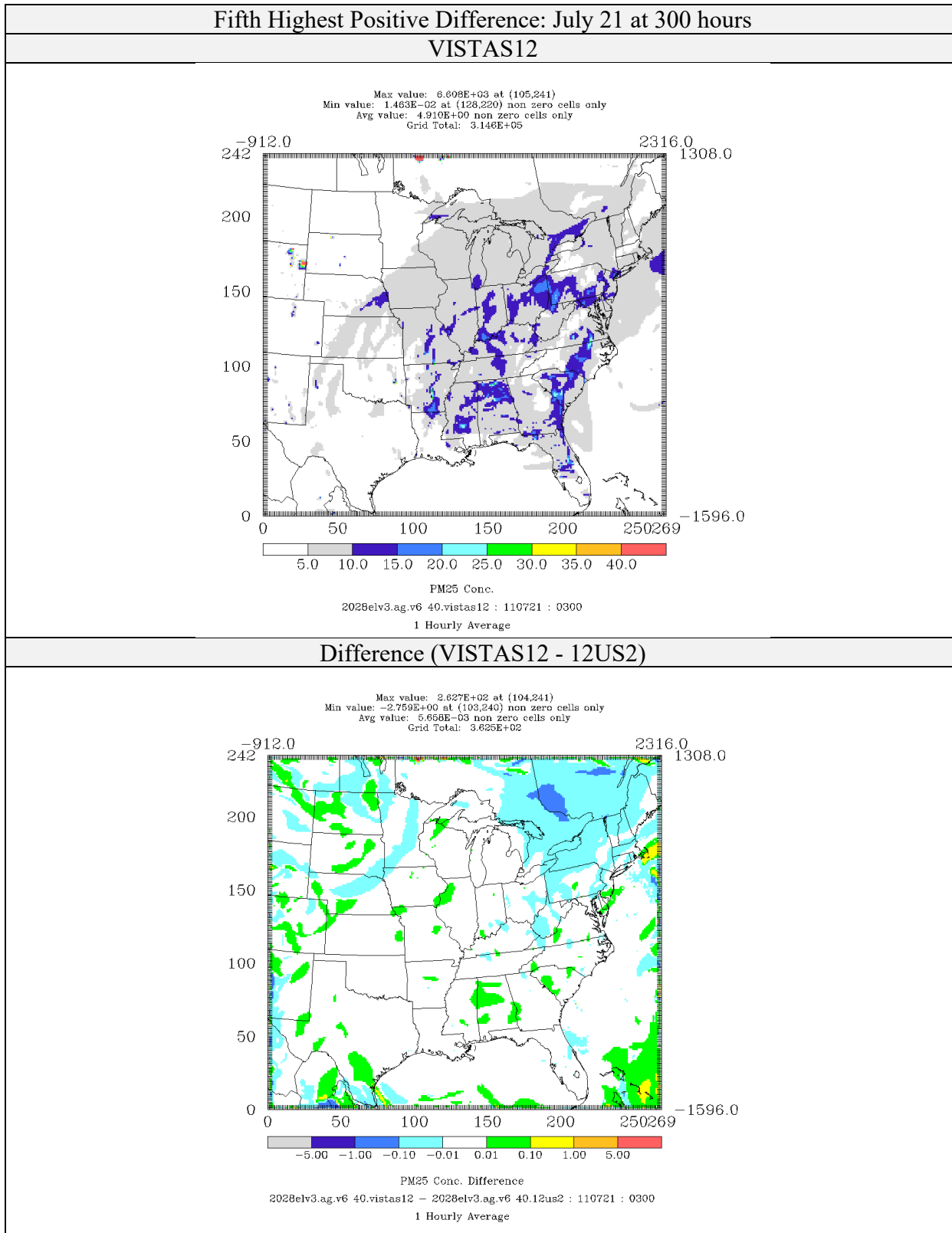


Figure 4-26: Comparison of PM_{2.5} Concentrations ($\mu\text{g}/\text{m}^3$) for CAMx 6.40 on VISTAS12 and 12US2 Domains 2028elv3 Simulations (Fifth Highest Positive Difference)

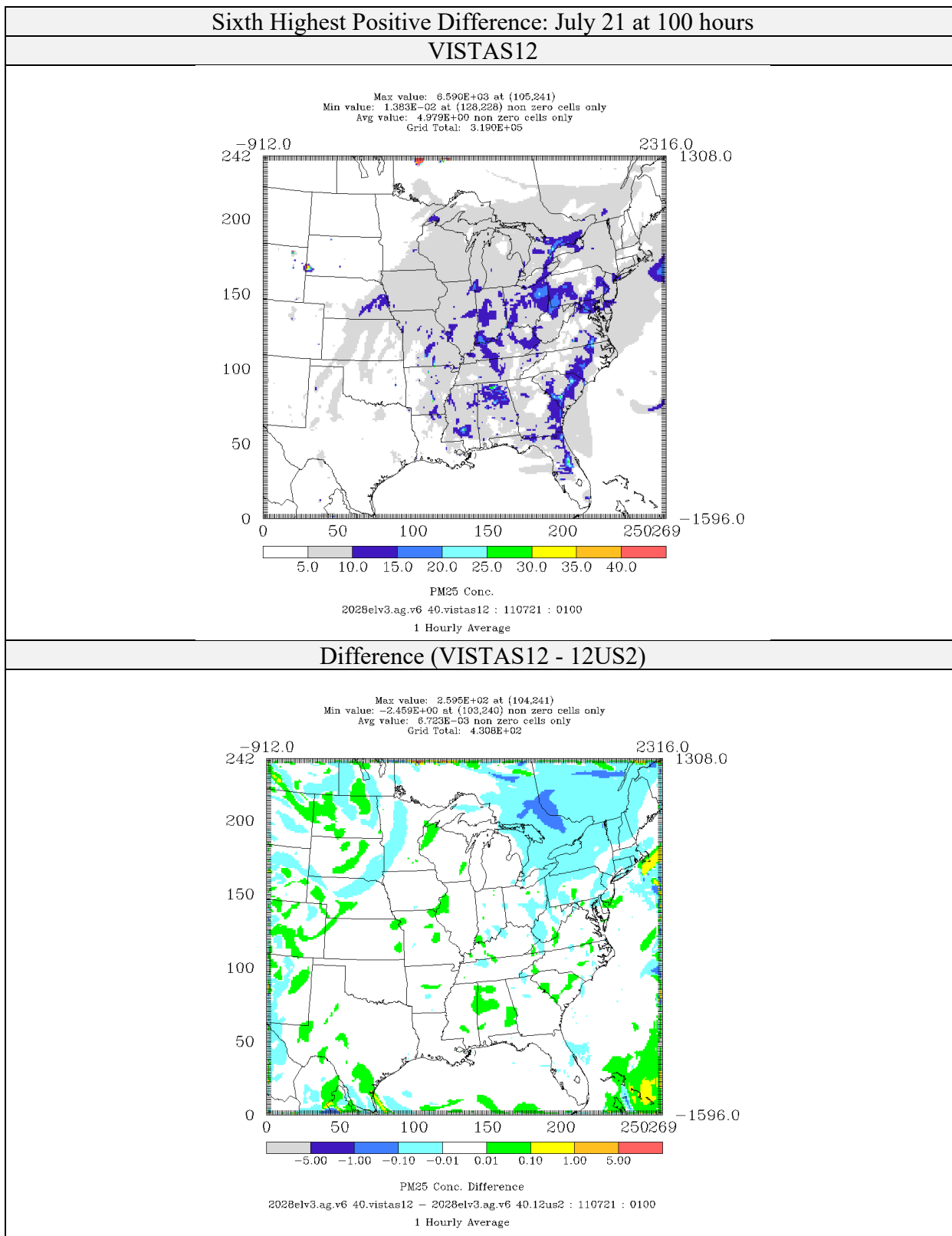


Figure 4-27: Comparison of PM_{2.5} Concentrations ($\mu\text{g}/\text{m}^3$) for CAMx 6.40 on VISTAS12 and 12US2 Domains 2028elv3 Simulations (Sixth Highest Positive Difference)

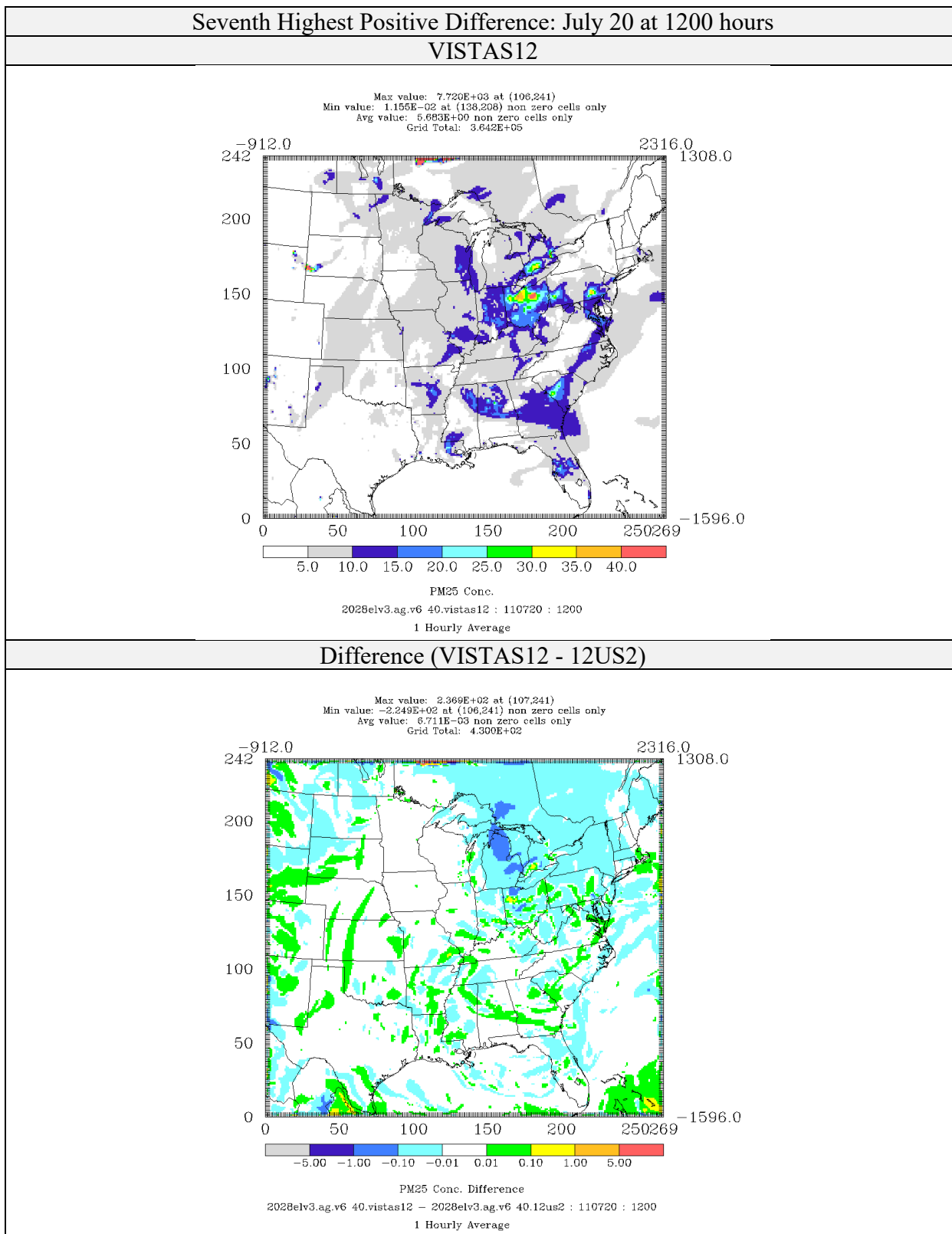


Figure 4-28: Comparison of PM_{2.5} Concentrations ($\mu\text{g}/\text{m}^3$) for CAMx 6.40 on VISTAS12 and 12US2 Domains 2028elv3 Simulations (Seventh Highest Positive Difference)

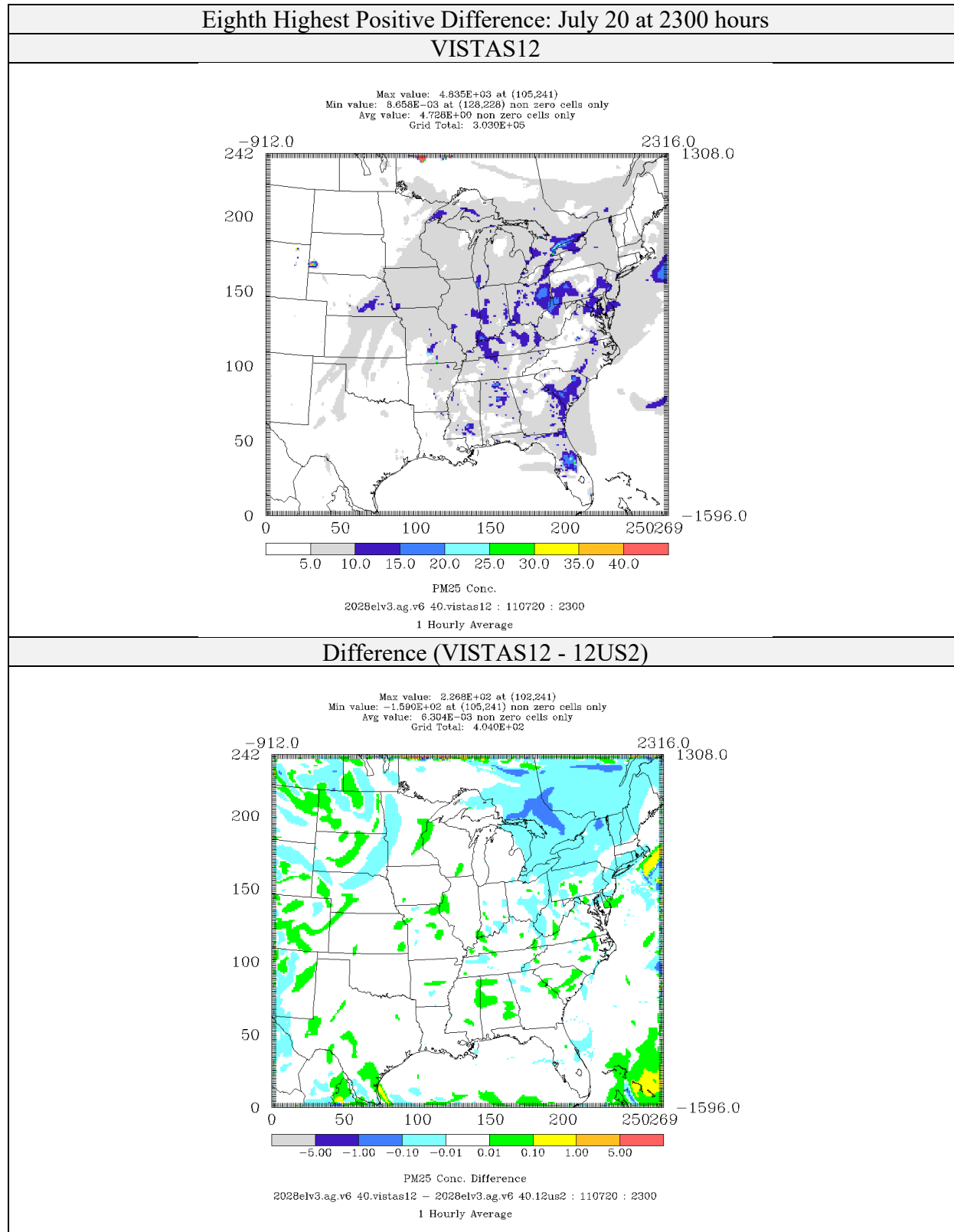


Figure 4-29: Comparison of PM_{2.5} Concentrations ($\mu\text{g}/\text{m}^3$) for CAMx 6.40 on VISTAS12 and 12US2 Domains 2028elv3 Simulations (Eighth Highest Positive Difference)

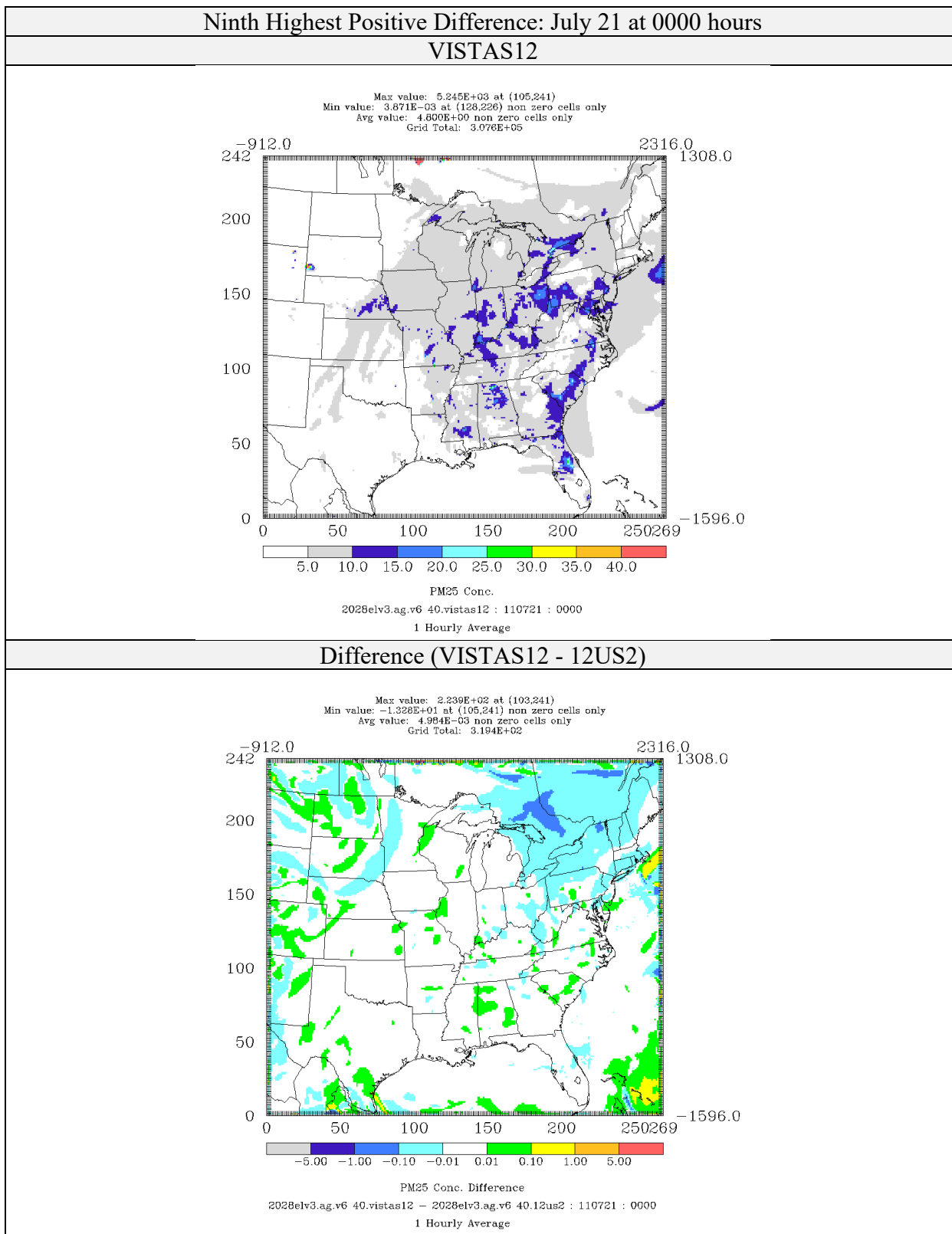


Figure 4-30: Comparison of PM_{2.5} Concentrations ($\mu\text{g}/\text{m}^3$) for CAMx 6.40 on VISTAS12 and 12US2 Domains 2028elv3 Simulations (Ninth Highest Positive Difference)

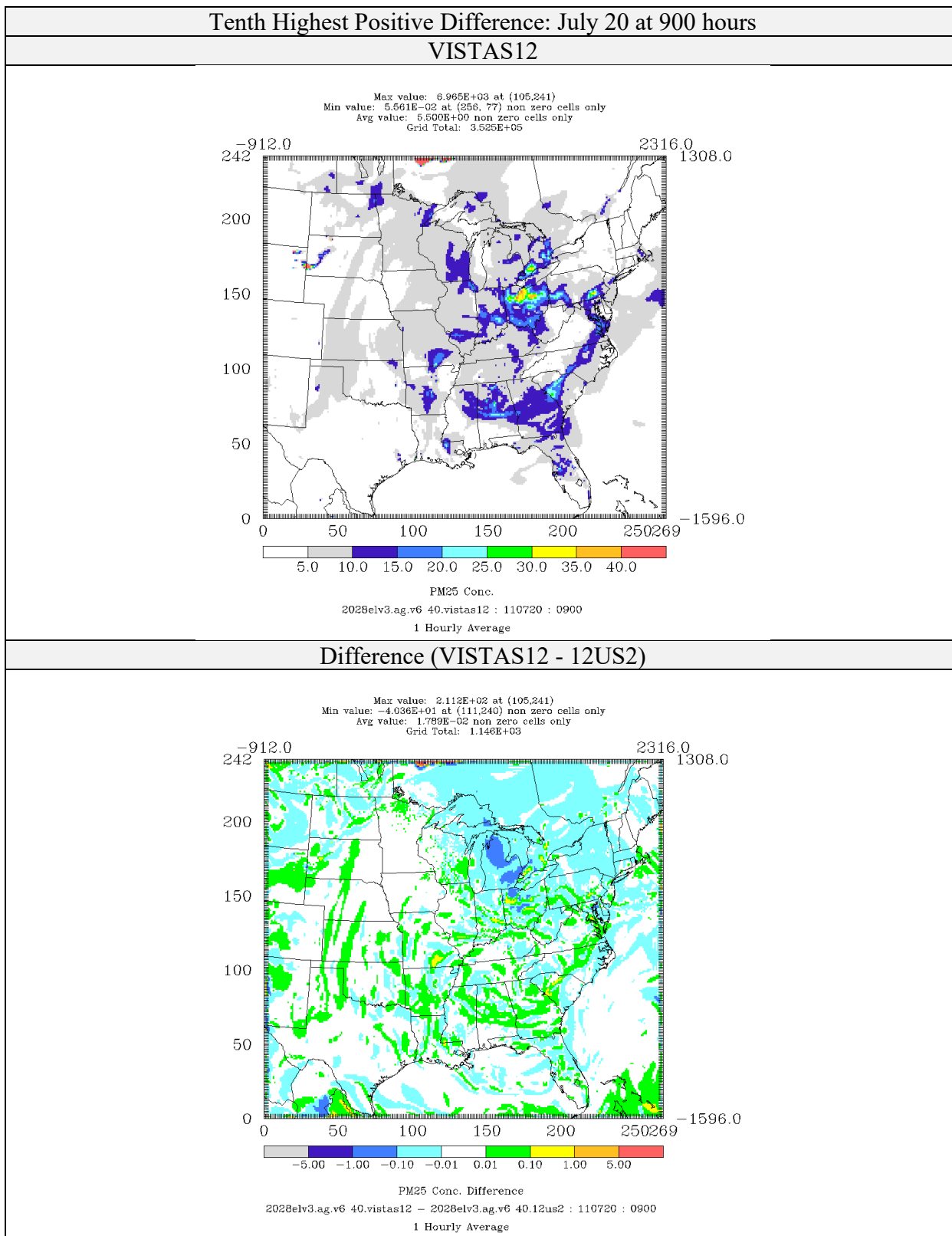


Figure 4-31: Comparison of PM_{2.5} Concentrations ($\mu\text{g}/\text{m}^3$) for CAMx 6.40 on VISTAS12 and 12US2 Domains 2028elv3 Simulations (Tenth Highest Positive Difference)

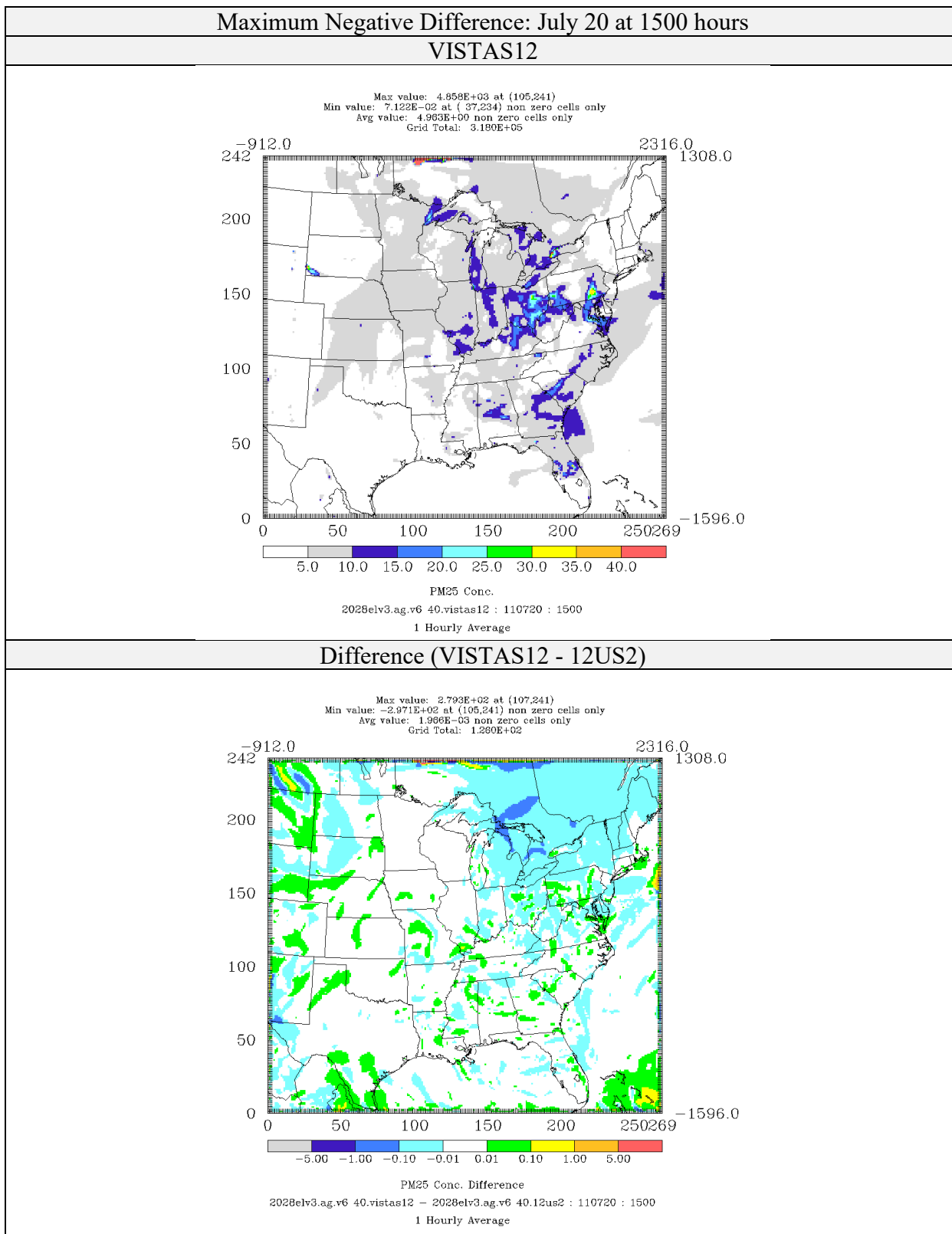


Figure 4-32: Comparison of PM_{2.5} Concentrations ($\mu\text{g}/\text{m}^3$) for CAMx 6.40 on VISTAS12 and 12US2 Domains 2028elv3 Simulations (Maximum Negative Difference)

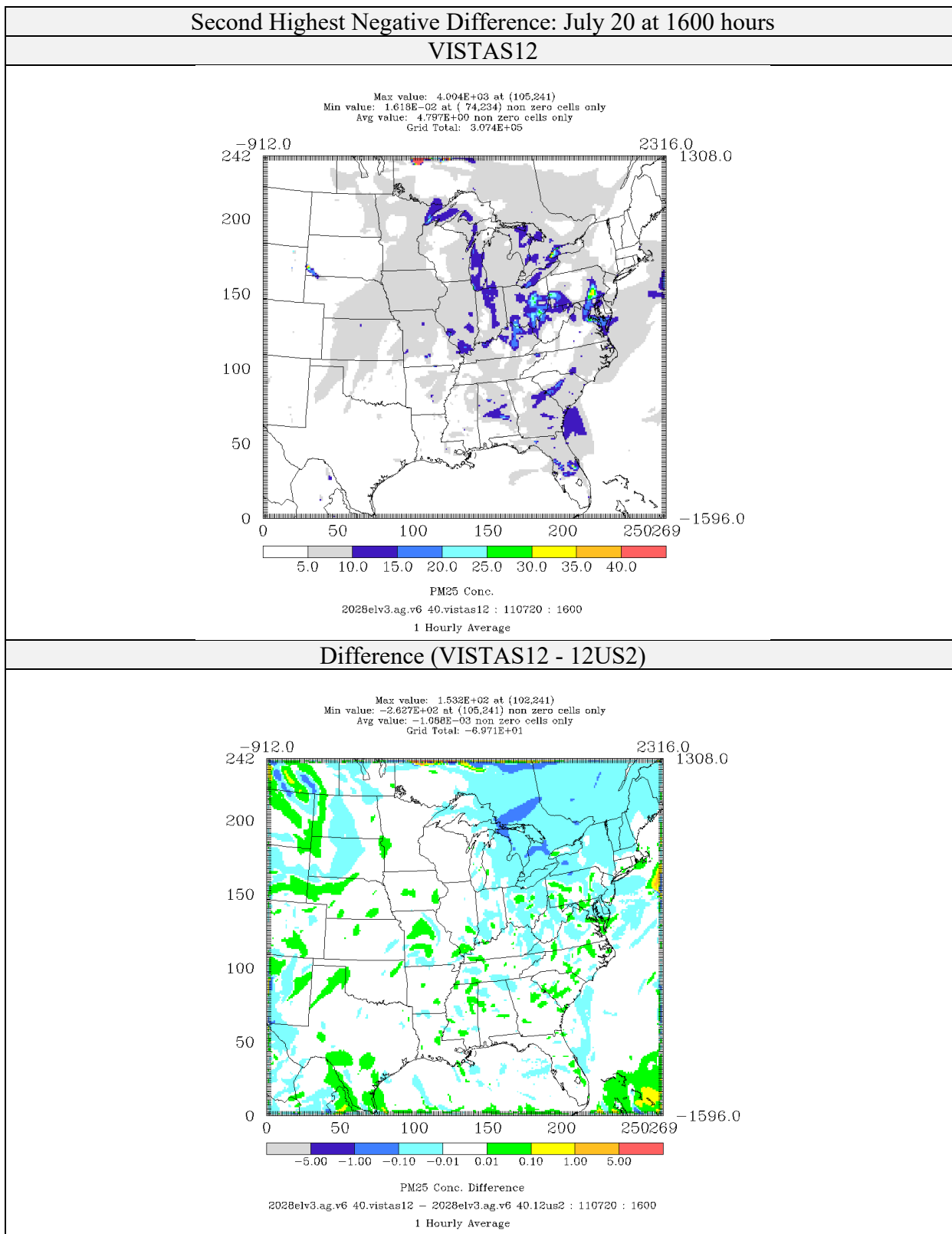


Figure 4-33: Comparison of PM_{2.5} Concentrations ($\mu\text{g}/\text{m}^3$) for CAMx 6.40 on VISTAS12 and 12US2 Domains 2028elv3 Simulations (Second Highest Negative Difference)

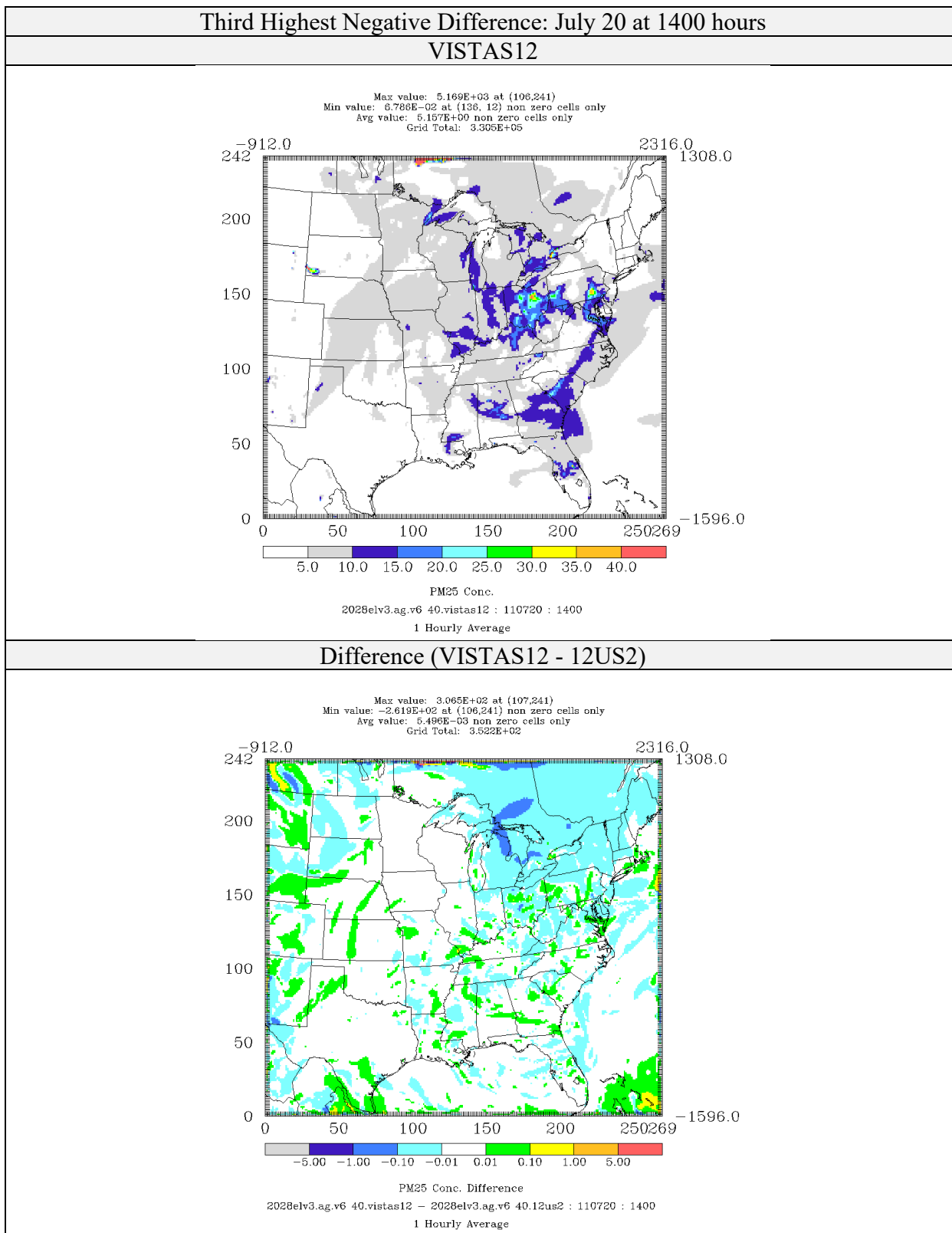


Figure 4-34: Comparison of PM_{2.5} Concentrations ($\mu\text{g}/\text{m}^3$) for CAMx 6.40 on VISTAS12 and 12US2 Domains 2028elv3 Simulations (Third Highest Negative Difference)

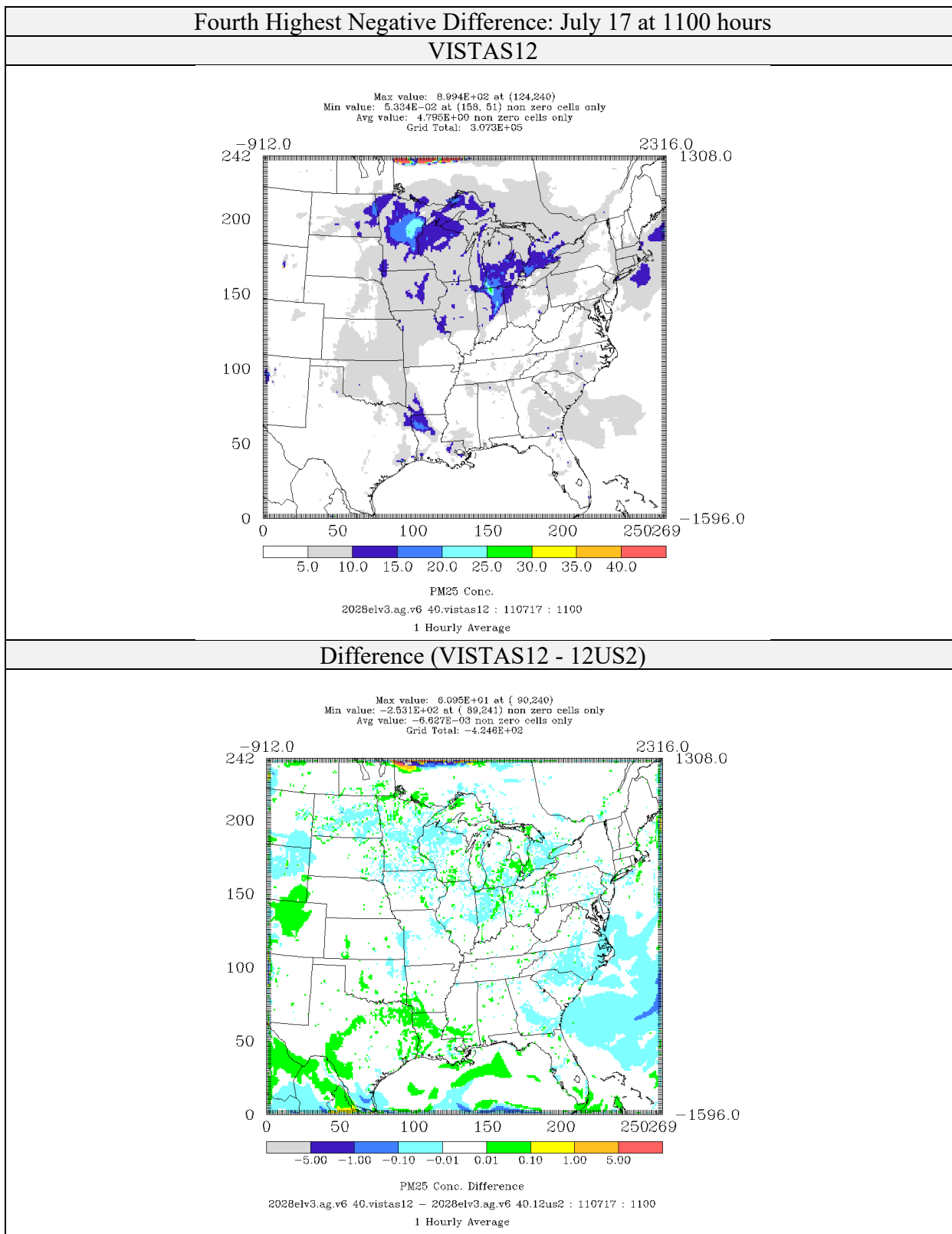


Figure 4-35: Comparison of PM_{2.5} Concentrations ($\mu\text{g}/\text{m}^3$) for CAMx 6.40 on VISTAS12 and 12US2 Domains 2028elv3 Simulations (Fourth Highest Negative Difference)

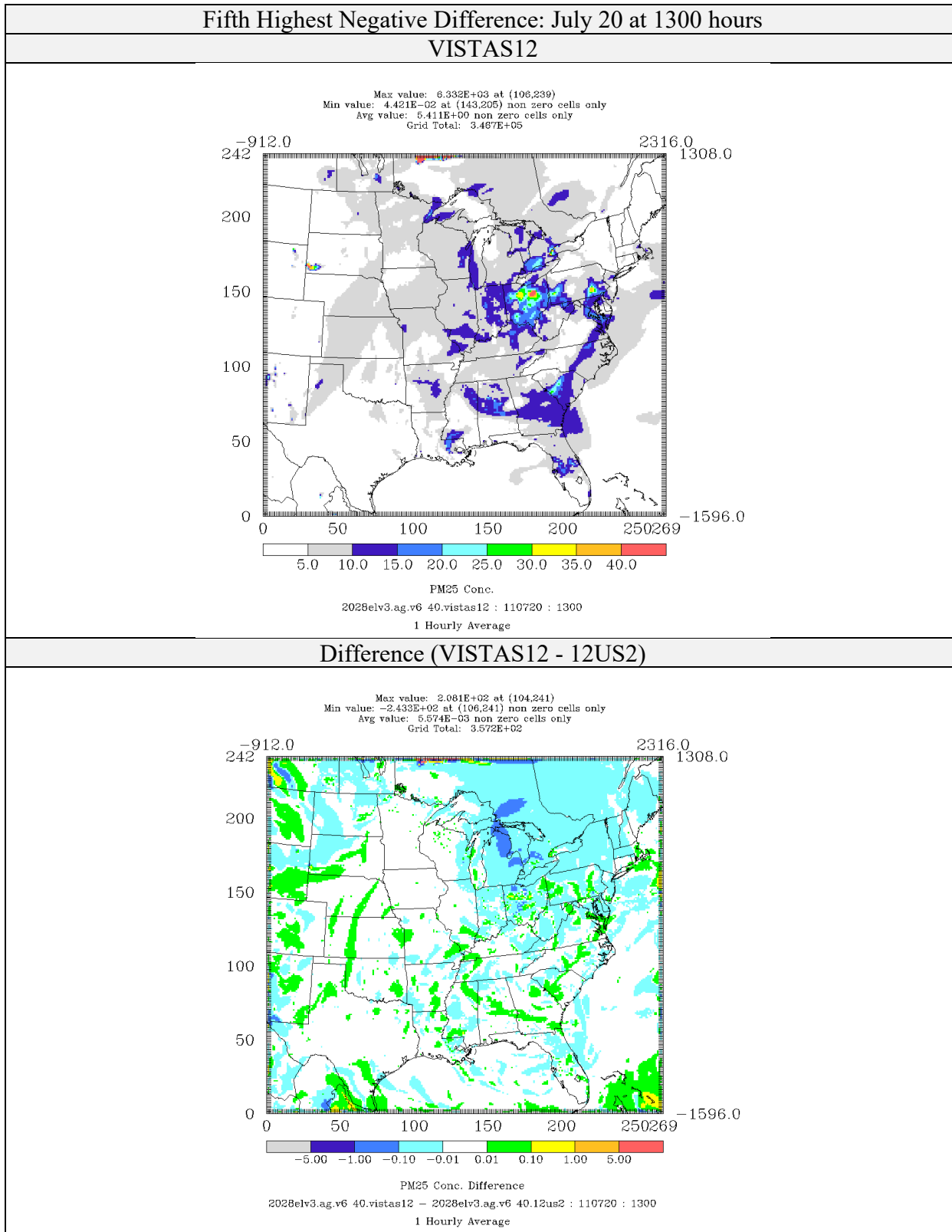


Figure 4-36: Comparison of PM_{2.5} Concentrations ($\mu\text{g}/\text{m}^3$) for CAMx 6.40 on VISTAS12 and 12US2 Domains 2028elv3 Simulations (Fifth Highest Negative Difference)

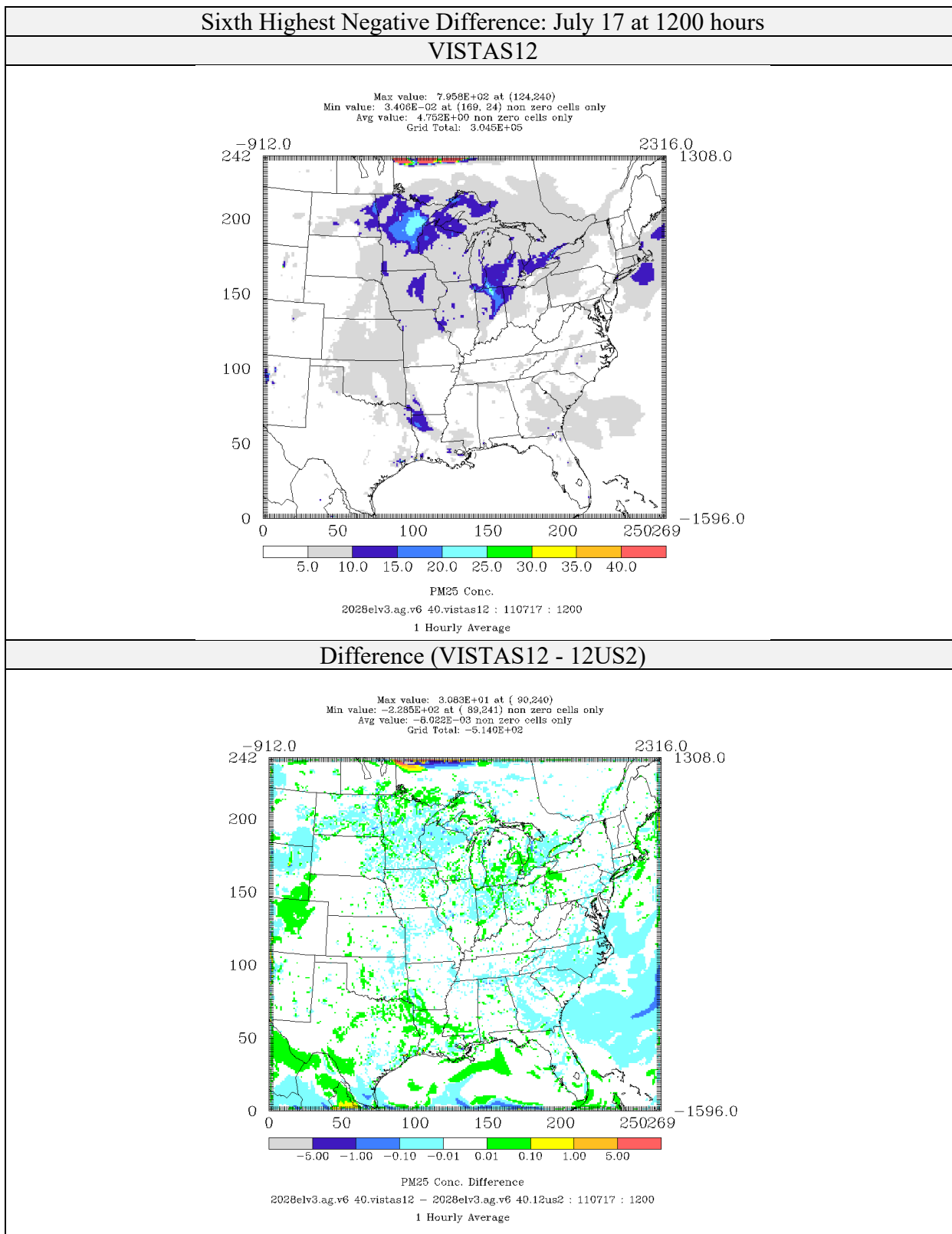


Figure 4-37: Comparison of PM_{2.5} Concentrations ($\mu\text{g}/\text{m}^3$) for CAMx 6.40 on VISTAS12 and 12US2 Domains 2028elv3 Simulations (Sixth Highest Negative Difference)

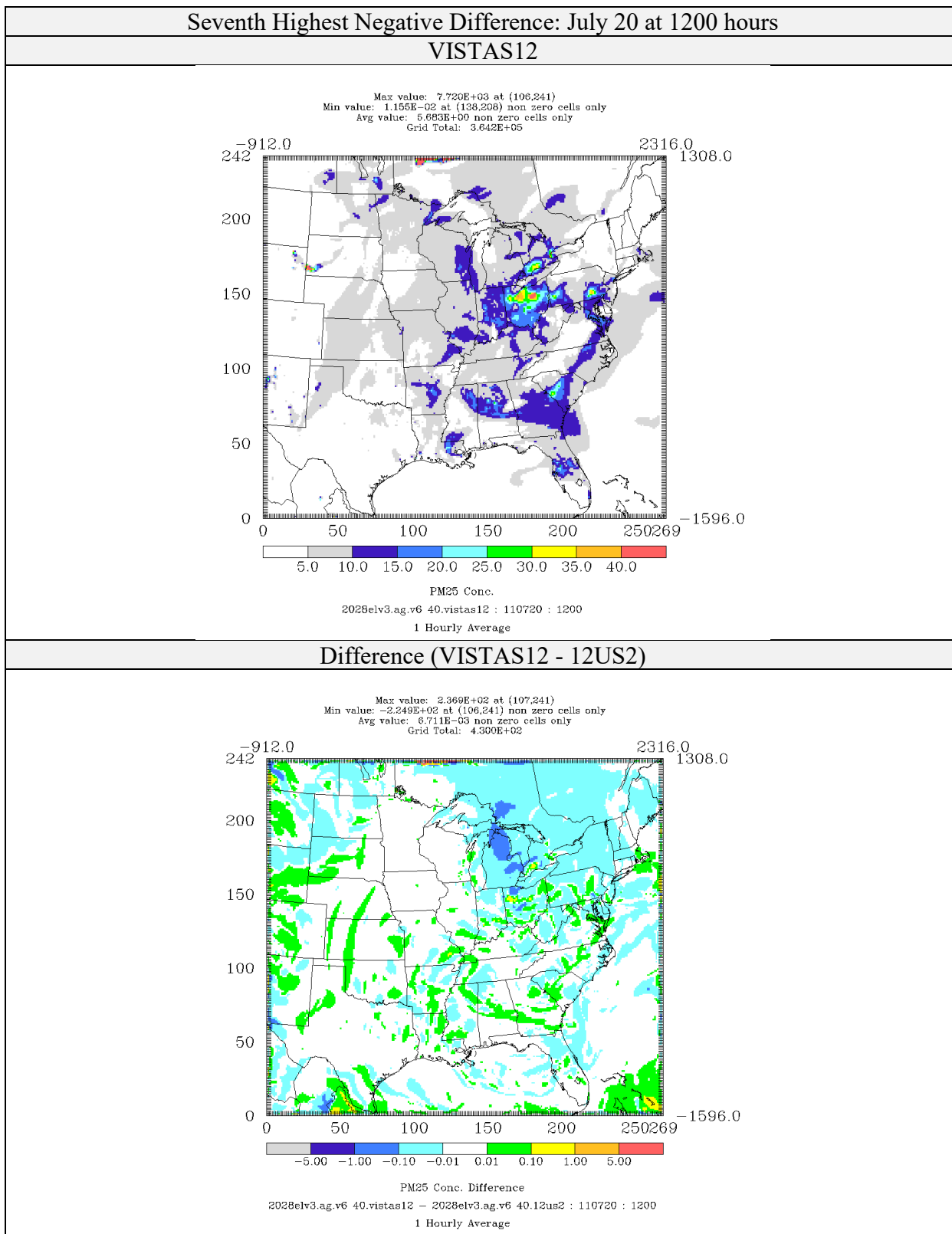


Figure 4-38: Comparison of PM_{2.5} Concentrations ($\mu\text{g}/\text{m}^3$) for CAMx 6.40 on VISTAS12 and 12US2 Domains 2028elv3 Simulations (Seventh Highest Negative Difference)

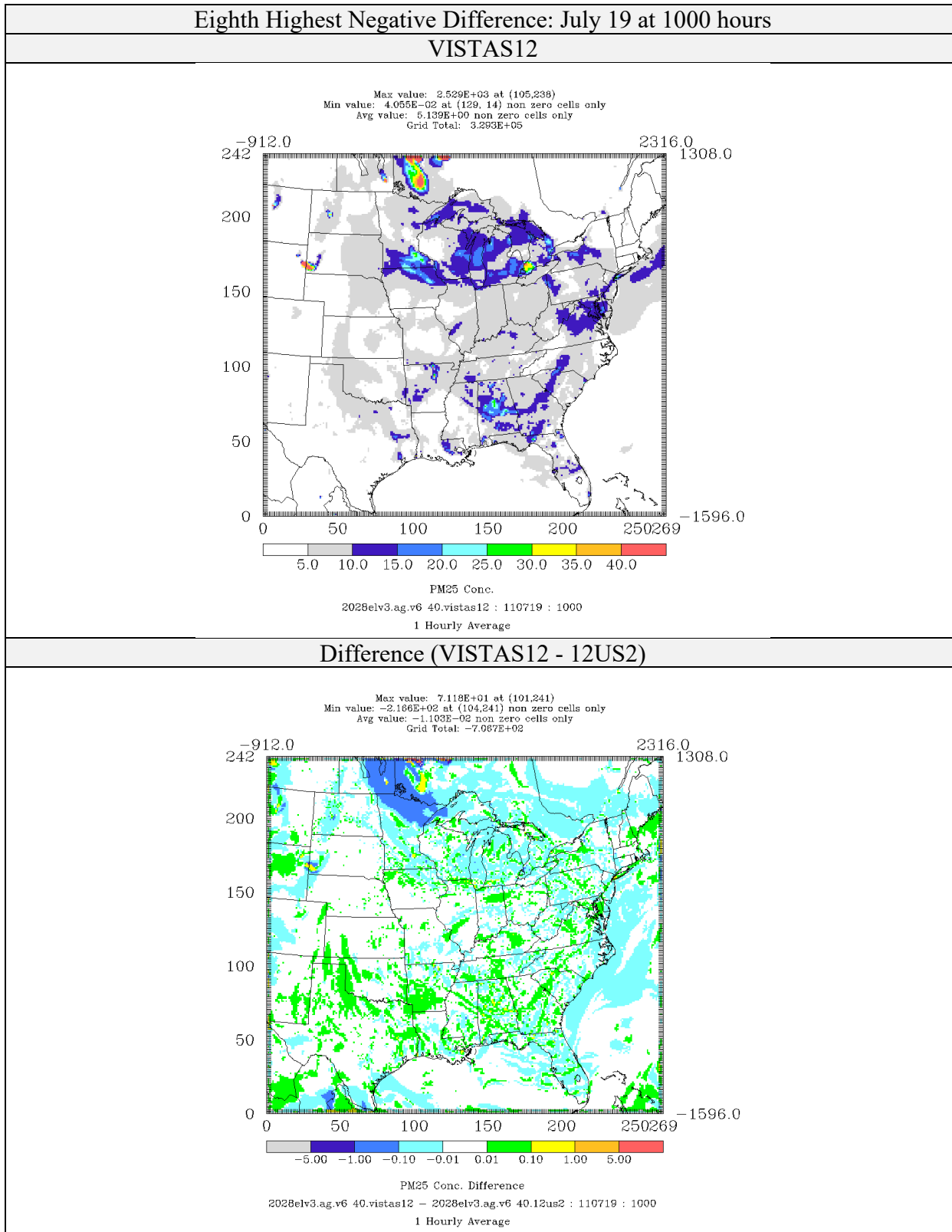


Figure 4-39: Comparison of PM_{2.5} Concentrations ($\mu\text{g}/\text{m}^3$) for CAMx 6.40 on VISTAS12 and 12US2 Domains 2028elv3 Simulations (Eighth Highest Negative Difference)

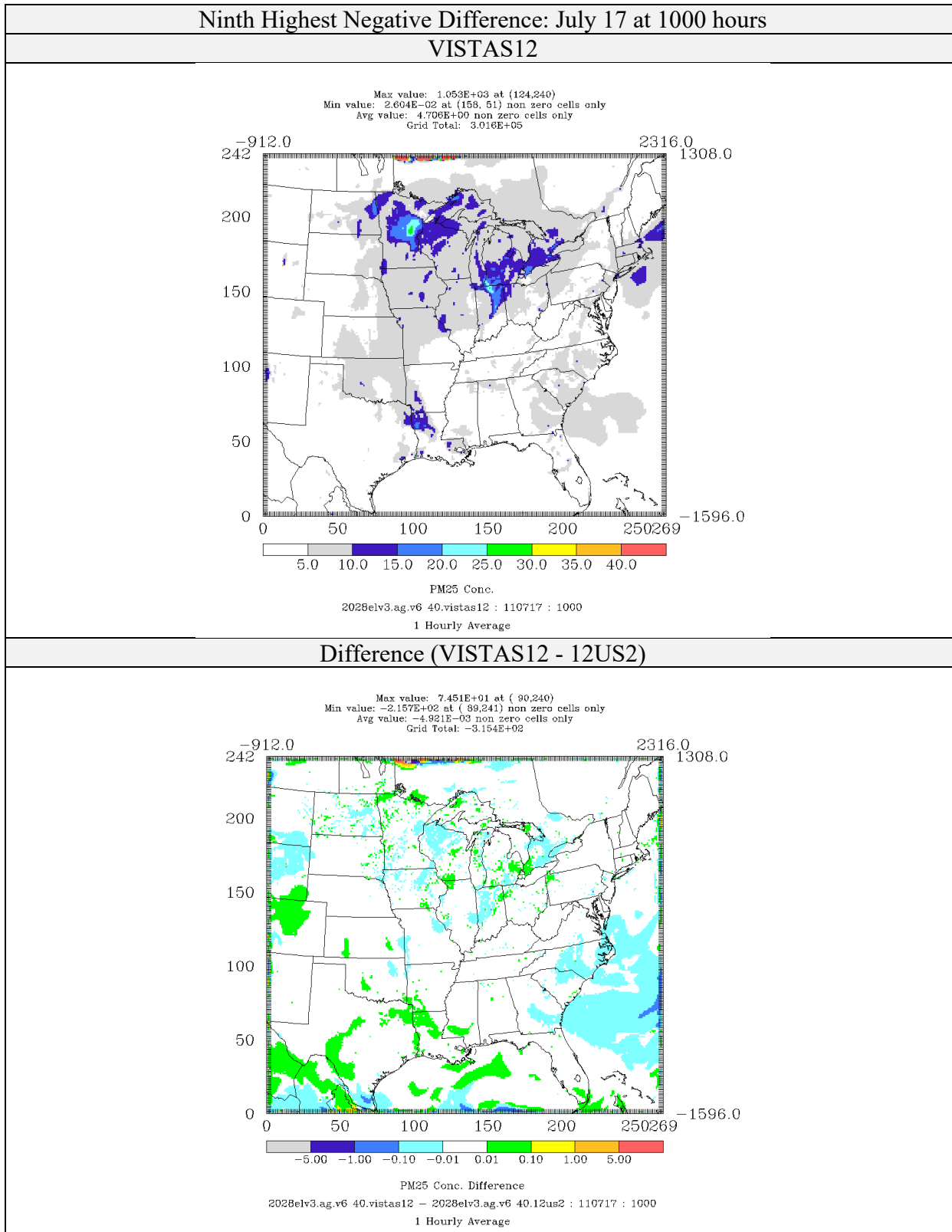


Figure 4-40: Comparison of PM_{2.5} Concentrations ($\mu\text{g}/\text{m}^3$) for CAMx 6.40 on VISTAS12 and 12US2 Domains 2028elv3 Simulations (Ninth Highest Negative Difference)

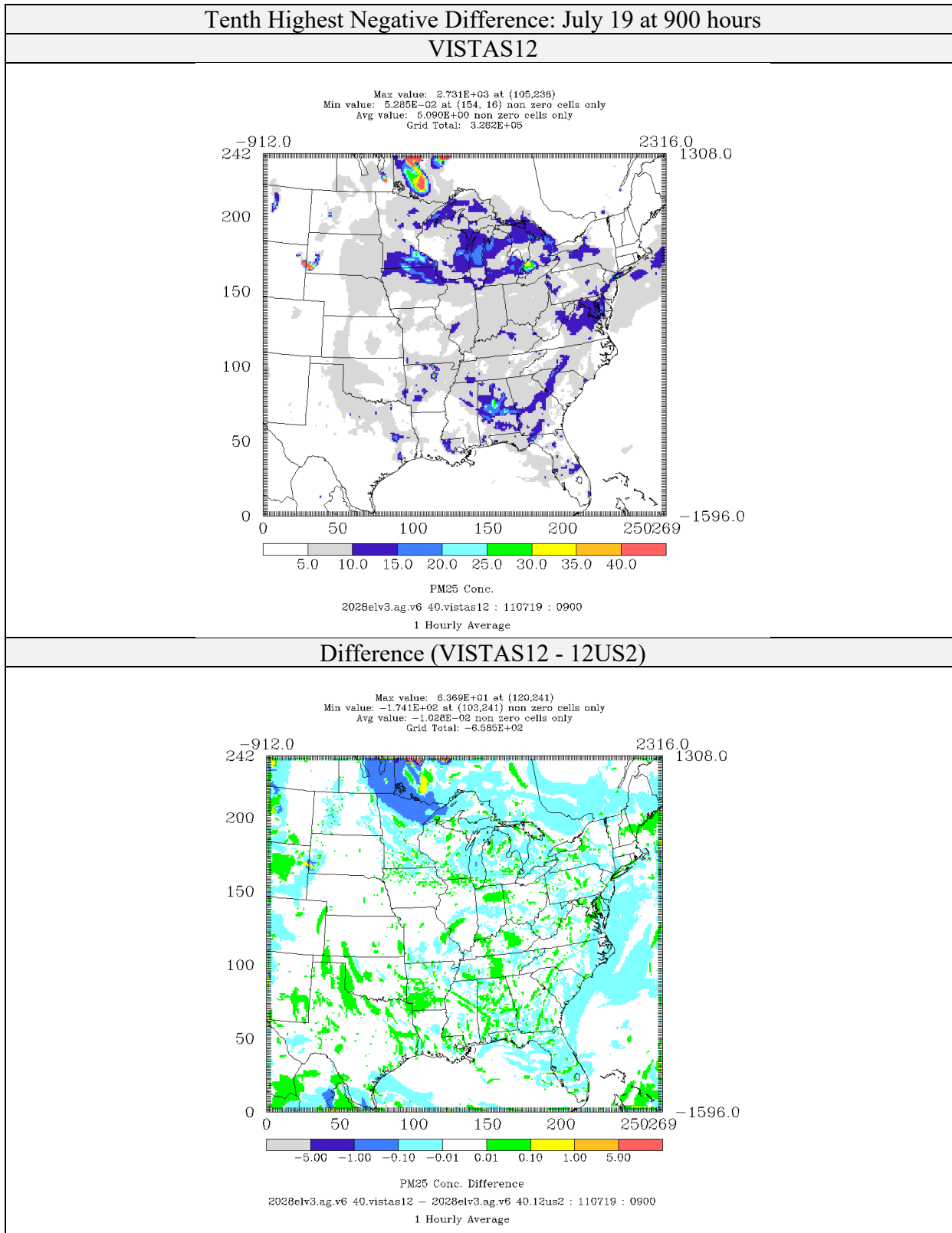


Figure 4-41: Comparison of PM_{2.5} Concentrations ($\mu\text{g}/\text{m}^3$) for CAMx 6.40 on VISTAS12 and 12US2 Domains 2028elv3 Simulations (Tenth Highest Negative Difference)

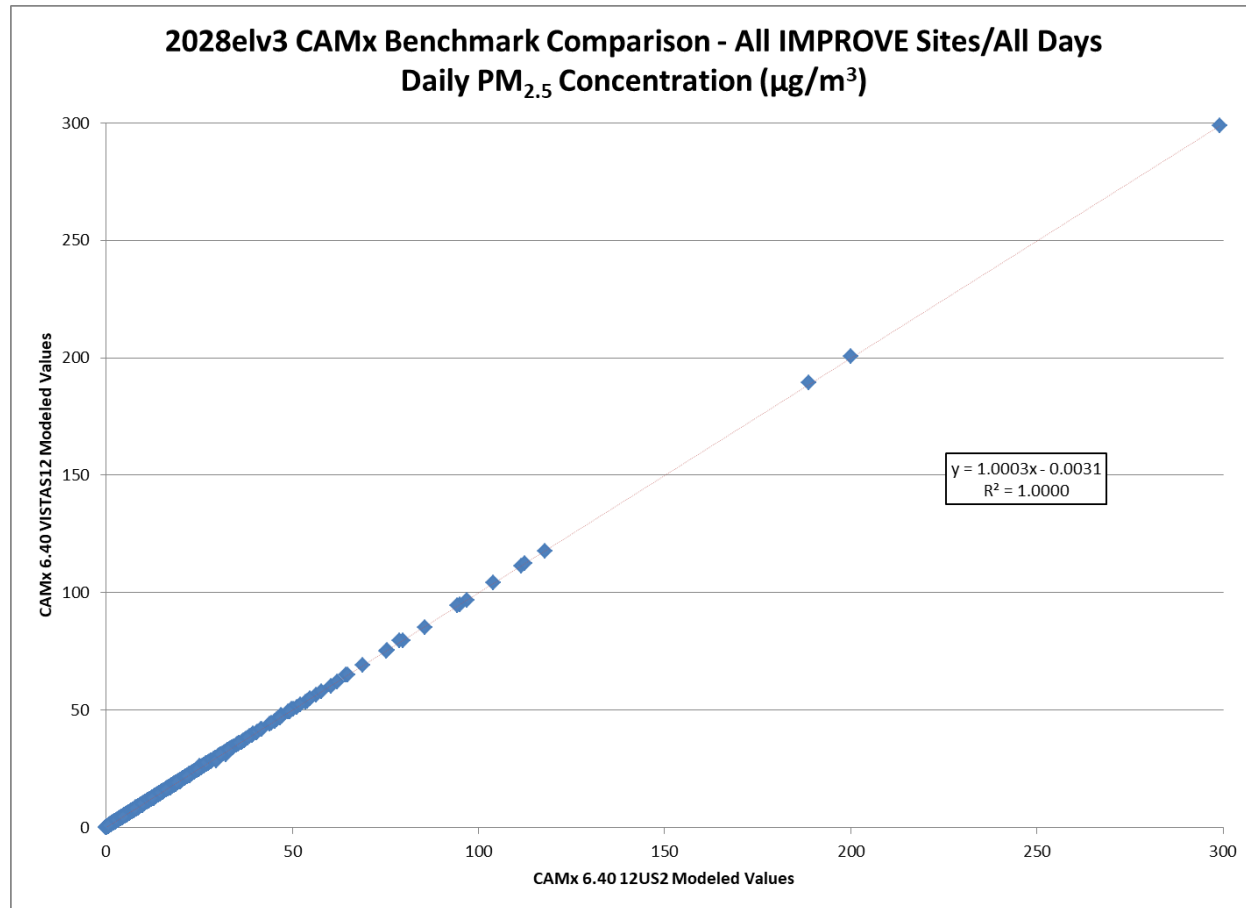


Figure 4-42: Scatterplot Comparing 24-hour Average Predicted PM_{2.5} Concentrations (μg/m³) for All Days at all IMPROVE Monitor Locations for CAMx 6.40 on VISTAS12 and 12US2 Domains 2028elv3 Simulations Performed by VISTAS (Alpine).

4.3 Sulfate

Sulfate results for the top 10 positive and negative hours are presented in tabular format in Table 4-3. The maximum positive difference is $5.76 \mu\text{g}/\text{m}^3$ falling to $3.43 \mu\text{g}/\text{m}^3$ for the 10th high. The maximum negative difference is $-4.57 \mu\text{g}/\text{m}^3$ falling to $-2.34 \mu\text{g}/\text{m}^3$ for the 10th high. The maximum positive percent difference on these days is 94.5% and negative percent difference of -32.7%.

As expected, the maximum impacts on the top 10 positive and negative hours are occurring very near the border. As was described in Section 2, the two CAMx simulations used the same input data, except that the pollutant concentrations on in-flow boundary cells. For the simulation on the VISTAS12 domain the in-flow concentrations are specified in hourly boundary conditions extracted from the 12US2 simulation. For the 12US2 simulation the in-flow concentrations were continuously updated from the cells outside the VISTAS12 domain. It would be expected that concentration differences would occur from the differences in hourly average concentrations, versus in the instantaneous concentrations. The top 10 positive difference hours are presented in Figures 4-43 through 4-52 and the top 10 negative difference hours are presented in Tables 4-53 through 4-62. The peak differences are occurring between July 17 and July 20. The area of the peak impact is very near the northern border, north of Minnesota.

Scatterplots of the daily average sulfate concentrations in local standard time at the IMPROVE monitors are presented in Figure 4-63. The 12US2 results are plotted on the x-axis and the VISTAS12 results are plotted on the y-axis. The data has a high degree of correlation with a line of best fit with a slope of 1.0019, an intercept of $0.0008 \mu\text{g}/\text{m}^3$ and an R^2 of 0.9999.

Examination of the difference animations often show differences along the boundary becoming lower as the plumes along the boundary move into the domain.

Table 4-3. Comparison of 2028elv3 CAMx 6.40 VISTAS12 and 12US2 Simulation of Sulfate Concentrations ($\mu\text{g}/\text{m}^3$). Hours with the top 10 maximum positive and maximum negative differences are shown.

Year	Month	Day	Hour	VISTAS12 Conc.	12US2 Conc.	Difference ($\mu\text{g}/\text{m}^3$)	Percent Difference	Column	Row
Maximum Positive									
2011	7	21	4	13.56	7.80	5.76	73.9%	104	241
2011	7	20	14	25.43	20.65	4.79	23.2%	107	241
2011	7	21	3	44.72	40.44	4.28	10.6%	104	241
2011	7	20	15	13.32	9.20	4.12	44.8%	107	241
2011	7	21	1	31.50	27.50	4.00	14.5%	104	241
2011	7	20	12	45.82	41.92	3.90	9.3%	107	241
2011	7	20	11	39.79	35.92	3.87	10.8%	107	241
2011	7	21	0	10.21	6.66	3.55	53.2%	103	241
2011	7	20	23	7.17	3.69	3.48	94.5%	102	241
2011	7	20	22	8.31	4.88	3.43	70.3%	102	241
Maximum Negative									
2011	7	20	14	73.45	78.03	-4.57	-5.9%	106	241
2011	7	20	15	66.90	71.41	-4.51	-6.3%	105	241
2011	7	20	13	88.61	92.84	-4.23	-4.6%	106	241
2011	7	20	16	54.97	59.00	-4.03	-6.8%	105	241
2011	7	20	12	112.23	116.24	-4.00	-3.4%	106	241
2011	7	17	11	6.88	10.22	-3.34	-32.7%	89	241
2011	7	17	12	6.87	9.91	-3.04	-30.7%	89	241
2011	7	19	10	11.25	14.18	-2.93	-20.6%	104	241
2011	7	17	10	5.80	8.59	-2.79	-32.5%	89	241
2011	7	19	9	11.52	13.86	-2.34	-16.9%	103	241

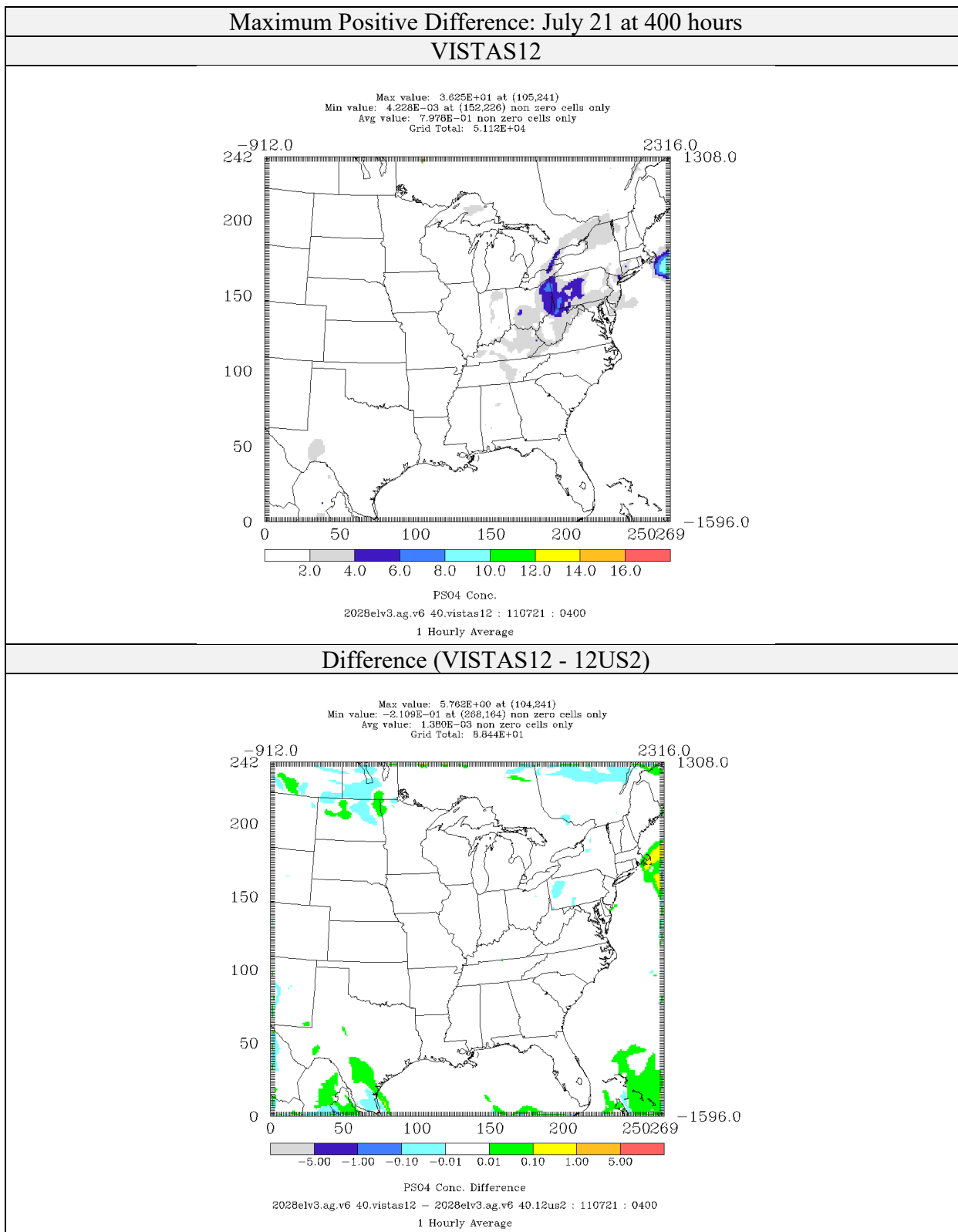


Figure 4-43: Comparison of Sulfate Concentrations ($\mu\text{g}/\text{m}^3$) for CAMx 6.40 on VISTAS12 and 12US2 Domains 2028elv3 Simulations (Maximum Positive Difference)

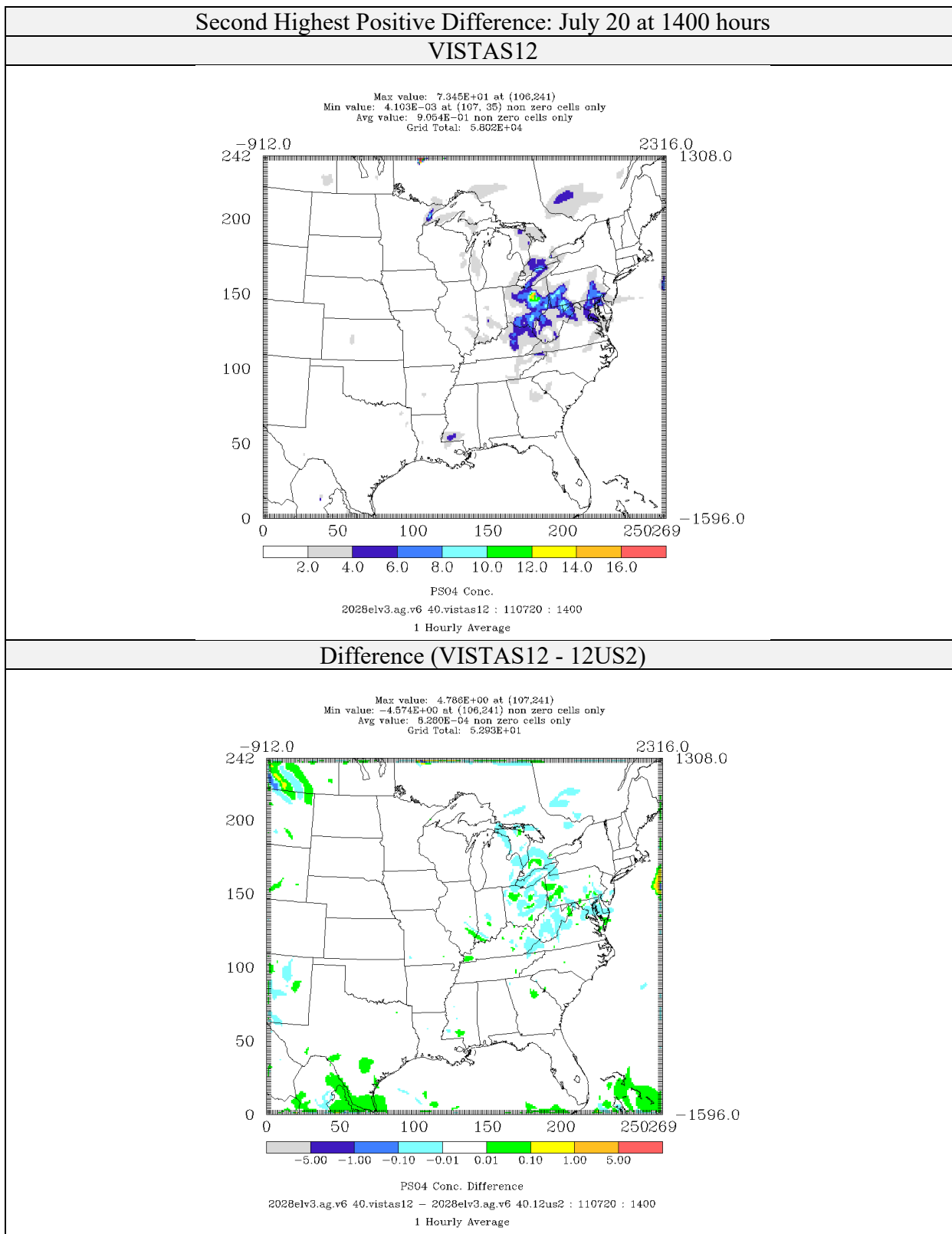


Figure 4-44: Comparison of Sulfate Concentrations ($\mu\text{g}/\text{m}^3$) for CAMx 6.40 on VISTAS12 and 12US2 Domains 2028elv3 Simulations (Second Highest Positive Difference)

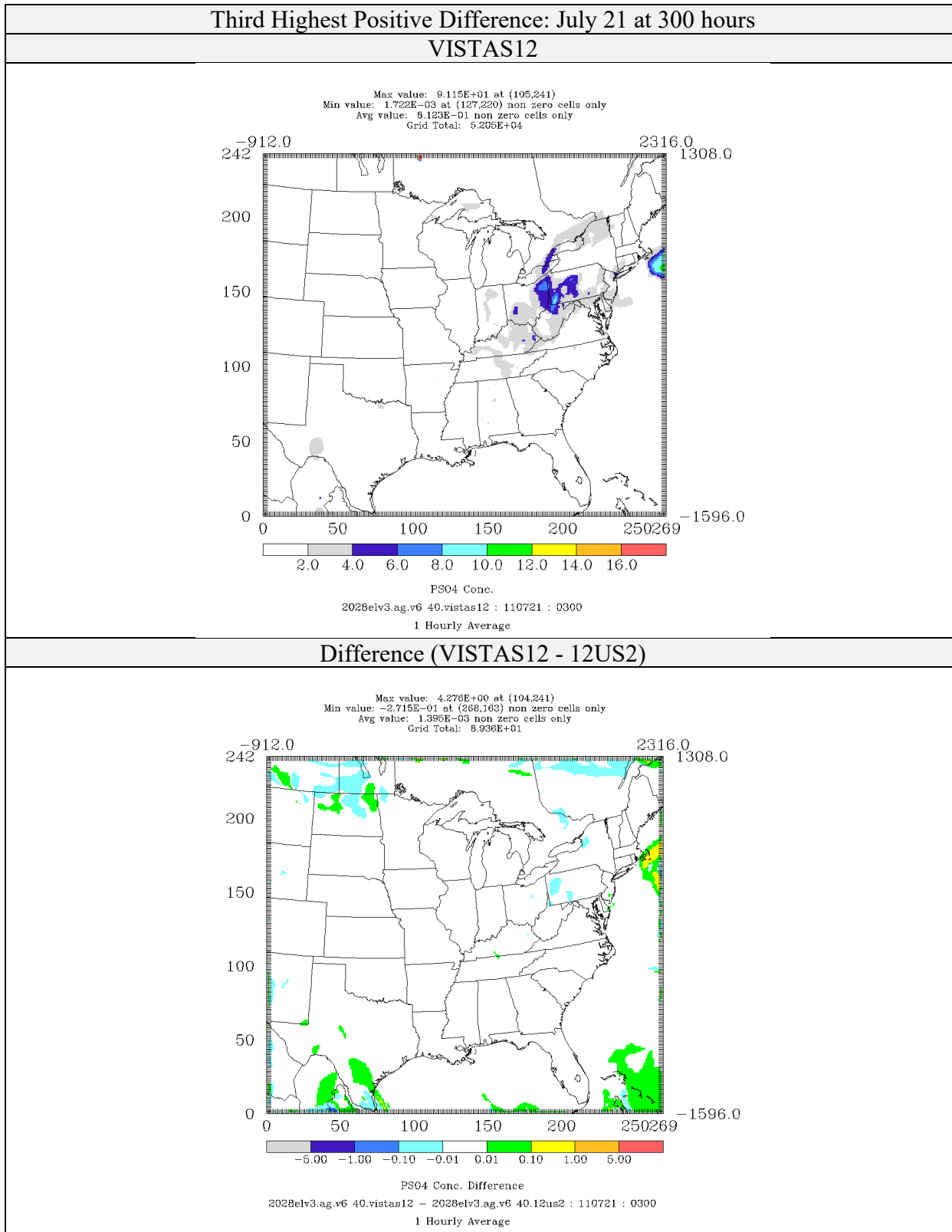


Figure 4-45: Comparison of Sulfate Concentrations ($\mu\text{g}/\text{m}^3$) for CAMx 6.40 on VISTAS12 and 12US2 Domains 2028elv3 Simulations (Third Highest Positive Difference)

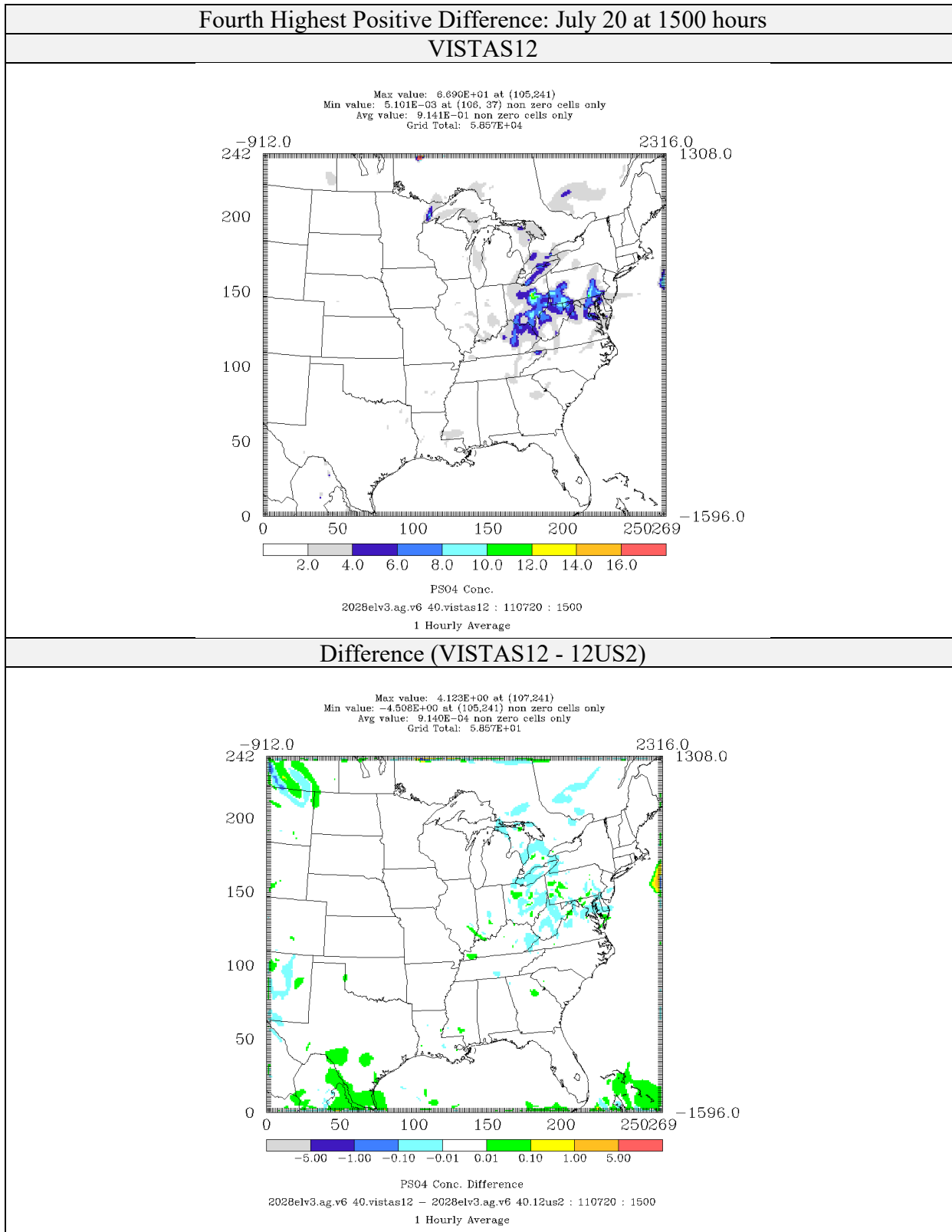


Figure 4-46: Comparison of Sulfate Concentrations ($\mu\text{g}/\text{m}^3$) for CAMx 6.40 on VISTAS12 and 12US2 Domains 2028elv3 Simulations (Fourth Highest Positive Difference)

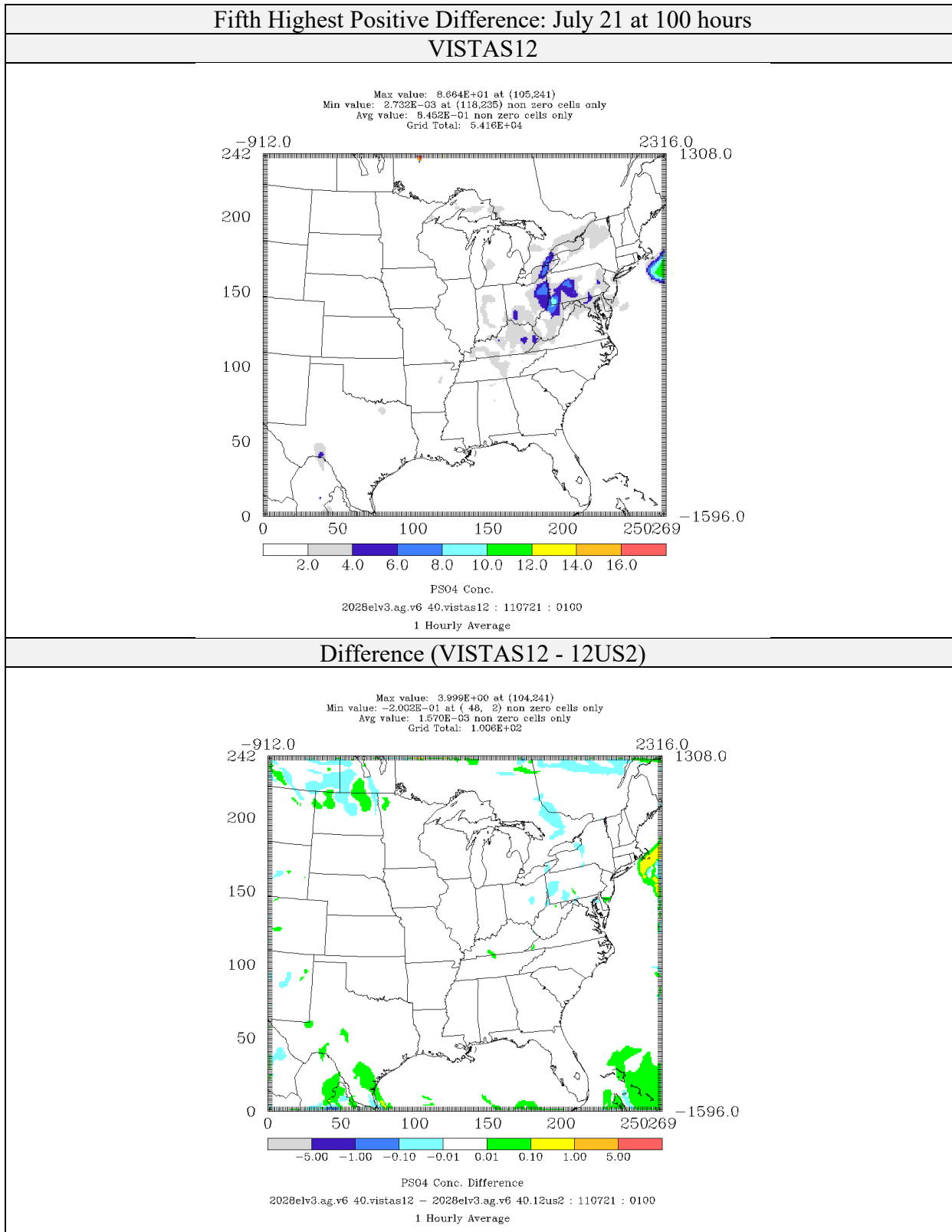


Figure 4-47: Comparison of Sulfate Concentrations ($\mu\text{g}/\text{m}^3$) for CAMx 6.40 on VISTAS12 and 12US2 Domains 2028elv3 Simulations (Fifth Highest Positive Difference)

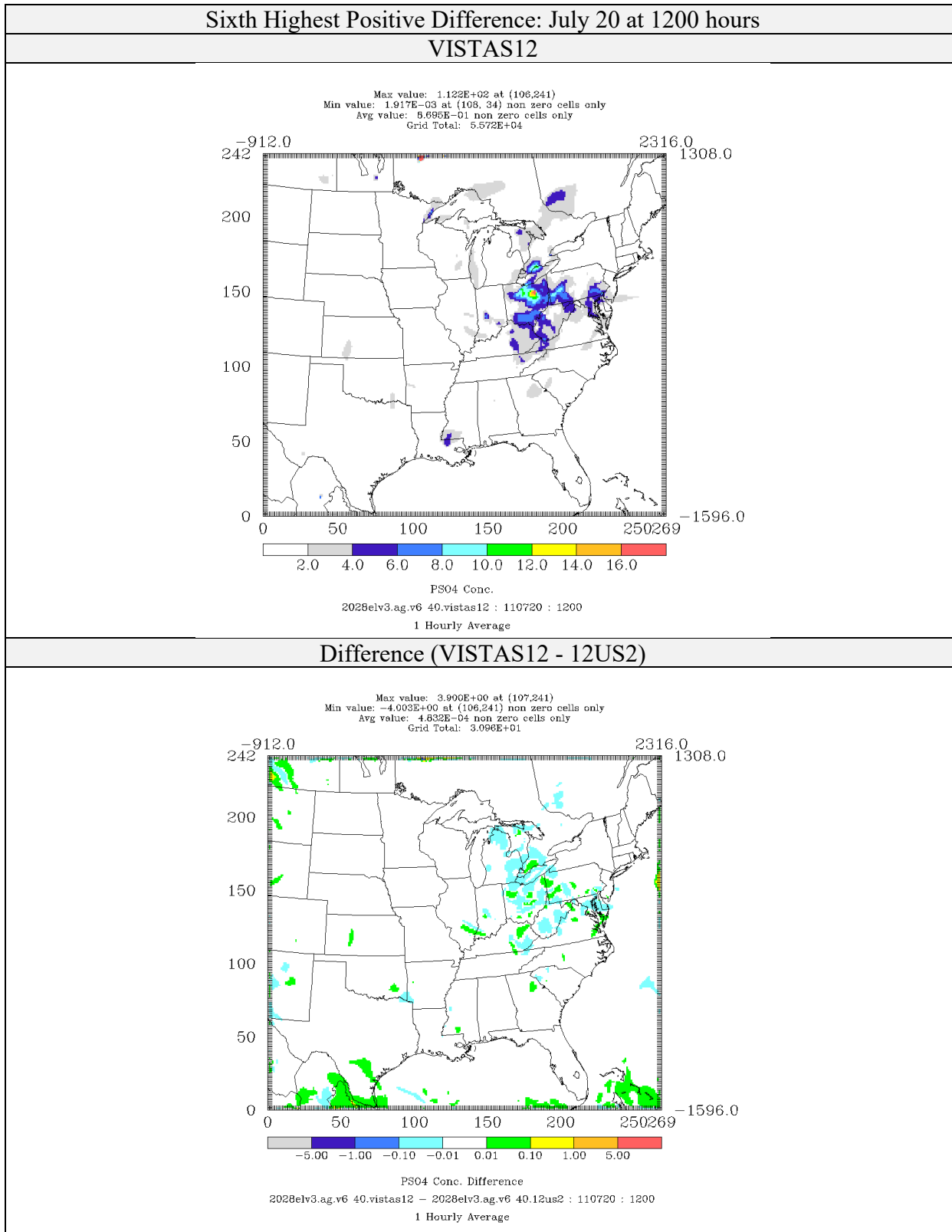


Figure 4-48: Comparison of Sulfate Concentrations ($\mu\text{g}/\text{m}^3$) for CAMx 6.40 on VISTAS12 and 12US2 Domains 2028elv3 Simulations (Sixth Highest Positive Difference)

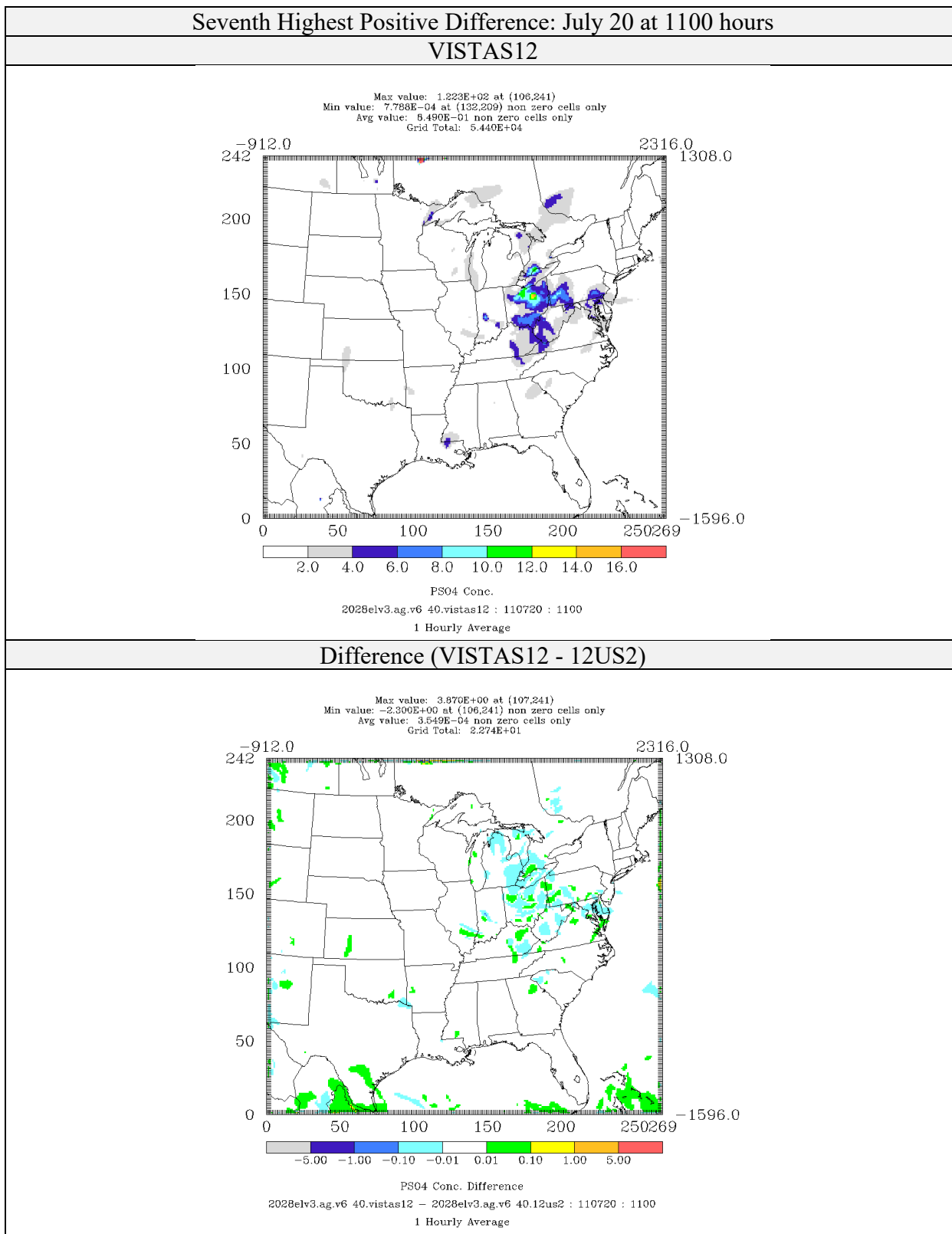


Figure 4-49: Comparison of Sulfate Concentrations ($\mu\text{g}/\text{m}^3$) for CAMx 6.40 on VISTAS12 and 12US2 Domains 2028elv3 Simulations

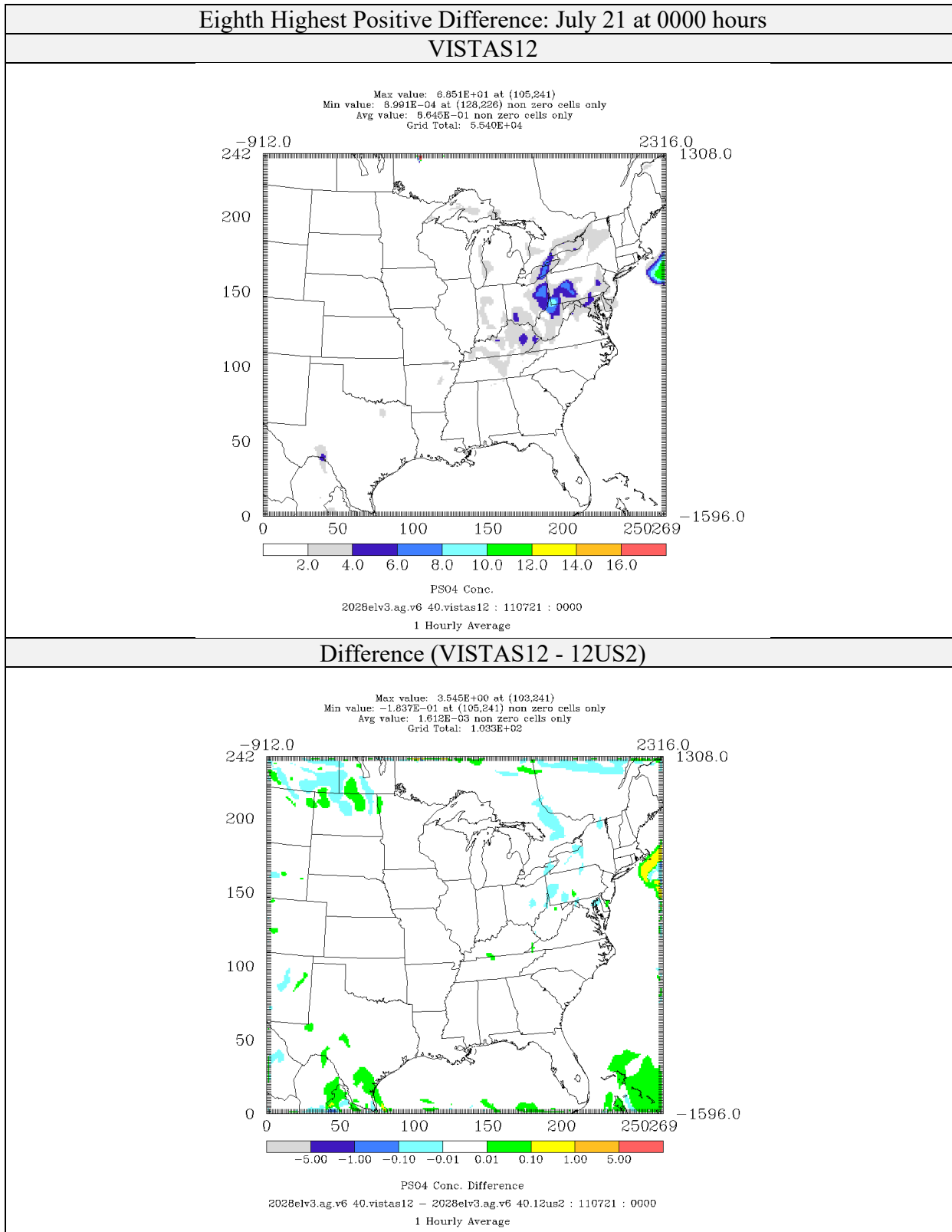


Figure 4-50: Comparison of Sulfate Concentrations ($\mu\text{g}/\text{m}^3$) for CAMx 6.40 on VISTAS12 and 12US2 Domains 2028elv3 Simulations (Eighth Highest Positive Difference)

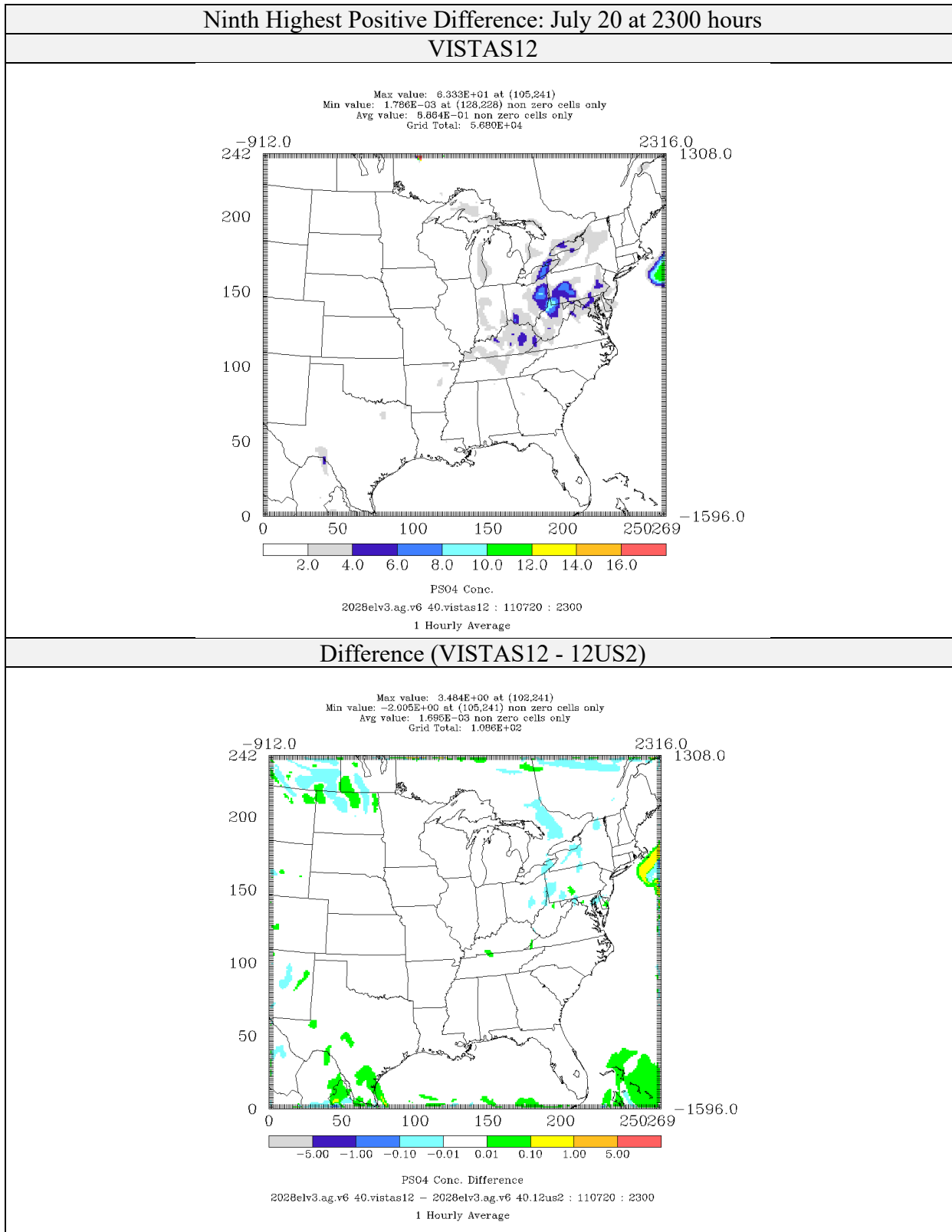


Figure 4-51: Comparison of Sulfate Concentrations ($\mu\text{g}/\text{m}^3$) for CAMx 6.40 on VISTAS12 and 12US2 Domains 2028elv3 Simulations (Ninth Highest Positive Difference)

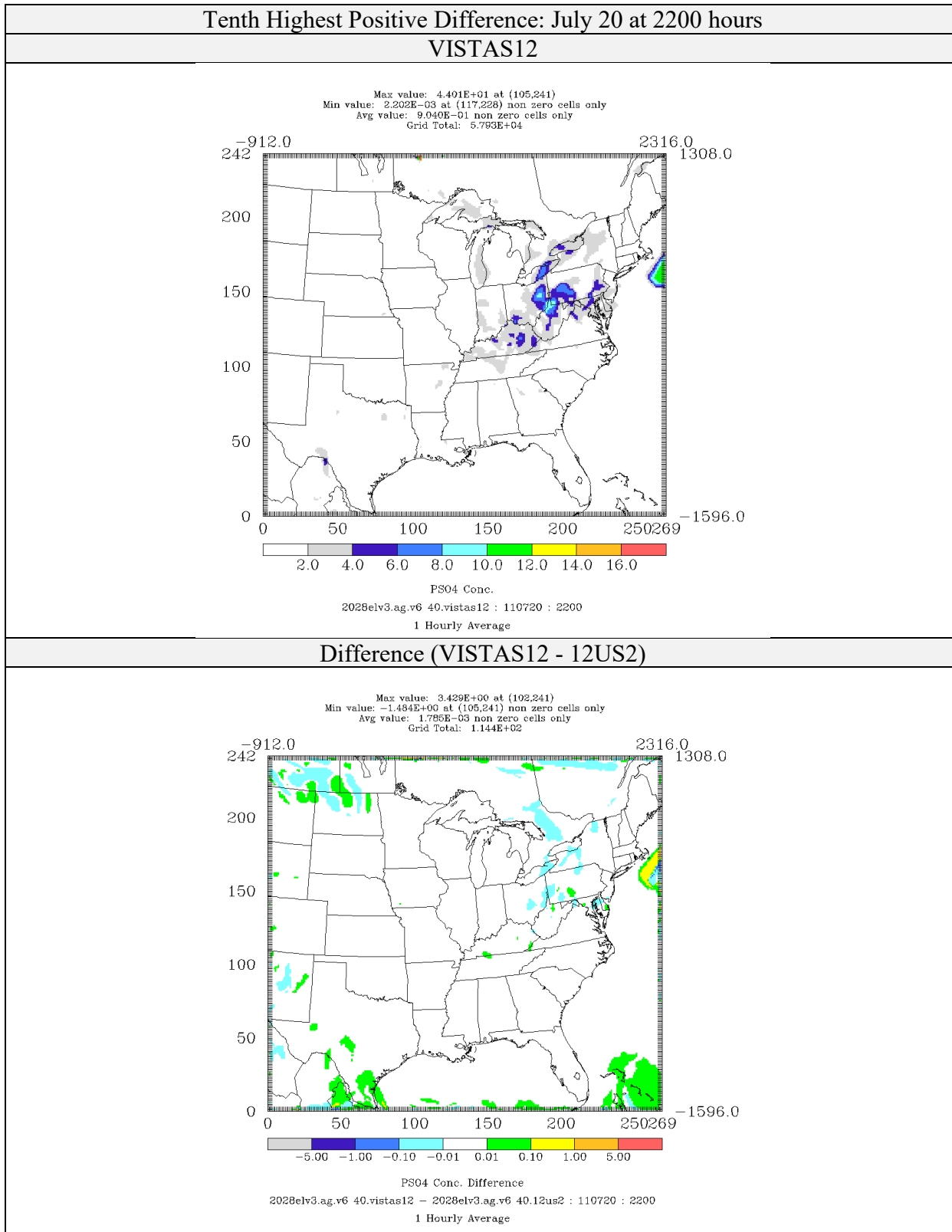


Figure 4-52: Comparison of Sulfate Concentrations ($\mu\text{g}/\text{m}^3$) for CAMx 6.40 on VISTAS12 and 12US2 Domains 2028elv3 Simulations (Tenth Highest Positive Difference)

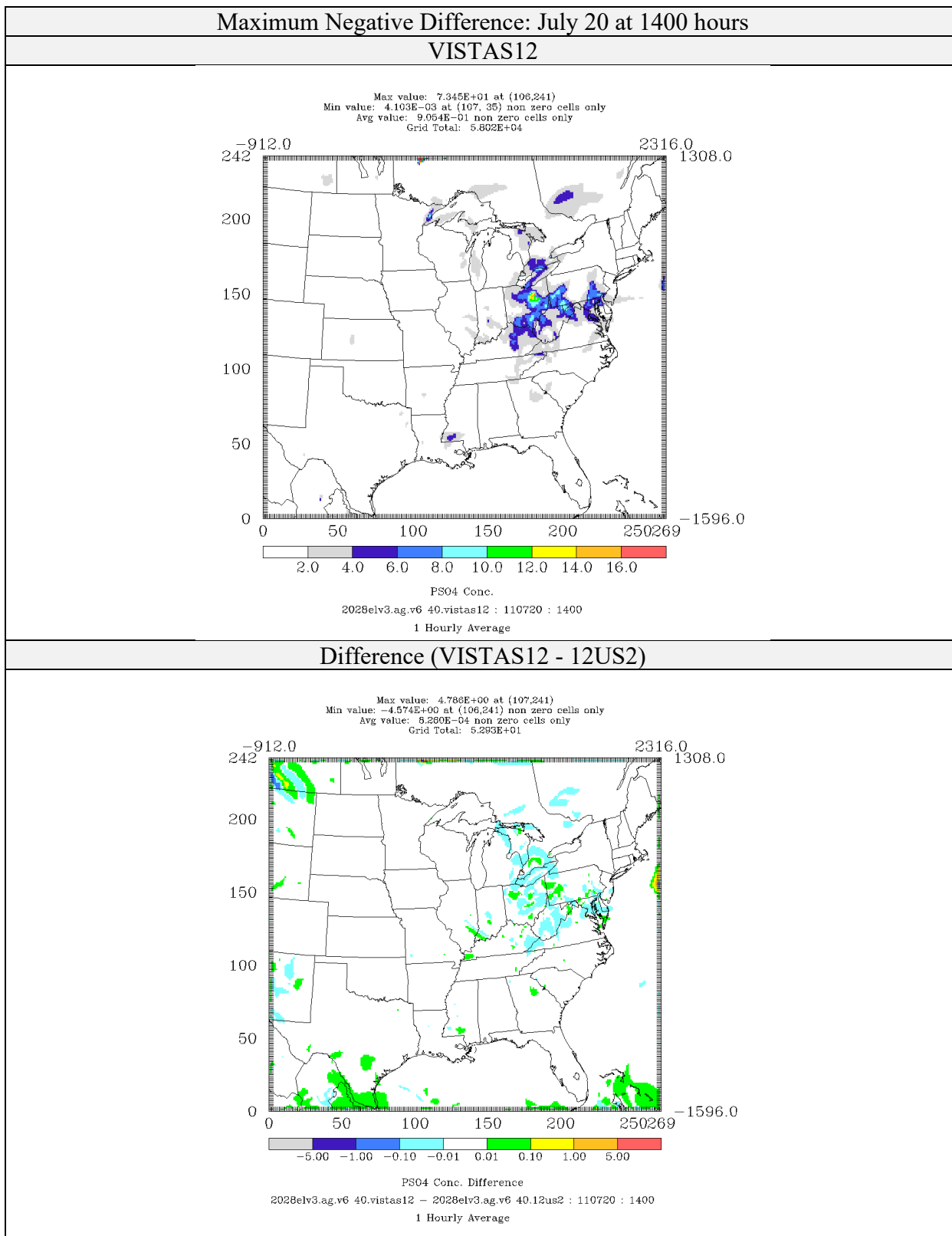


Figure 4-53: Comparison of Sulfate Concentrations ($\mu\text{g}/\text{m}^3$) for CAMx 6.40 on VISTAS12 and 12US2 Domains 2028elv3 Simulations (Maximum Negative Difference)

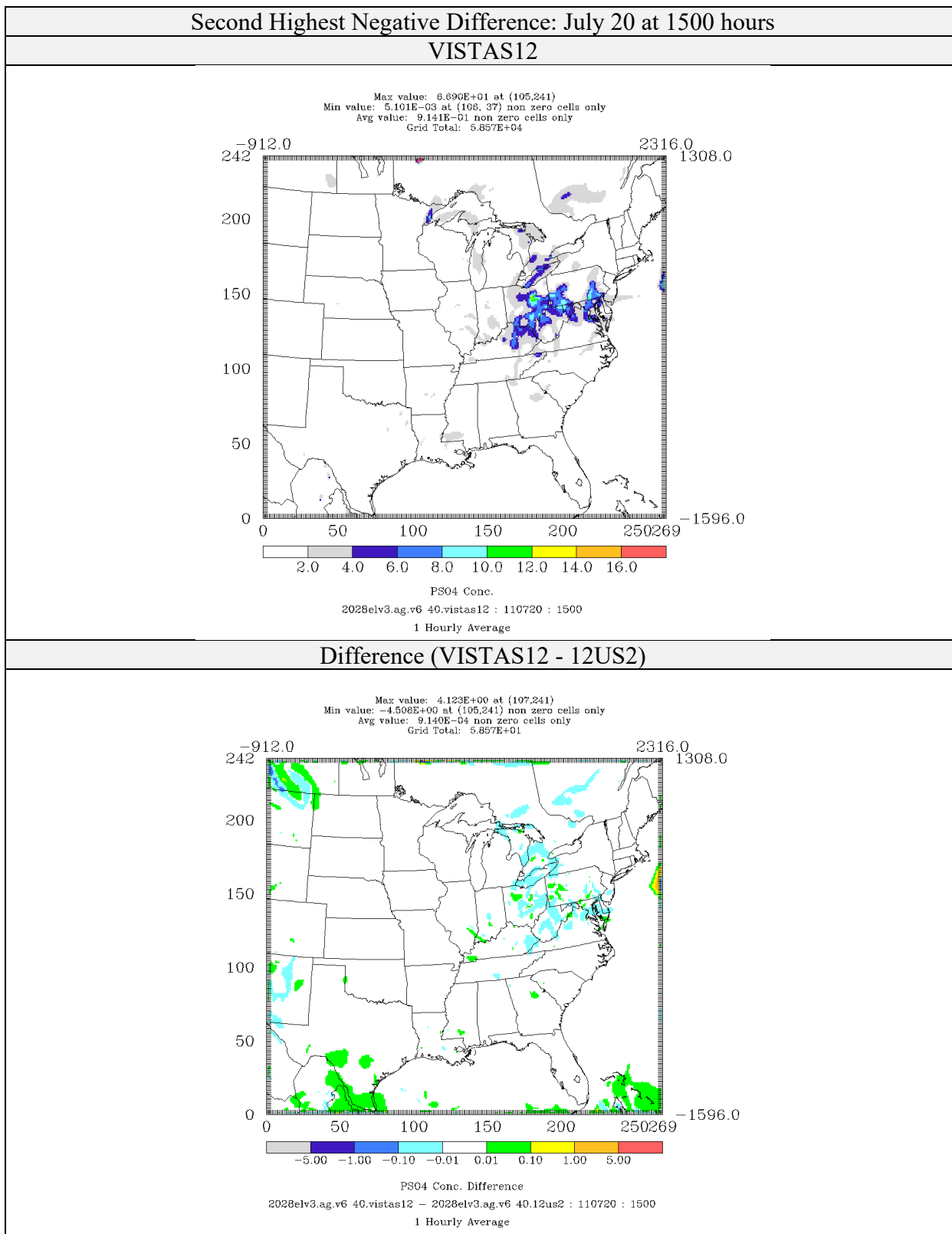


Figure 4-54: Comparison of Sulfate Concentrations ($\mu\text{g}/\text{m}^3$) for CAMx 6.40 on VISTAS12 and 12US2 Domains 2028elv3 Simulations (Second Highest Negative Difference)

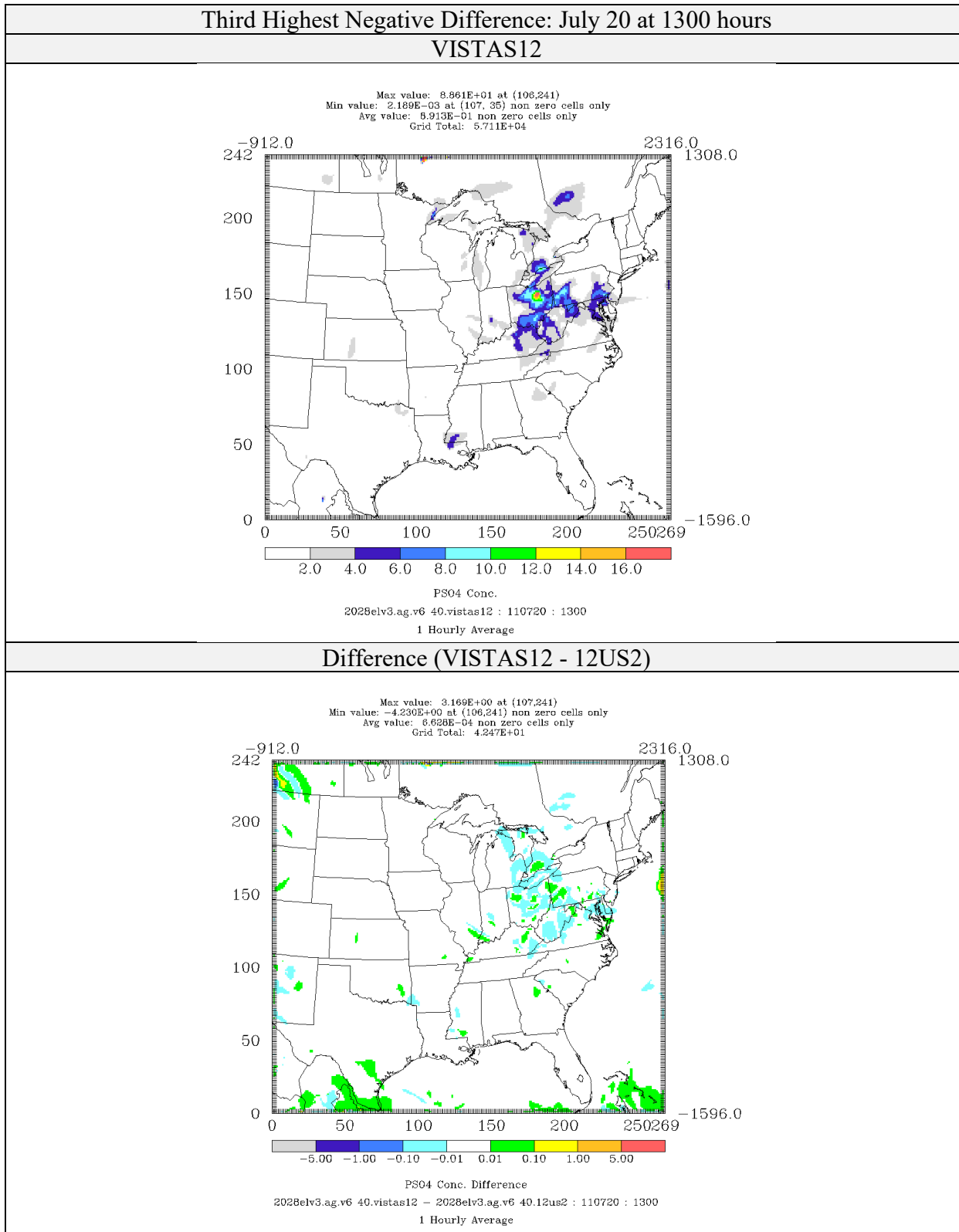


Figure 4-55: Comparison of Sulfate Concentrations ($\mu\text{g}/\text{m}^3$) for CAMx 6.40 on VISTAS12 and 12US2 Domains 2028elv3 Simulations (Third Highest Negative Difference)

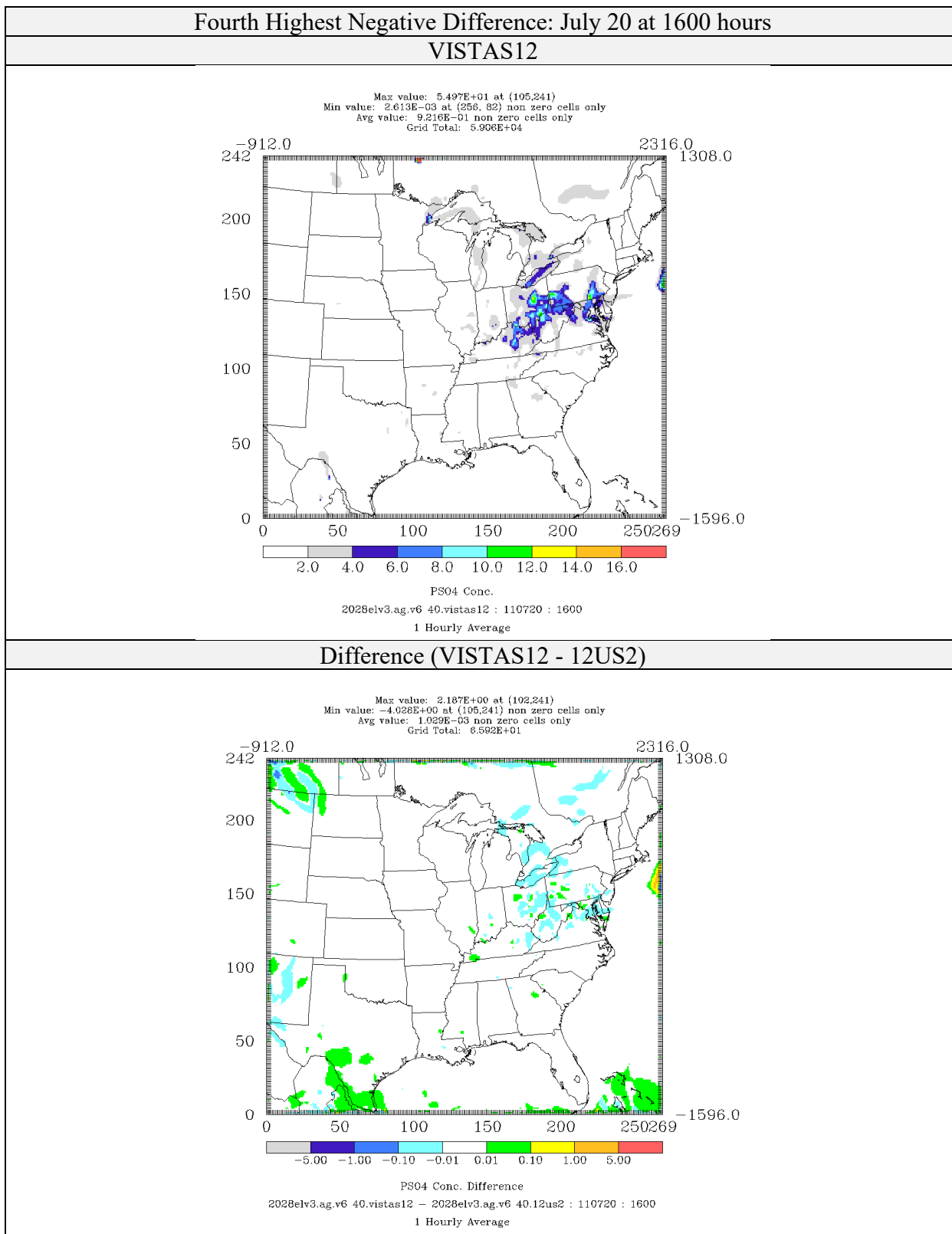


Figure 4-56: Comparison of Sulfate Concentrations ($\mu\text{g}/\text{m}^3$) for CAMx 6.40 on VISTAS12 and 12US2 Domains 2028elv3 Simulations (Fourth Highest Negative Difference)

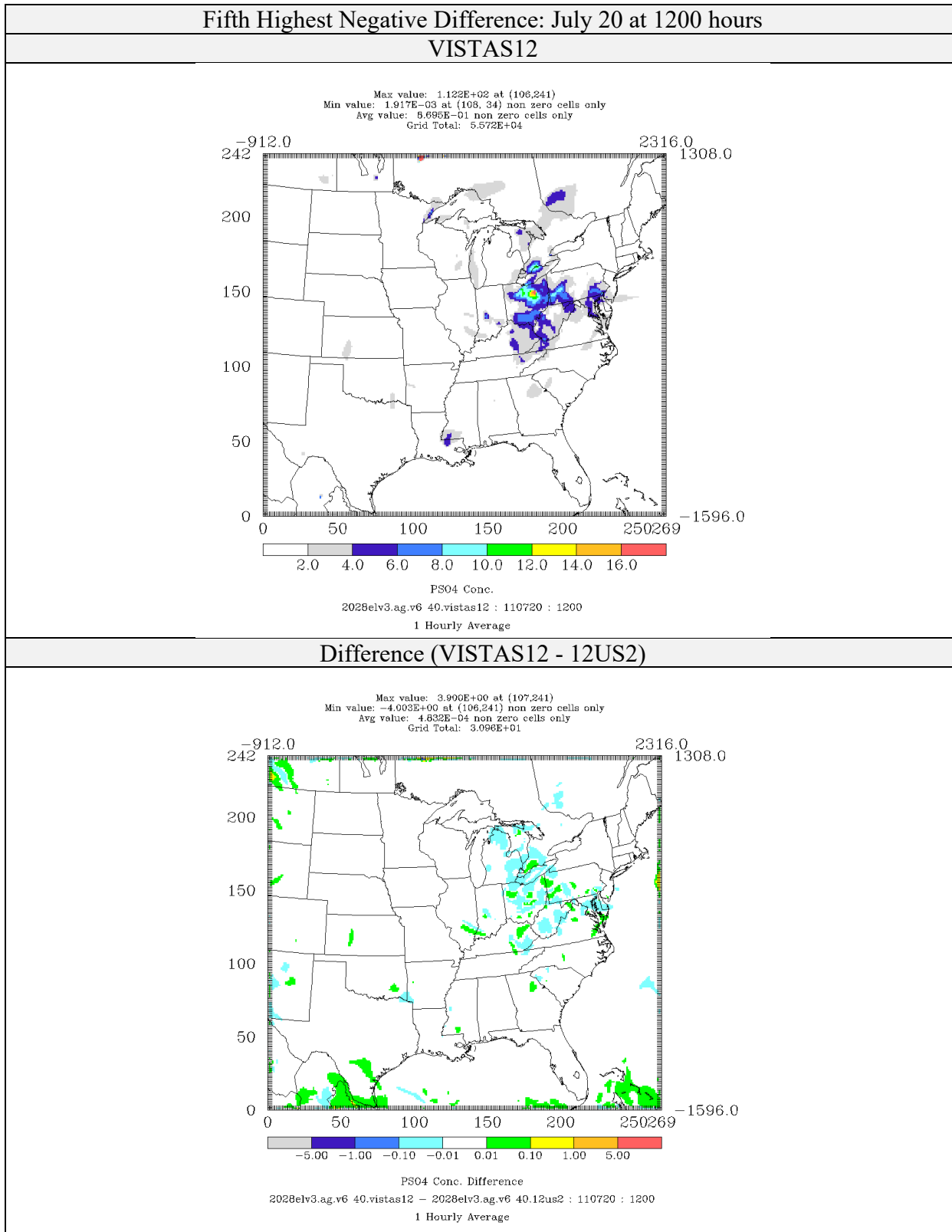


Figure 4-57: Comparison of Sulfate Concentrations ($\mu\text{g}/\text{m}^3$) for CAMx 6.40 on VISTAS12 and 12US2 Domains 2028elv3 Simulations (Fifth Highest Negative Difference)

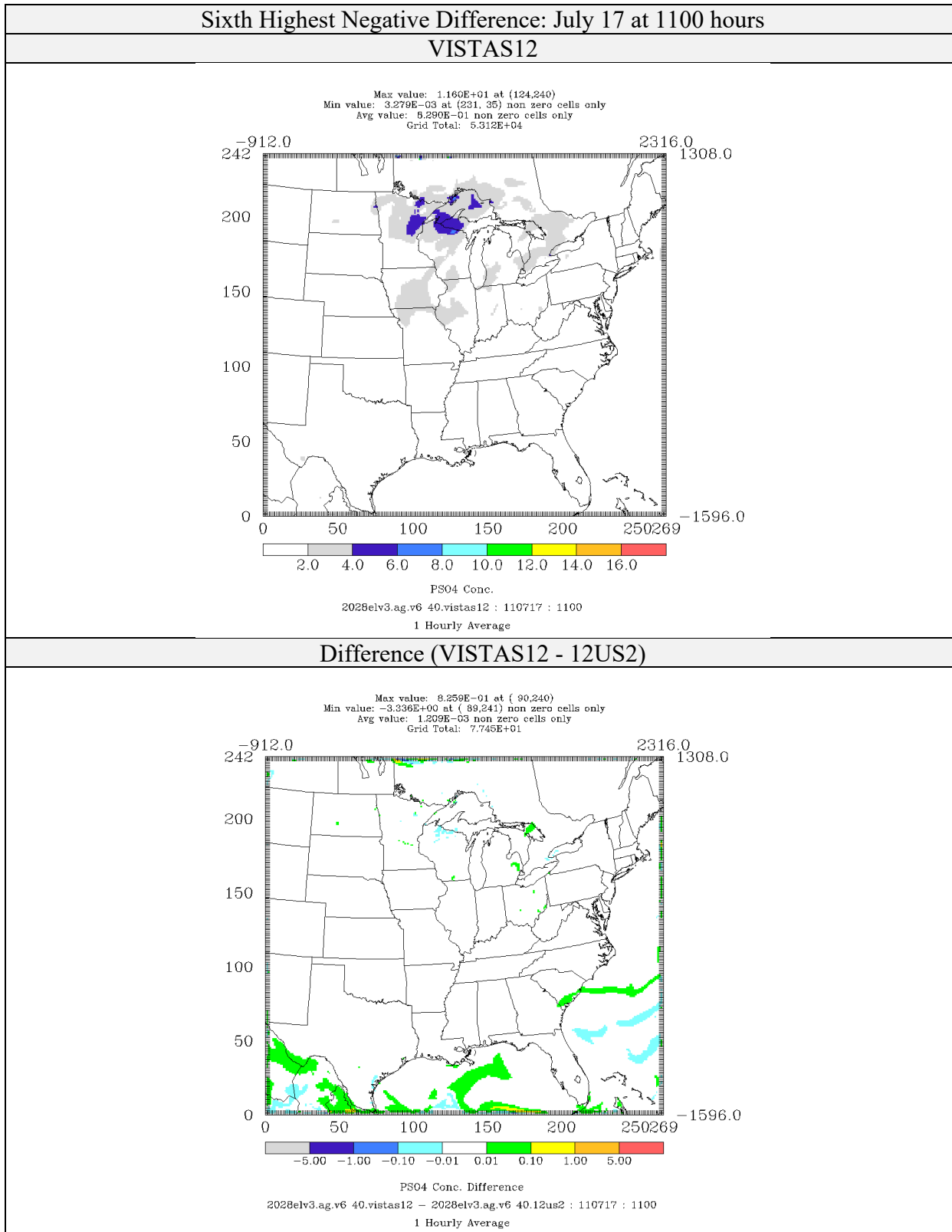


Figure 4-58: Comparison of Sulfate Concentrations ($\mu\text{g}/\text{m}^3$) for CAMx 6.40 on VISTAS12 and 12US2 Domains 2028elv3 Simulations (Sixth Highest Negative Difference)

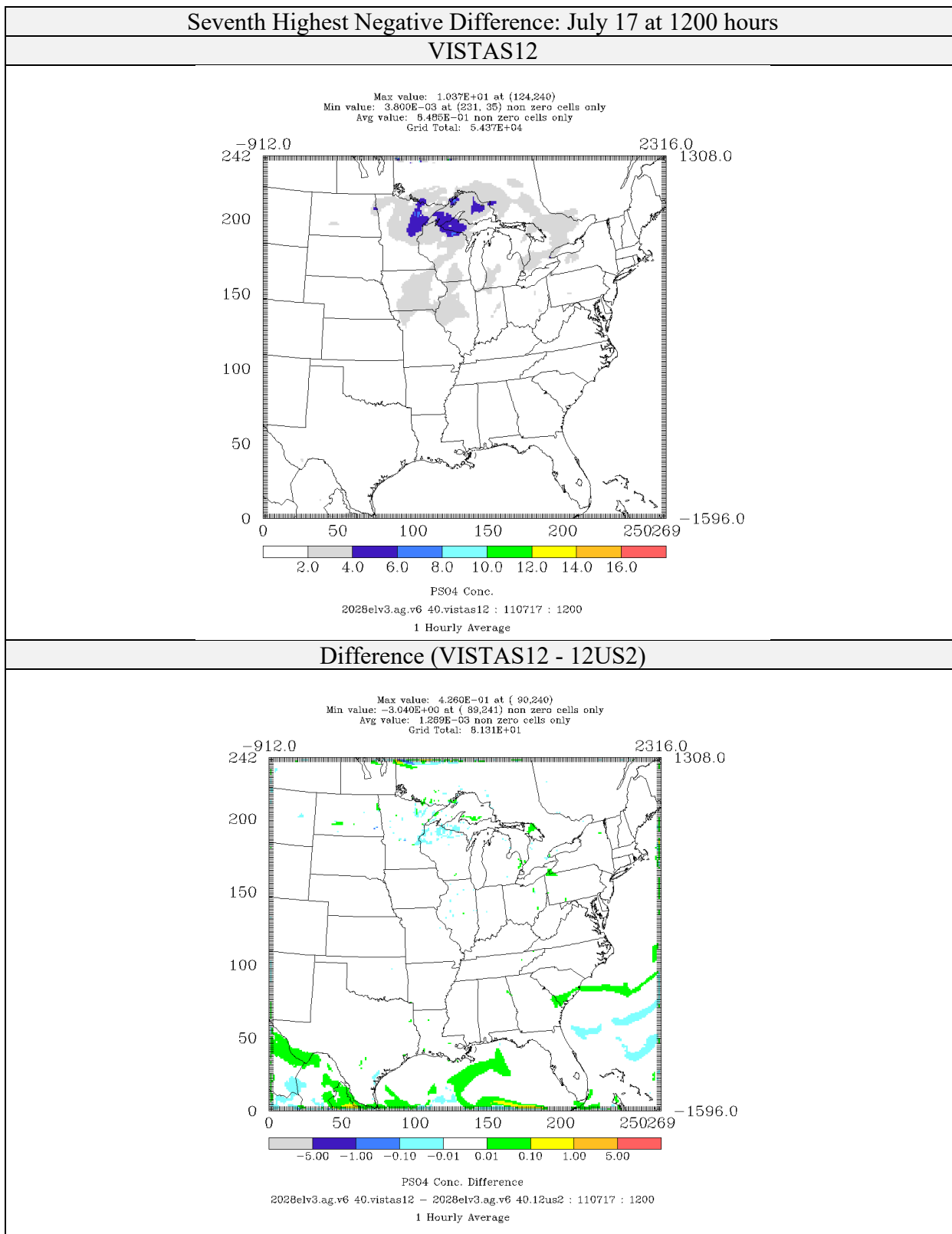


Figure 4-59: Comparison of Sulfate Concentrations ($\mu\text{g}/\text{m}^3$) for CAMx 6.40 on VISTAS12 and 12US2 Domains 2028elv3 Simulations (Seventh Highest Negative Difference)

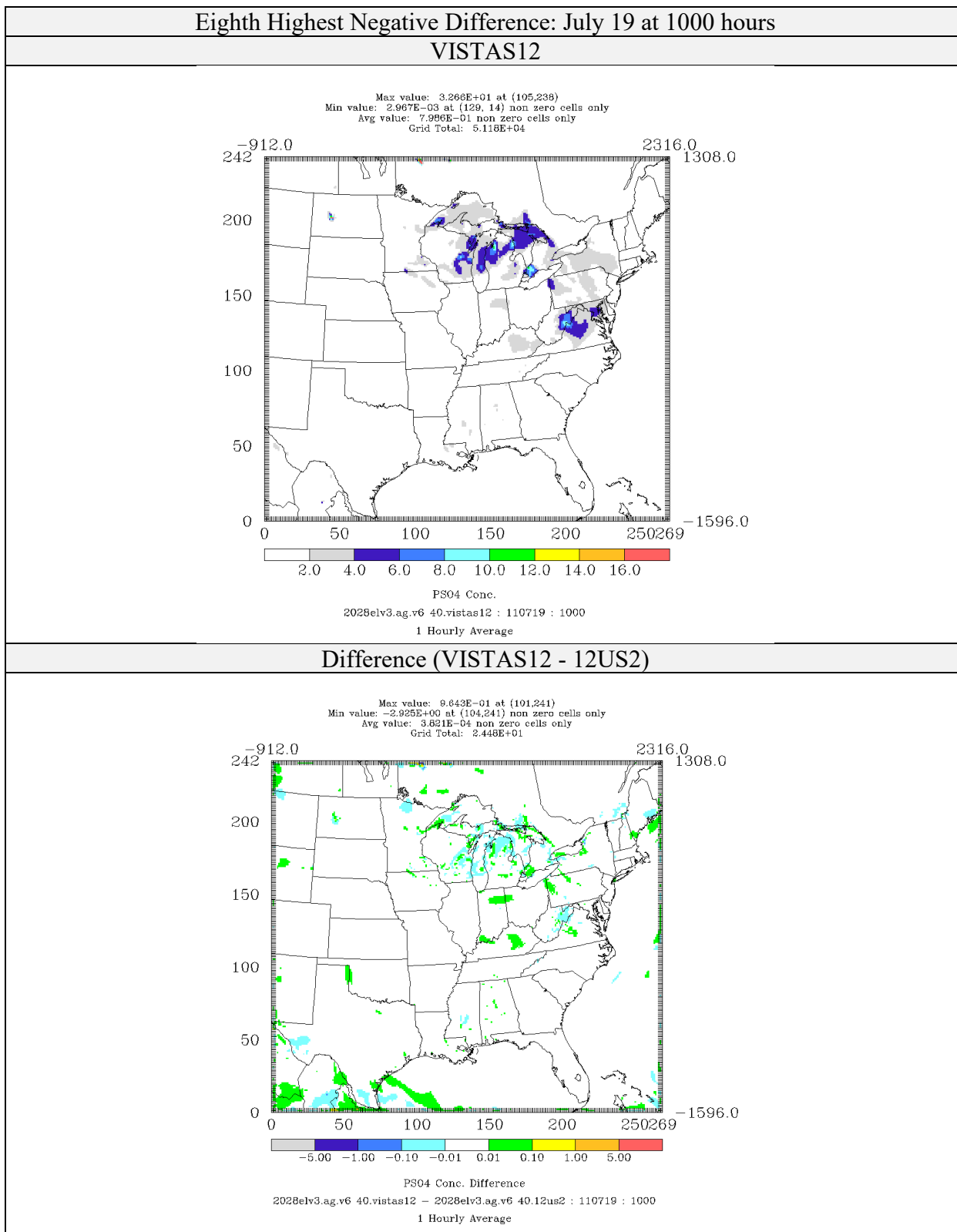


Figure 4-60: Comparison of Sulfate Concentrations ($\mu\text{g}/\text{m}^3$) for CAMx 6.40 on VISTAS12 and 12US2 Domains 2028elv3 Simulations (Eighth Highest Negative Difference)

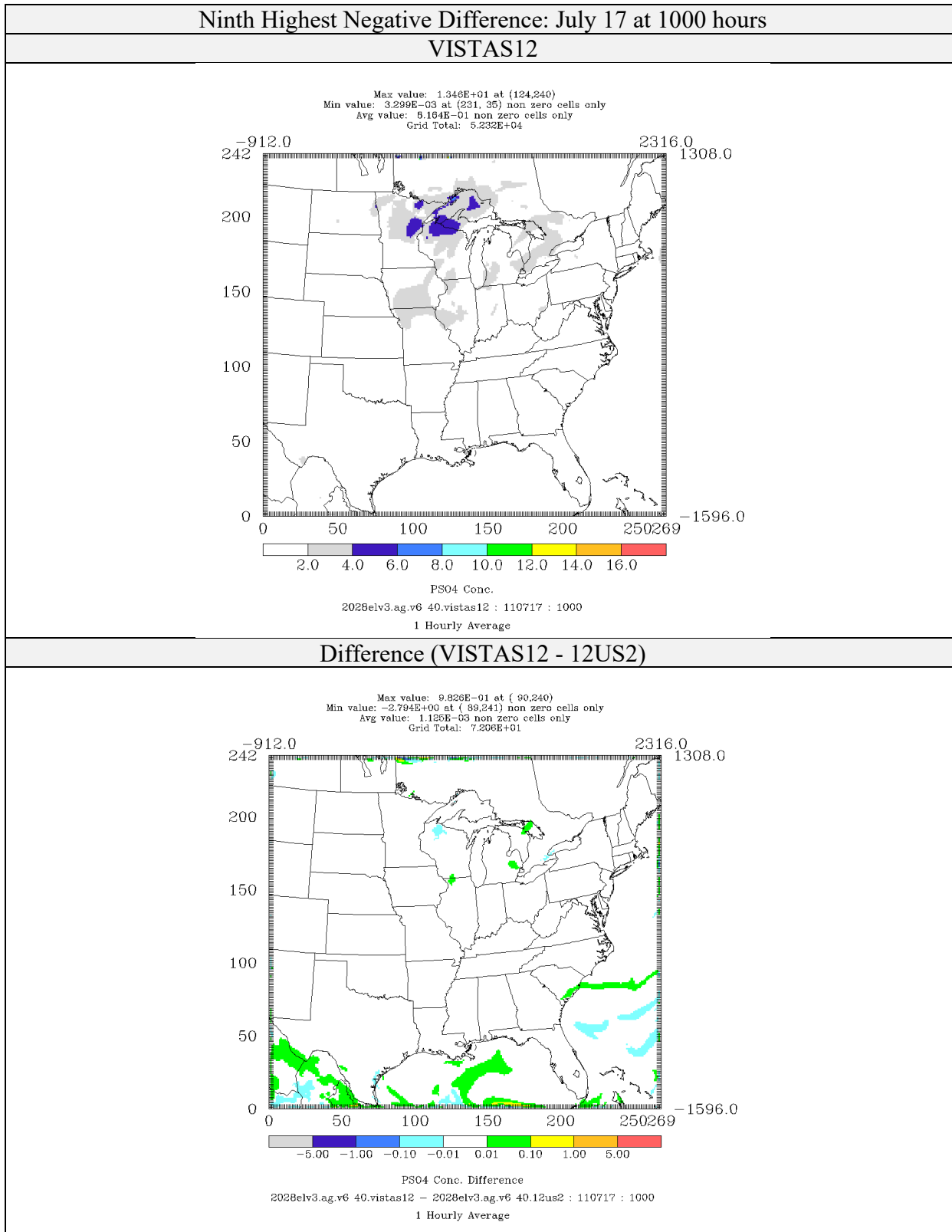


Figure 4-61: Comparison of Sulfate Concentrations ($\mu\text{g}/\text{m}^3$) for CAMx 6.40 on VISTAS12 and 12US2 Domains 2028elv3 Simulations (Ninth Highest Negative Difference)

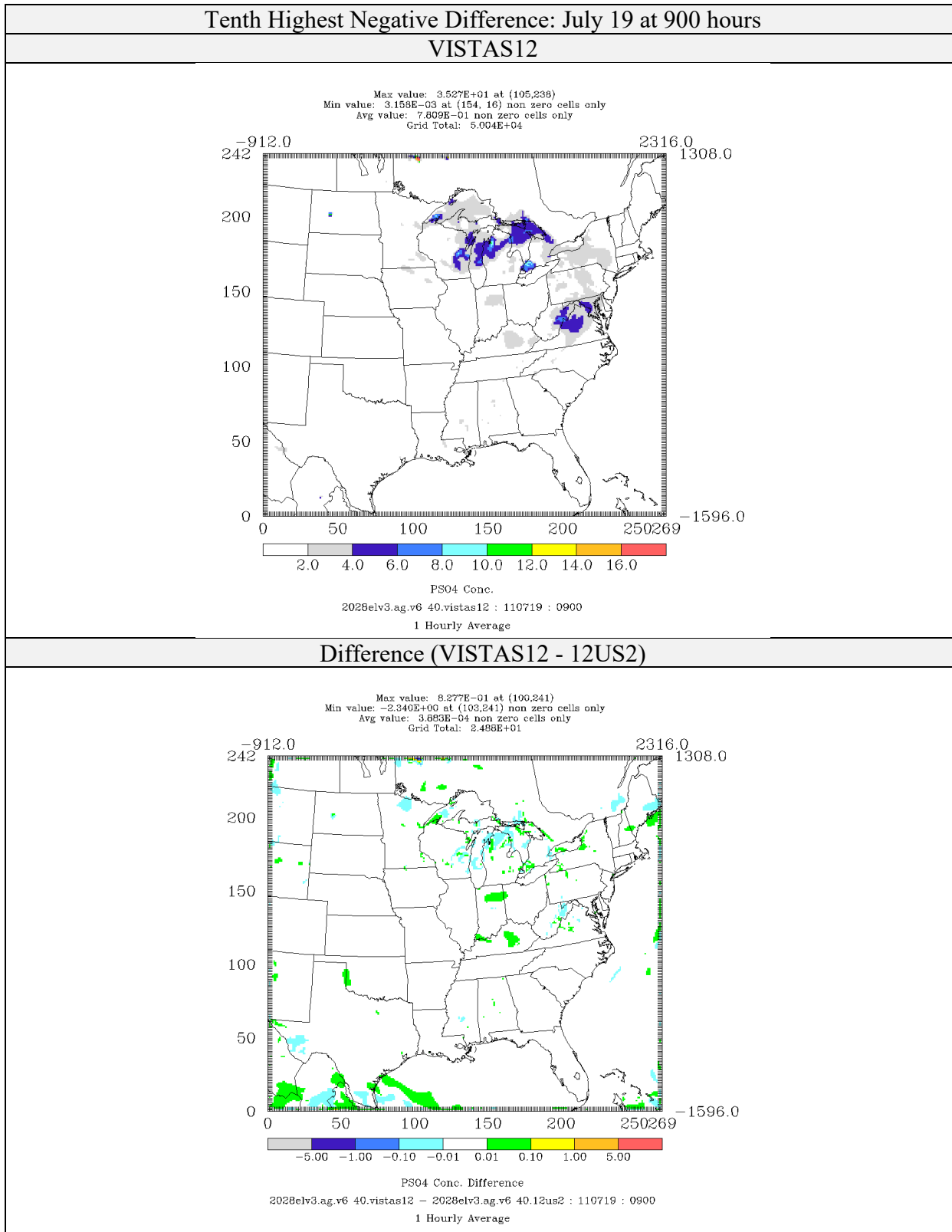


Figure 4-62: Comparison of Sulfate Concentrations ($\mu\text{g}/\text{m}^3$) for CAMx 6.40 on VISTAS12 and 12US2 Domains 2028elv3 Simulations (Tenth Highest Negative Difference)

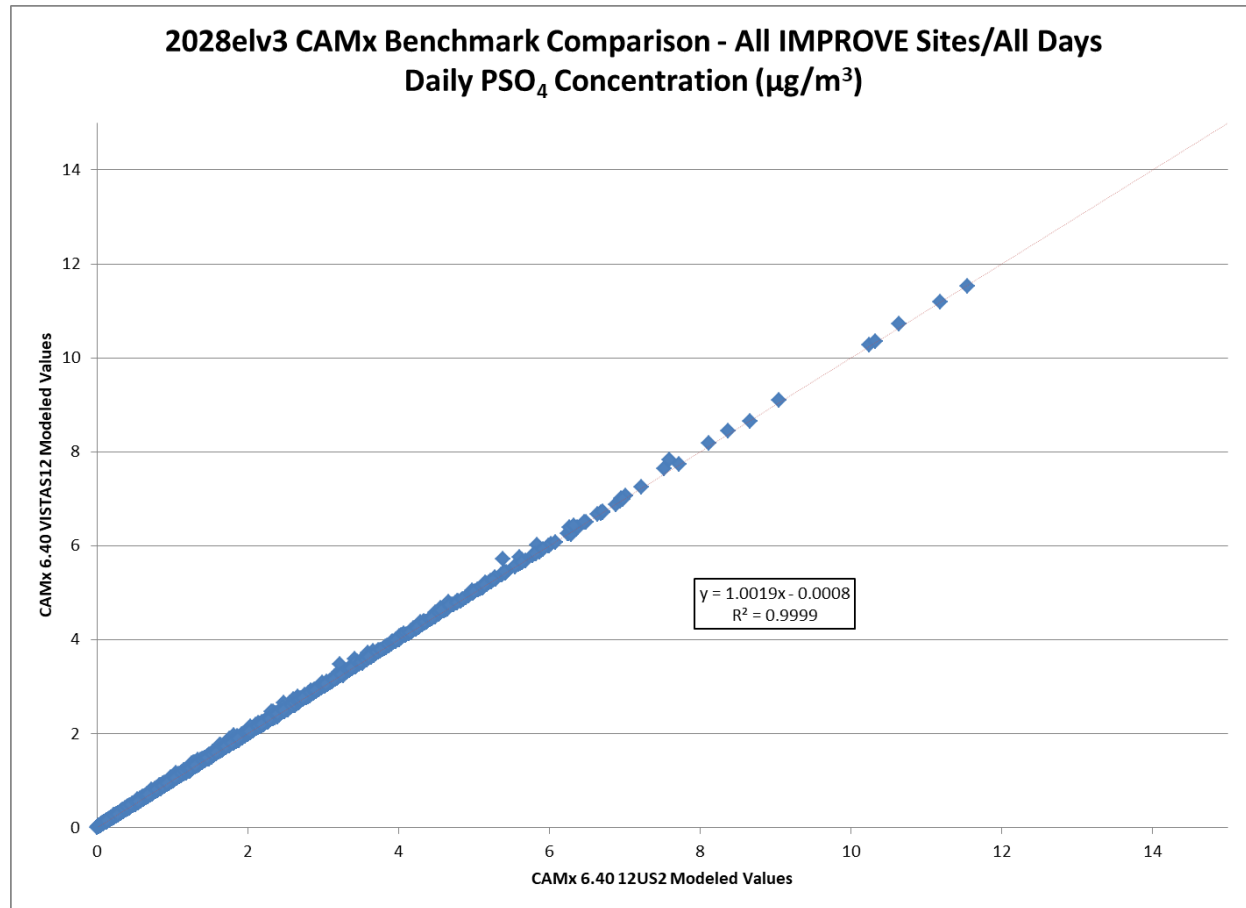


Figure 4-63: Scatterplot Comparing 24-hour Average Predicted Sulfate Concentrations ($\mu\text{g}/\text{m}^3$) for All Days at all IMPROVE Monitor Locations for CAMx 6.40 on VISTAS12 and 12US2 Domains 2028elv3 Simulations Performed by VISTAS (Alpine).

4.4 Nitrate

Nitrate results for the top 10 positive and negative hours are presented in tabular format in Table 4-4. The maximum positive difference is $7.21 \mu\text{g}/\text{m}^3$ falling to $4.22 \mu\text{g}/\text{m}^3$ for the 10th high. The maximum negative difference is $-4.63 \mu\text{g}/\text{m}^3$ falling to $-2.96 \mu\text{g}/\text{m}^3$ for the 10th high. The maximum positive percent difference from these days is 130.1% and negative percent difference of -49.2%.

As expected, the maximum impacts on the top 10 positive and negative hours are occurring very near the border. As was described in Section 2, the two CAMx simulations used the same input data, except that the pollutant concentrations on in-flow boundary cells. For the simulation on the VISTAS12 domain the in-flow concentrations are specified in hourly boundary conditions extracted from the 12US2 simulation. For the 12US2 simulation the in-flow concentrations were continuously updated from the cells outside the VISTAS12 domain. It would be expected that concentration differences would occur from the differences in hourly average concentrations, versus in the instantaneous concentrations.

The top 10 positive difference hours are presented in Figures 4-64 through 4-73 and the top 10 negative difference hours are presented in Figures 4-74 through 4-83. The peak differences are generally occurring on January 3, July 17 and July 20. On January 3 the area of the difference is generally in the north western portion of the domain in an area of a plume entering the domain from Canada. On July 20 the differences are along the northern border, north of Minnesota.

Scatterplots of the daily average nitrate concentrations in local standard time at the IMPROVE monitors are presented in Figure 4-83. The 12US2 results are plotted on the x-axis and the VISTAS12 results are plotted on the y-axis. The data has a high degree of correlation with a line of best fit with a slope of 0.9996, an intercept of $0.0006 \mu\text{g}/\text{m}^3$ and an R^2 of 1.0000.

Examination of the difference animations often show differences along the boundary becoming lower as the plumes along the boundary move into the domain.

Table 4-4. Comparison of 2028elv3 CAMx 6.40 VISTAS12 and 12US2 Simulation of Nitrate Concentrations ($\mu\text{g}/\text{m}^3$). Hours with the top 10 maximum positive and maximum negative differences are shown.

Year	Month	Day	Hour	VISTAS12 Conc.	12US2 Conc.	Difference ($\mu\text{g}/\text{m}^3$)	Percent Difference	Column	Row
Maximum Positive									
2011	1	3	7	26.59	19.38	7.21	37.2%	32	235
2011	1	3	6	26.46	19.29	7.16	37.1%	32	235
2011	1	3	5	26.34	19.24	7.10	36.9%	32	235
2011	7	20	20	10.58	4.60	5.98	130.1%	99	241
2011	1	3	10	27.68	21.79	5.89	27.0%	33	235
2011	1	3	8	26.83	21.02	5.81	27.6%	32	235
2011	7	20	15	25.48	20.00	5.47	27.4%	107	241
2011	1	3	4	26.62	21.41	5.21	24.3%	32	235
2011	1	3	12	20.45	15.87	4.59	28.9%	16	241
2011	7	20	19	14.19	9.98	4.22	42.3%	99	241
Maximum Negative									
2011	1	3	8	18.88	23.51	-4.63	-19.7%	33	233
2011	7	17	15	4.64	9.14	-4.49	-49.2%	90	241
2011	1	3	7	18.28	22.49	-4.21	-18.7%	33	233
2011	7	17	14	9.10	13.25	-4.15	-31.3%	90	241
2011	1	27	10	3.73	7.31	-3.58	-49.0%	224	241
2011	1	3	10	24.33	27.81	-3.48	-12.5%	30	233
2011	1	3	12	16.46	19.80	-3.33	-16.8%	13	240
2011	1	27	11	3.62	6.74	-3.12	-46.3%	224	241
2011	1	3	9	21.84	24.86	-3.02	-12.2%	33	234
2011	7	17	16	2.29	5.25	-2.96	-56.4%	91	241

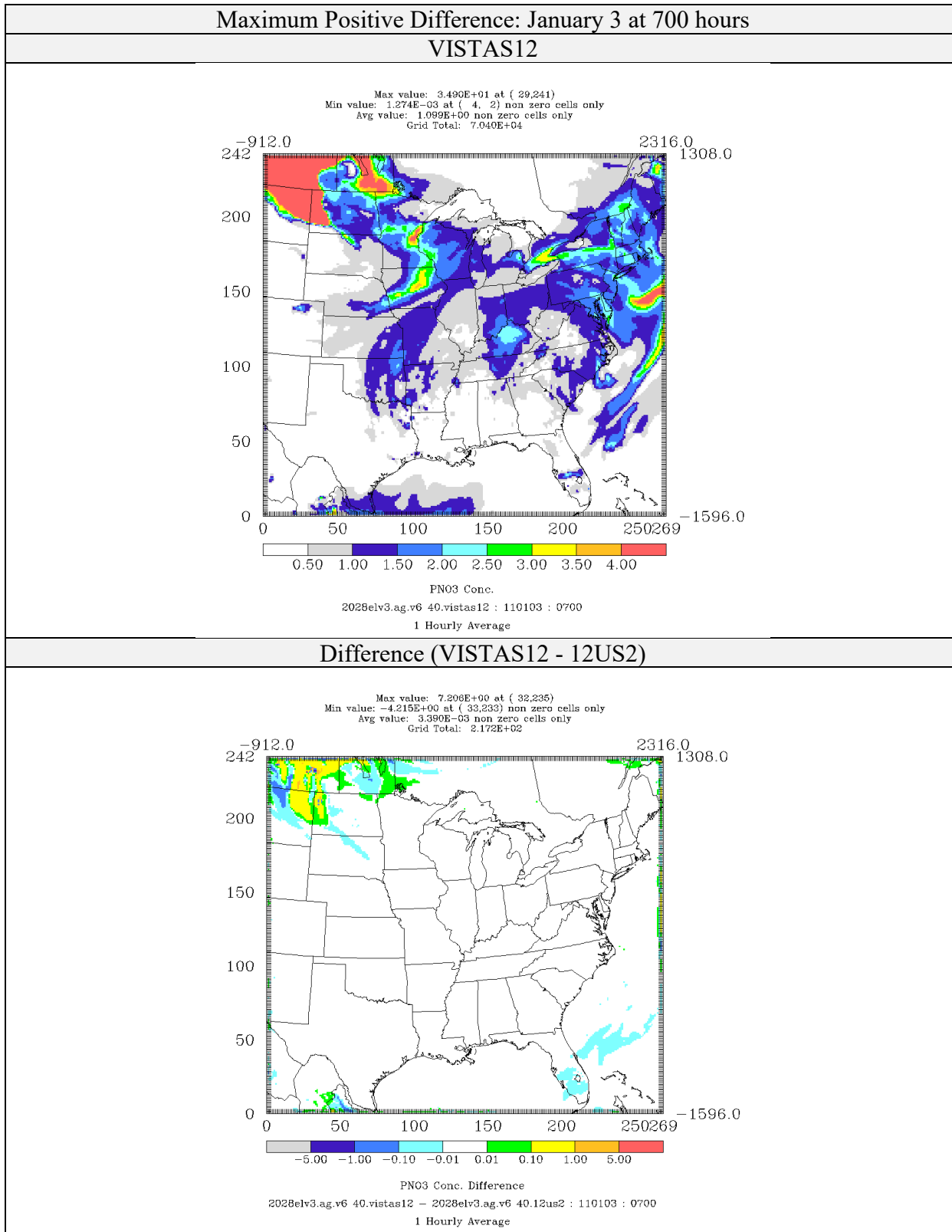


Figure 4-64: Comparison of Nitrate Concentrations ($\mu\text{g}/\text{m}^3$) for CAMx 6.40 on VISTAS12 and 12US2 Domains 2028elv3 Simulations (Maximum Positive Difference)

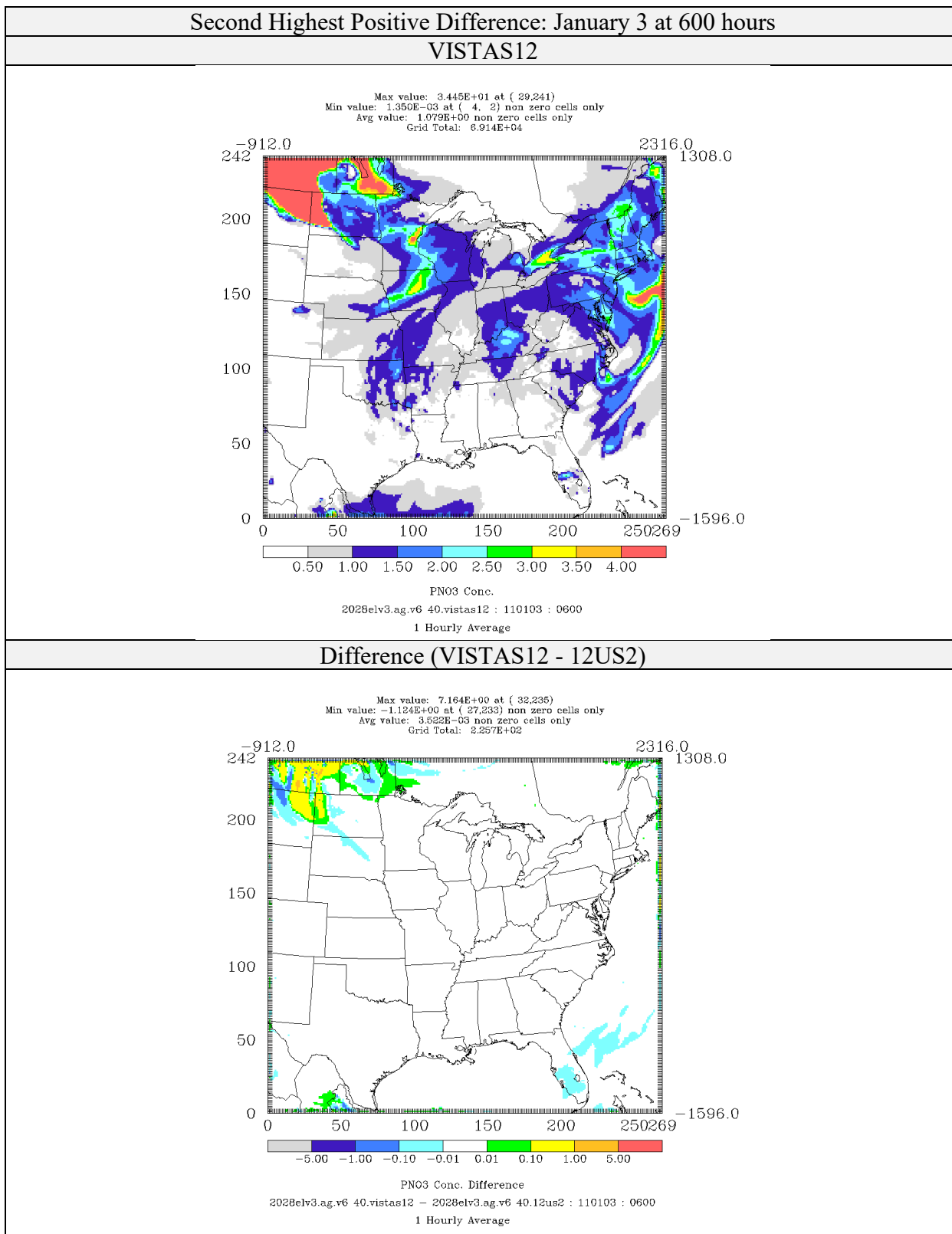


Figure 4-65: Comparison of Nitrate Concentrations ($\mu\text{g}/\text{m}^3$) for CAMx 6.40 on VISTAS12 and 12US2 Domains 2028elv3 Simulations (Second Highest Positive Difference)

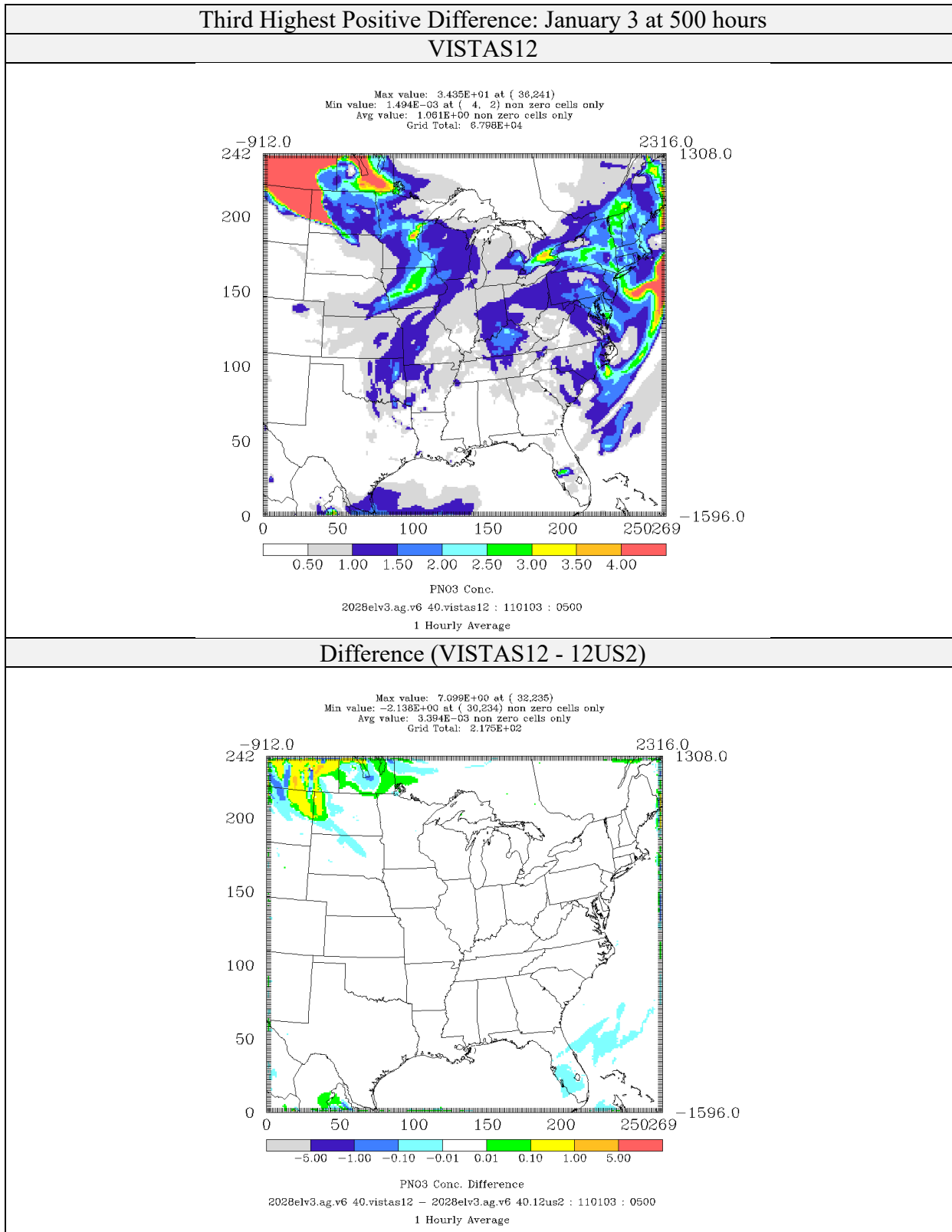


Figure 4-66: Comparison of Nitrate Concentrations ($\mu\text{g}/\text{m}^3$) for CAMx 6.40 on VISTAS12 and 12US2 Domains 2028elv3 Simulations (Third Highest Positive Difference)

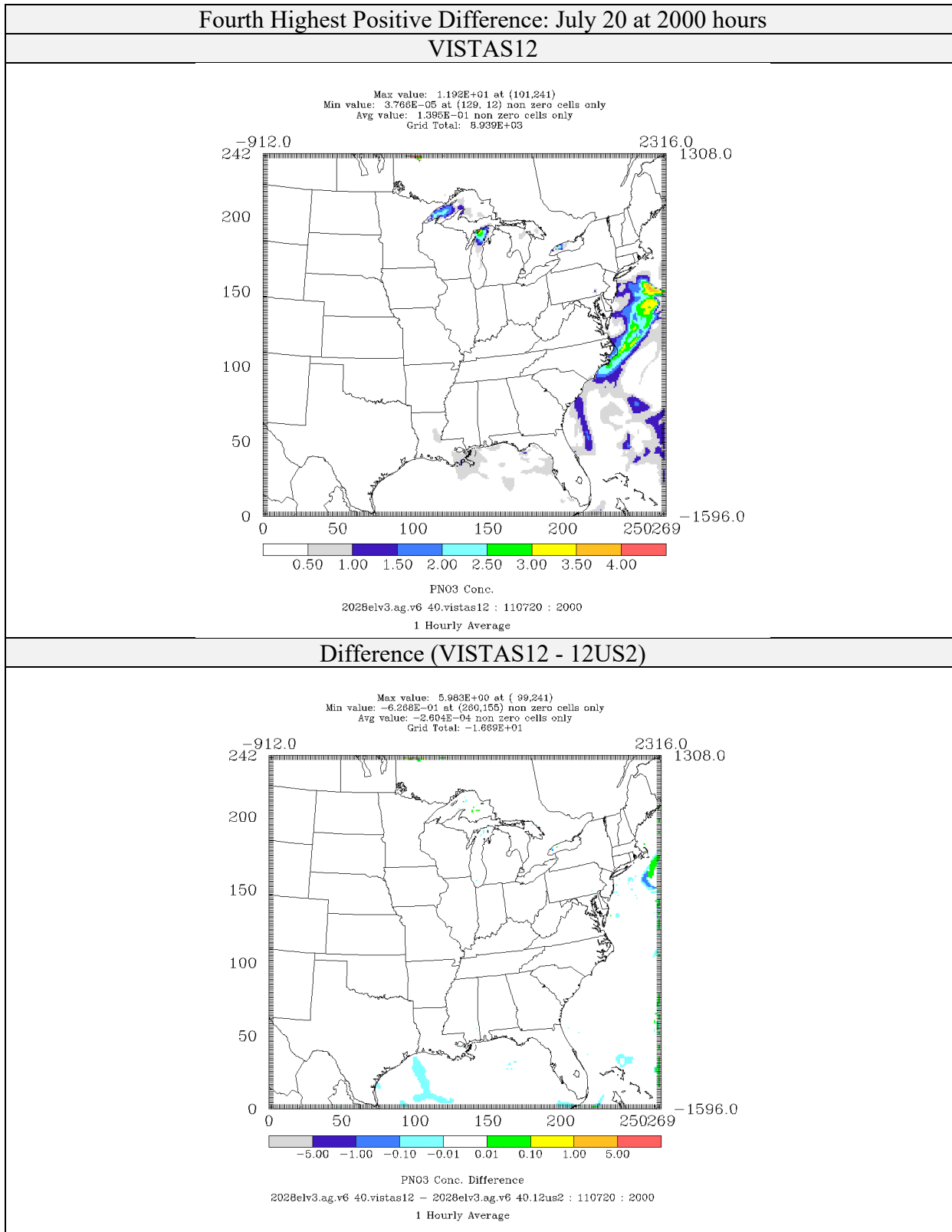


Figure 4-67: Comparison of Nitrate Concentrations ($\mu\text{g}/\text{m}^3$) for CAMx 6.40 on VISTAS12 and 12US2 Domains 2028elv3 Simulations (Fourth Highest Positive Difference)

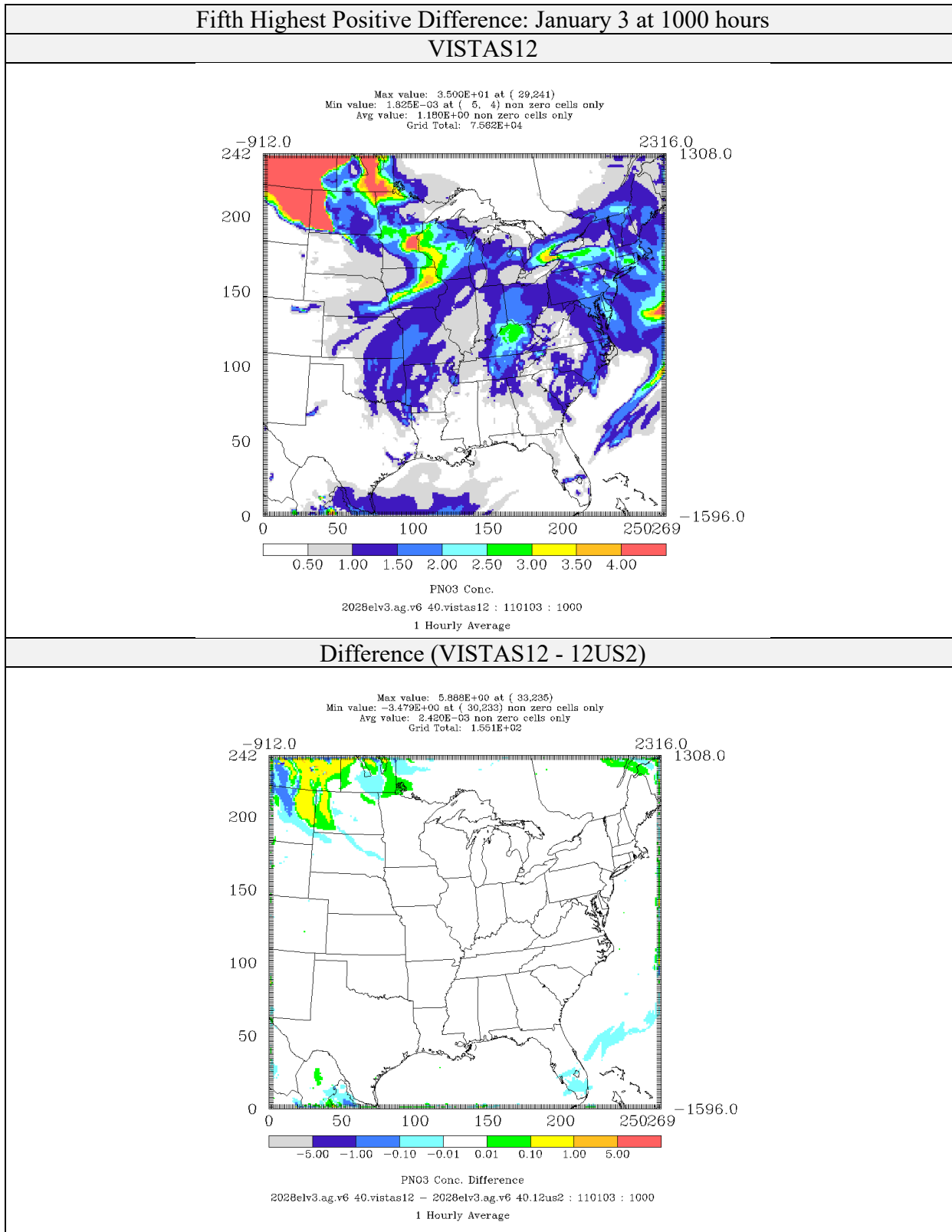


Figure 4-68: Comparison of Nitrate Concentrations ($\mu\text{g}/\text{m}^3$) for CAMx 6.40 on VISTAS12 and 12US2 Domains 2028elv3 Simulations (Fifth Highest Positive Difference)

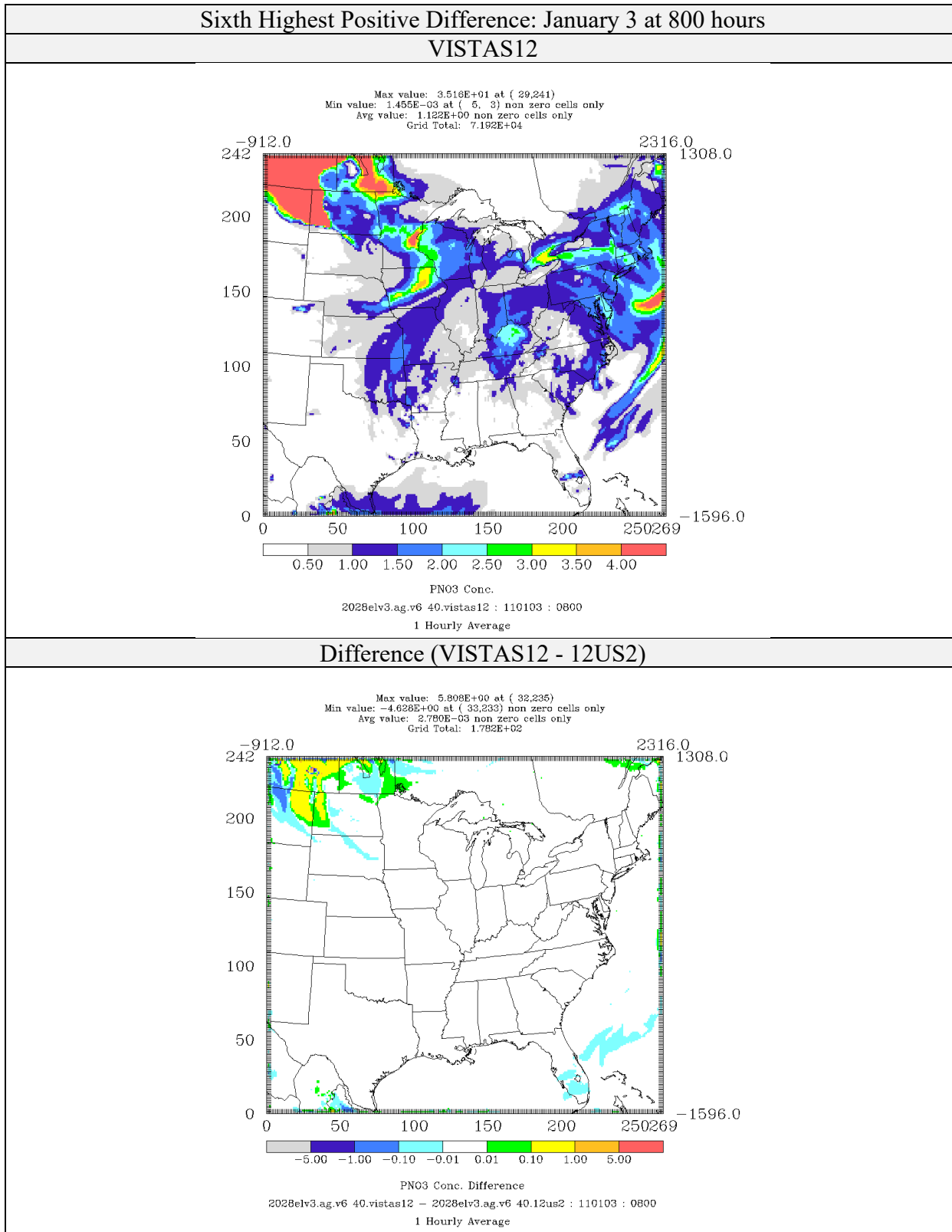


Figure 4-69: Comparison of Nitrate Concentrations ($\mu\text{g}/\text{m}^3$) for CAMx 6.40 on VISTAS12 and 12US2 Domains 2028elv3 Simulations (Sixth Highest Positive Difference)

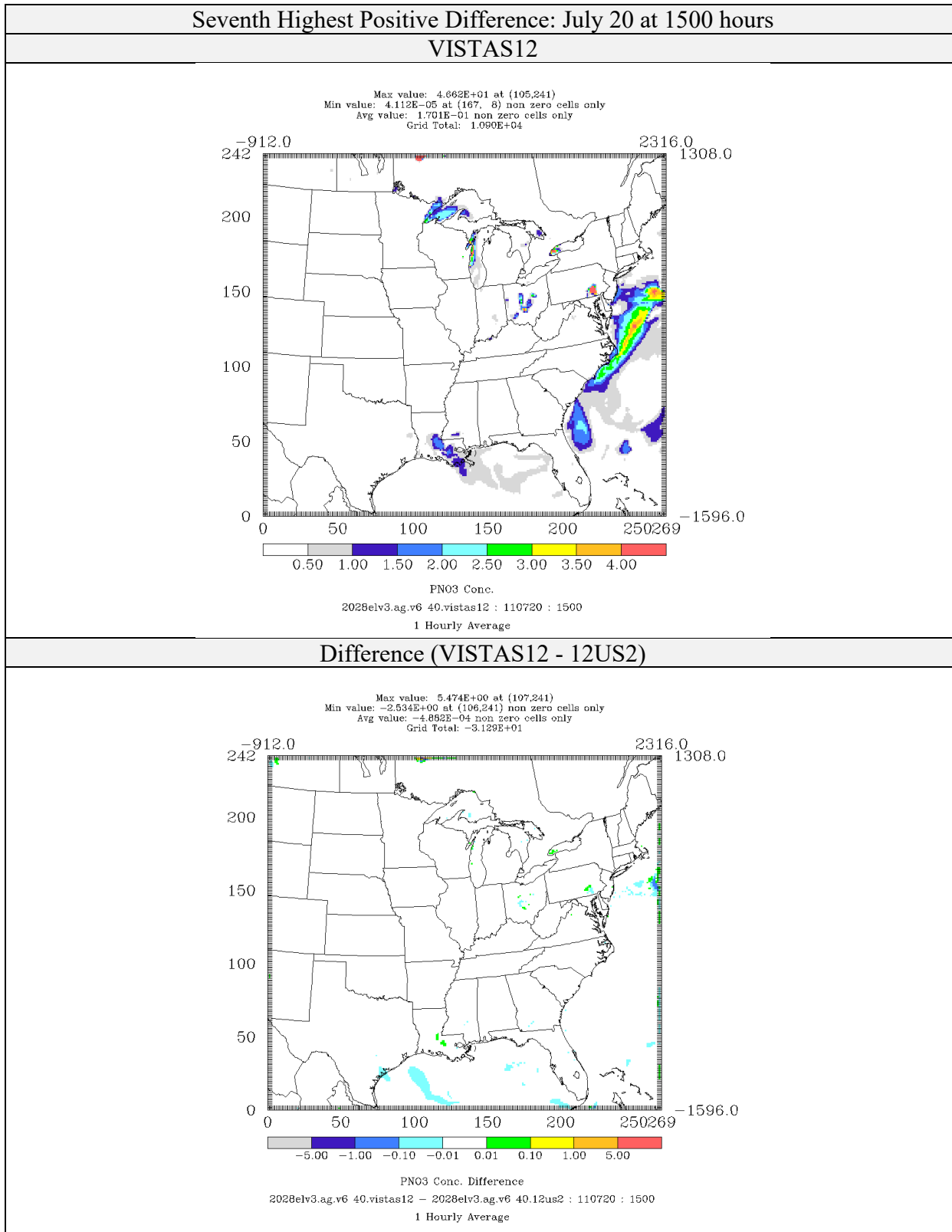


Figure 4-70: Comparison of Nitrate Concentrations ($\mu\text{g}/\text{m}^3$) for CAMx 6.40 on VISTAS12 and 12US2 Domains 2028elv3 Simulations (Seventh Highest Positive Difference)

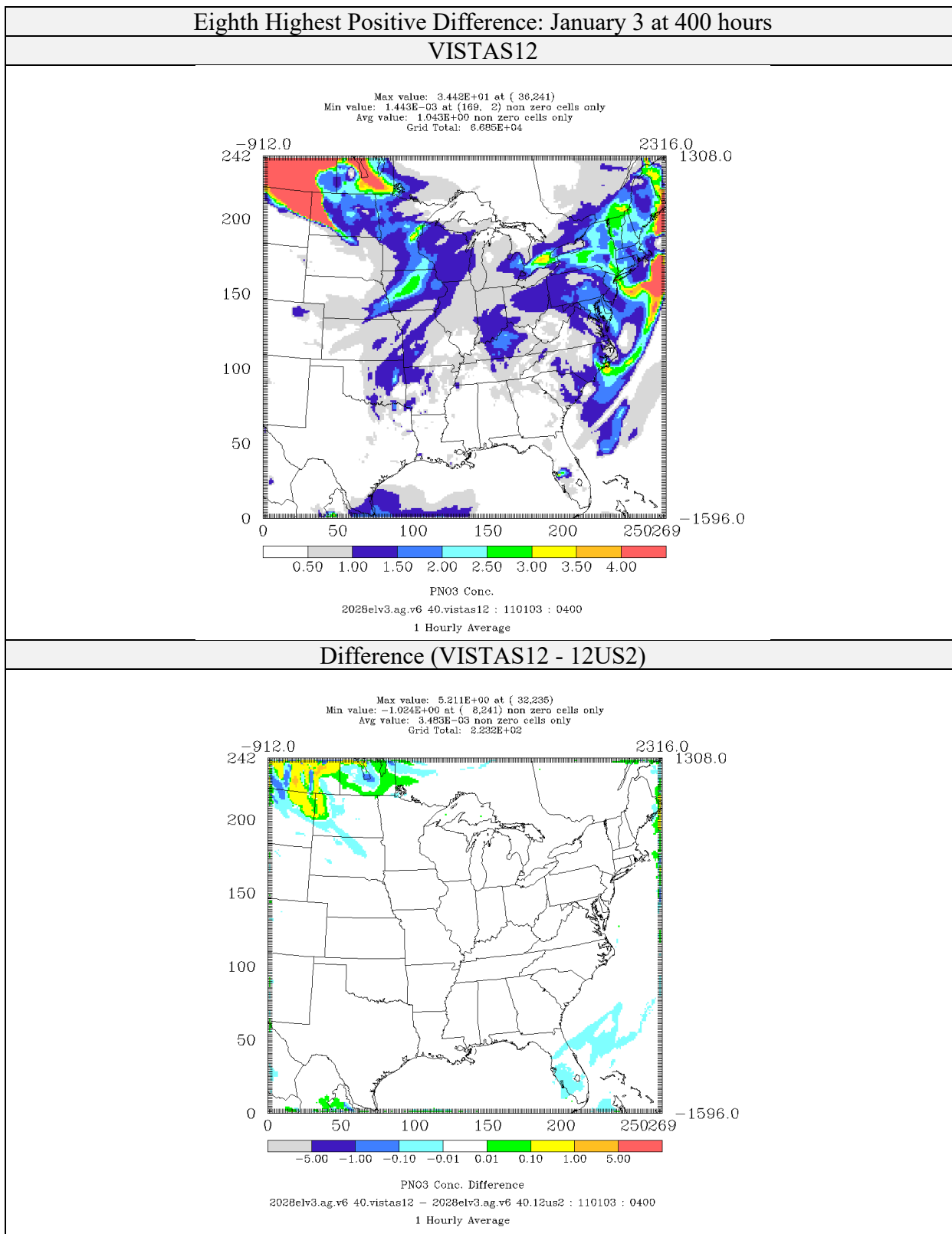


Figure 4-71: Comparison of Nitrate Concentrations ($\mu\text{g}/\text{m}^3$) for CAMx 6.40 on VISTAS12 and 12US2 Domains 2028elv3 Simulations (Eighth Highest Positive Difference)

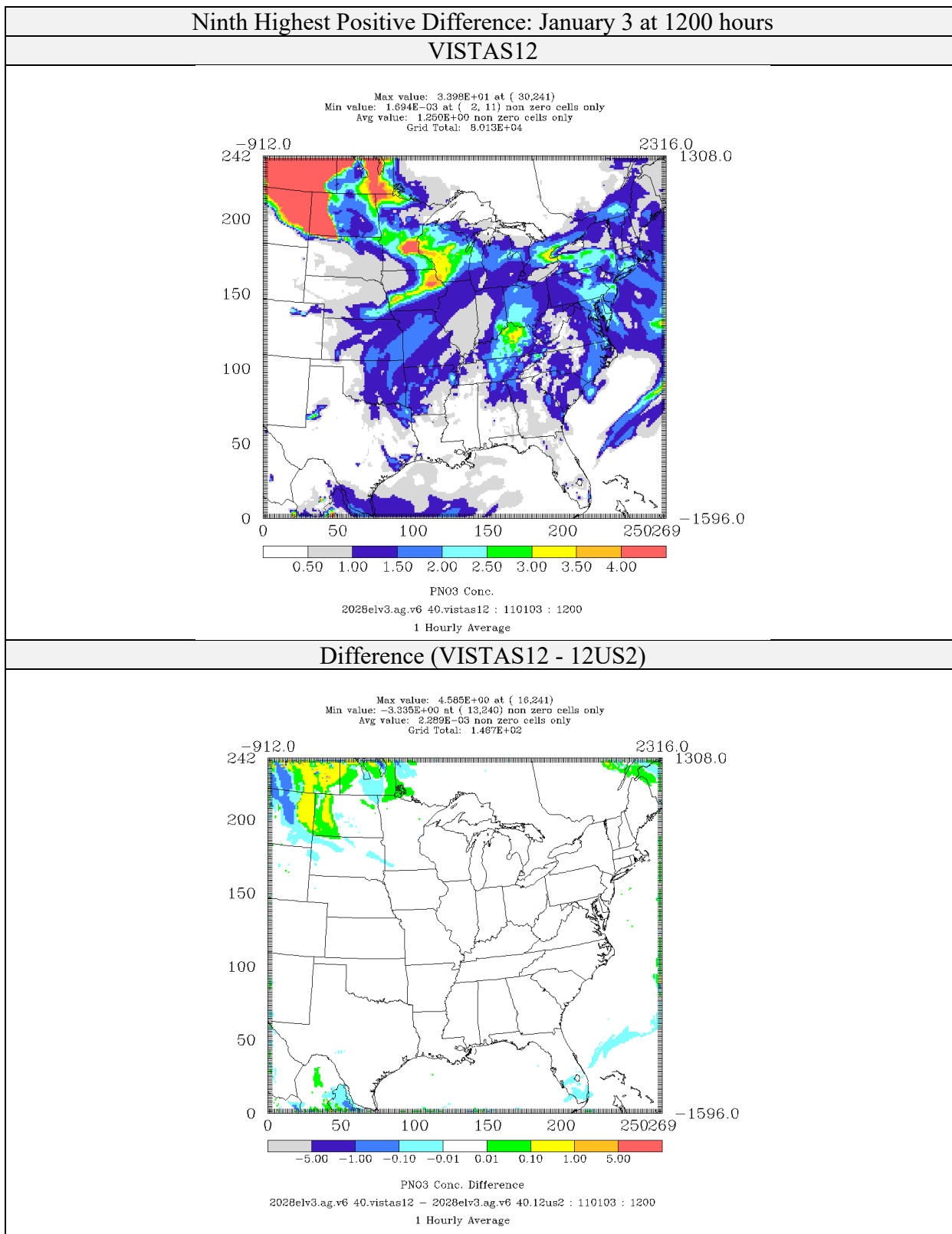


Figure 4-72: Comparison of Nitrate Concentrations ($\mu\text{g}/\text{m}^3$) for CAMx 6.40 on VISTAS12 and 12US2 Domains 2028elv3 Simulations (Ninth Highest Positive Difference)

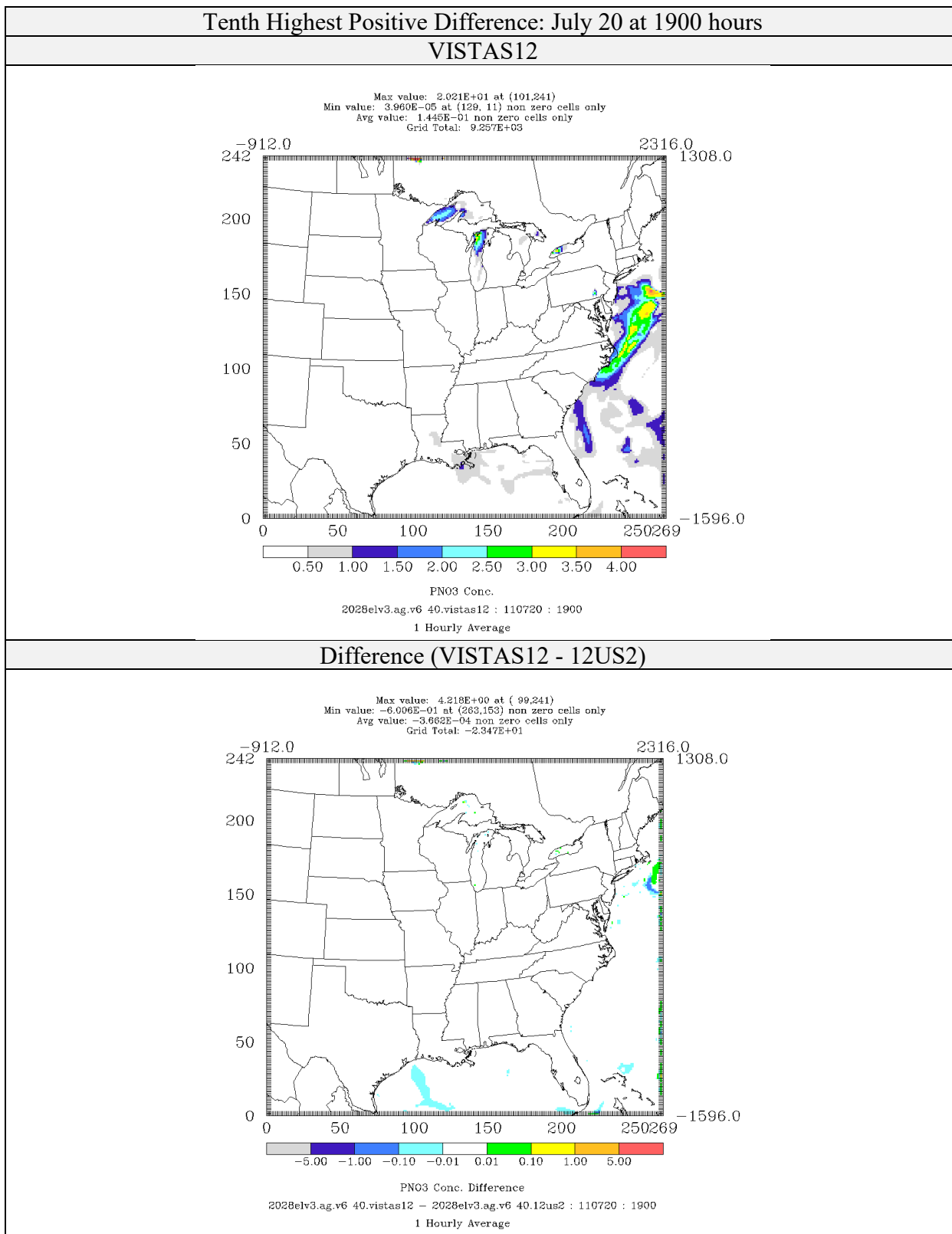


Figure 4-73: Comparison of Nitrate Concentrations ($\mu\text{g}/\text{m}^3$) for CAMx 6.40 on VISTAS12 and 12US2 Domains 2028elv3 Simulations (Tenth Highest Positive Difference)

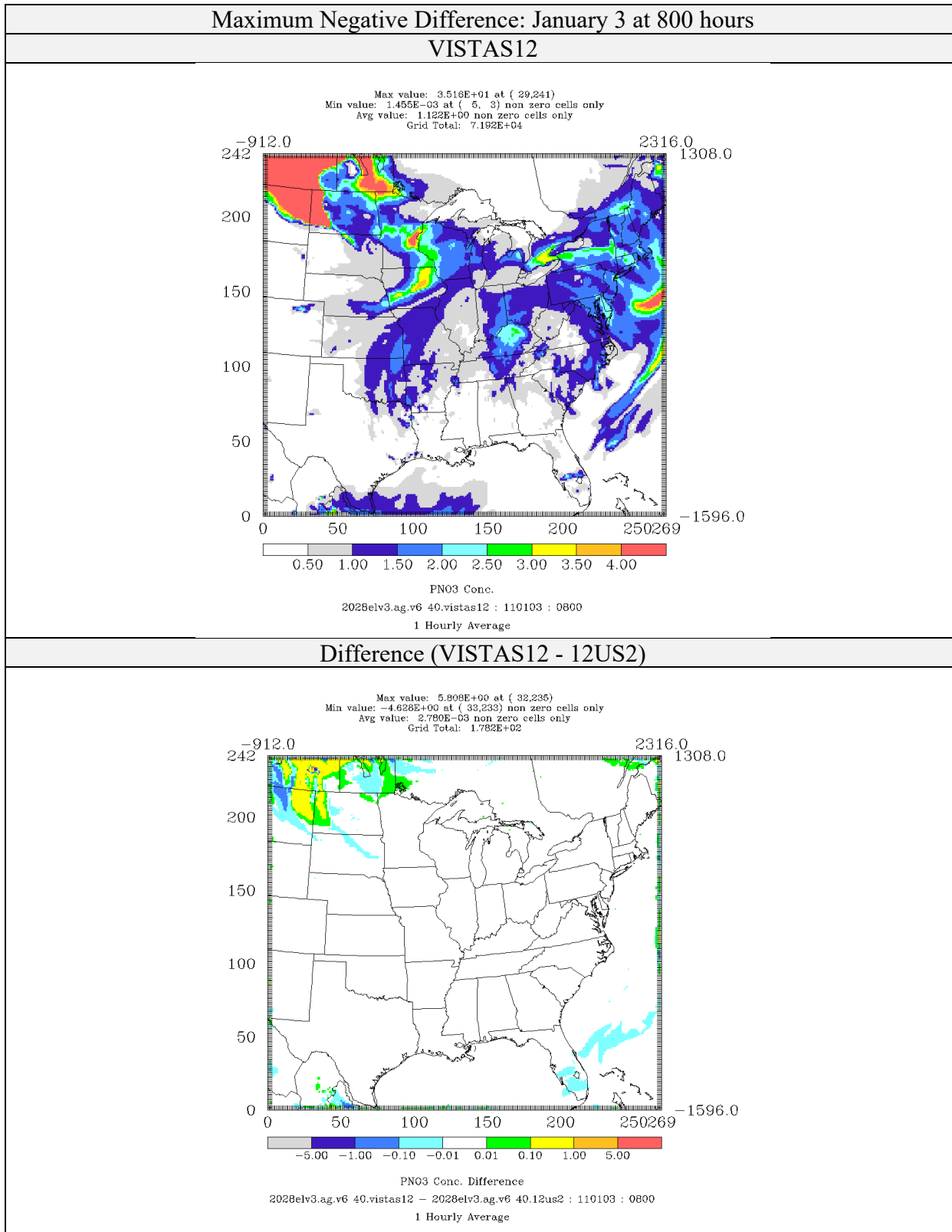


Figure 4-74: Comparison of Nitrate Concentrations ($\mu\text{g}/\text{m}^3$) for CAMx 6.40 on VISTAS12 and 12US2 Domains 2028elv3 Simulations (Maximum Negative Difference)

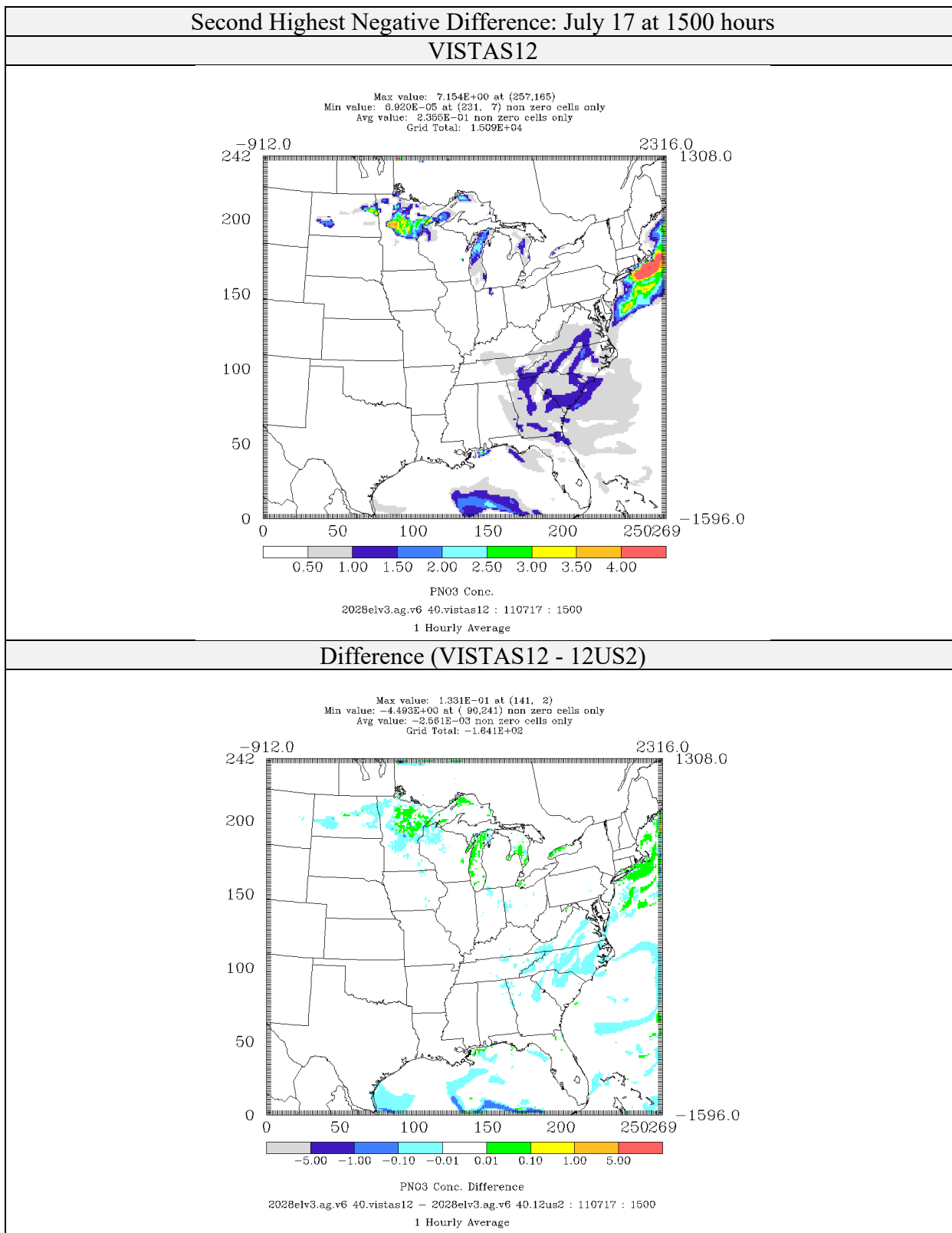


Figure 4-75: Comparison of Nitrate Concentrations ($\mu\text{g}/\text{m}^3$) for CAMx 6.40 on VISTAS12 and 12US2 Domains 2028elv3 Simulations (Second Highest Negative Difference)

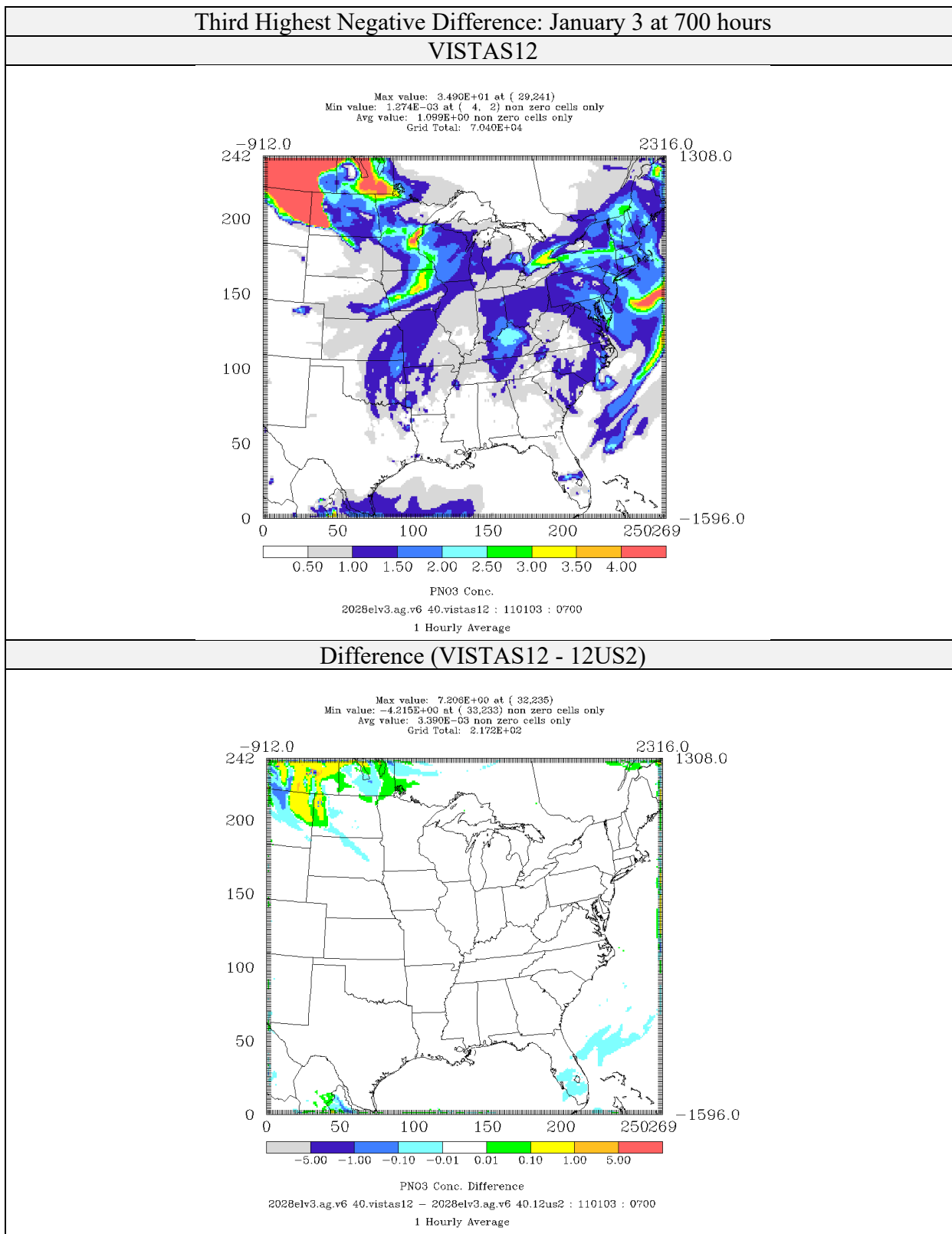


Figure 4-76: Comparison of Nitrate Concentrations ($\mu\text{g}/\text{m}^3$) for CAMx 6.40 on VISTAS12 and 12US2 Domains 2028elv3 Simulations (Third Highest Negative Difference)

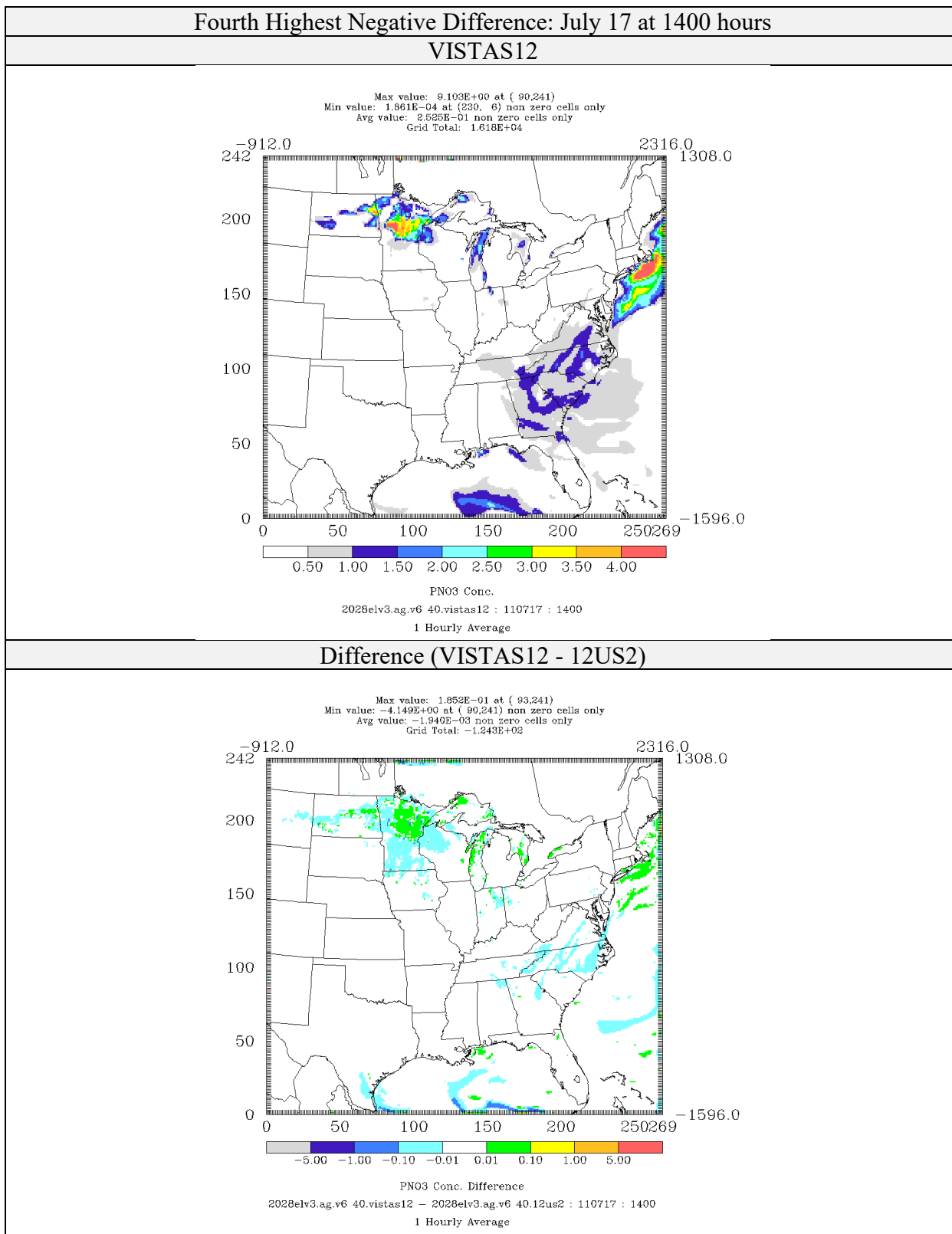


Figure 4-77: Comparison of Nitrate Concentrations ($\mu\text{g}/\text{m}^3$) for CAMx 6.40 on VISTAS12 and 12US2 Domains 2028elv3 Simulations (Fourth Highest Negative Difference)

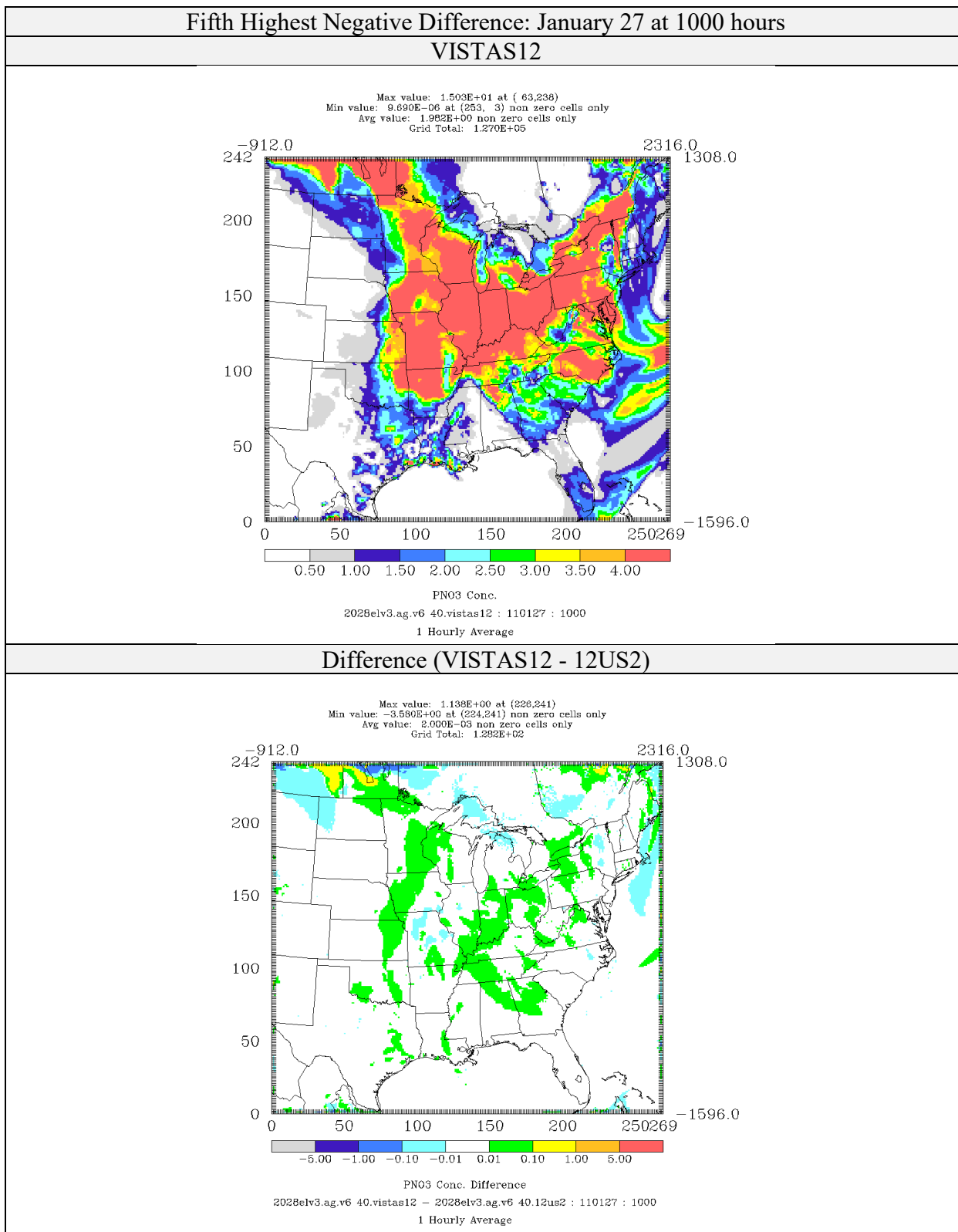


Figure 4-78: Comparison of Nitrate Concentrations ($\mu\text{g}/\text{m}^3$) for CAMx 6.40 on VISTAS12 and 12US2 Domains 2028elv3 Simulations (Fifth Highest Negative Difference)

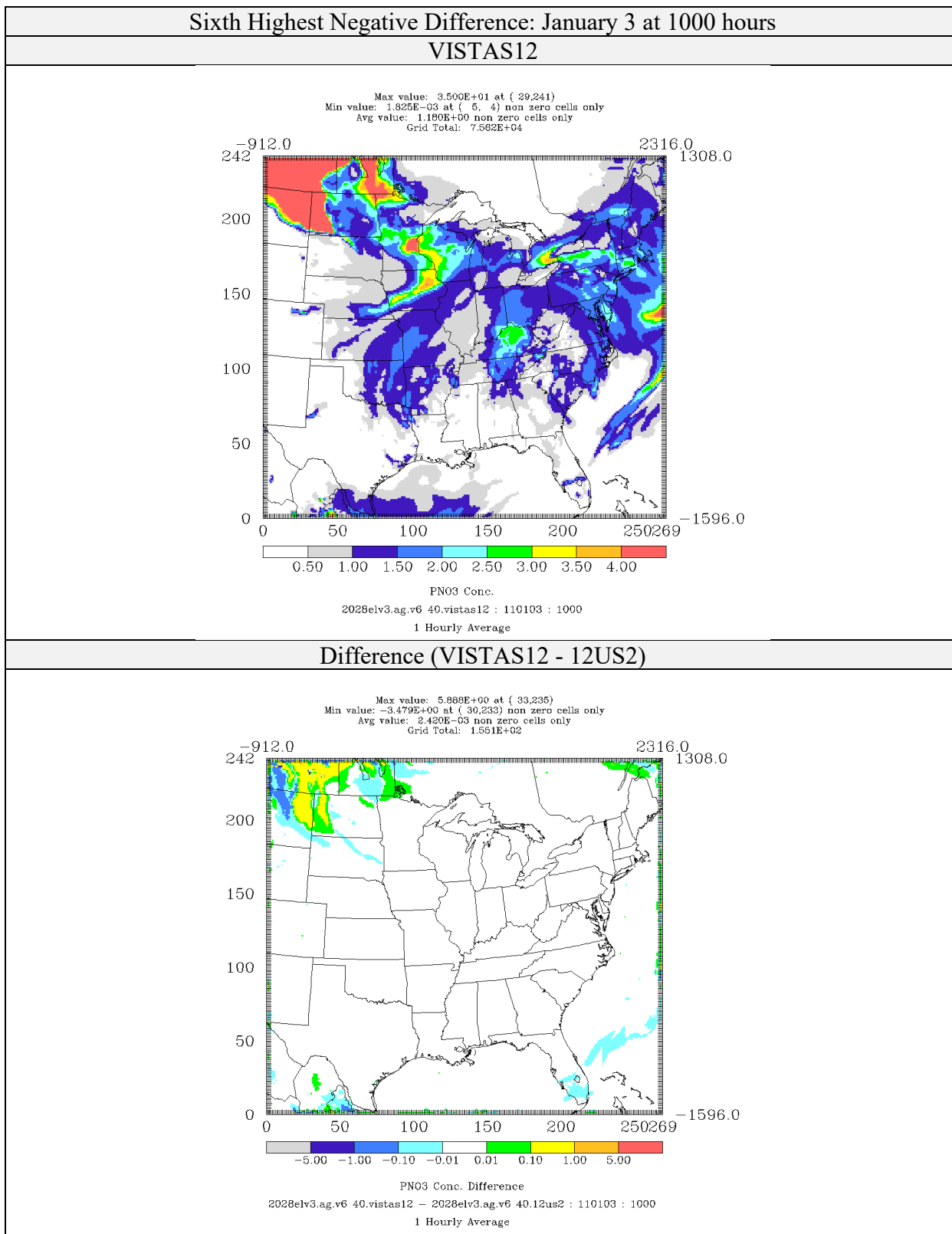


Figure 4-79: Comparison of Nitrate Concentrations ($\mu\text{g}/\text{m}^3$) for CAMx 6.40 on VISTAS12 and 12US2 Domains 2028elv3 Simulations (Sixth Highest Negative Difference)

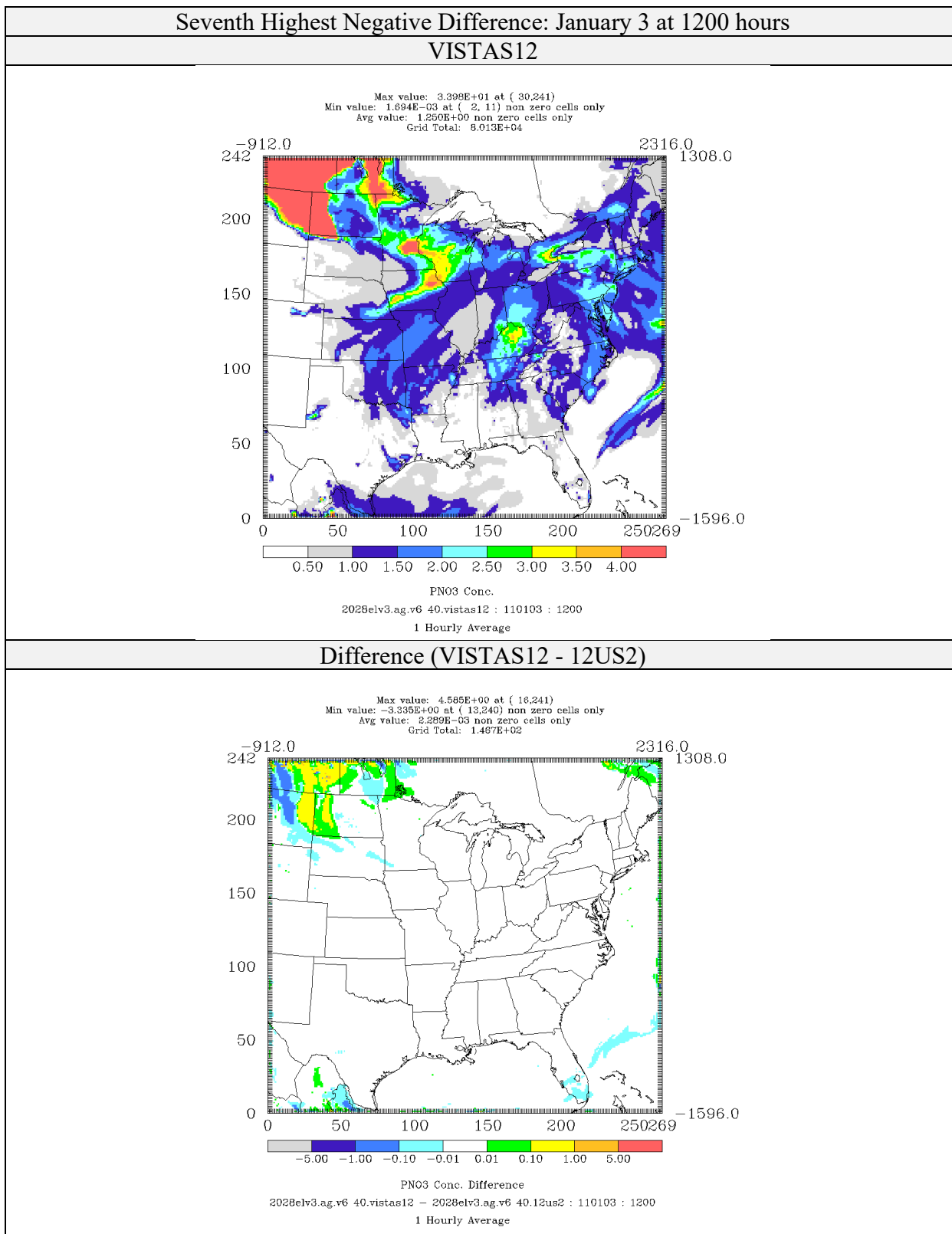


Figure 4-80: Comparison of Nitrate Concentrations ($\mu\text{g}/\text{m}^3$) for CAMx 6.40 on VISTAS12 and 12US2 Domains 2028elv3 Simulations (Seventh Highest Negative Difference)

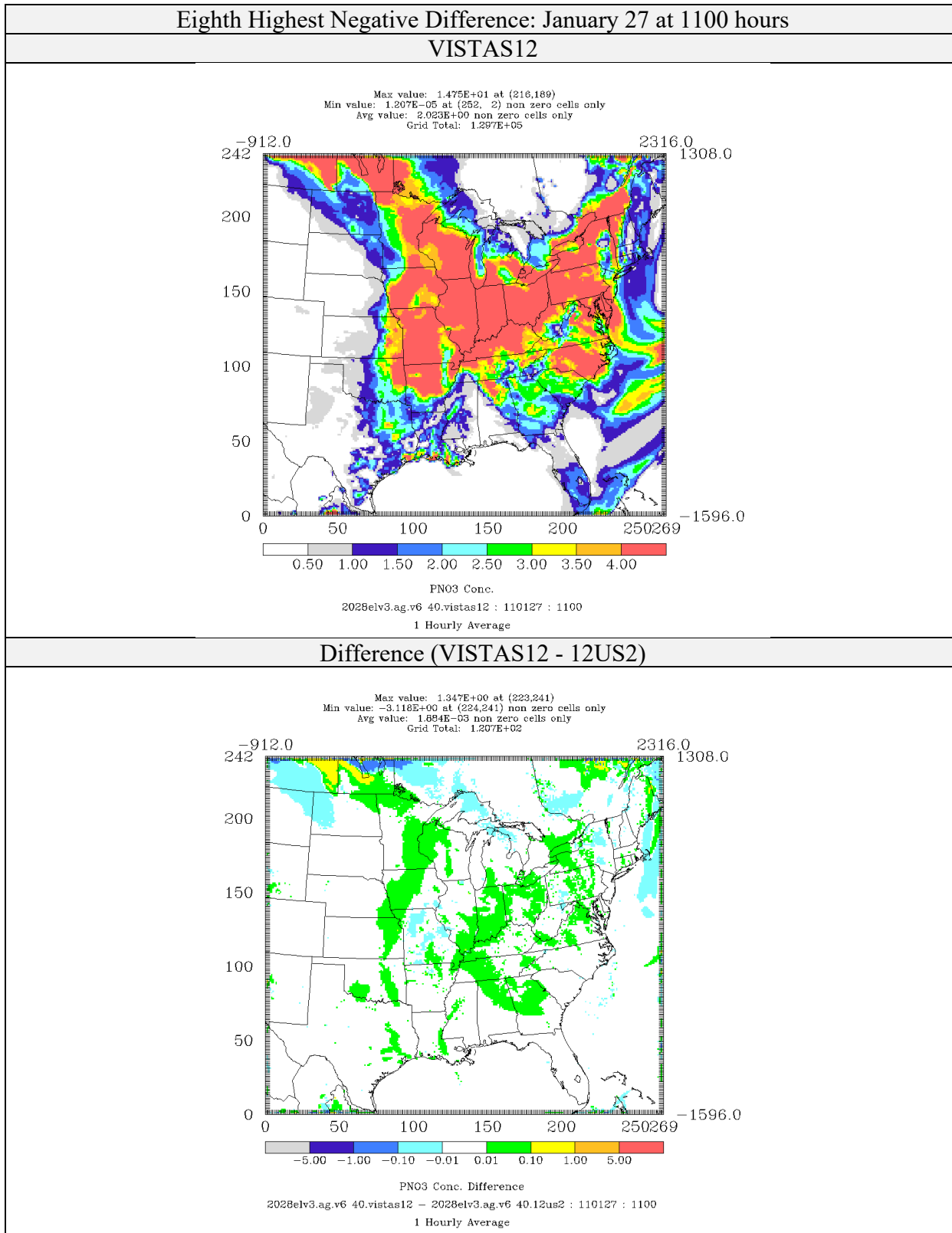


Figure 4-81: Comparison of Nitrate Concentrations ($\mu\text{g}/\text{m}^3$) for CAMx 6.40 on VISTAS12 and 12US2 Domains 2028elv3 Simulations (Eighth Highest Negative Difference)

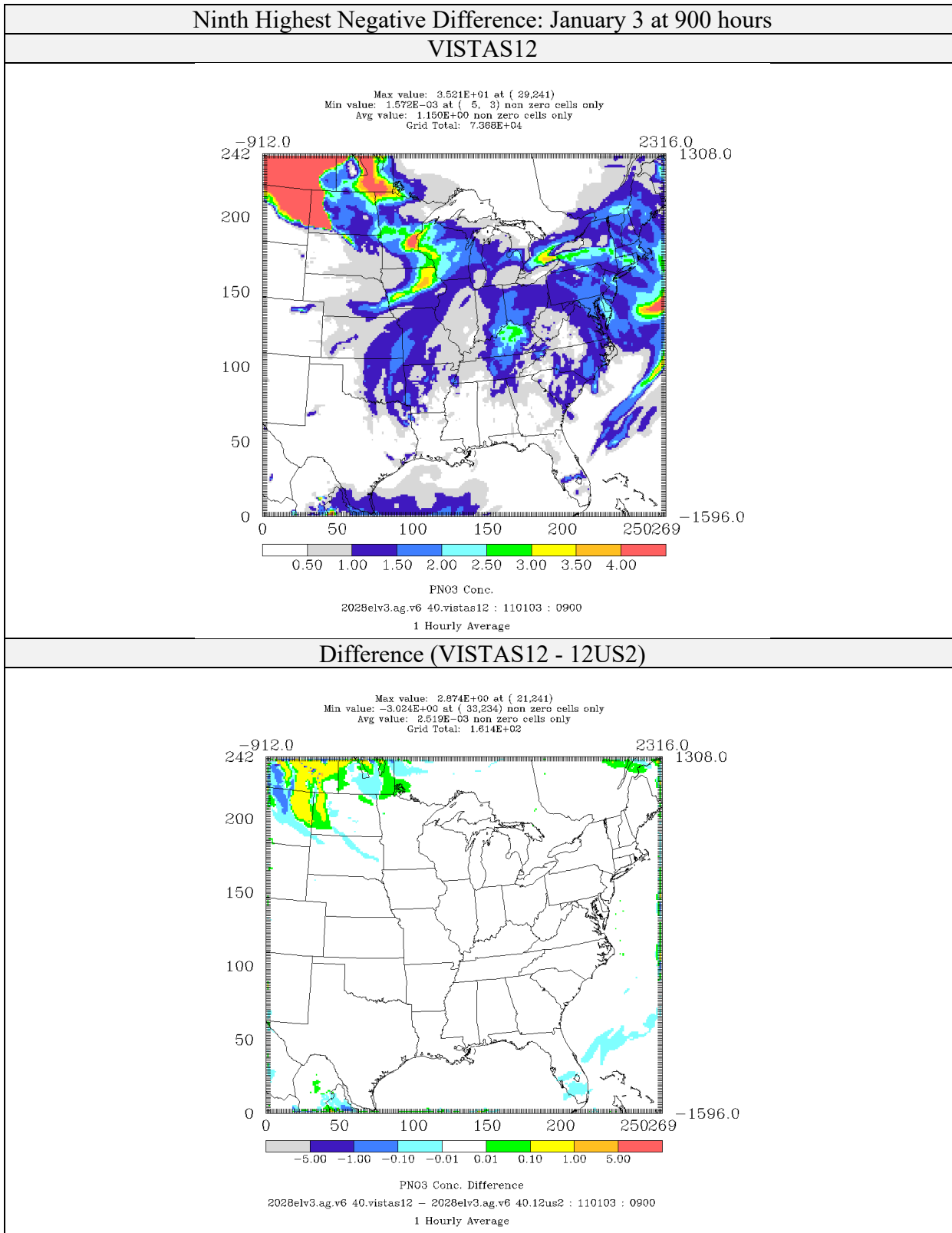


Figure 4-82: Comparison of Nitrate Concentrations ($\mu\text{g}/\text{m}^3$) for CAMx 6.40 on VISTAS12 and 12US2 Domains 2028elv3 Simulations (Ninth Highest Negative Difference)

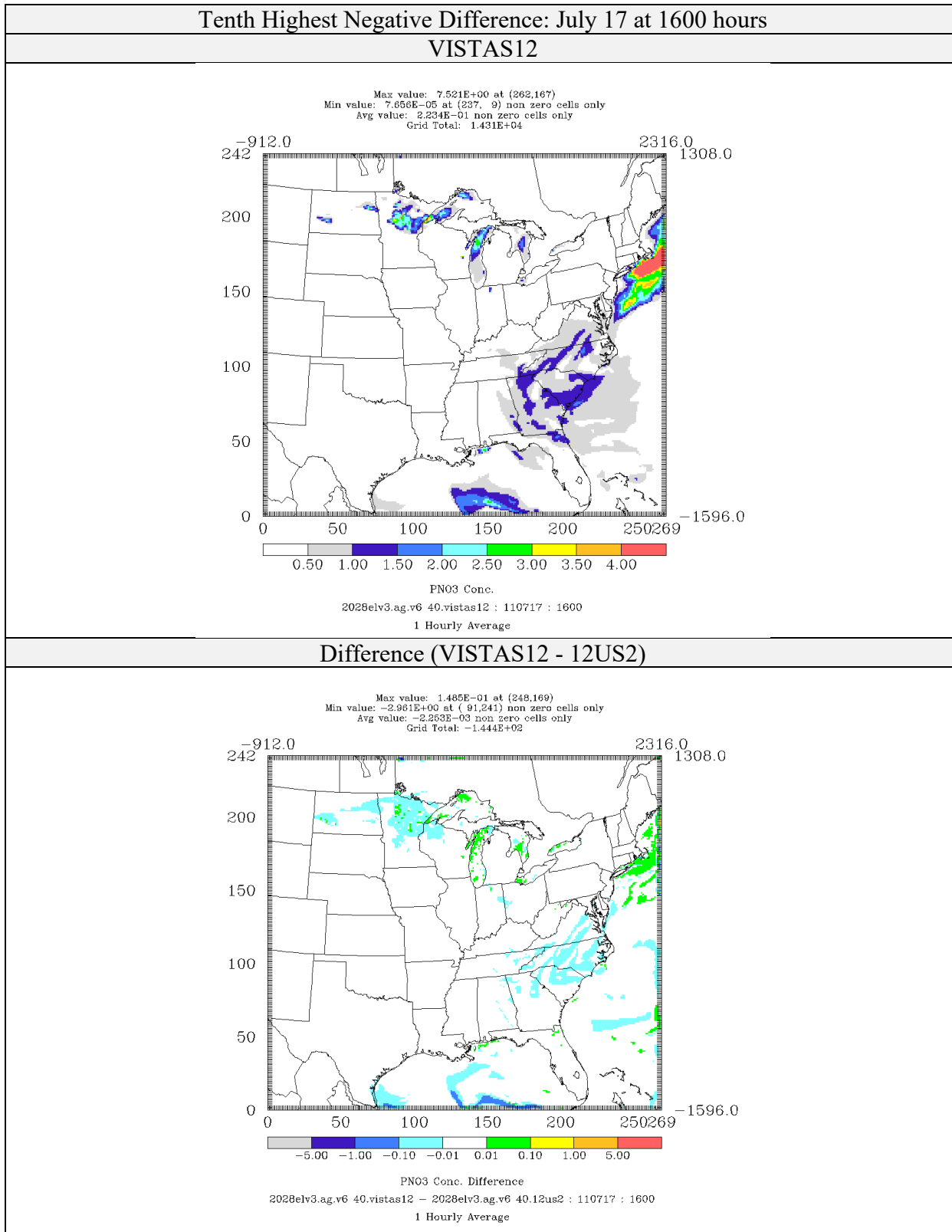


Figure 4-83: Comparison of Nitrate Concentrations ($\mu\text{g}/\text{m}^3$) for CAMx 6.40 on VISTAS12 and 12US2 Domains 2028elv3 Simulations (Tenth Highest Negative Difference)

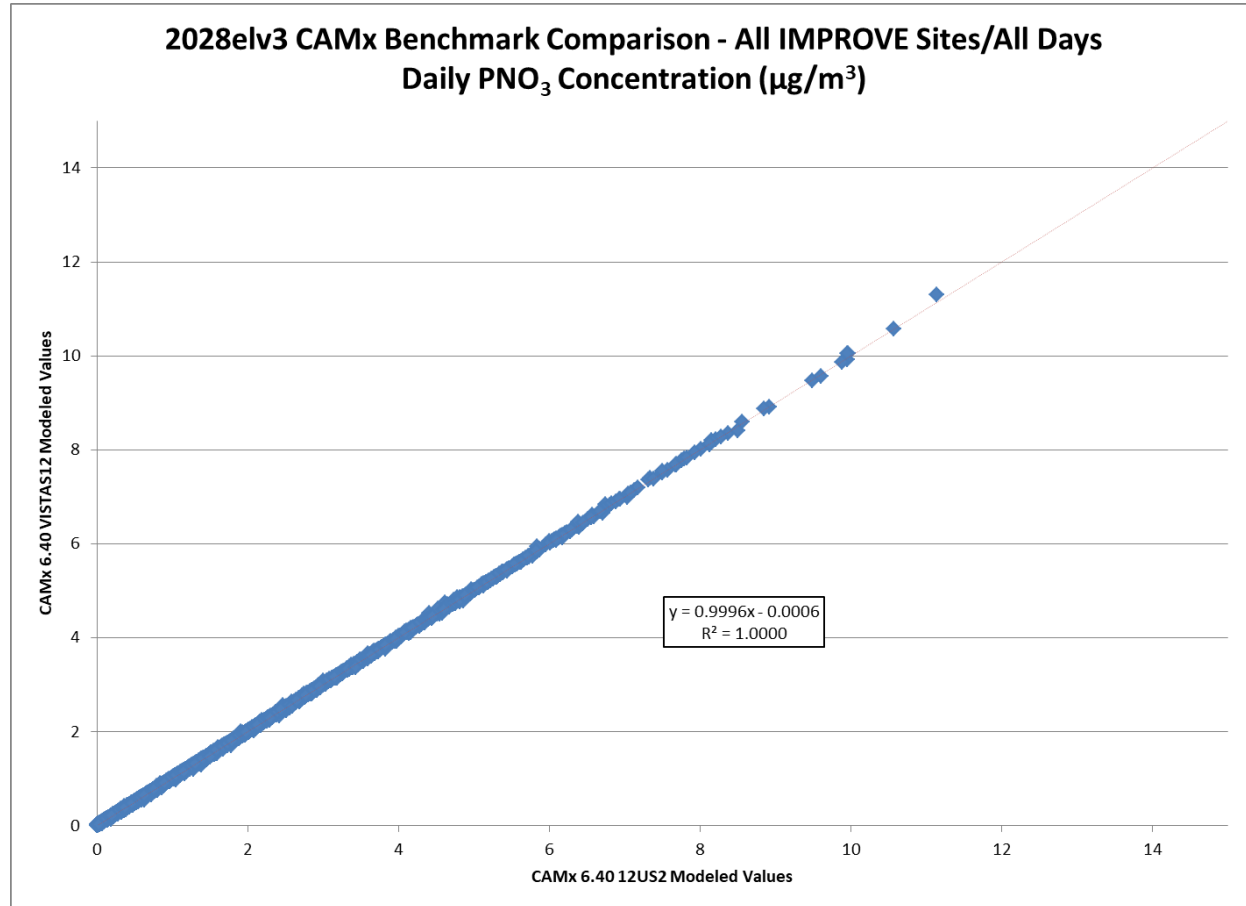


Figure 4-84: Scatterplot Comparing 24-hour Average Predicted Nitrate Concentrations (μg/m³) for All Days at all IMPROVE Monitor Locations for CAMx 6.40 on VISTAS12 and 12US2 Domains 2028elv3 Simulations Performed by VISTAS (Alpine).

4.5 Organic Matter (OM)

Organic Matter (OM) results for the top 10 positive and negative hours are presented in tabular format in Table 4-5. The maximum positive difference is 296.00 $\mu\text{g}/\text{m}^3$ falling to 161.83 $\mu\text{g}/\text{m}^3$ for the 10th high. The maximum negative difference is -228.07 $\mu\text{g}/\text{m}^3$ falling to -134.62 $\mu\text{g}/\text{m}^3$ for the 10th high. The maximum positive percent difference from these days is 97.4% and negative percent difference of -33.7%.

As expected, the maximum impacts on the top 10 positive and negative hours are occurring very near the border. As was described in Section 2, the two CAMx simulations used the same input data, except that the pollutant concentrations on in-flow boundary cells. For the simulation on the VISTAS12 domain the in-flow concentrations are specified in hourly boundary conditions extracted from the 12US2 simulation. For the 12US2 simulation the in-flow concentrations were continuously updated from the cells outside the VISTAS12 domain. It would be expected that concentration differences would occur from the differences in hourly average concentrations, versus in the instantaneous concentrations.

The top 10 positive difference hours are presented in Figures 4-85 through 4-94 and the top 10 negative impact hours are presented in Tables 4-95 through 4-104. As with sulfate, the peak differences are occurring between July 17 and July 20. The area of the peak impact is very near the northern border, north of Minnesota. This is an area where CAMx simulations are showing very high OC concentrations in an area heavily influenced by boundary conditions.

Scatterplots of the daily average OM concentrations in local standard time at the IMPROVE monitors are presented in Figure 4-105. The 12US2 results are plotted on the x-axis and the VISTAS12 results are plotted on the y-axis. The data has a high degree of correlation with a line of best fit with a slope of 1.0004, an intercept of 0.0017 $\mu\text{g}/\text{m}^3$ and an R^2 of 1.0000.

Table 4-5. Comparison of 2028elv3 CAMx 6.40 VISTAS12 and 12US2 Simulation of Organic Matter Concentrations ($\mu\text{g}/\text{m}^3$). Hours with the top 10 maximum positive and maximum negative differences are shown.

Year	Month	Day	Hour	VISTAS12 Conc.	12US2 Conc.	Difference ($\mu\text{g}/\text{m}^3$)	Percent Difference	Column	Row
<i>Maximum Positive</i>									
2011	7	21	4	735.71	439.71	296.00	67.3%	104	241
2011	7	20	14	1262.44	1025.84	236.60	23.1%	107	241
2011	7	20	15	633.93	422.81	211.12	49.9%	107	241
2011	7	20	11	2118.91	1910.65	208.27	10.9%	107	241
2011	7	21	3	2457.80	2255.25	202.56	9.0%	104	241
2011	7	21	1	1835.92	1635.03	200.90	12.3%	104	241
2011	7	20	12	2332.91	2150.04	182.88	8.5%	107	241
2011	7	20	23	352.04	178.32	173.73	97.4%	102	241
2011	7	21	0	568.80	396.74	172.07	43.4%	103	241
2011	7	20	9	5412.29	5250.46	161.83	3.1%	105	241
<i>Maximum Negative</i>									
2011	7	20	15	3744.14	3972.21	-228.07	-5.7%	105	241
2011	7	20	16	3083.95	3285.59	-201.64	-6.1%	105	241
2011	7	20	14	3985.64	4186.45	-200.81	-4.8%	106	241
2011	7	17	11	396.17	591.55	-195.38	-33.0%	89	241
2011	7	20	13	4751.92	4939.42	-187.49	-3.8%	106	241
2011	7	17	12	386.67	562.26	-175.59	-31.2%	89	241
2011	7	20	12	5973.55	6146.67	-173.11	-2.8%	106	241
2011	7	19	10	634.35	802.35	-168.00	-20.9%	104	241
2011	7	17	10	335.13	501.78	-166.65	-33.2%	89	241
2011	7	17	9	265.14	399.76	-134.62	-33.7%	89	241

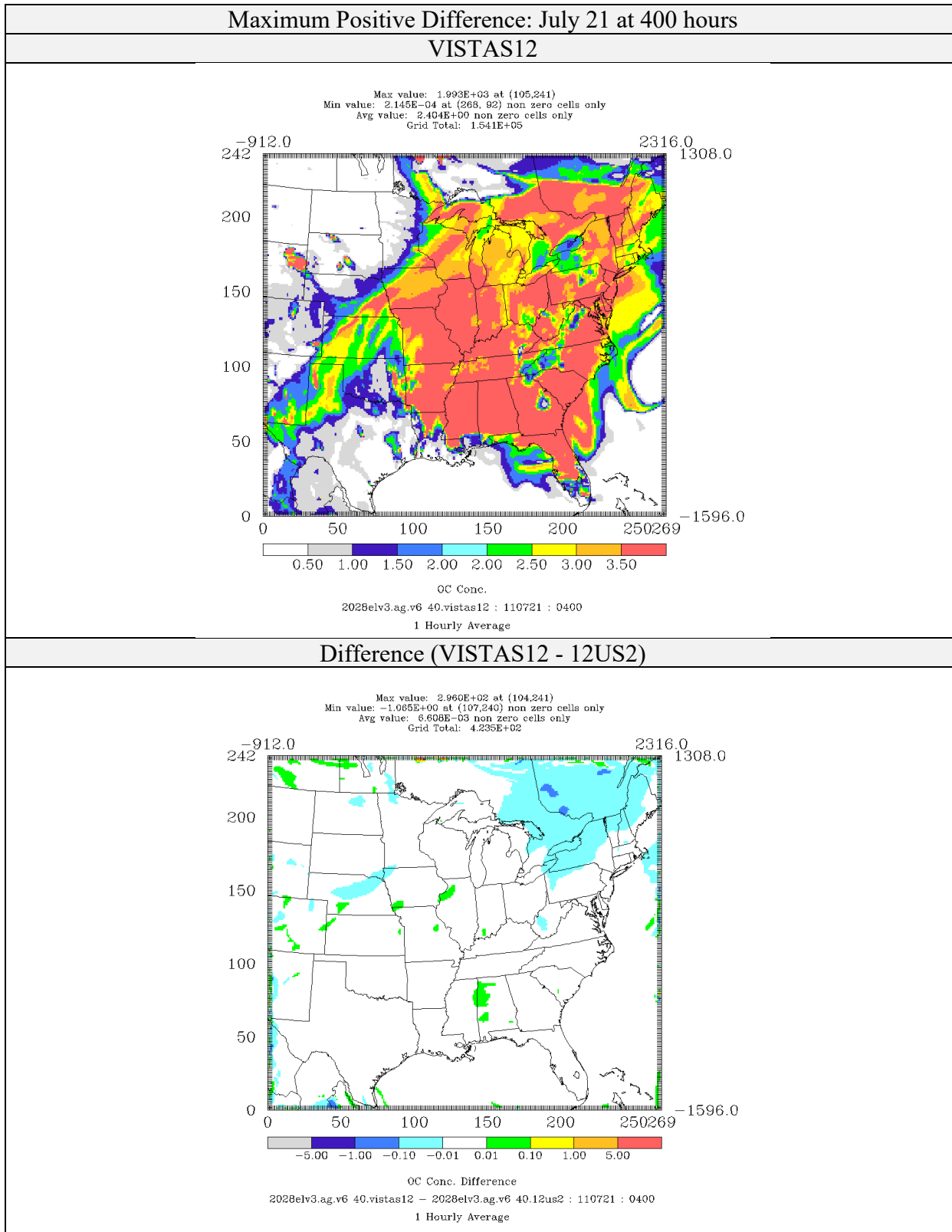


Figure 4-85: Comparison of Organic Matter Concentrations ($\mu\text{g}/\text{m}^3$) for CAMx 6.40 on VISTAS12 and 12US2 Domains 2028elv3 Simulations (Maximum Positive Difference)

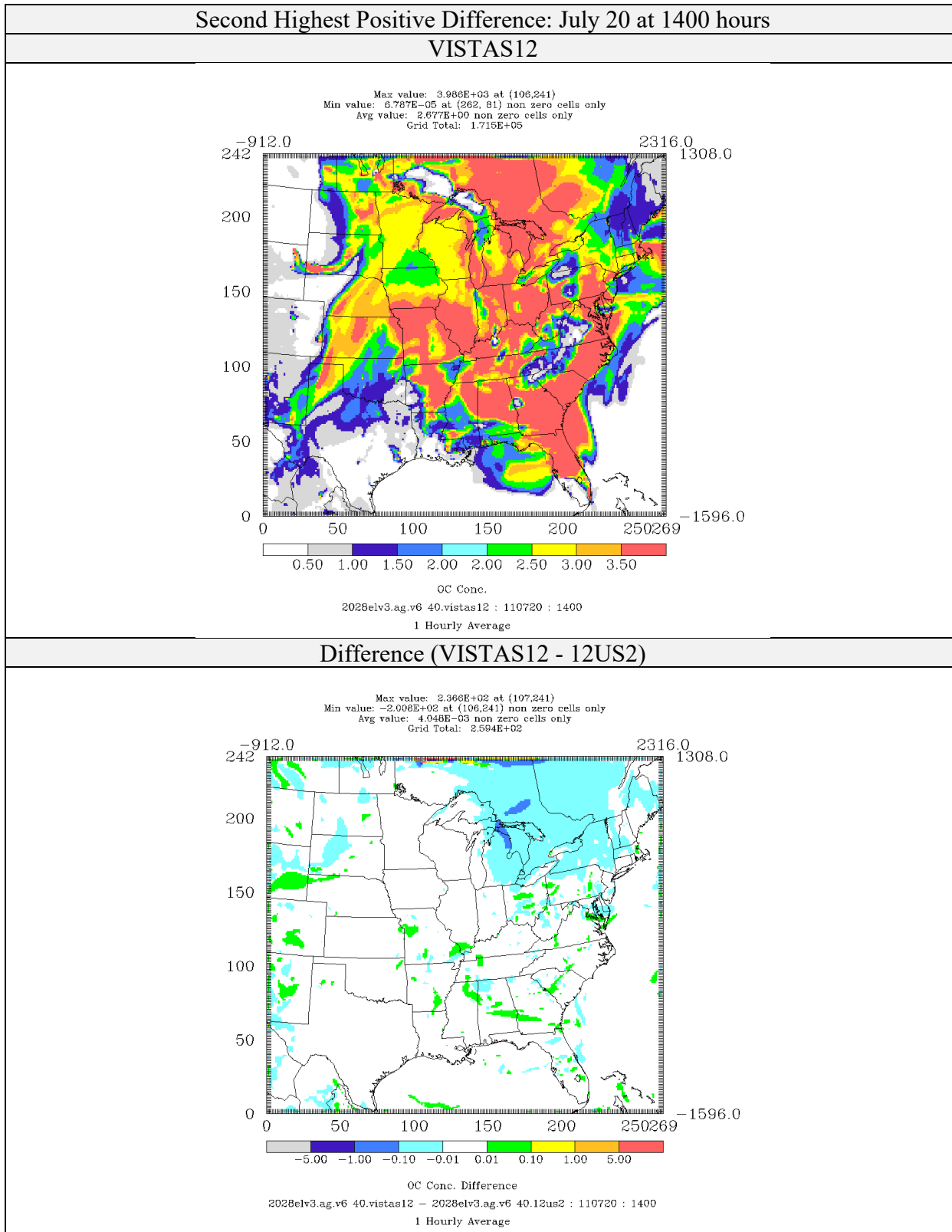


Figure 4-86: Comparison of Organic Matter Concentrations ($\mu\text{g}/\text{m}^3$) for CAMx 6.40 on VISTAS12 and 12US2 Domains 2028elv3 Simulations (Second Highest Positive Difference)

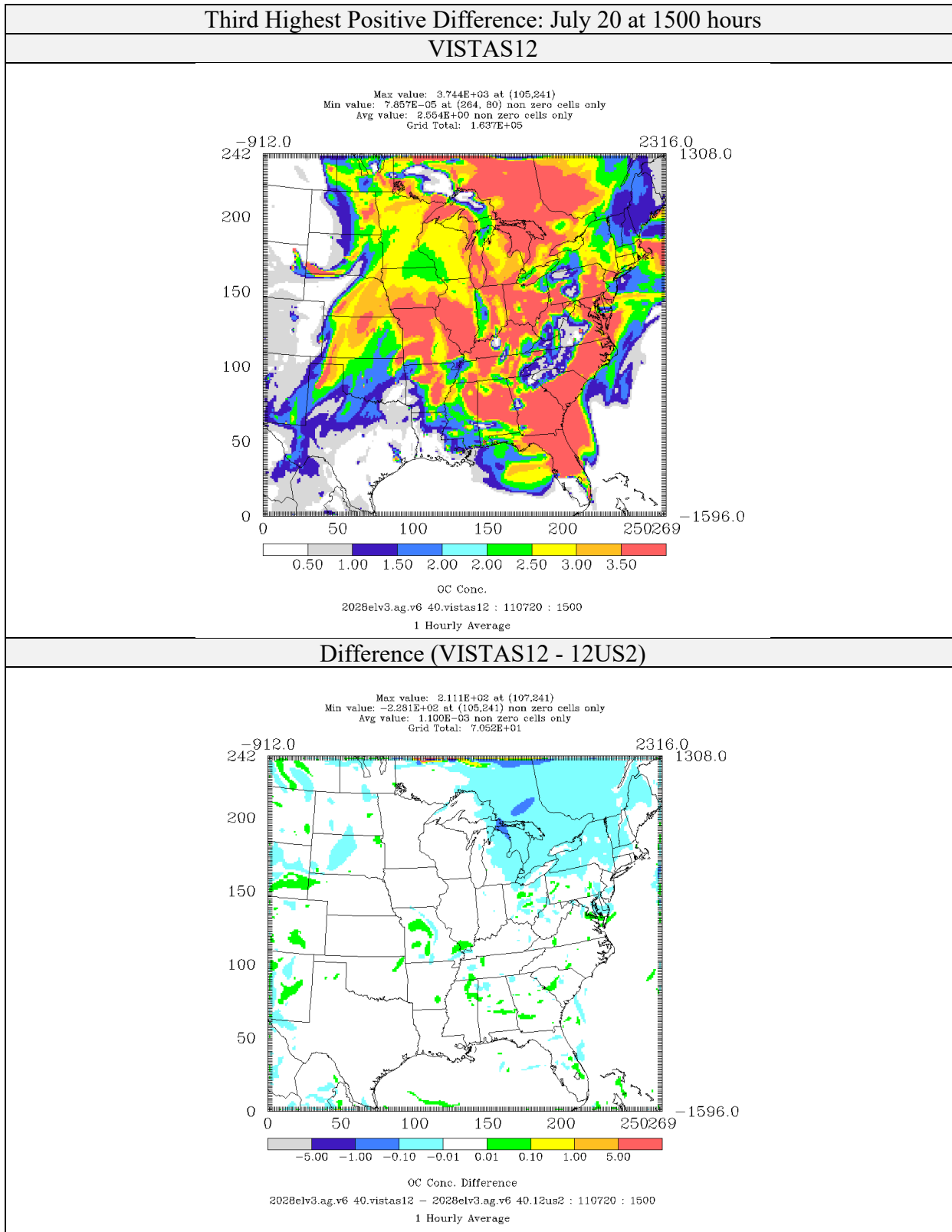


Figure 4-87: Comparison of Organic Matter Concentrations ($\mu\text{g}/\text{m}^3$) for CAMx 6.40 on VISTAS12 and 12US2 Domains 2028elv3 Simulations (Third Highest Positive Difference)

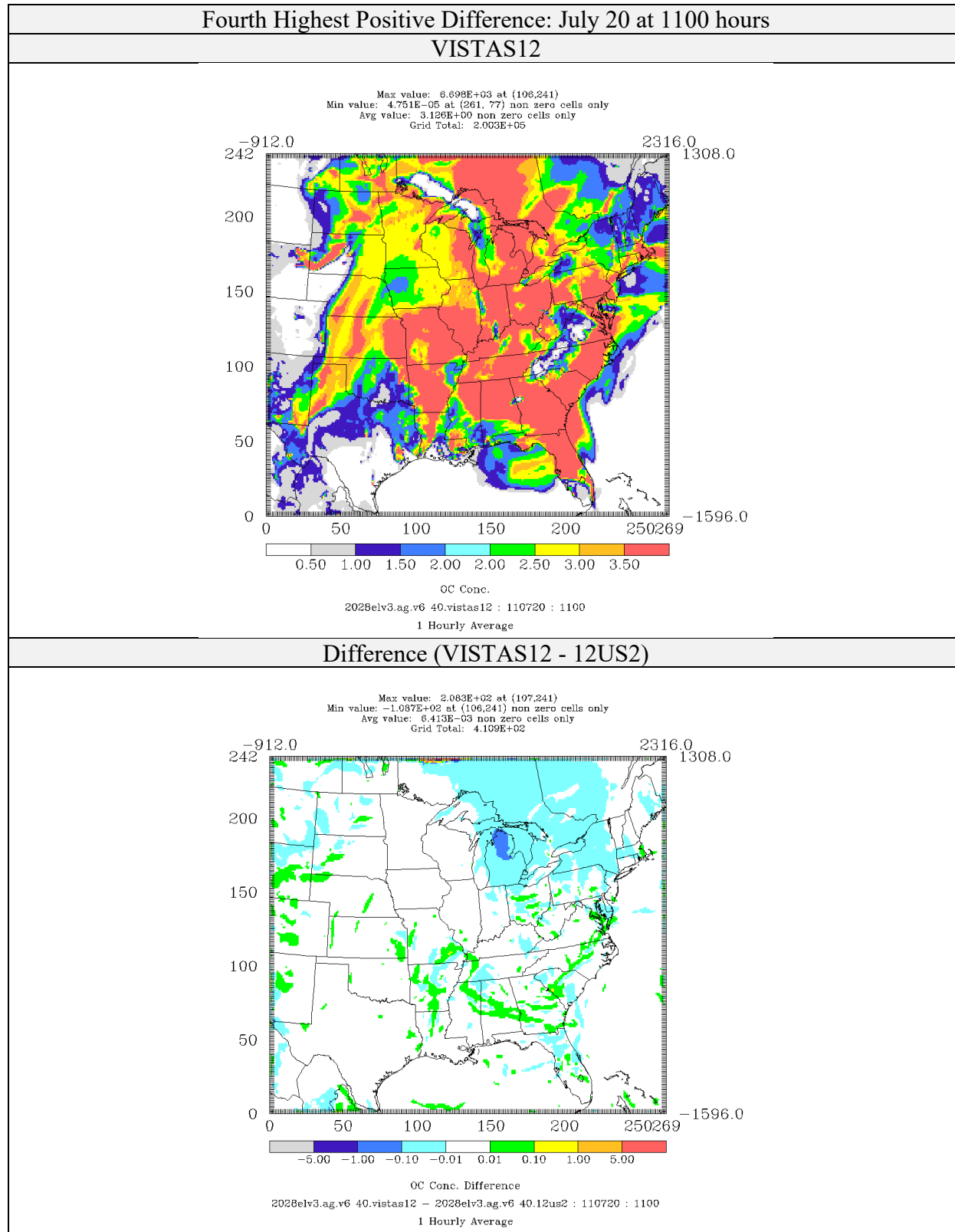


Figure 4-88: Comparison of Organic Matter Concentrations ($\mu\text{g}/\text{m}^3$) for CAMx 6.40 on VISTAS12 and 12US2 Domains 2028elv3 Simulations (Fourth Highest Positive Difference)

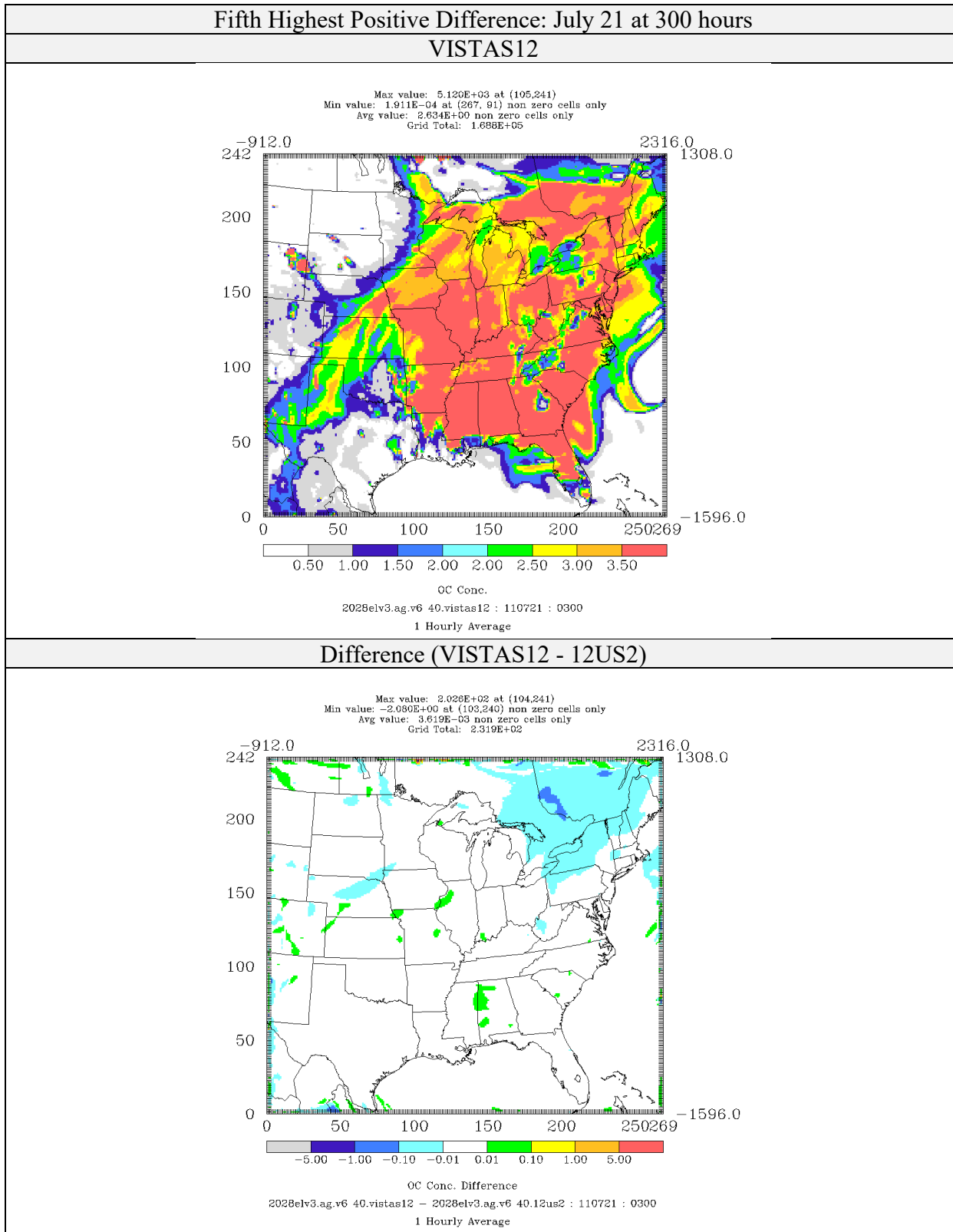


Figure 4-89: Comparison of Organic Matter Concentrations ($\mu\text{g}/\text{m}^3$) for CAMx 6.40 on VISTAS12 and 12US2 Domains 2028elv3 Simulations (Fifth Highest Positive Difference)

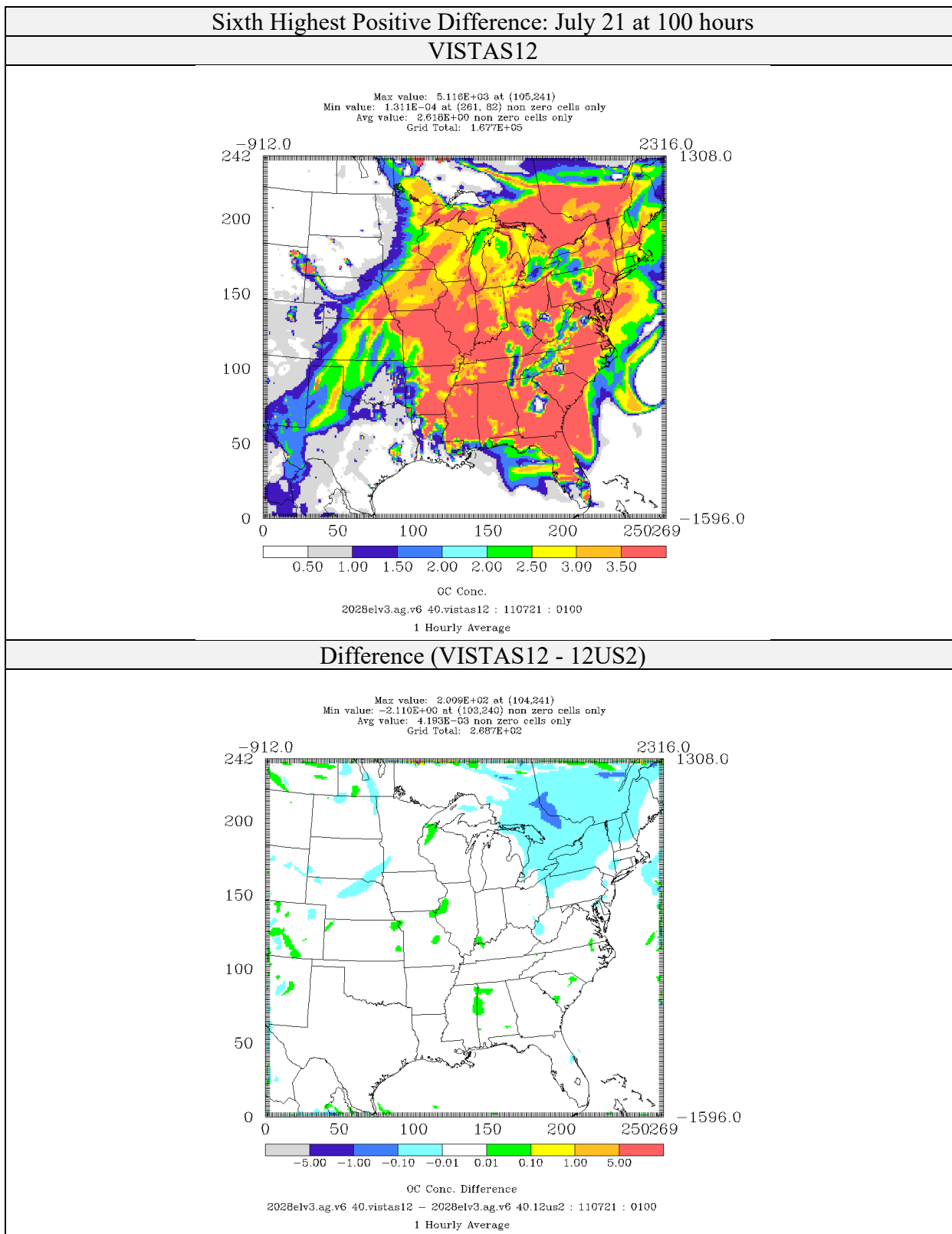


Figure 4-90: Comparison of Organic Matter Concentrations ($\mu\text{g}/\text{m}^3$) for CAMx 6.40 on VISTAS12 and 12US2 Domains 2028elv3 Simulations (Sixth Highest Positive Difference)

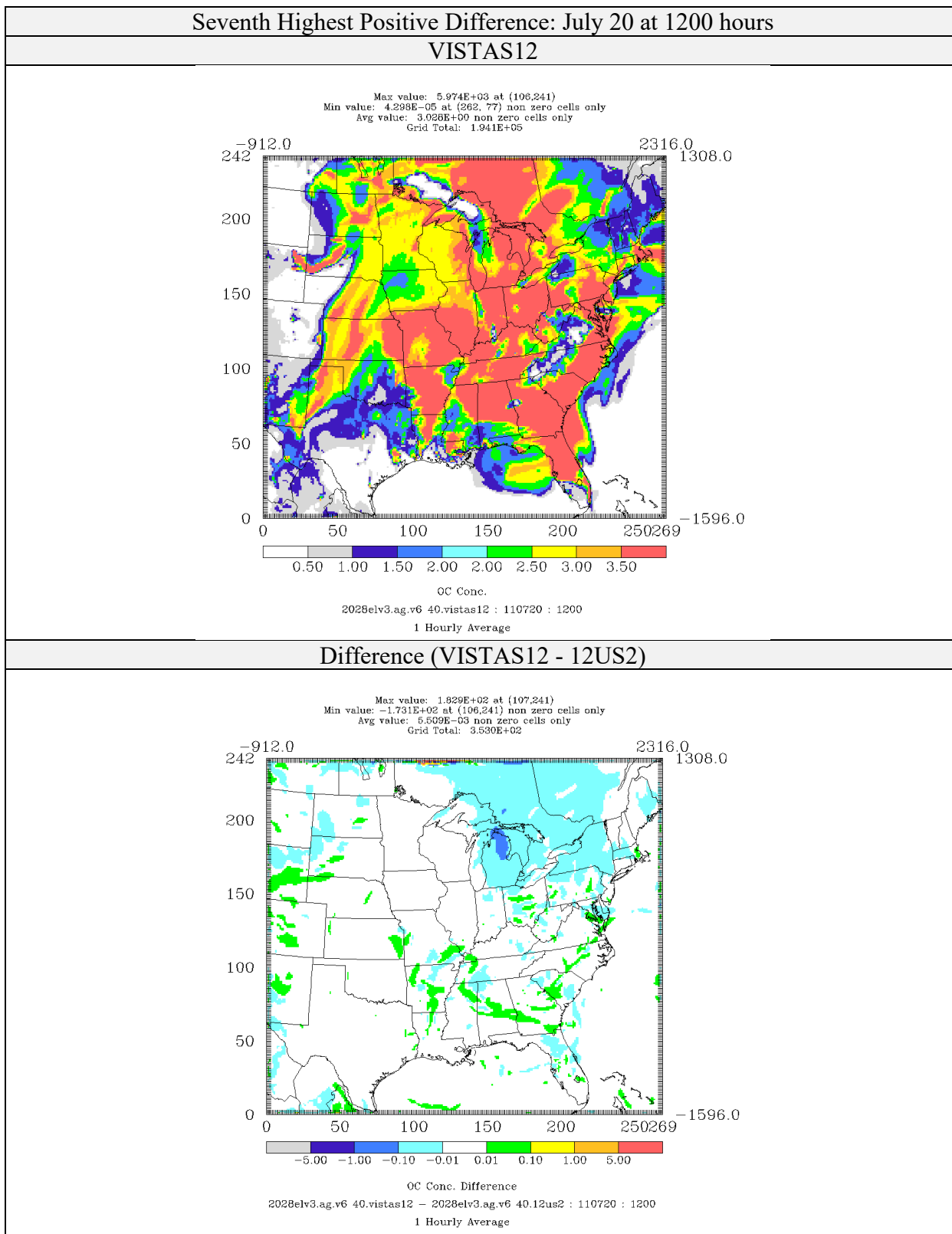


Figure 4-91: Comparison of Organic Matter Concentrations ($\mu\text{g}/\text{m}^3$) for CAMx 6.40 on VISTAS12 and 12US2 Domains 2028elv3 Simulations (Seventh Highest Positive Difference)

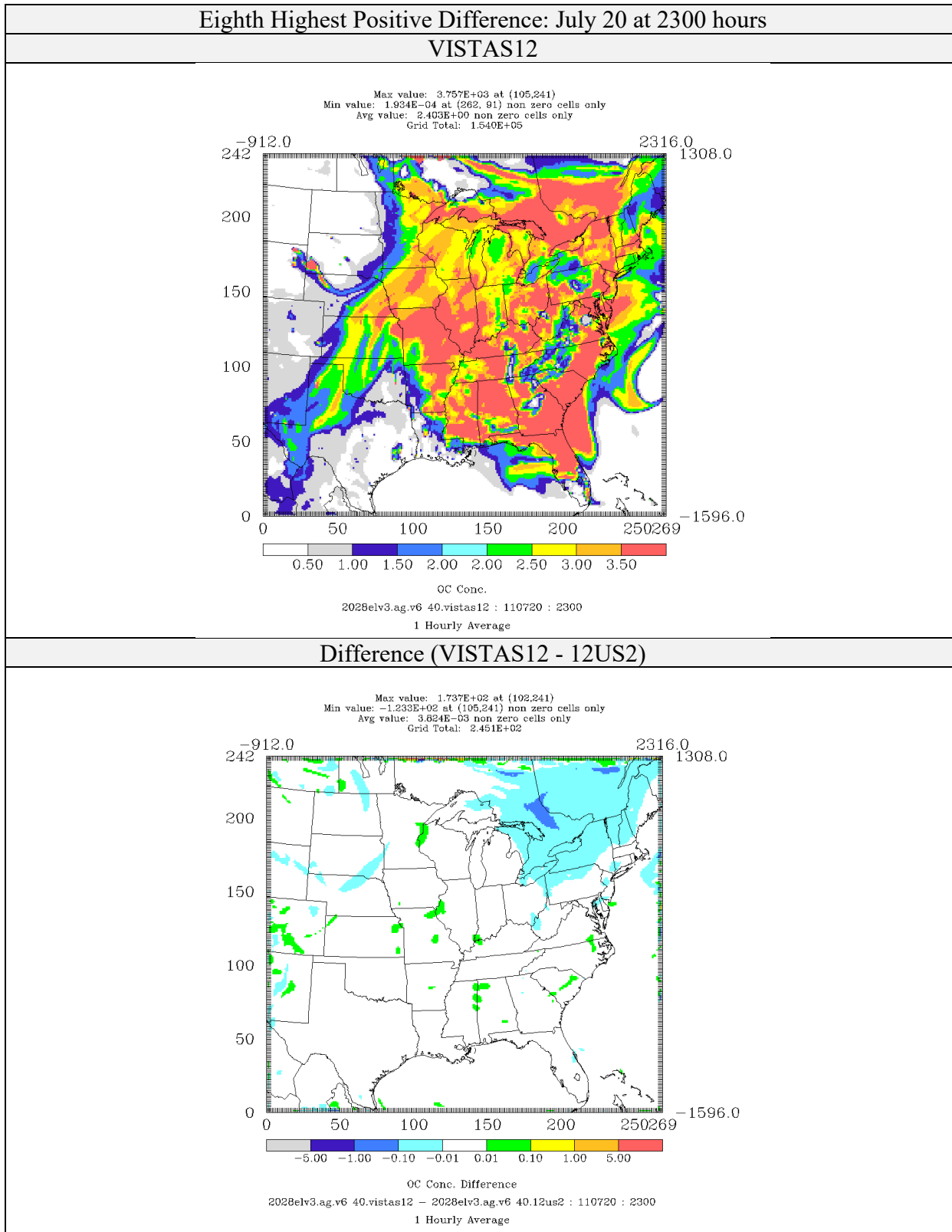


Figure 4-92: Comparison of Organic Matter Concentrations ($\mu\text{g}/\text{m}^3$) for CAMx 6.40 on VISTAS12 and 12US2 Domains 2028elv3 Simulations (Eighth Highest Positive Difference)

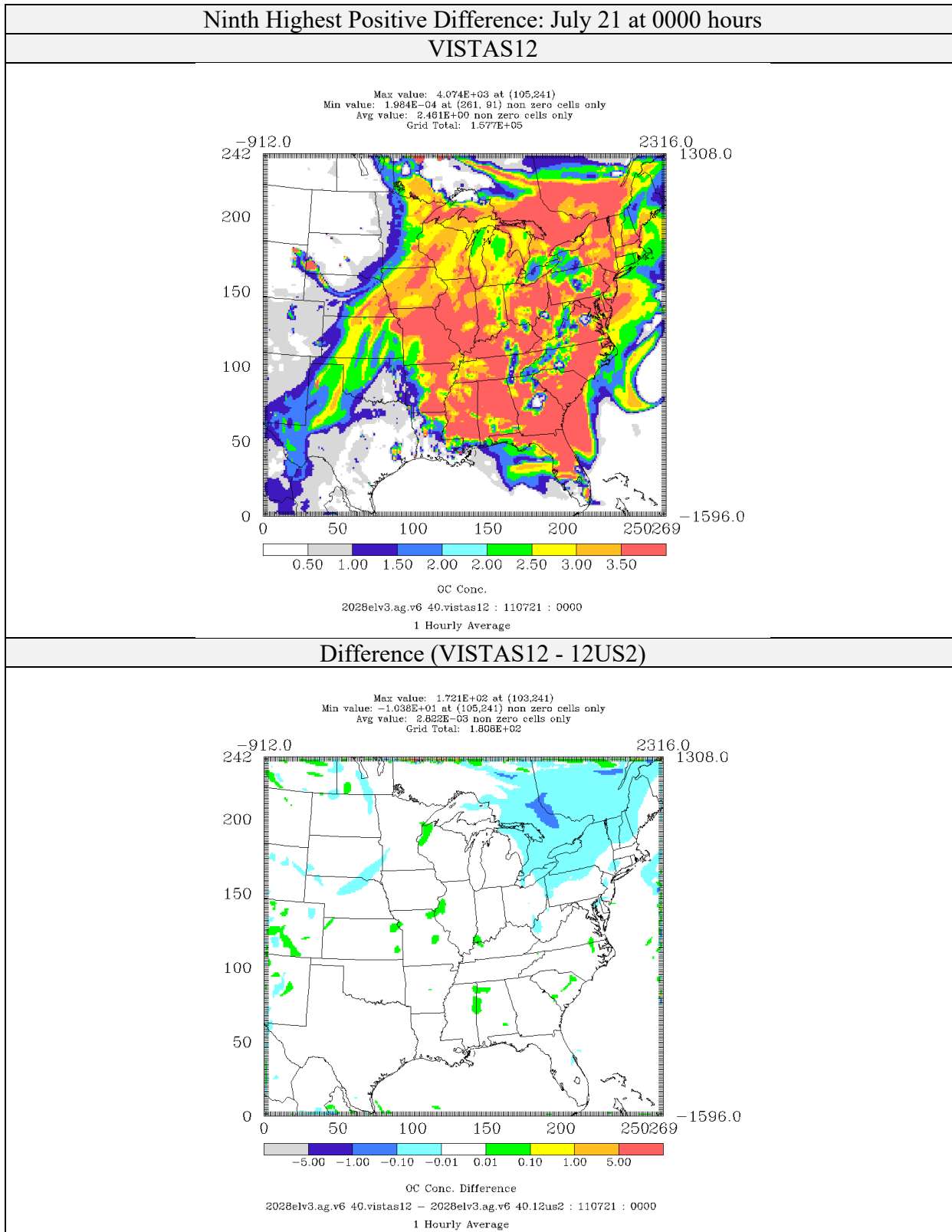


Figure 4-93: Comparison of Organic Matter Concentrations ($\mu\text{g}/\text{m}^3$) for CAMx 6.40 on VISTAS12 and 12US2 Domains 2028elv3 Simulations (Ninth Highest Positive Difference)

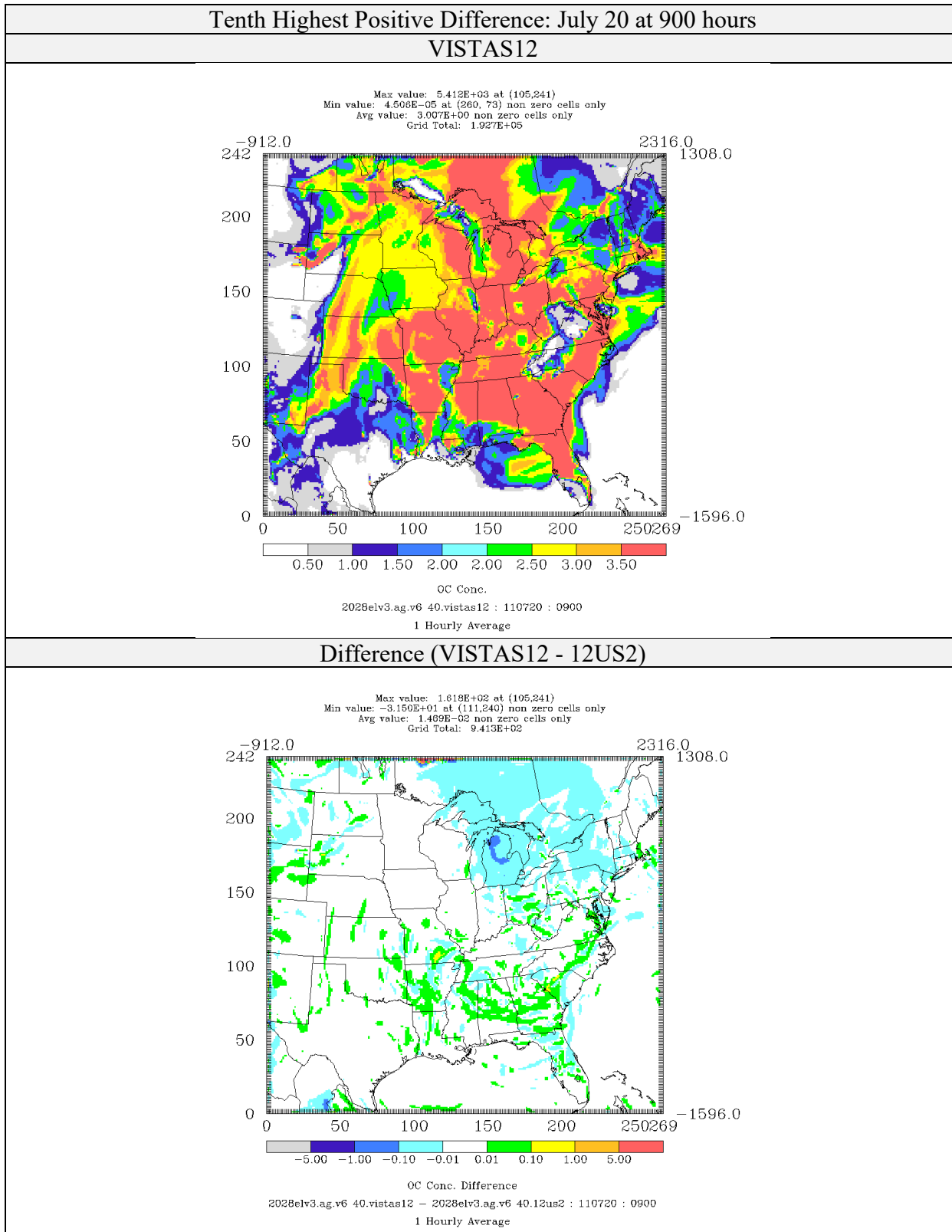


Figure 4-94: Comparison of Organic Matter Concentrations ($\mu\text{g}/\text{m}^3$) for CAMx 6.40 on VISTAS12 and 12US2 Domains 2028elv3 Simulations (Tenth Highest Positive Difference)

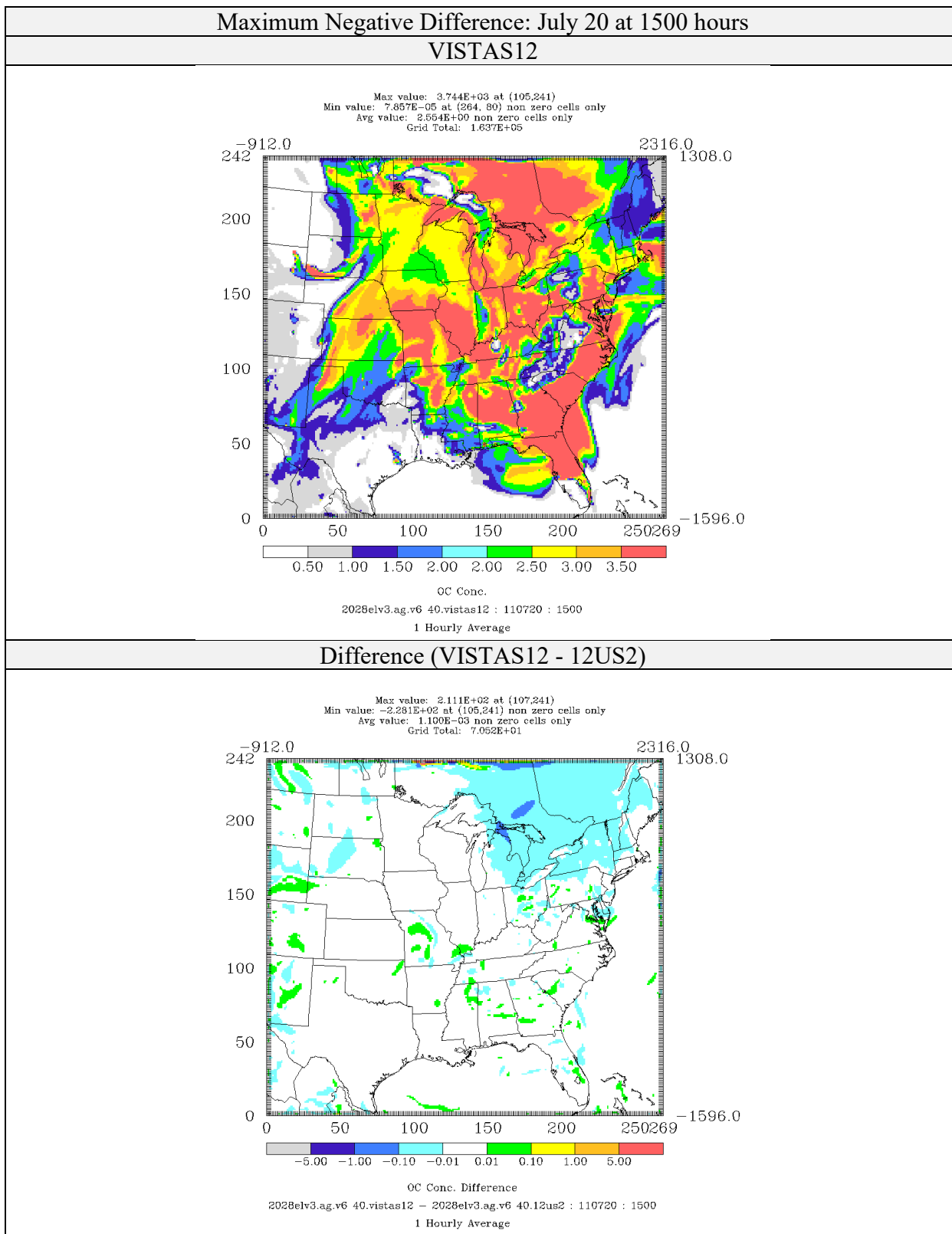


Figure 4-95: Comparison of Organic Matter Concentrations ($\mu\text{g}/\text{m}^3$) for CAMx 6.40 on VISTAS12 and 12US2 Domains 2028elv3 Simulations (Maximum Negative Difference)

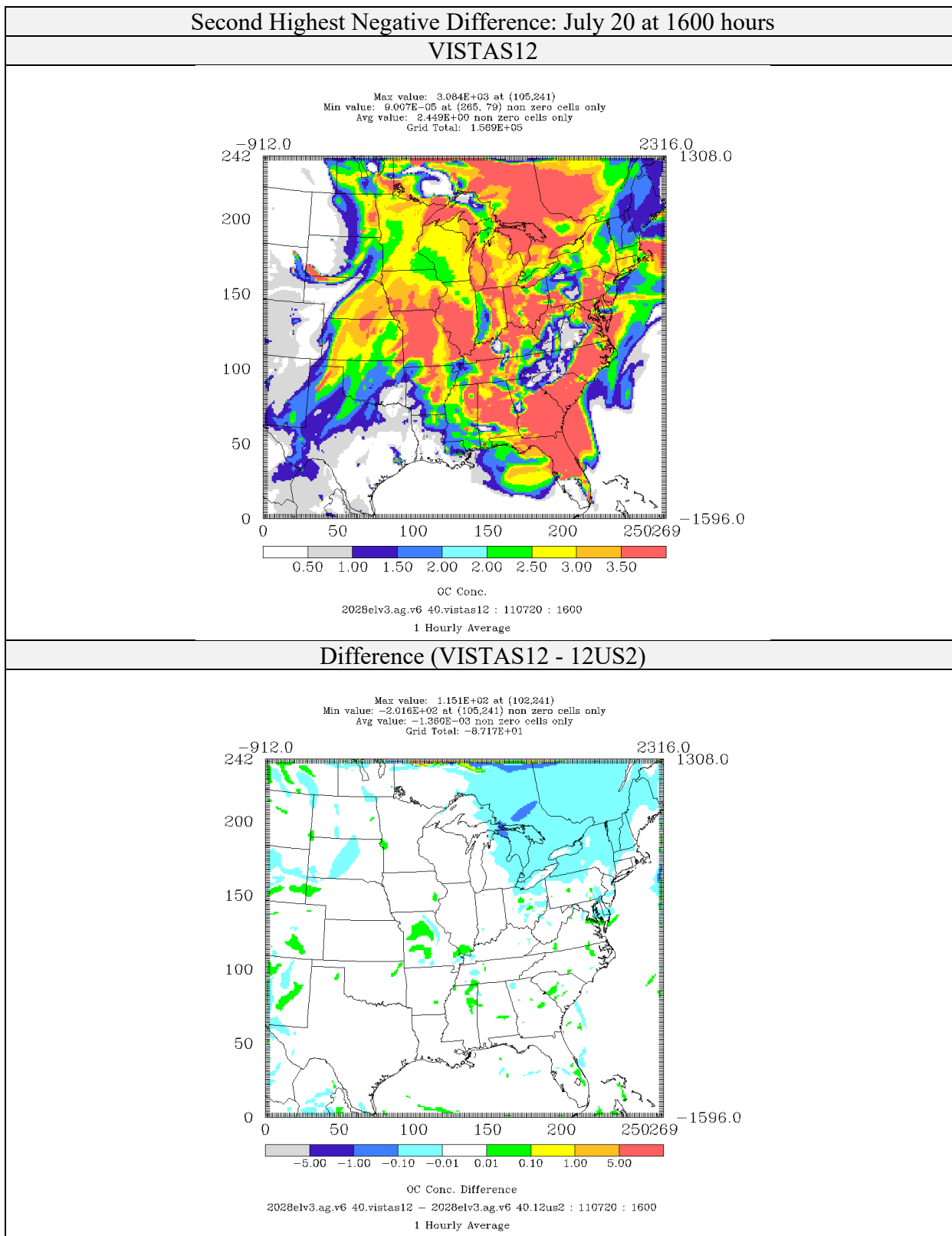


Figure 4-96: Comparison of Organic Matter Concentrations ($\mu\text{g}/\text{m}^3$) for CAMx 6.40 on VISTAS12 and 12US2 Domains 2028elv3 Simulations (Second Highest Negative Difference)

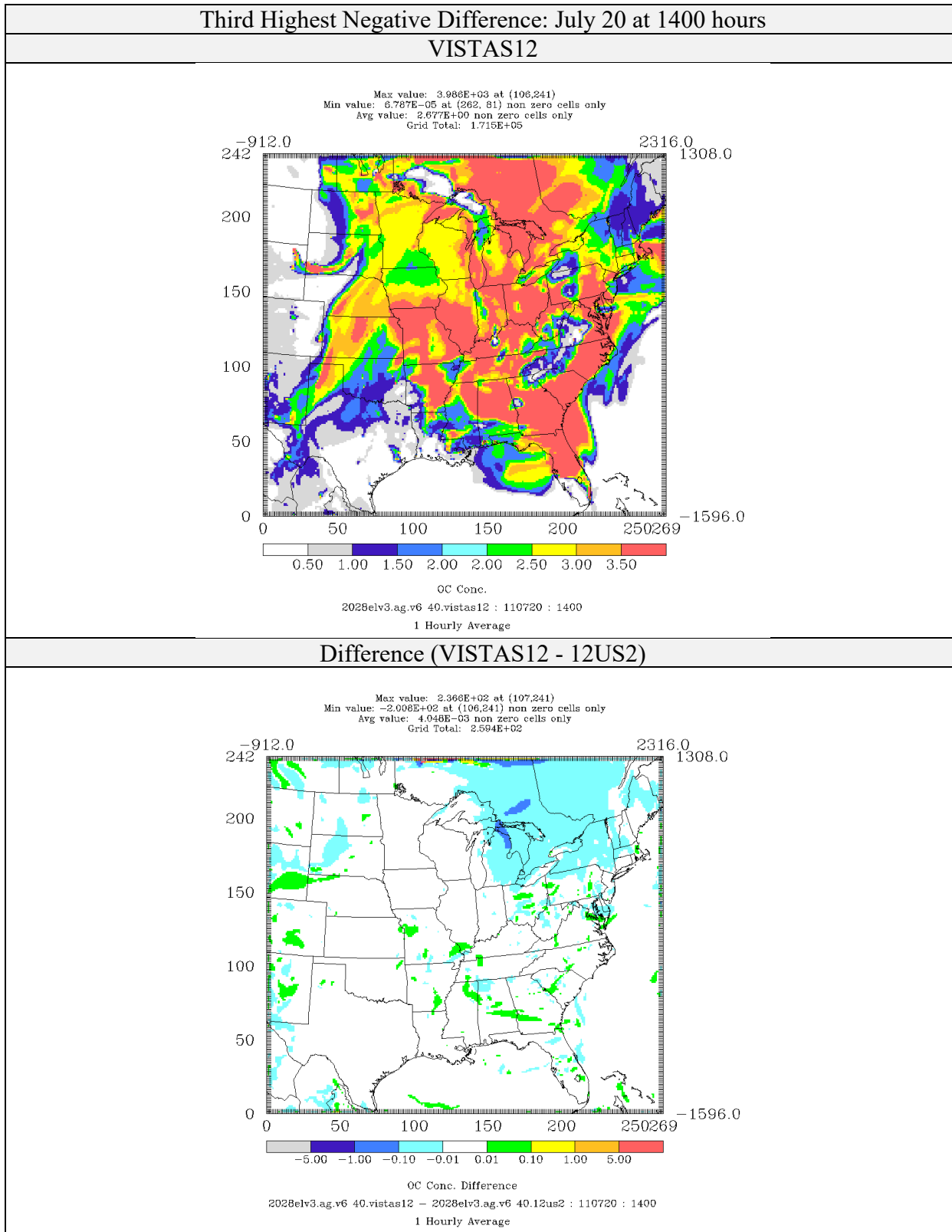


Figure 4-97: Comparison of Organic Matter Concentrations ($\mu\text{g}/\text{m}^3$) for CAMx 6.40 on VISTAS12 and 12US2 Domains 2028elv3 Simulations (Third Highest Negative Difference)

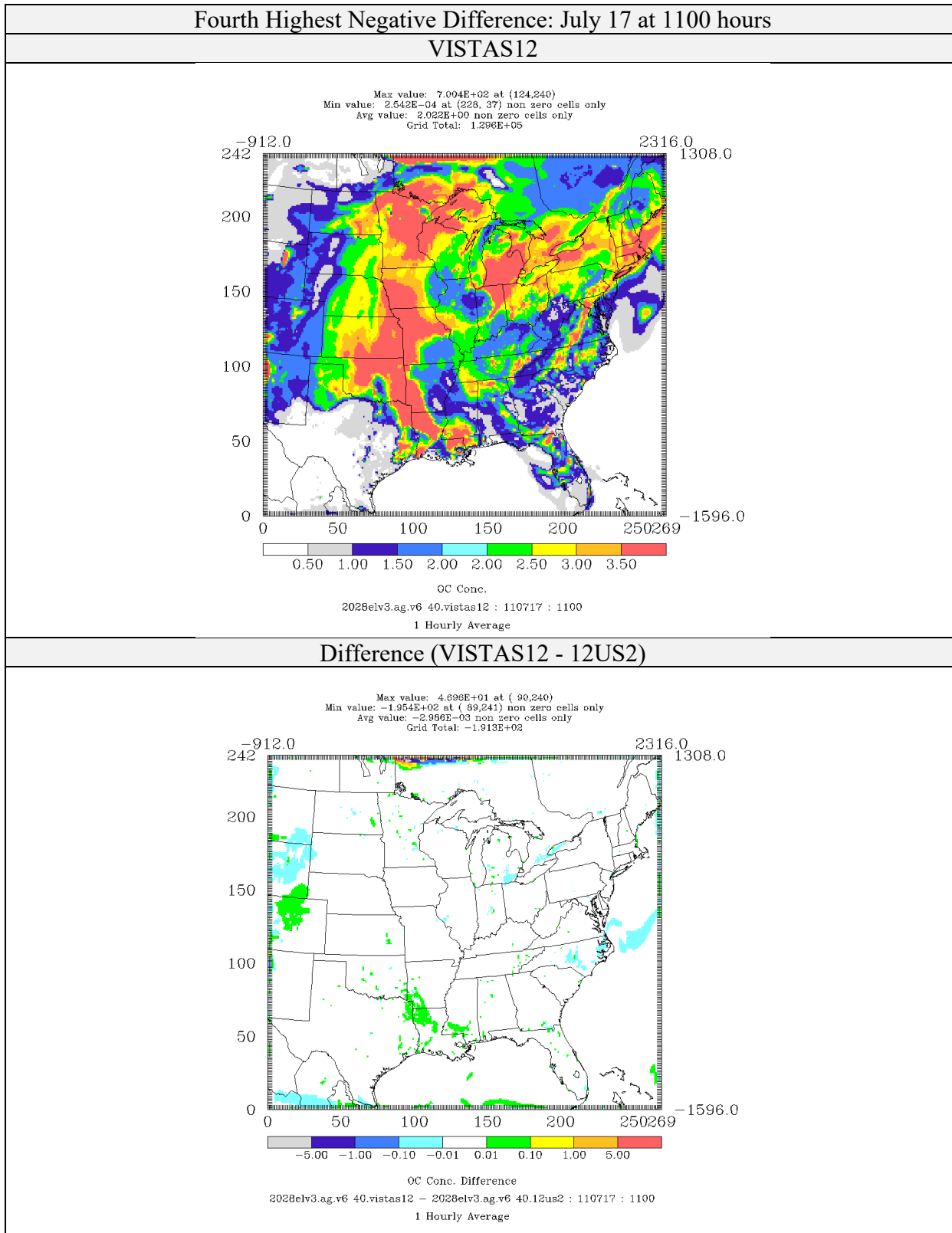


Figure 4-98: Comparison of Organic Matter Concentrations ($\mu\text{g}/\text{m}^3$) for CAMx 6.40 on VISTAS12 and 12US2 Domains 2028elv3 Simulations (Fourth Highest Negative Difference)

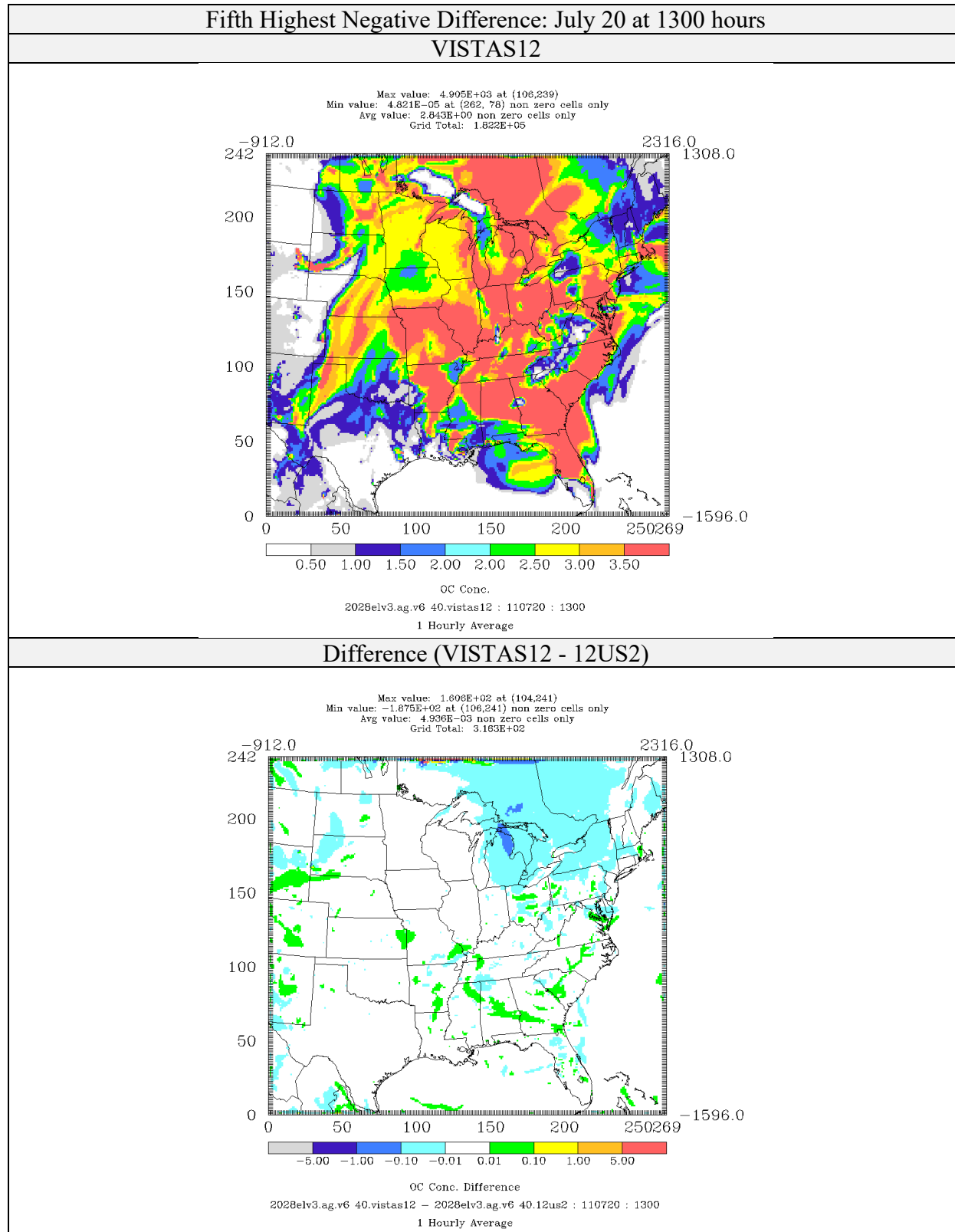


Figure 4-99: Comparison of Organic Matter Concentrations ($\mu\text{g}/\text{m}^3$) for CAMx 6.40 on VISTAS12 and 12US2 Domains 2028elv3 Simulations (Fifth Highest Negative Difference)

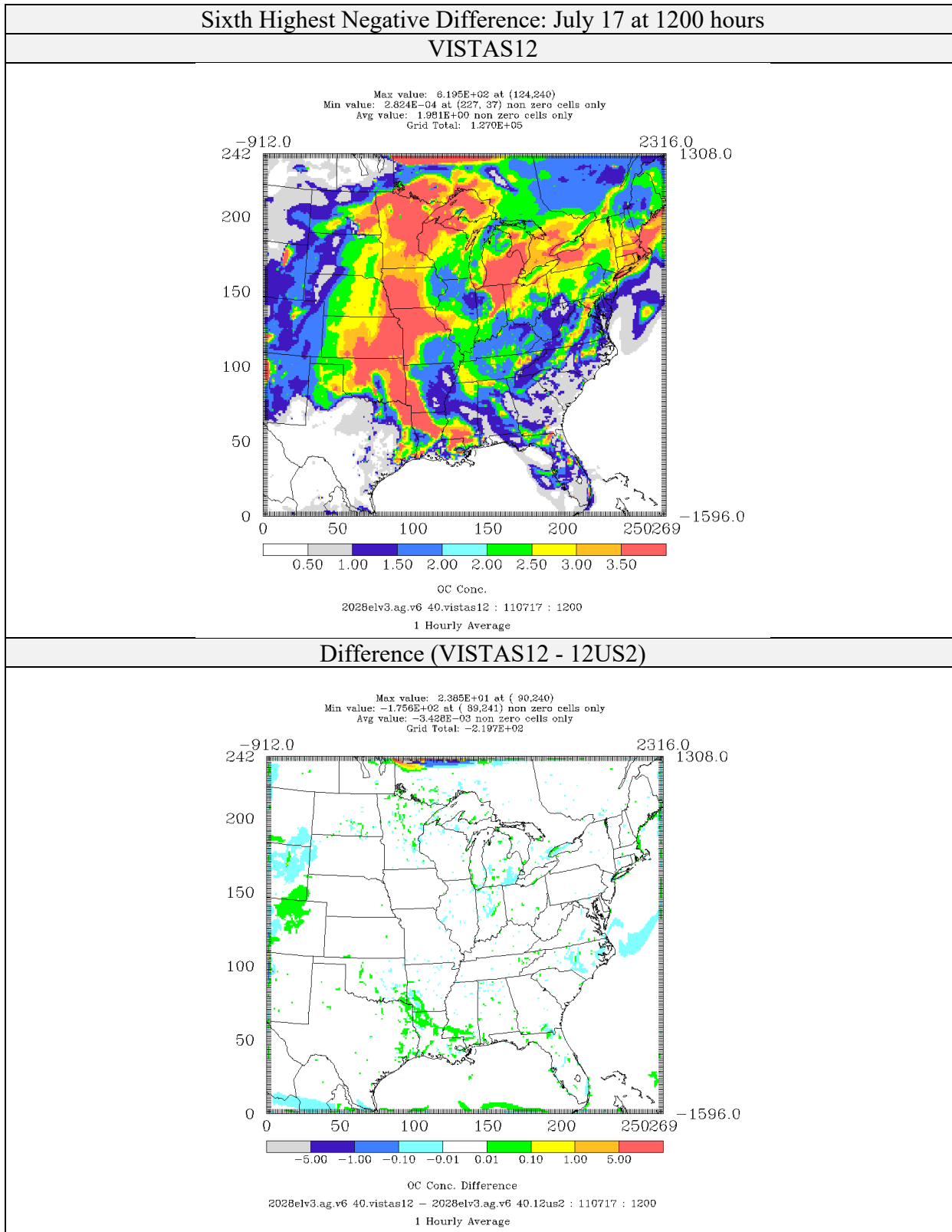


Figure 4-100: Comparison of Organic Matter Concentrations ($\mu\text{g}/\text{m}^3$) for CAMx 6.40 on VISTAS12 and 12US2 Domains 2028elv3 Simulations (Sixth Highest Negative Difference)

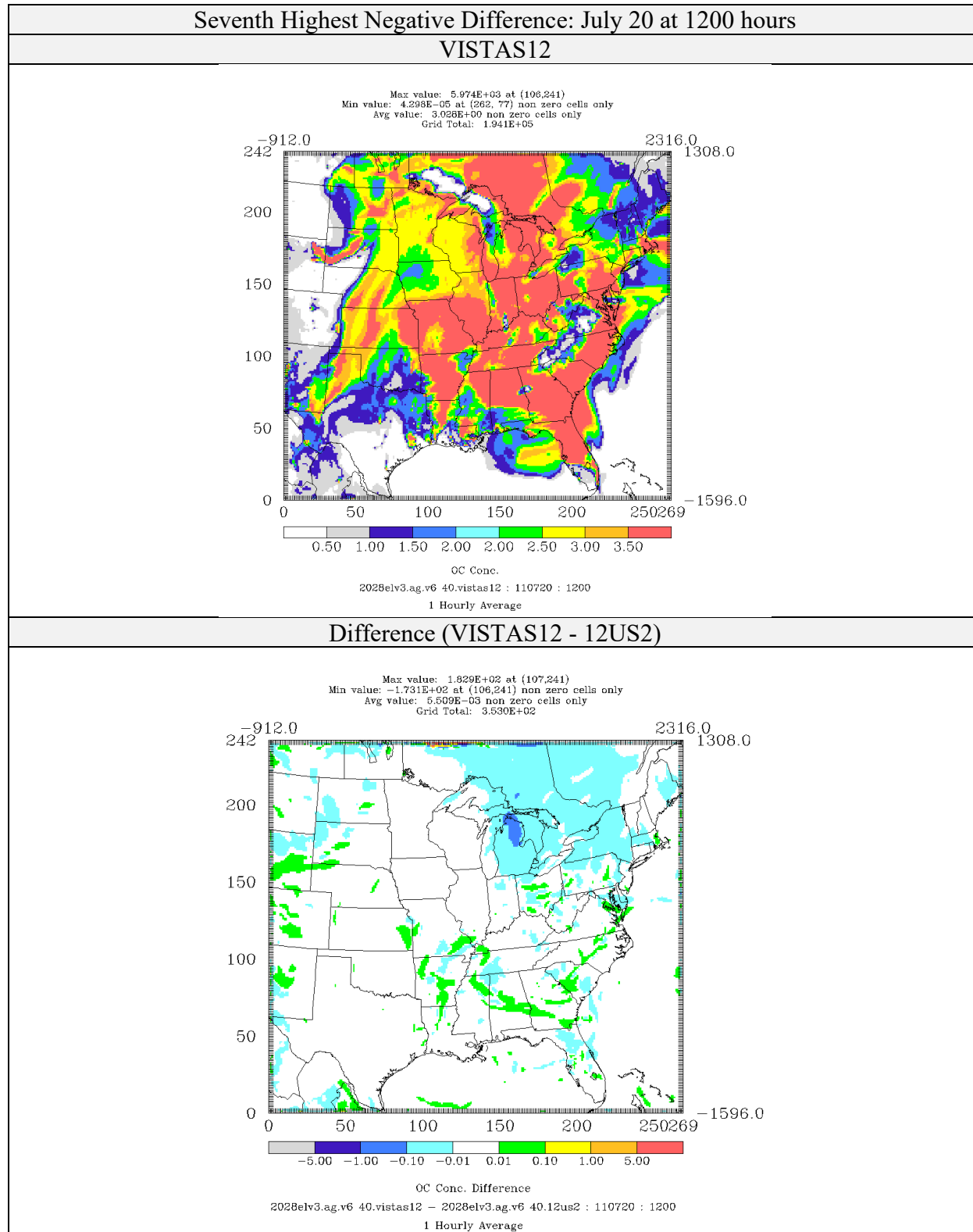


Figure 4-101: Comparison of Organic Matter Concentrations ($\mu\text{g}/\text{m}^3$) for CAMx 6.40 on VISTAS12 and 12US2 Domains 2028elv3 Simulations (Seventh Highest Negative Difference)

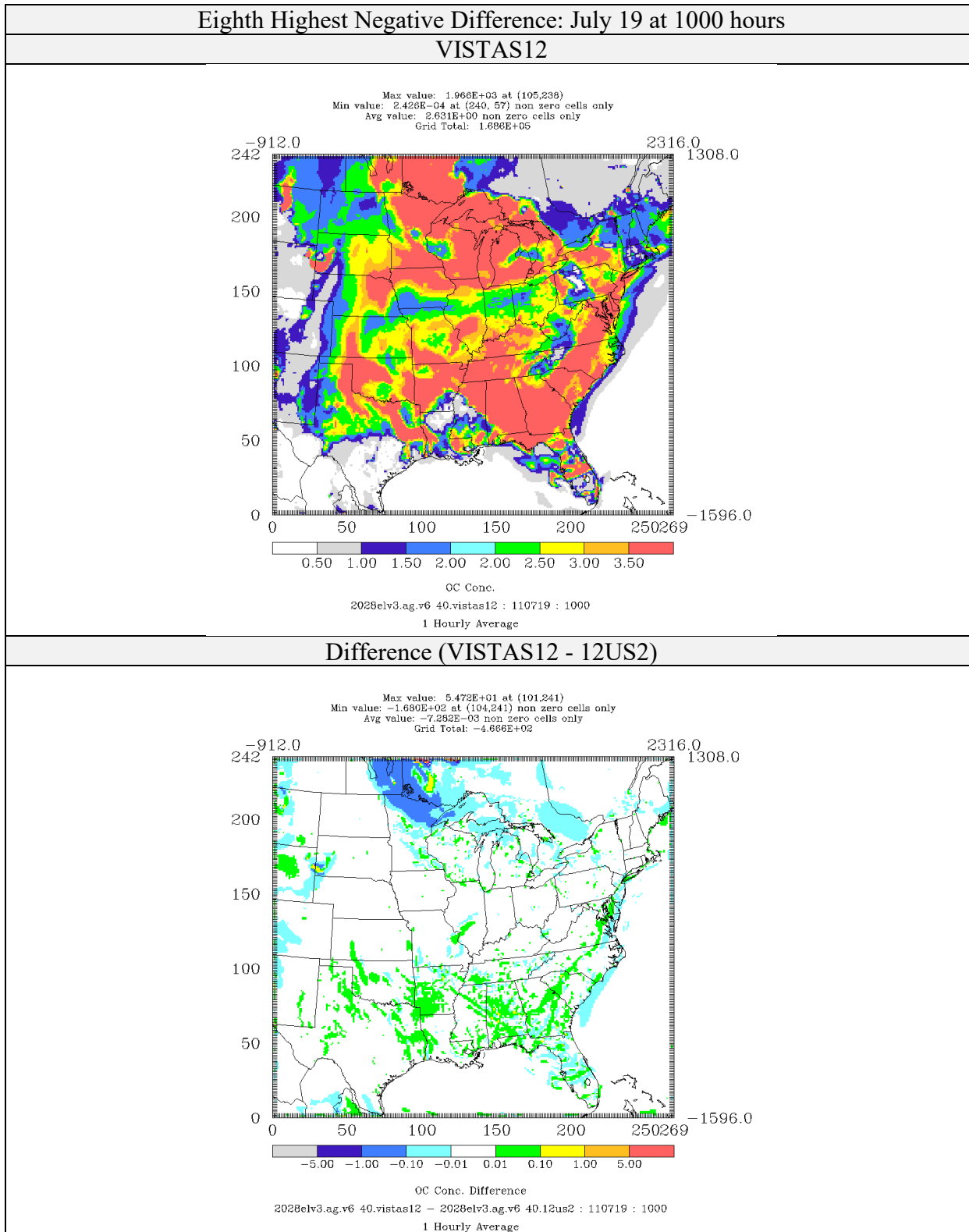


Figure 4-102: Comparison of Organic Matter Concentrations ($\mu\text{g}/\text{m}^3$) for CAMx 6.40 on VISTAS12 and 12US2 Domains 2028elv3 Simulations (Eighth Highest Negative Difference)

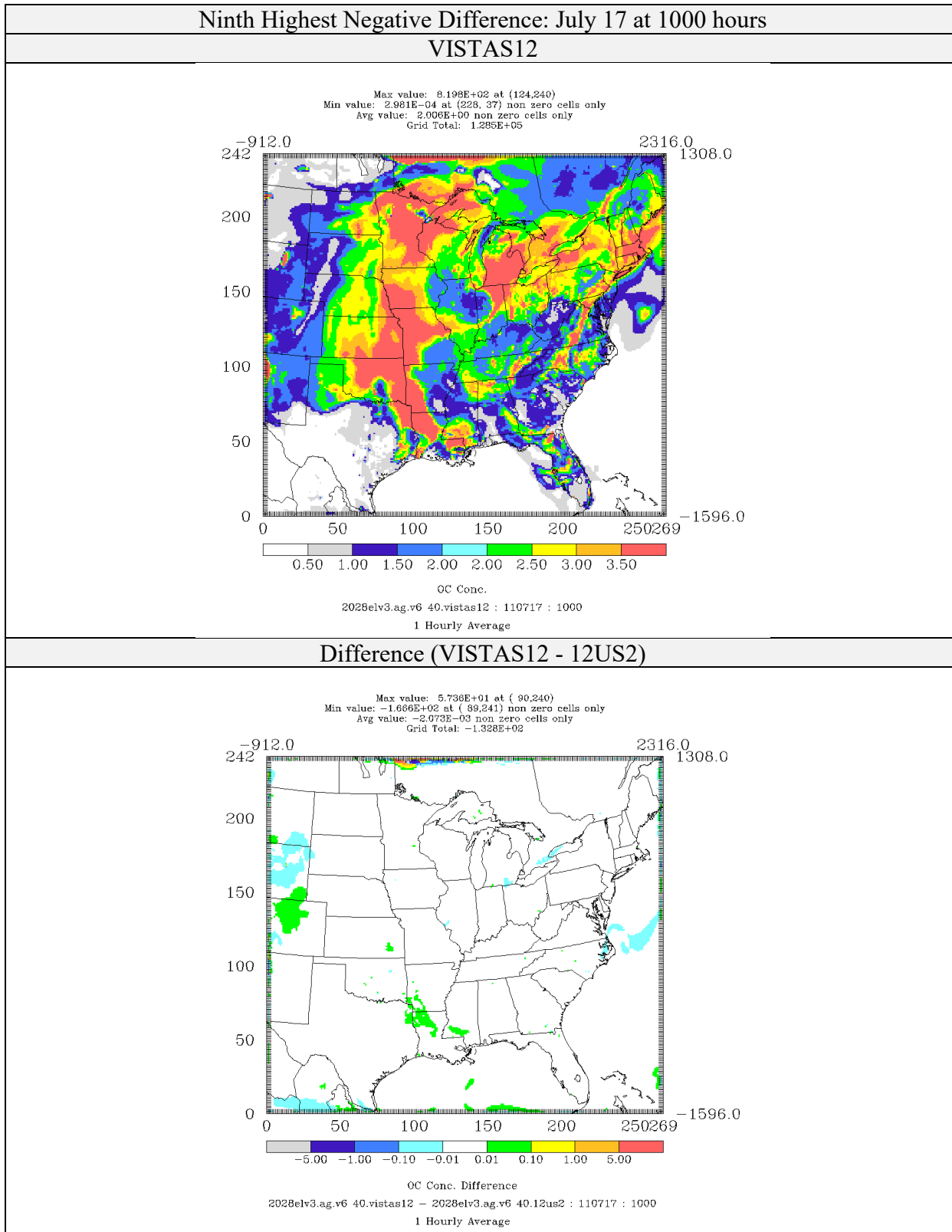


Figure 4-103: Comparison of Organic Matter Concentrations ($\mu\text{g}/\text{m}^3$) for CAMx 6.40 on VISTAS12 and 12US2 Domains 2028elv3 Simulations (Ninth Highest Negative Difference)

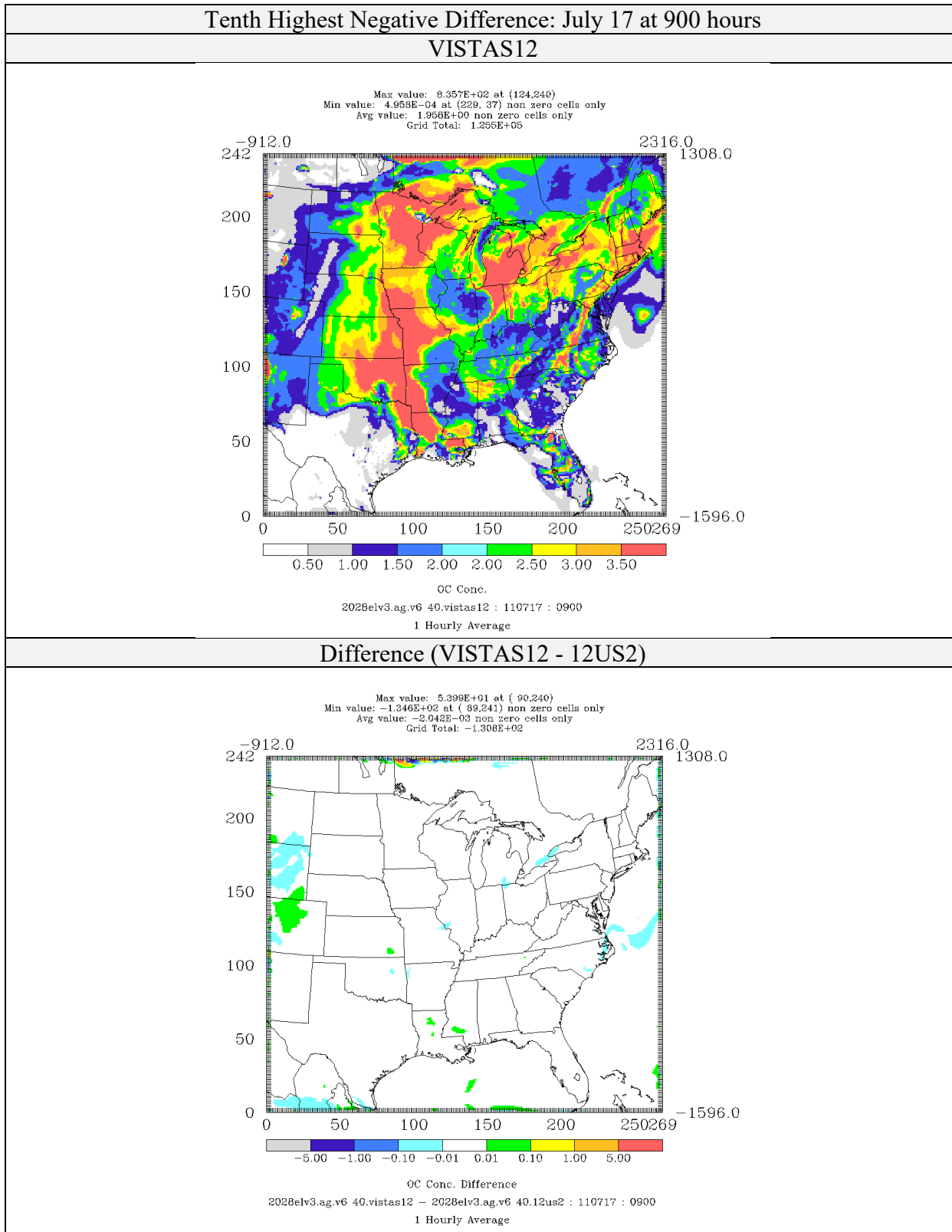


Figure 4-104: Comparison of Organic Matter Concentrations ($\mu\text{g}/\text{m}^3$) for CAMx 6.40 on VISTAS12 and 12US2 Domains 2028elv3 Simulations (Tenth Highest Negative Difference)

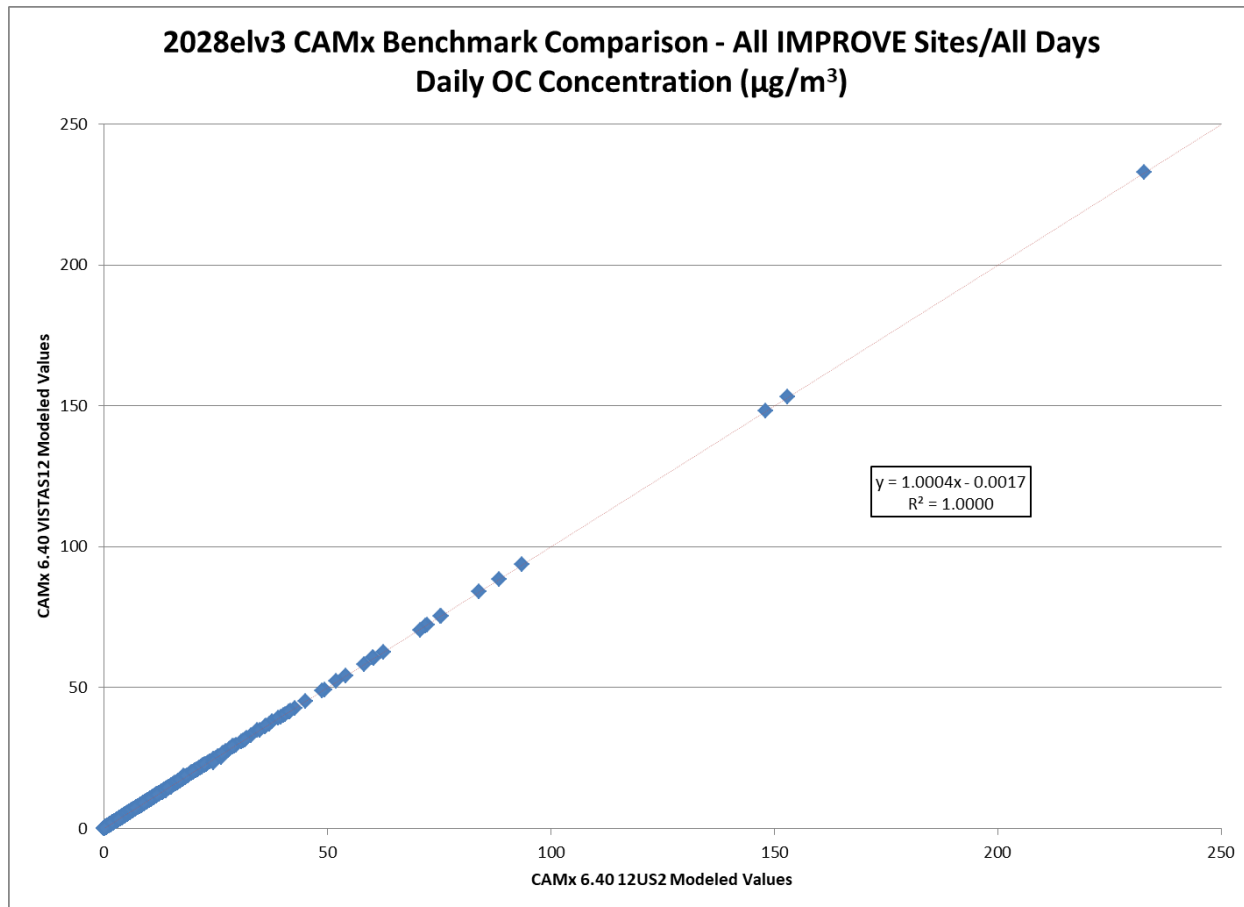


Figure 4-105: Scatterplot Comparing 24-hour Average Predicted Organic Matter Concentrations ($\mu\text{g}/\text{m}^3$) for All Days at all IMPROVE Monitor Locations for CAMx 6.40 on VISTAS12 and 12US2 Domains 2028elv3 Simulations Performed by VISTAS (Alpine).

5.0 CONCLUSIONS

A comparison has been made between CAMx 6.40 simulations using EPA's 2028el modeling platform as performed on the Alpine Geophysics computer system for the VISTAS12 and EPA continental US 12km (12US2) grid. The comparison was conducted for ozone, PM_{2.5}, sulfate, nitrate and organic carbon and included an examination both of hourly gridded concentrations and at daily average concentrations at the IMPROVE monitors. The hourly gridded comparison showed areas of maximum differences along the border with the differences decreasing with distance into the VISTAS12 domain.

Two issues have been identified that have noted impact on the use of the VISTAS12 domain relative to the 12US2 domain. The first, and likely the most significant issue is a time-step difference at the boundary where concentration conditions from outside of the domain are injected into the modeling domain at one hour intervals compared to the model generated (sub-hourly) time-step interval within the modeling domain. These differences can create initial, significant concentration gradients along the boundary that can be carried through the episode and transported to grid cells within the modeling domain. The second issue is related to the time step in the model. The time step is determined by the maximum wind in the modeling domain. If the highest wind in the 12US2 domain occurs somewhere outside the VISTAS12 domain, the time step in the 12US2 simulation will be longer than in the VISTAS12 domain.

We note that in modeling the VISTAS12 domain with 12US2 boundary conditions, both of these issues are exacerbated in the modeling due to large emission sources located near the boundary of the 12US2/VISTAS12 boundary. A comparison of the daily average concentrations at the IMPROVE monitors showed very small differences with an R² of no less than 0.9999 for all pollutants.

Alpine Geophysics does not see any features in the modeling that would preclude the use of the VISTAS12 modeling domain for use in the VISTAS air quality planning, yet recognizes the impacts related to the current configuration of the VISTAS12 domain and issues related to border grid cells. While the analysis at the IMPROVE monitors has shown that the impact is negligible at the IMPROVE monitors, if these differences are unacceptable to SESARM, SESARM should consider using the 12US2 domain for regional haze modeling.